# MUD VOLCANOES ON THE DRY LAND OF NIGERIA

**BY**

**MUSA OJOCHENEMI KIZITO**

**DEPARTMENT OF GEOLOGY**

**FACULTY OF SCIENCE,**

**AHMADU BELLO UNIVERSITY,**

**ZARIA, NIGERIA.**

**SEPTEMBER, 2015**

# MUD VOLCANOES ON THE DRY LAND OF NIGERIA

**BY**

**MUSA OJOCHENEMI KIZITO**

**B.Sc., M.Sc. Geology, A.B.U, ZARIA.**

**(Ph.D/SCIE/08597/2010-2011)**

**A DISSERTATION SUBMITTED TO POSTGRADUATE SCHOOL, AHMADU BELLO UNIVERSITY,**

**ZARIA, NIGERIA.**

**IN PARTIAL FULFILLMENT OF THE REQUIREMENTS FOR THE AWARD OF DOCTOR OF PHILOSOPHY DEGREE IN GEOLOGY**

**DEPARTMENT OF GEOLOGY**

**AHMADU BELLO UNIVERSITY,**

**ZARIA, NIGERIA**

**SEPTEMBER, 2015**

## DECLARATION

I declare that this dissertation titled "Mud volcanoes on the dry land of Nigeria" has been done by me in the Department of Geology, Ahmadu Bello University, Zaria, under the academic linkage between Ahmadu Bello University, Zaria, Nigeria and the University of Silesia, Katowice, Poland, under the supervision of Dr Ewa Kurowska, Professor Krzysztof Schoeneich, and Professor S.A Alagbe. All the information derived from literature has been duly acknowledged in the text and a list of references provided. No part of this dissertation was previously presented for another degree or diploma at this University or any other institution of higher learning.

Musa Ojochenemi Kizito

| _____ | _____ | _____ |
|---|---|---|
| Name of Student | Signature | Date |

## CERTIFICATION

This dissertation titled "MUD VOLCANOES ON THE DRY LAND OF NIGERIA" meets the regulations governing the award of degree of Doctor of Philosophy in Geology from Ahmadu Bello University, Zaria, and is approved for its contribution to knowledge and literary presentation.

| | | |
|---|---|---|
| Dr Ewa Kurowska | E. Kurowska | 1/10/2015 |
| Chairman, Supervisory Committee | Signature | Date |
| Professor Krzysztof Schoeneich | _____ | _____ |
| Member, Supervisory Committee | Signature | Date |
| Professor Solomon A. Alagbe | _____ | _____ |
| Member, Supervisory Committee | Signature | Date |
| Dr .Halidu Hamza | _____ | _____ |
| Head of Department | Signature | Date |
| Professor Kabiru Bala | _____ | _____ |
| Dean, Postgraduate School | Signature | Date |

## ACKNOWLEDGEMENT

My sincere gratitude goes to the Almighty God, who in his infinite mercy has seen me through this academic programme despite all the challenges.

My gratitude goes to the chairman of the supervisory committee Dr Ewa Kurowska, who facilitated some of the analysis in this work. Also, her suggestions, criticism, critical review of the dissertation, made the work a huge success. I am also indebted to Professor Krzysztof Schoeneich and Professor S. A. Alagbe, members of the supervisory committee who were consistently made remarkable contributions and suggestions that have improved the quality of this work.

I am equally grateful to the Head and staff of Geology Department, Ahmadu Bello University, Zaria, for their useful comments, discussions, suggestions and encouragement to this research work. My thanks go to the Dean of Science, Federal University Lokoja, Professor Patrick Audu for his useful advice, support and encouragement. My gratitude goes to the Head of Geology Department, Federal University Lokoja, Professor Abdullahi Emmanuel Bala, for his useful comments, discussions, suggestions and encouragement to this research work. Also, am grateful to Dr. Jerry Ayok for all his meaningful suggestions and contributions rendered to make this work a huge success.

I acknowledge the prayers, love, advice and moral support from my wife and sons, Mrs. Abigail Ojogbane Musa, Joseph Akoji Musa (Jnr) and Joshua Onucheojo Musa, Mum (Mrs. Agnes Musa), Professor Patrick Audu's family, Mr. and Mrs. Alfred Musa, Mr. and Mrs. Patrick Musa, Mrs Josephine Ademu, Mr and Mrs Jomomoh, Rev. Sis. Mary Musa, Mr and Mrs. Jones Negedu, Mr and Mrs Johnpaul Musa, My Inlaws (Mr. and Mrs. T.A Okeme), Mr. and Mrs Mathias Ojih, Ojochegbe Musa, Divine Jomomoh,

Enyojo Musa, James Jomomoh, Joseph Musa, Jason Jomomoh, Michel Negedu and Sheila Musa.

My regards goes to my field assistant, Mr Husseini Ahmed residence of Lallapido village and all my colleagues and friends who have made the programme very interesting for me, Dibal Usman, Fabian Ohiemi, Thaddeus Akuh, Charles Okeme, Romanus Adejo, Umaru Musa, Engr. George Okpanachi, Ebenezer Kudamnya, Efenji Godwin, Silas Joshua, John Onah, Ishiaku David Shilte, and Saleh (Kura).

I also remain grateful to 400 level students during the 2012 fieldwork under the supervision of Professor Krzysztof Schoeneich. The village heads and the people of the following communities: Lallaipido, Todi, Kurum, Lachikoltok, Biliri, Gujuba, Pamadu, Lashadar, Leturu, Jenye, Lakaturu, Digga and Latatar. I sincere acknowledge the support from TET Fund through the management of Federal University Lokoja, for providing staff fellowship grant. I wish to acknowledge the academic linkage between Ahmadu Bello University, Zaria, Nigeria and the University of Silesia, Katowice (Poland), for making this research work possible.

Finally, am eternally grateful to my late Dad, Sir J.A. Musa, you were the first person that educated, inspired and encouraged me on the need to further my studies after my B.Sc degree. As i celebrate today, I only wish you were here on earth because i know you would have gone out of your ways to host me. By accomplishing what we started some years ago, I know i have made you proud even as your gentle soul is resting at the bossom of the lord.

## ABSTRACT

Mud volcanoes are some of the most mysterious geological features. Occurrence of mud volcanoes could signify presence of hydrocarbons or sudden endogenetic events. Mud volcanoes exist worldwide in areas of rapid sedimentation, lateral tectonic compression and recent magmatic activity or hydrocarbon occurrence. In this study, about 200 of onshore mud volcanoes were found and documented in Nigeria.A critical study on the occurrence of recently found onshore mud volcanoes in Nigeria was undertaken with emphasis on documentation and mapping of the onshore mud volcanoes with the view of understanding the geological control on their distribution. The study approach involves reconnaissance survey, fieldwork, field sampling and insitu measurement of physico – chemical parameters. In this study, through reconnaissance survey, about 200 of onshore mud volcanoes were investigated and documented in Nigeria. The fieldwork revealed that onshore mud volcanoes are located within Cretaceous Upper Benue Trough, filled with Early Cretceous continental deposits and Late Cretaceous marine deposits, having a history of magmatism dating from Albian to Pleistocene. The onshore mud volcanoes occur mostly on Yolde Formation and Upper Bima Sandstone in groups of 5 – 30 volcanoes (mud volcano fields). They occur along the NE – SW trending Kaltungo fault zone and other minor N – S and NW –SE trending faults. The physical characteristic of the onshore mud volcanoes found are mostly of small sizes, having cones not exceeding one and half metres in height and diameters ranging from 0.5 m to 8 m at base, with pools of water and mudflows from the craters. Temperature of the mud at the neck of the volcano ranges between 22°C to 26°C which is below the local mean annual temperature of the surrounding at 29°C. The XRD analysis of the clays from the mud volcanoes reveal the presence of traces of marine mineral content such as smectite, bentonite, calcite and evaporites in the clay in some of the mud volcanoes, and complete absence of the listed elements in other mud volcanoes reveals that the clays being extruded by the mud volcanoes are mostly from the Yolde Formation and the Upper Bima Sandstone. Results of hydrochemical analysis on the water samples from 14 mud volcano fields show that the cationic and anionic concentration varies as follows: $Ca^{2+}$ (8.26 to 46.4 mg/l), $Mg^{2+}$ (1.16 to 20 mg/l), $Na^{+}$(18.6 to 4789 mg/l), $K^{+}$ (9.4 to 134 mg/l), Fe (0.02 to 5.74 mg/l), $HC0_3$– (126 to 3111 mg/l), $Cl^{-}$ (5 to 2625 mg/l), $S0_4^{2-}$ (12.5 to 16.9mg/l), $C0_3^{2-}$ (3 to 2040 mg/l) and $SiO_2$ (7 to 45.6 mg/l). Physico - chemical parameters of water from the mud volcanoes, is most highly alkaline (pH ranges from 7.94 to 8.99), saline (TDS varies from 249 to 12757 mg/l), very hard (TH varies from 102 to 1180 mg/l $CaCO_3$). The dominant hydrochemical facies is Na (K) – $HCO_3$ while Ca–Na–$HCO_3$ is the minor water type. The chemical composition of water from the mud volcanoes shows high mineralisation which is an indication of connate mixed with meteoric water. With the exception of $Ca^{2+}$, $Mg^{2+}$ and $S0_4^{2-}$, all other parameters are far above the World Health Organization (WHO) and Nigerian Industrial Standard (NIS) standards for drinking water which may be important in environmental context as the local people sometimes drink the water. This group of onshore mud volcanoes found in Nigeria are structurally controlled and characterised as small mud or often sand volcanoes from which material ejected to the surface is derived from shallow depths, usually only a few tens of metres. The occurrences of onshore mud volcanoes along the fault zones within the study area suggest a surface manifestation of neotectonism in the area.

## TABLE OF CONTENT

PAGE

Tittle Page - - - - - - - - - i

Declaration - - - - - - - - - ii

Certification - - - - - - - - - iii

Acknowledgement - - - - - - - - - iv

Abstract - - - - - - - - - vi

Table of Contents - - - - - - - - - vii

List of Tables - - - - - - - - - - xi

List of Maps and Figures - - - - - - - - xii

List of Plates - - - - - - - - - - xvi

List of Appendices - - - - - - - - - xxv

**CHAPTER ONE: GENERAL INTRODUCTION**

1.1 Background to the Study - - - - - - - - 1

1.2 Aim and Objectives of the Study - - - - - - 3

1.3 Justification of the Study - - - - - - - 3

1.4 Scope of the Study - - - - - - - - 4

1.5 Concept and Origin of Mud Volcanoes - - - - - 5

1.6 Classification of Mud Volcanoes - - - - - 9

1.7 Global Distribution of Mud Volcanoes - - - - 10

1.7.1 Mud Volcanoes in Africa - - - - - - 11

1.7.2 Mud Volcanoes in Nigeria - - - - - - 13

## CHAPTER TWO: LOCATION AND GEOLOGY OF SURROUNDING AREA OF MUD VOLCANOES


2.1 Location and Accessibility of Onshore Mud Volcanoes in Nigeria - 15

2.2 Climate and Vegetation of the Area of Occurrence of Mud Volcanoes 15

2.3 Relief and Drainage of the Area of Occurrence of Mud Volcanoes - 17

2.4 People and Settlement of the Area of Occurrence of Mud Volcanoes 17

2.5 Geological Background of the Area of Occurrence of Mud Volcanoes 20

2.5.1 History of the Benue Trough of Nigeria - - - - 20

2.5.2 Origin of the Benue Trough of Nigeria- - - - - 21

2.6 Palaeogeographic History of the Benue Trough of Nigeria- - - 23

2.6.1 Albian Transgression - - - - - - 23

2.6.2 Late Albian to Cenomanian Regression - - - - 24

2.6.3 Late Cenomanian to Early Turonian Transgression - - - 24

2.6.4 Middle Turonian Regression - - - - 25

2.6.5 Late Turonian to Coniacian Transgression - - - - 25

2.6.6 Santonian - - - - - - - - 25

2.6.7 Late Campanian to Maastrichtian Transgression - - - 26

2.6.8 Palaeocene Transgression - - - - - - 26

2.7 The Upper Benue Trough - - - - - - 27

2.7.1 Introduction - - - - - - - - 27

2.8 Stratigraphic Succession - - - - - - 28

2.8.1 Bima Group - - - - - - - - 32

2.8.2 Yolde Formation - - - - - - - 34

2.8.3 Pindiga Formation - - - - - - 36

2.8.4 Gombe Formation - - - - - - 43

2.8.5 Kerri-Kerri Formation- - - - - - - 43

2.8.6 Biu Basalt - - - - - - - - 44

2.8.7 Alluvium - - - - - - - - 45

2.9 Structure of the Upper Benue Trough- - - - - 45

2.9.1 Faults - - - - - - - - 48

2.9.2 Folds - - - - - - - - - 49

**CHAPTER THREE: METHODOLOGY**

3.0 Introduction - - - - - - - - 52

3.1 Desk Study - - - - - - - - 52

3.2 Reconnaissance Survey - - - - - - 52

3.3 Interpretation of Satellite Images - - - - - 52

3.4 Fieldwork - - - - - - - - 53

3.5 Laboratory Sample Preparation and Analysis - - - 54

3.5.1 Granulometric Analysis - - - - - - 54

3.5.2 X-Ray Diffractometer (XRD) Analysis - - - - 55

3.5.3 Water Analysis - - - - - - - - 57

3.6 Statistical Analysis of Results and Interpretation - - - 58

**CHAPTER FOUR: RESULTS AND DISCUSSION**

4.1 The Geology of the Surrounding Area of Mud Volcanoes - - 61

4.1.1 Stratigraphy of the Study Area - - - - - 61

4.1.2 Geological Structures in the Study Area - - - - 67

4.2 Physical Characteristics of Onshore Mud Volcanoes Documented

in the Study Area - - - - - - - 72

4.3 Distribution of Onshore Mud Volcanoes in the Study Area - - 118

4.4 Granulometric Analysis - - - - - - 120

4.5 X –Ray Diffractogram (XRD) Analysis on Extruded Clays - 131

4.6 Hydrochemistry of Water from Onshore Mud Volcanoes in the Study Area - - - - - - - - 137

4.5.1 The Summary of Hydrochemical Parameters of Water from Mud Volcanoes - - - - - - - 140

4.5.2 Water Type - - - - - - - 145

4.5.3 Correlation Analysis - - - - - - - 148

4.5.4 Classification of Water from Mud Volcanoes as Mineral Water - 150

**CHAPTER FIVE: SYNTHESIS AND EVOLUTIONAL MODEL OF MUD VOLCANOES**

5.1 Mud Volcano Morphology in the Study Area - - - 155

5.2 Mechanisms of Volcanic Mud Formation in the Study Area - 157

5.3 Similarities between Onshore Mud Volcanoes in Nigeria and those in other Parts of the World - - - - - - 157

**CHAPTER SIX: SUMMARY, CONCLUSION AND** RECOMMENDATIONS

6.1 Summary and Conclusion - - - - - - 161

6.2 Recommendations - - - - - 163

References - - - - - - - - - 165

Appendix A - - - - - - - - - 175

Appendix B - - - - - - - - - 190

Appendix C - - - - - - - - - 211

Appendix D - - - - - - - - - 213

## LIST OF TABLES

Table1: Lithostratigraphic Subdivision of the Gongola Basin by Various Authors - - - - - - - - 31

Table 2: XRD Sample Pairs with Description from Labels on Sample Containers - - - - - - - - 55

Table 3: X-Ray Diffractometer Specification - - - 56

Table 4: Interpretation Scale of Graphic Mean (M) - - - 58

Table 5: Interpretation Scale for Graphic Sorting (Δ) -- - - 59

Table 6: Interpretation Scale of Graphic Skewness (Ski) - - - 59

Table 7: Interpretation Scale of Graphic Kurtosis (KG) - - - 60

Table 8: Location and Physical Description of the Onshore Mud Volcanoes in Nigeria - - - - - - 73

Table 9: Tabulated Result for Sieve Size Analysis - - - - 121

Table 10: Calculated Values for Grain Size Parameters of Sandstone within the Areas of Occurrence of Mud Volcanoes and their Interpretation 129

Table 11: Physico - Chemical Parameters of Water from Mud Volcanoes in the Area - - - - - - - - 137

Table 12: Hydrochemical Parameters Analysed in Water from Onshore Mud volcanoes in Nigeria - - - - - - 138

Table 13: Comparison of the Hydrochemical Data from all Mud Volcanoes - - - - - - - - 141

Table 14: Comparison of the Physico – Chemical Characteristics of Water from the Mud Volcanoes and the various Geological Formations - - - - - - 142

Table 15: Percentage of Hardness of the Water from the Mud Volcanoes - 143

Table 16: Classification of Water from Mud Volcanoes in the Study Area - 148

Table 17: Correlation Matrix of Hydrochemical Data in the Study Area - 148

Table18: Criteria for Mineral Waters in Accordance With the EU Mineral Water Directive - - - - - - 150
Table19: Classification of Mineral Waters from Mud Volcanoes in the Study Area - - - - - - - 150
Table 20: Classification System for Mineral Waters Based on Concentration of Chloride (Mg/L) - - - - - - 151
Table 21: Classification of Waters based on Chloride from the Study Area - 151

## LIST OF FIGURES

Figure 1: Basic Mud Volcano Formations - - - - - 7

Figure 2: Schematic Diagrams of (A) Cone-Shaped and (B) Pie-Shaped Mud Feature - - - - - - - - 10

Figure 3: Occurrence and Distribution of Mud Volcanoes on Earth - - 12

Figure 4: Location Map Showing the Area of Occurrence of Onshore Mud Volcanoes in Nigeria - - - - - - 16

Figure 5: Topographical Map of the Area of Occurrence of Onshore Mud Volcanoes Showing Relief and Settlements - - - 18

Figure 6: Drainage Map of the Area of Occurrence of Onshore Mud Volcanoes - - - - - - - 19

Figure 7: Outline Geological Map Showing the Main Features of the Upper Benue Trough Region - - - - - - 20

Figure 8: Geological Map of the Area of Occurrence of Mud Volcanoes modified after Benkhelil (1985) - - - - - 30

Figure 9: Generalized Lithostratigraphic Profile of Bima Group - - 32

Figure 10: Section of Yolde Formation; Exposed 750 M North of Ruwan Kuka - - - - - - - 35

Figure 11: Pindiga Formation (Kanawa Member) - - - - 37

Figure 12: Pindiga Formations (Gulani Member) - - - - 39

Figure 13: Pindiga Formation (Deba Fulani Member) - - - 40

Figure 14: Pindiga Formation (Dumbuluwa Member). Complete Fining - Upward Cycle, Doro Hill - - - - 41

Figure 15: Gombe Formation, Lithofacies Recognizable Within the Formation - - - - - - - 44

Figure 16: Map Showing the Main Structural Features of the Outcropping Cretaceous Gongola Basin (After Zaborski Et Al., 1998) - 47

Figure 17: The Geological Map of the Area of Occurrence of Mud Volcanoes Showing Most of the Mud Volcanoes on the Yolde Formation - 62

Figure 18: The Structural Map of the Area of Occurrence of Mud Volcanoes Locating the Mud Volcanoes on Faults - - - - 68

Figure 19: Rose Diagram Showing the Trends of Faults in the Study Area - 69

Figure 20: Satellite Image of the Area Showing Mud Volcanoes and the Trend of Some of the Faults - - - - - 69

Figure 21: Dadiya Syncline from Satellite Image - - - - 72

Figure 22: Lallapido Mud Volcanoes on the Background of Geological Map after Benkhelil (1985) - - - - - 75

Figure 23: Gujuba Mud Volcanoes on the Background of Geological Map after Benkhelil (1985) - - - - - 79

Figure 24: Jenye Mud Volcanoes Located on the Background of Geological Map after Benkhelil (1985) - - - - - 83

Figure 25: Pamadu Mud Volcanoes Located on the Background of Geological Map after Benkhelil (1985) - - - - 86

Figure 26: Lashadar Mud Volcanoes Located on the Background of Geological Map after Benkhelil (1985) - - - - 89

Figure 27: Lakaturu Mud Volcanoes Located on the Background of Geological Map after Benkhelil (1985) - - - 92

Figure 28: Digga Mud Volcanoes Located on the Background of Geological Map after Benkhelil (1985) - - - - - 96

Figure 29: Kurum Mud Volcanoes Located on the Background of Geological Map after Benkhelil (1985) - - - - - 98

Figure 30: Lawampe Mud Volcanoes Located on the Background of Geological Map after Benkhelil (1985) - - - - 101

Figure 31: Kolokwani Mud Volcanoes Located on the Background of Geological Map after Benkhelil (1985) - - - 103

Figure 32: Lashuwa Volcanoes on the Background of Geological Map after Benkhelil (1985) - - - - - 104

Figure 33: Todi Mud Volcanoes Located on the Background of Geological Map after Benkhelil (1985) - - - - - 106

Figure 34: Konta Mud Volcanoes Located on the Background of Geological Map after Benkhelil (1985) - - - - - 109

Figure 35: Lachikoltok Mud Volcanoes Located on the Background of Geological Map after Benkhelil (1985) - - - - 111

Figure 36: Sasanyi Mud Volcanoes Located on the Background of Geological Map after Benkhelil (1985) - - - - - 113

Figure 37: Fokata Mud Volcanoes Located on the Background of Geological Map after Benkhelil (1985) - - - - - 115

Figure 38: A Faulted Zone from Satellite Image Showing Trend of NE – SW 119

Figure 39: Cumulative Frequency Curve for Lap 1 - - - - 123

Figure 40: Cumulative Frequency Curve for Tod 1 - - - - 124

Figure 41: Cumulative Frequency Curve for Tod 2 - - - - 124

Figure 42: Cumulative Frequency Curve for Lak 1 - - - - 125

Figure 43: Cumulative Frequency Curve for Kur 1 - - - - 125

Figure 44: Cumulative Frequency Curve for Lap 2 - - - - 126

Figure 45: Cumulative Frequency Curve for Lash 1 - - - - 126

Figure 46: Cumulative Frequency Curve for Pam 1 - - - - 127

Figure 47: Cumulative Frequency Curve for Kur 2 - - - - 127

Figure 48: Cumulative Frequency Curve for Jen 1 - - - - 128

Figure 49: Measured XRD Pattern (Diffractogram) of Clays at Kurum - 131

Figure 50: Measured XRD Pattern (Diffractogram) of Clays at Lashadar - 132

Figure 51: Measured XRD Pattern (Diffractogram) of Clays at Lakaturu - 133

Figure 52: Measured XRD Pattern (Diffractogram) of Clays at Pamadu - 135

Figure 53: Measured XRD Pattern (Diffractogram) of Clays at Jenye - 136

Figure 54: Piper Trilinear Diagram Used for Water Classification - - 146

Figure 55: Schoeller Diagram for Water Samples from the Study Area - 147

Figure 56: Pie Chart Showing the Classification of Mineral Water Based on TDS - - - - - - - 153

Figure 57: Pie Chart Showing the Classification of Mineral Water Based on Cl - - - - - - - 154

Figure 58: Pie Chart Showing the Classification of Mineral Water Based on Bicarbonate - - - - - - 154

Figure 59: Schematic Diagram Showing the External Morphology of a Mud Volcano in the Study Area - - - - - - - 156
Figure 60: Schematic Diagram Showing the Process of Volcanic Mud Formation in the Study Area - - - - - - - 156

## LIST OF PLATES

Plate 1: Azimuth Map of 3d Seabed Reflector Showing Faults, Pockmarks and Mud Volcano - - - - - - 14

Plate 2: An Outcrop of Upper Bima Sandstone (b 3) at South of Todi Village 63

Plate 3: An Outcrop of Upper Bima Sandstone (B 3) at South of Todi Village Showing Tabular Cross - Bedding - - - - - 63

Plate 4: Yolde Formation at Kurum Showing Flat Lying Outcrop of Fine Grained Sandstone - - - - - - 65

Plate 5: Yolde Formation at Lakaturu Showing Convolute Bedding - - 65

Plate 6: Kanawa Member of the Pindiga Formation at Kurum Showing Regoliths of Fossiliferous Limestones with Ammonites - - 66

Plate 7: Kanawa Member of the Pindiga Formation at Kurum Showing Intense Bioturbation of Thalassinoids - - - - - 66

Plate 8: Olivine Basalt at Pokata Showing Fine Grained Crystalline Texture - 67

Plate 9: A Fault Zone within the Upper Bima Formation at Lallapido Showing NE – SW Trend - - - - - - 71

Plate 10: A Fault Zone within the Upper Bima Formation at Todi Showing NE – SW Trend - - - - - - 71

Plate 11: A Mud Volcano Occurrence at Lallapido, Showing the Angle of Slope, Dry Mud and Fresh Mud Flowing from the Crater - 76

Plate 12: A Mud Volcano Occurrence at Lallapido, Small Cone with Fresh Mud Flowing from the Crater - - - - - - 76

Plate 13: A Mud Volcano Occurrence at Lallapido, Showing the Angle of Slope, Dry Mud and Fresh Mud Flowing from the Crater - - - 77

Plate 14: A Mud Volcano Occurrence at Lallapido, Showing the Angle of Slope, with Fresh Mud Flowing from the Crater - - - 77

Plate 15: A Mud Volcano at Gujuba with Slurry of Mud and Water Seeping from the Crater - - - - - - 80

Plate 16: A Mud Volcano at Gujuba with Slurry of Mud and Water Seeping from the Crater - - - - - - 80

Plate 17: A Mud Volcano at Gujuba with Slurry of Mud and Water Seeping from the Crater - - - - - - 81

Plate 18: A Mud Volcano at Gujuba with Slurry of Mud and Water Seeping from the Crater - - - - - - 81

Plate 19: A Mud Volcano at Jenye with Slurry of Mud and Water Seeping from the Crater - - - - - - 84

Plate 20: A Mud Volcano at Jenye with Slurry of Mud and Water Seeping from the Crater - - - - - - - 84

Plate 21: A Mud Volcano at Jenye with Slurry of Mud and Water Seeping from the Crater - - - - - - 85

Plate 22: A Cow Being Rescued from a Mud Volcano at Jenye - - 85

Plate 23: A Mud Volcano at Pamadu with Slurry of Mud and Water Seeping from the Crater with Precipitated Salt - - - - 87

Plate 24: A Mud Volcano at Pamadu with Water Seeping from the Crater with Grasses and Precipitated Salt - - - - 87

Plate 25: A Mud Volcano at Pamadu with Slurry of Mud and Water Seeping from the Crater with Precipitated Salt- - - - 88

Plate 26: A Mud Volcano at Pamadu, Massive with Slurry of Mud and Water Seeping from the Crater with Precipitated Salt - - 88

Plate 27: A Mud Volcano at Lashadar with Slurry of Mud and Water Seeping from the Crater - - - - - 90

Plate 28: A Mud Volcano at Lashadar with Slurry of Mud and Water Seeping from the Crater - - - - - 90

Plate 29: A Mud Volcano at Lashadar with Little Dry Slurry of Mud and water Around the Crater -- - - - - 91

Plate 30: A Mud Volcano at Lashadar with Slurry of Mud and Water Seeping from the Crater - - - - - 91

Plate 31: A Mud Volcano at Lakaturu with Slurry of Mud and Water Seeping from the Crater - - - - - - 93

Plate 32: A Mud Volcano at Lakaturu with Slurry of Mud and Water Seeping from the Crater - - - - - - 93

Plate 33: A Mud Volcano at Lakaturu with Slurry of Mud and Water Seeping from the Crater- - - - - - - 94

Plate 34: The Result of Mistakenly Stepping into the Edge of a Mud Volcano at Lakaturu in Upper Benue Trough of Nigeria - - 94

Plate 35: Photograph of Water Volcano at Chengau - - - - 95

Plate 36: Volcano of Water Variety Seeping Out Water at Digga - - 97

Plate 37: Volcano of Water Variety Seeping Out Water at Digga - - 97

Plate 38: A Mud Volcano at Kurum with Slurry of Mud and Water - 99

Plate 39: A Mud Volcano of Two Craters at Kurum with Slurry of Mud and Water Seeping from the Crater - - - - 99

Plate 40: A Volcano of Water Variety at Kurum with Water Seeping from the Crater - - - - - - - 100

Plate 41: A Mud Volcano at Kurum with Slurry of Mud and Water Seeping from the Crater - - - - - - 100

Plate 42: A Mud Volcano at Lawampe with Slurry of Mud and Water - 102

Plate 43: A Mud Volcano at Kolokwami with Slurry of Mud and Water - 103

Plate 44: A Volcano of Water Variety at Lashuwo with Water from the Crater - - - - - - - - 105

Plate 45: A Mud Volcano of Multi Crater at Todi with Slurry of Mud and Water - - - - - - - 107

Plate 46: A Mud Volcano at Todi with Slurry of Mud and Water - - 107

Plate 47: A Mud Volcano at Todi with Slurry of Mud and Water - - 108

Plate 48: A Mud Volcano at Todi with Slurry of Mud and Water - - 108

Plate 49: A Volcano of Water Variety at Konta with Water from the Crater- 110

Plate 50: A Mud Volcano at Lachikoltok with Slurry of Mud and Water - 111

Plate 51: A Mud Volcano at Lachikoltok with Water Seeping from the Crater 112

Plate 52: A Volcano of Water Variety at Sasanyi with Water Seeping from the Crater - - - - - - - 114

Plate 53: A Volcano of Water Variety at Sasanyi with Water Seeping from the Crater - - - - - - - - 114

Plate 54: A Volcano of Water Variety at Fokata with Water Seeping from the Crater - - - - - - - 116

Plate 55: A Warm Spring at Leturu with Warm Water Seeping from the Crater - - - - - - - - 117

Plate 56: A Warm Spring at Lakomji with Warm Water Seeping from the Crater - - - - - - - - 117

Plate 57: Faulted Yolde Formation at Lakaturu Showing Trend of NE – SW 119

Plate 58: The Photo of Similar Mud Volcano in Trinidad and Tobago Showing Precipitated Salt - - - - - - 159

Plate 59: Photo of Similar Mud Volcano in Baratang, Andaman Islands and India 160

Plate 60: Photo of Similar Mud Volcano in Monagas, Venezuela Showing Mud Flow from the Crater - - - - - - 160

## LIST OF APPENDIXES

Location and Physical Description of the Onshore Mud Volcanoes in the Study Area - - - - - - - - - 175

Photographs of Mud Volcanoes - - - - - - 190

Physico - chemical Parameters of Water from Onshore Mud Volcanoes in Nigeria- - - - - - - - - - 211

Results of Hydrochemical Analysis of Water Sample from Mud Volcanoes 213

# CHAPTER ONE

# INTRODUCTION

## 1.1 Background to the Study

Mud volcanoes are some of the most mysterious geological features. Thousands of mud volcanoes exist worldwide in areas of rapid sedimentation, hydrocarbon occurrence, lateral tectonic compression, and recent magmatic activity (Dimitrov, 2002). The number of known mud volcanoes is growing with both onshore and offshore discoveries. About 2000 mud volcanoes have been confirmed onshore and over 700,000 have been estimated to be discovered offshore globally (Dimitrov, 2002; Milkov, 2000; Judd, 2005). Whitten and Brooks (1972) define a mud volcano as a type of spring, with a positive topographic feature in form of a cone having varying sizes from a fraction of metre to over one kilometre, in which is incorporated argillaceous materials or volcanic ash to produce a boiling mass of mud. Springs are defined as places where groundwater flows naturally from a rock sediment or soil onto the land surface or into a body of surface water. Their occurrence is not limited to rocks of a particular age or type or to any specific geological or topographic setting. The diversity of springs is indicative of the wide array of geological and hydrological conditions which lead to their occurrence (Pitt and Alfaro, 2001).

According to Keilhack (1912) classification of springs into descending springs and ascending springs based on the path of the water to the surface and not the origin of the water. Mud volcanoes are ascending springs with low conical mounds having a crater at the top through which the water rises-are built up when water containing clay or fine sand rises to the surface under pressure. As the water spreads out of the vent it loses velocity and therefore deposits the matter it had carried in suspension. Such deposits are

made by the temporary springs formed along fissures in unconsolidated rocks during earthquake (Kirk, 1919).

Offshore mud volcanoes in Nigeria in the Niger Delta have been reported as circular features from the upper continental slope (Graue, 2000, Heggland, 2001). However, onshore mud volcanoes were only reported at Todi village in the Cretaceous Upper Benue Trough of Nigeria (Umaru, 2000). Later on (2009 - 2011), Professor Schoeneich of the Department of Geology, Ahmadu Bello University Zaria, Nigeria, in company of Dr Ewa Kurowska from University of Silesia, Poland, visited the area and found other mud volcanoes in Todi and Lallapido villages. However, occurrence of mud volcanoes was not mentioned in previous scientific works on the Upper Benue Trough and southern Borno Basin by Falconer (1911), Jones (1932), Raeburn and Jones (1934), Barber *et al*. (1954), Carter *et al.* (1963), Allix (1983), Benkhelil (1985; 1986; 1988), Popoff (1988), Guiraud (1989) and Zaborski *et al*. (1998). That discovery by Umaru (2000) brought to limelight the occurrence of onshore mud volcanoes in Nigeria and there is need to critical study and document the onshore mud volcanoes in Nigeria. Therefore, this study is aimed at documenting and mapping the occurrences of the onshore mud volcanoes in Nigeria with the view of understanding the geological control on their distribution. Reconnaissance investigation in finding more onshore mud volcanoes were carried out in the Lower Benue Trough, Middle Benue Trough and Upper Benue Trough and the Niger Delta Basin. However, more of the onshore mud volcanoes were recorded in parts of the Upper Benue Trough of Nigeria. Therefore, this study is aimed at documenting and mapping the occurrences of the onshore mud volcanoes in Nigeria with the view of understanding the geological control on their distribution. Also, this study will establish if there are similarities between onshore mud volcanoes discovered on land in Nigeria and those on land in other countries such as

India, Venezuela, Trinidad and Tobago, Mongolia and California in terms of their height, shape, size, precipitated salt, mud flow from the crater.

## 1.2 Aim and Objectives of the Study

The research work is aimed at documenting and mapping the occurrences of onshore mud volcanoes in Nigeria, with the view of understanding the geological control on their distribution. The objectives are:

i. To document all the mud volcanoes found onshore Nigeria.
ii. To carry out a detailed geological mapping of surrounding areas of the onshore mud volcanoes.
iii. To establish the possible geological control on their occurrences and distribution.
iv. To carry out a mineralogical and hydro-chemical analyses of the mud and water directly flowing from volcanoes.

## 1.3 Justification of the Study

Onshore mud volcanoes are rare geological phenomena and are only being reported in Nigeria for the first time. A distribution map of mud volcanoes in the world does not show the occurrences of onshore mud volcanoes in Nigeria. The occurrences of mud volcanoes are always attributed to areas of tectonic activity such as rapid sedimentation, hydrocarbon occurrence and lateral tectonic compression. The Distribution of onshore mud volcanoes along faults may also reveal if the mud volcanoes are structurally controlled.

Therefore, documentation and mapping of onshore mud volcanoes in Nigeria will help in integrating the onshore mud volcanoes into the world distribution map of mud volcanoes. Exploration for oil in the Benue Trough has been on-going, it is important to know if onshore mud volcanoes are possible indication of hydrocarbon in the Benue

Trough. Mud volcanoes also signify manifestation of earthquakes or sudden endogenetic events. Knowing the relationship of onshore mud volcanoes in Nigeria to earthquakes or endogenetic events will also be useful to avoid sudden environmental hazard in surrounding areas where the mud volcanoes are occurring.

## 1.4 Scope of the Study

The Scope of the study is as follows:

1) Desk study: entails literature survey for previous work on mud volcanoes with emphasis on onshore mud volcanoes. Also, acquisition of satellite data and interpretation of same.
2) Reconnaissance survey: reconnaissance survey will be carried out within the Upper Benue Trough and other basins such as Middle Benue Trough, Lower Benue Trough and the Niger Delta with possibilities of documenting more onshore mud volcanoes.

**3)** Fieldwork: detail geological mapping of surrounding areas of the onshore mud volcanoes will be done to delineate the different lithologies and structural features of the area.

4) Laboratory analyses which involves the following:
    i) Grain size analysis on the sediments from the surrounding areas of onshore mud volcanoes will be done in order to determine particle size distribution other grain size parameters such as mean, sorting, skewness and kurtosis.
    ii) X-ray diffractometer analysis will be carried out on clay samples extruded from the mud volcanoes and the sorrowing overburden.

iii) Water Analysis will be carried out on water issuing out from the craters of the mud volcanoes from each of the fourteen fields of the mud volcanoes for hydrochemical analysis.

5) Statistical data evaluation / processing

The textural properties of the sediments surrounding the area of occurrences of onshore mud volcanoes will be determine from cumulative frequency curves. The hydrochemical facies of the water issuing from the crater of the onshore mud volcanoes are determined from Piper and Schoeller diagrams.

## 1.5 Concept and Origin of Mud Volcanoes

According to Fowler *et al*. (2000), mud volcanoes often result from the presence of under compacted mudstones and over pressured multi-phase pore fluids, brine and methane. Mud volcanoes may also be described as features closely related to ‘‘clay or mud diapirs’’. By definition, the Greek “diapeirein” means “to pierce” and was first used by Mrazec (1915). However, Mrazec's (1915) definition of diapirism as the process of forceful movement of a more or less plastic body from areas of higher pressure to areas of lower pressure has since then been widely accepted. It has often been restricted to salt structures, although some workers used it for effusive or intrusive magmatic processes (Wegmann, 1930).

According to Brown (1990), the formation of diatremes is often associated with mud diapirism. However, they can be formed above any stratigraphic or structural conduit that rapidly expels fluids into the base of an unlithified sediment column leading to fluidization. In mud diapirism, the mud is assumed to be driven upward by buoyancy forces resulting from the bulk density contrast between an overpressured muddy mass and an overburden of greater density. As the mud reaches depths of around one or two kilometres, rapid expansion of the dissolved gas as it comes out of solution increases the

buoyancy effects and the stress on the surrounding sediments which can lead to fluidization. Migration pathways are quickly formed to the surface, typically along lines of weakness associated with localized extensional tectonics over the top of the underlying diapir, resulting in eruptions of gas charged mud and water at the surface creating a mud volcano (Brown 1990).

Although the driving mechanisms are different, both diapirs and diatremes involve mud and overpressured multiphase pore fluids and in some cases are often morphologically similar. Eruptions may vary from gentle extrusions of mud to violent explosions of gas and mud. Essentially all reported mud volcanoes are associated with thick sequences of overpressured, organic and clay-rich sediments (Hedberg, 1974; 1980).

According to Graue (2000), based on the large differences observed in shape, size and eruption styles of mud volcanoes, it is clear that there is no exact model that can explain their origin. Ultimately, mud volcanoes form either as clay diapirs that reach and pierce the ground-surface or as fluidized argillaceous sediments, together with water and various amounts of hydrocarbon gases which are extruded along structural weaknesses (conduits) within subsurface sediments/rocks (Milkov, 2000; Figure 1 ). The fundamental requisite for mud volcanism is the existence of a potential source domain and solitary or interconnected argillaceous carrier beds for migrating fluids and gases. However, for actual volcanic processes to commence and continue, that is, for gases to form and/or for the source material to move, rise and eventually extrude from the subsurface – additional forces are required.

According to Rukavičková and Hanžl (2008), mud volcanoes, regardless of comparable morphology and manifestation on the Earth's surface, may also be of variable origins. Rukavičková and Hanžl (2008) further described three fundamental groups based on the genesis of the mud volcanoes: (a) mud volcanoes *sensu stricto* linked with hydrocarbon

gas release (Dimitrov, 2002; *fide:* Rukavičková and Hanžl 2008); (b) hydrothermal mud volcanoes (Pitt and Hutchinson, 1982; *fide:* Rukavičková and Hanžl 2008); (c) mud volcanoes as a manifestation of an earthquake or a sudden exogenetic event (Rogozhin *et al*., 2007; *fide:* Rukavičková and Hanžl (2008).

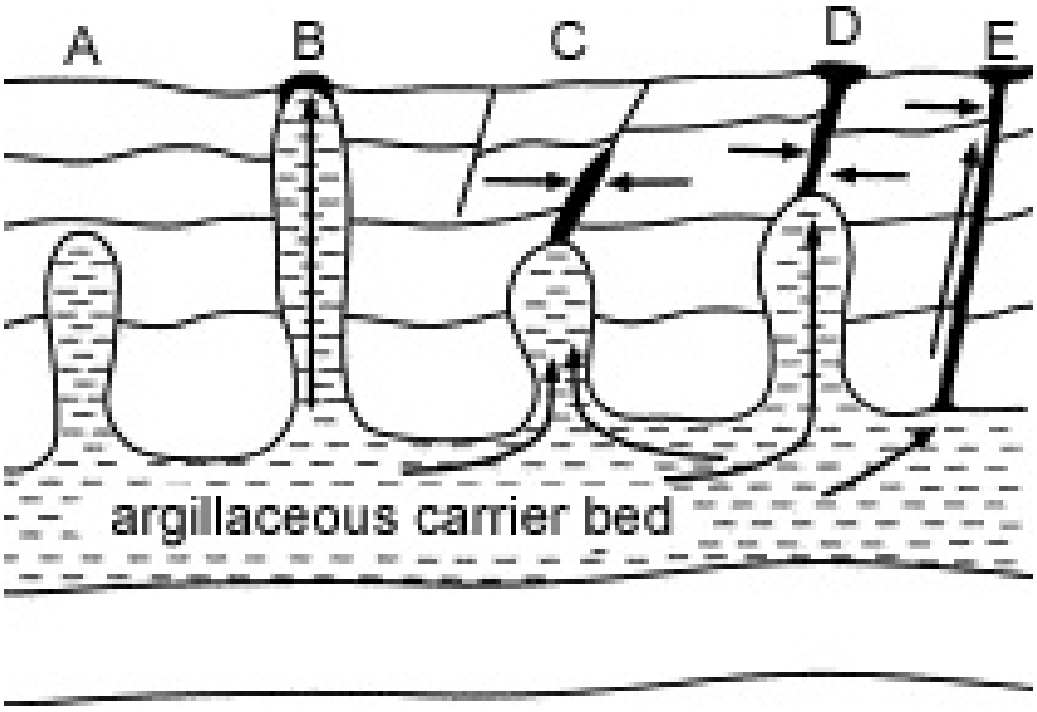



Figure 1: Basic mud volcano formation. Explaination: A; clay diaper, B; seafloor-piercing clay diapir - a mud volcano, C; seafloor seepage D and E; mud volcanoes formed due to rise of fluidized sediments along faults (after: Milkov, 2000).

**Mud volcanoes sensu stricto linked with hydrocarbon gas release** (Dimitrov, 2002; *fide:* Rukavičková and Hanžl, 2008). These mud volcanoes are usually associated with deposits of hydrocarbon. Gases formed during hydrocarbon formation processes and available water, forces the mud ascent to the Earth's surface. The mud volcanoes range in size from small gryphons of about one meter in diameter to several kilometres, and with average heights of hundreds of metres (Dimitrov, 2002; Kholodov, 2002; *fide* Rukavičková and Hanžl 2008). They are irregularly clustered in separated areas forming belts, which coincide with active areas of the continental plate boundaries and zones of

young orogenic structures (Dimitrov, 2002). Examples of this type of mud volcanoes are located in eastern Azerbaijan and the Caspian Sea region (Panahi, 2005; *fide* Rukavičková and Hanžl 2008).

**Hydrothermal mud volcanoes (**Pitt and Hutchinson, 1982; *fide:* Rukavičková and Hanžl 2008) are usually found in regions characterised by recent volcanic activity. Volcanic gas and hot water rising to the surface detach and entrain fine-grained particles of adjacent rocks. The mud cones, usually not more than one or two metres in height, mud cauldrons and fumaroles are all apparent results of these geologic processes. The characteristic of these mud volcanoes includes high water temperature, formation of large volumes of water vapour and absence of hydrocarbon gases (Kholodov, 2002; *fide:* Rukavičková and Hanžl 2008). 'Mud pot' is an alternative term used for hydrothermal mud volcanoes, which are in fact recognized to be thermal springs. Examples of known hydrothermal mud pots occur in Yellowstone National Park in USA (Pitt and Hutchinson, 1982).

**Mud volcanoes as manifestation of earthquake or sudden exogenetic events** (Rogozhin *et al*., 2007; *fide:* Rukavičková and Hanžl 2008). These mud volcanoes occur as small mud or often sand volcanoes, which are caused by constant effects of earthquakes or floods, which can lead to rapid increase in strain in rocks or abrupt change in piezometric pressure in aquifers. The major characteristics that differentiate this type of mud volcanoes with the previous two groups of mud volcanoes is that, ejected material to the surface are derived from shallow depths, usually only a few tens of metres. The height of this type of mud volcanoes reaches generally several decimetres, rarely above one metre; their diameter may attain several metres.

## 1.6 Classification of Mud Volcanoes

In the classification of mud volcanoes, few classification schemes exist and have been developed by the use of different approaches and criteria namely: the shape and size of mud volcano construction (Gubkin and Federov, 1940, Jakubov *et al*., 1971, Ivanov *et al*., 1996); the correlation of mud volcanoes with local geological structures such as faults and folding (Arkhangelski, 1932). However, Kalinko (1964) generalized the data on numerous mud volcanoes to construct a classification system based on the character of their activity with respect to morphological expression.

The submarine mud volcanoes are difficult to classify but assumptions can be made by studying their morphology: shape of the body, structure of the crater and mud flows. The recent activity of submarine mud volcanoes can be judged by several peculiarities, most prominent at the summit of the mud volcanoes (Ivanov *et al*., 1996)

Kopf (2002) said that because of the variety of mud volcanoes, no strict classification seems useful or possible. However, he gave two typical features which are schematically referred to below as mud dome and mud pie (Figure 2). The differences between cones (domes) and pies are made on the grounds of angle of the flanks. Pies generally have <5° slopes.

The feeder, or conduit, is the central feature through which mud extrusion is facilitated. It may be either cylindrical, irregularly shaped, or a slit (i.e., a fracture or fault). The area where the central conduit crops out at the surface is called the crest, being generally the most elevated point. If the crest region shows a depression, this is referred to as the crater. If this crater is filled with soupy mud, this feature is called a mud pool. Sometimes, if the main conduit of the mud volcano terminates as a crater, it may also have been termed a pingo or cauldron (Portuguese for caldera). Splays of the main conduit may result in small craters somewhere off the centre (or even on the flank) and

are referred to as gryphons. Both the main conduit and the gryphons are the locations from which mudflows originate (Kopf, 2002).

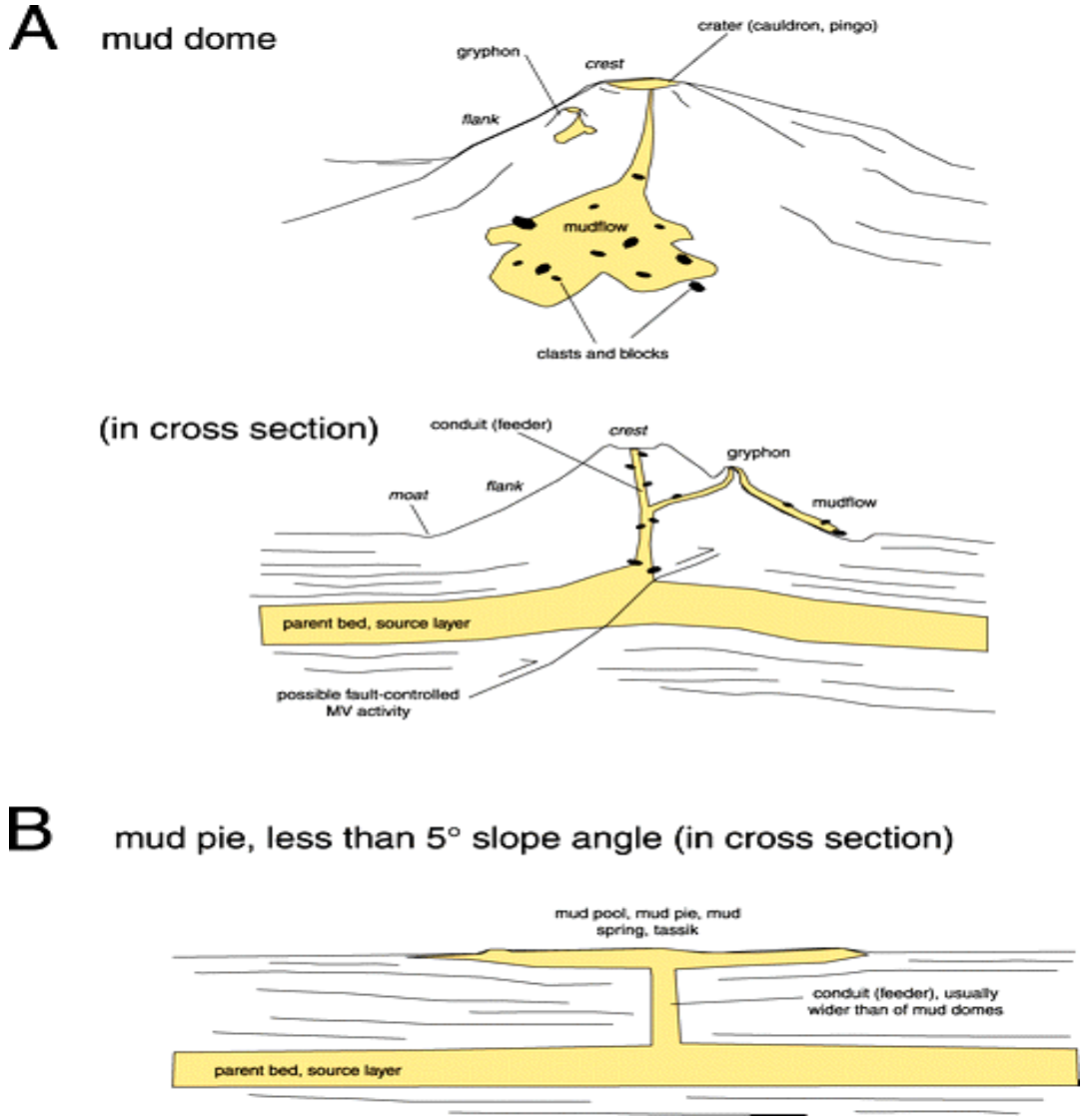



Figure 2: Schematic diagrams of (A) cone-shaped and (B) pie-shaped mud feature (After Kopf, 2002).

## 1.7 Global Distribution of Mud Volcanoes

Mud volcanoes are distributed worldwide and are located in a wide variety of tectonic environments, including passive continental margins and continental interiors, as well as convergent plate boundaries, where fluid rich sediments and volatiles are released due to increasing compactional stress and temperature (Reed *et al.*, 1990; Hedberg,

1980). About 2,000 mud volcanoes have been so far discovered onshore according to Dimitrov (2002). It is estimated that the mud volcanoes worldwide are from 7,000 to 1,000 000 in number (Milkov, 2000; Judd, 2005; *fide* Akesson, 2008).

Figure 3 shows the distribution of the most distinct and relatively well known mud volcano examples: Italy (Deecke, 1897; Chiodini *et al.*, 1996), Burma (Pascoe, 1912; Chhibber, 1934), Java, Sumatra, and Borneo (Blumer, 1922; Reinhard and Wenk, 1951), Trinidad (Kugler, 1933; Birchwood, 1965), Azerbaijan (Goubkin and Federov, 1940; Kugler, 1939; Jakubov *et al.*, 1971), the Makran coast of Iran and Pakistan (Harrison, 1944; Snead, 1964), Colombia (Gansser, 1960), Timor (Audley-Charles, 1968) and Venezuela (Higgins and Saunders, 1973). Smaller numbers of mud volcanoes have also been described from the Netherlands (Paine, 1968), the Mississippi and the Nile deltas (Hovland and *et al*., 1997), the North Sea (Vogt *et al*., 1997), Lake Michigan and the Greenland (Kopf, 2002).

About 150 onshore single mud volcanoes were found in Taiwan, the Marianas, Malaysia, Samoa and Australia to New Zealand (Kopf, 2002; Dimitrov, 2003).

The number of mud volcanoes on the eastern coast of the Pacific Ocean is much less, however examples are known from and around the Aleutian Trench, Alaska, British Columbia, California, Costa Rica, Ecuador and Peru (Kopf, 2002; Dimitrov, 2003). The Atlantic Ocean comprises several hundred of both onshore and offshore mud volcanoes. With the vast majority concentrated along the Caribbean thrust belts and within the Barbados accretionary zone (Dimitrov, 2003).

### 1.7.1 Mud volcanoes in Africa

Since 1999, many mud volcanoes and diapirs were discovered in the Gulf of Cadiz and North Atlantic Moroccan margin. The Gulf of Cadiz is located in a tectonically active area in front of the Betic - Rifain arc. It is bounded by the Iberian Peninsula to the North

and the African continent to the South (Mhammedi *et al.*, 2008). The research conducted by Gardner, 2000; Gutscher *et al*., 2007and Garàcia *et al*., 2003 (*fide* Mhammedi *et al.*, 2008) showed that the extensive occurrence of mud volcanoes in the Gulf of Cadiz are located in the shallowest part of the accretionary wedge and they result from neotectonics.

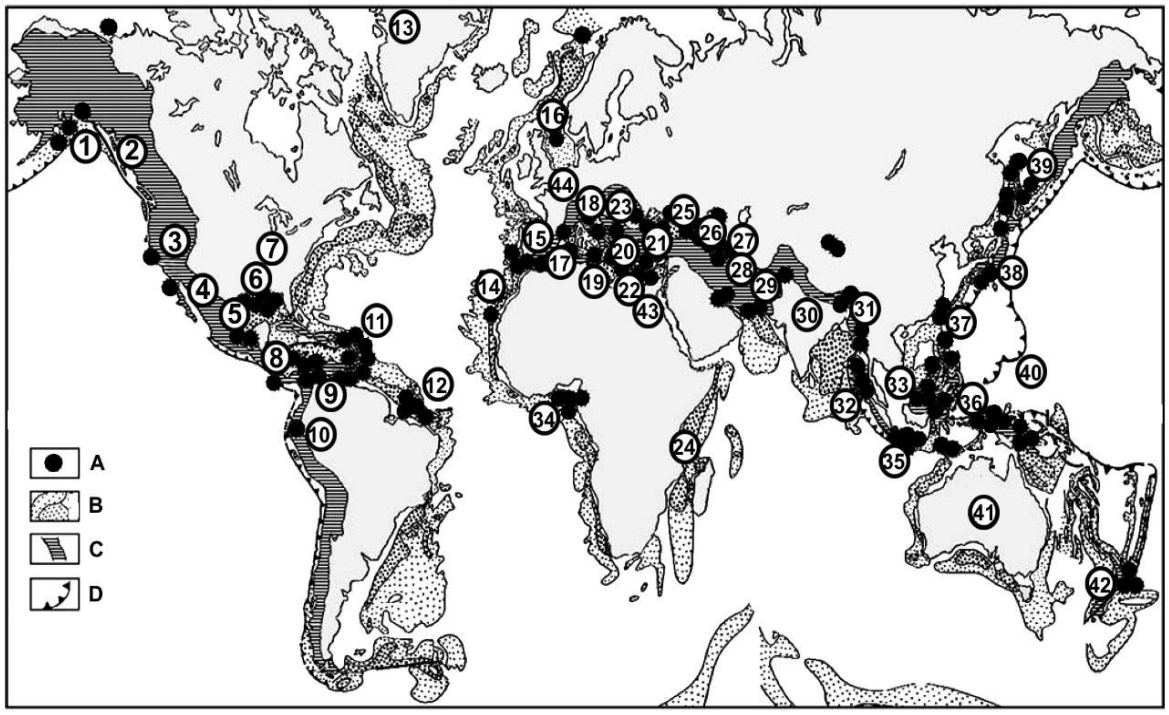



Figure 3: Occurrence and distribution of mud volcanoes on Earth (modified after Dimitrov, **2003 and Kopf, 2002):** 1 Aleutian Trench, Alaska Margin: Copper River Basin,2 British Columbia, Canada,3 Cascadia (Oregon, Washington), 4 California, Nevada, 5 Gulf of Mexico, 6 Texas, Mississippi, Louisiana, 7 Lake Michigan, 8 Colombia, 9 Costa Rica, ,10 Ecuador, 11 Barbados,12 Venezuela and Trinidad, 13 Greenland, North Atlantic, 14 Morocco/North Africa, ,15 Spain, 16 Barents Sea, North Sea, Baltic Sea, 17 Alboran Sea, 18 Western Alps, Appennines/Italy,19 Sicily, 20 Peloponnesus/ Greece, Adriatic Sea, 21 Aegean Sea, 22 Eastern Mediterranean Sea, 23 Romania, 24 Tanzania/East Africa, 25 Black Sea, Kerch Crimea Peninsulas, 26 Caucasus (Taman, Georgia, Azerbaijan), 27 Caspian Sea, 28 Iran, Turkmenistan, 29 Makran and Pakistan, 30 India, 31 Burma, 32 Sumatra, Java, 33 Borneo, Brunei, Sabah/Malaysia, 34 Gulf of Guinea, 35 Timor-Ceram Arc, 36 Irian Raya, Papua New Guinea, 37 Taiwan, 38 Ryukyu Trench, Nankai, Japan Trench, Japan, 39 Sakhalin Island/ Sea of Ochotsk, 40 Marianas, 41 Australia, 42 New Zeland, 43 Libyan Desert, Egypt, 44 Netherlands; *A* - single mud volcanoes, mud volcano belts or separated areas, *B* - sediments in the areas out of the continental shelves, *C* – active compressional areas, *D* - subduction zones.

### 1.7.2 Mud Volcanoes in Nigeria

Little has been published on mud volcanoes in Nigeria. They occur offshore of Nigeria, in the Niger Delta where, according to Graue (2000), numerous circular features have been reported from the upper continental slope. They were investigated using geophysical techniques and it was found that the domes are active or dormant, usually 1–2 km in diameter. Some features overlie rolling anticlines and the others juxtapose diapirs. Core samples from the deep, exploration wells revealed oil, gas, and clasts of shale and sandstone in the mud. Some rare carbonate nodules have also been found. The age of the mud volcanoes material is Pliocene and Pleistocene (Graue, 2000). The geophysical investigation and cores analyses revealed that the source bed to the mud volcanoes consists of over-pressured shale, which is overlain by low-integrity sediments. In the result of high pressure forces some of the shale intrudes into the overburden forming mud domes, while other features are formed from high fluid discharge from an underlying sediment wedge and appear as circular depressions in the surrounding seafloor.

Also, according to Heggland *et al.* (2001), seismic data from the Nigerian continental slope show indications of fluid flow to the seabed through faults. Plate 1 shows an azimuth map of the 3D seabed reflector. The water depth varies from approx. 300 m in the NE to 800 m in the SW. Pockmarks are visible along seabed fault lines indicating fluid flow through the faults. Mud volcanoes also seem to be associated with the faults. Rapid sedimentation and slumping of unconsolidated sediments along with high gas content in the sediments is believed to have caused the generation of the mud volcanoes (Heggland *et al.* 2001).

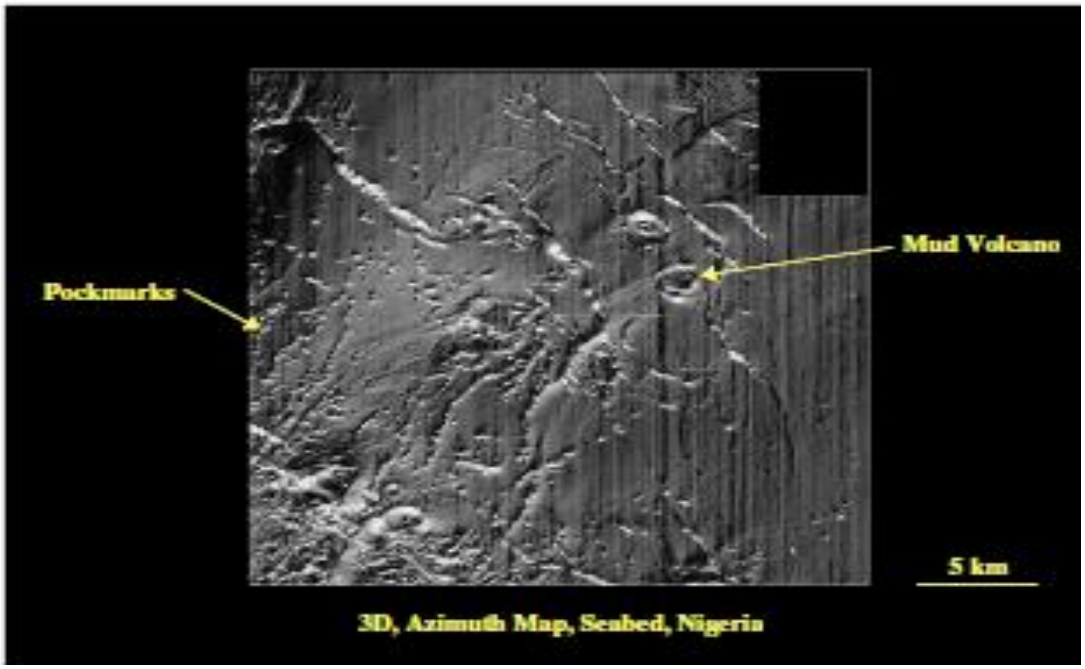



Plate 1: Azimuth map of the 3D seabed reflector showing faults, pockmarks and mud volcanoes (Heggland et al. 2001)

# CHAPTER TWO

# LOCATION AND GEOLOGY OF SURROUNDING AREA OF MUD VOLCANOES

## 2.1 Location and Accessibility of Onshore Mud Volcanoes in Nigeria

All documented areas of occurrences of onshore mud volcanoes in Nigeria are located within the southern part of Gombe State in the Upper Benue Trough. The area falls within latitudinal range $09^0$ 30'00" – $10^0$ 00'00" and longitudinal range $11^0$ 00'00" – $11^0$ 15'00", and is located on a Federal Surveys of Nigeria (1975) 1: 50,000 topographical maps sheet 173 (Kaltungo) SW and NW (Figure 4). The area is accessible from the north by Billiri – Filiya, from the northwest by Shela - Todi and from the northeast by Kaltungo - Lallapido secondary tarred roads. The stream channels and the footpaths in the area served as access routes during the fieldwork.

## 2.2 Climate and Vegetation on the Area of Occurrence of Mud Volcanoes

The area of occurrence of mud volcanoes falls within the humid tropical climatic zone of Nigeria, in Sudan Savannah with alternating rainy and dry seasons. The mean annual rainfall of the area is 900mm, which lasts from May to October, while the dry season starts from October to April (Schoeneich and Garba, 2010). The highest rainfall is recorded in the months of July and August. Mean annual temperature ranges from $26^oC$ to $27^oC$ (Schoeneich and Garba, 2010).

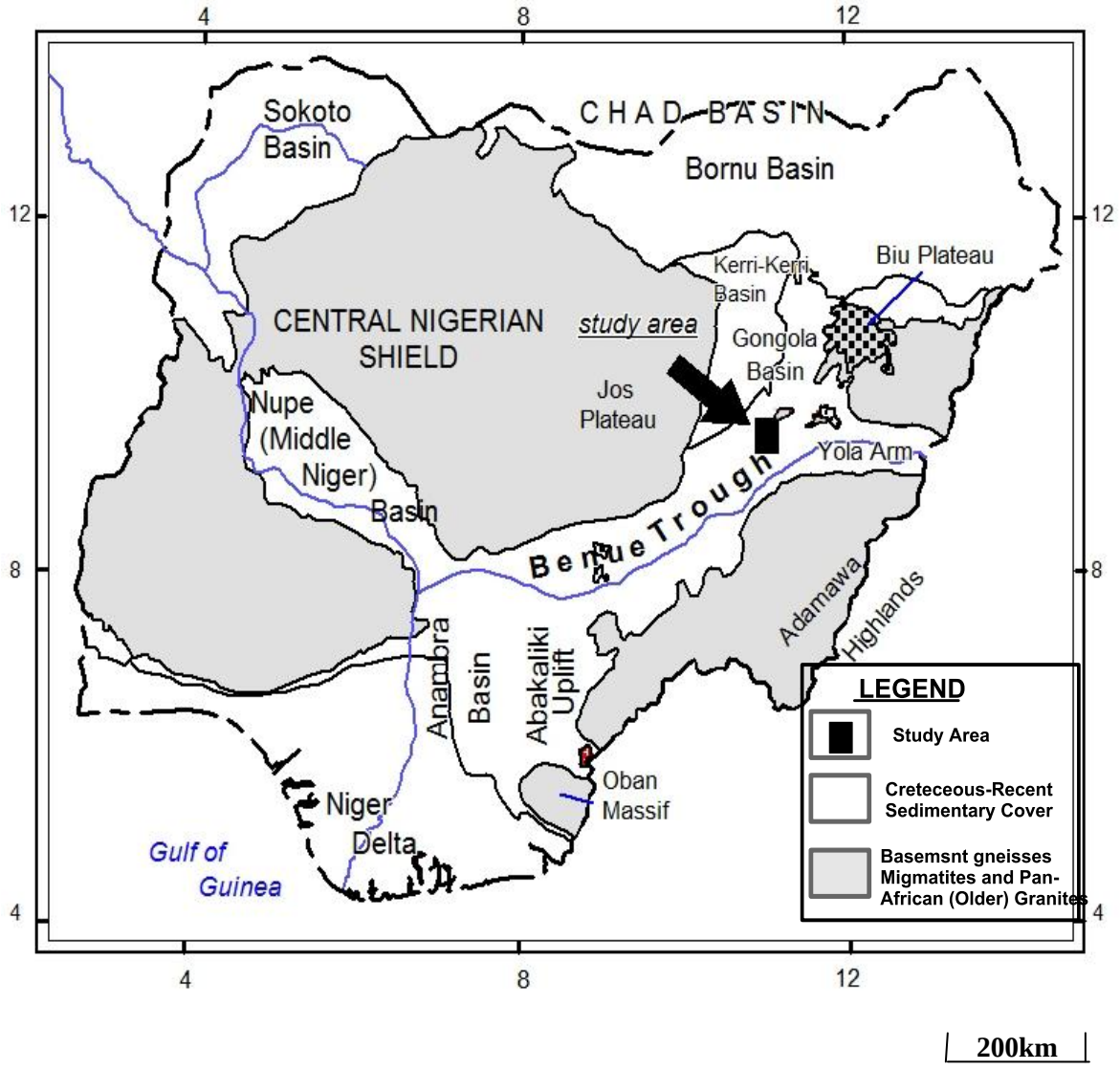



Figure 4: Geological sketch map of Nigeria modified from Obaje (2009) showing the area of occurrence of onshore mud volcanoes in Nigeria.

The vegetation within the area where mud volcanoes occur is characterized by sparsely distributed trees, showing a stunted growth. Continuous cover of grasses, trees with thorns, thick barks and tall leaves, characterises the vegetation. Trees found there include mango, neem, and baobab. Deforestation and farming has affected the natural vegetation leading to erosion in some parts.

## 2.3 Relief and Drainage of the Area of Occurrence of Mud Volcanoes

The prominent topographical features of the area are towards the north eastern part, south eastern part and the southern part within the Bima Formation while the Yolde Formation forms gently undulating hills at the south – western part of the area (Figure 5). The general topography of the area is associated with watershed which produces river channels and exposes the successions it cross cut. The magma volcanic intrusions into the Cretaceous sandstone form prominent hills with sharp peak. The area is drained by tributaries of the River Lakukus, River Jallang, River Tibalni, River Wale and River Yaudi. Most of them are seasonal while some are perennial forming dendritic drainage pattern (Figure 6).

## 2.4 People and Settlements of the Area of Occurrence of Mud Volcanoes

The area of occurrence of mud volcanoes is inhabited by the Tangale, Shongom, and the Fulani speaking people. The choice of site for settlements in the study area depends on the geology, topography, and availability of water and arable farm land. Major settlements connected by motorable roads are: Lallapido, Todi, Billiri, Kurum and Lakaturu (Figure 5).

The soil types in the area is good for the cultivation of crops like millet, guinea corn, maize and cotton especially on the rich dark grey to black clayey soils of the Bima Sandstone and part of the Yolde Formation. Also, grazing of animals and excavation of clays for construction purposes are carried out by the people.

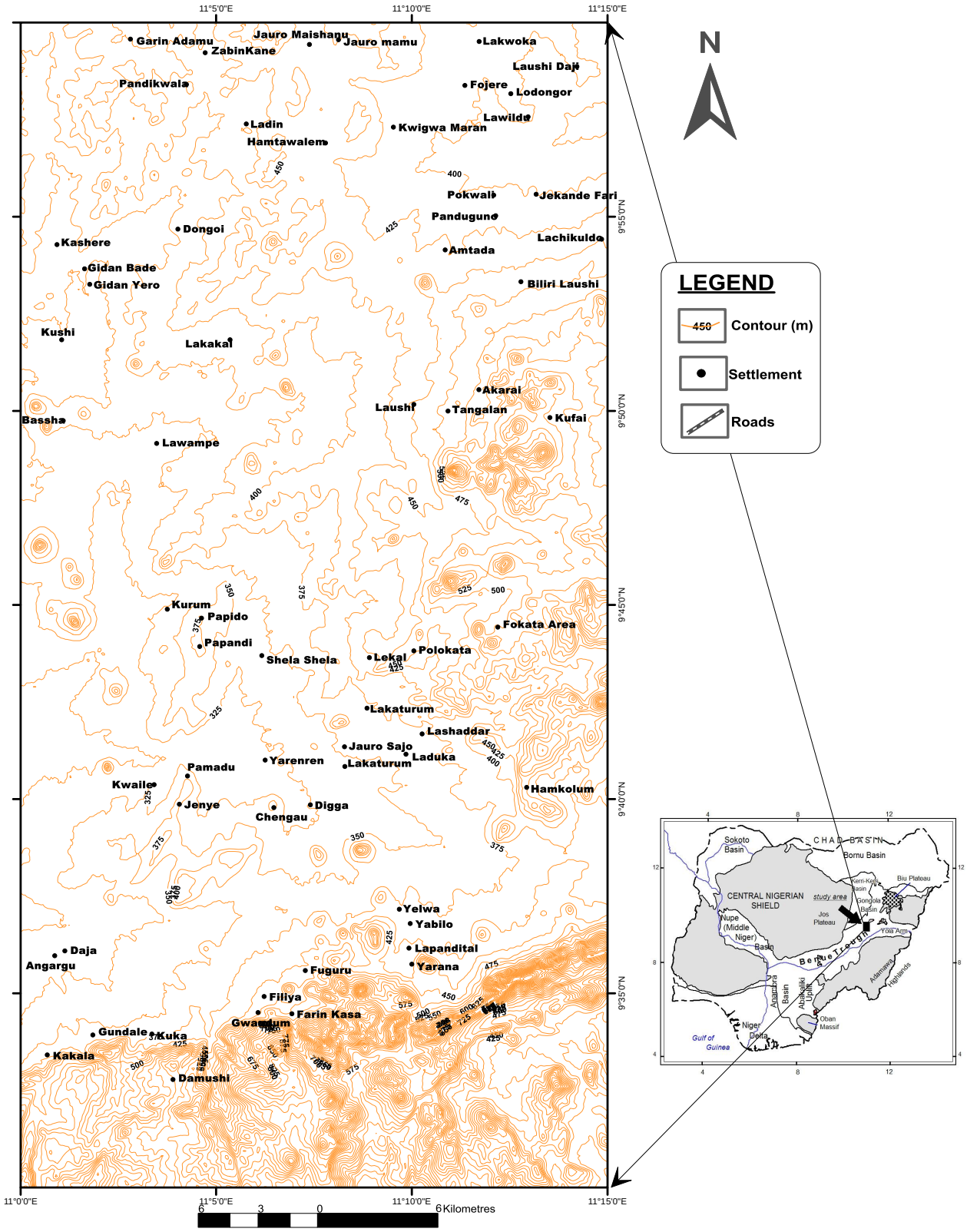



Figure 5: Topographical map of the surrounding area of onshore mud volcanoes showing relief and settlements (Source: Federal Surveys, Nigeria, 1975)

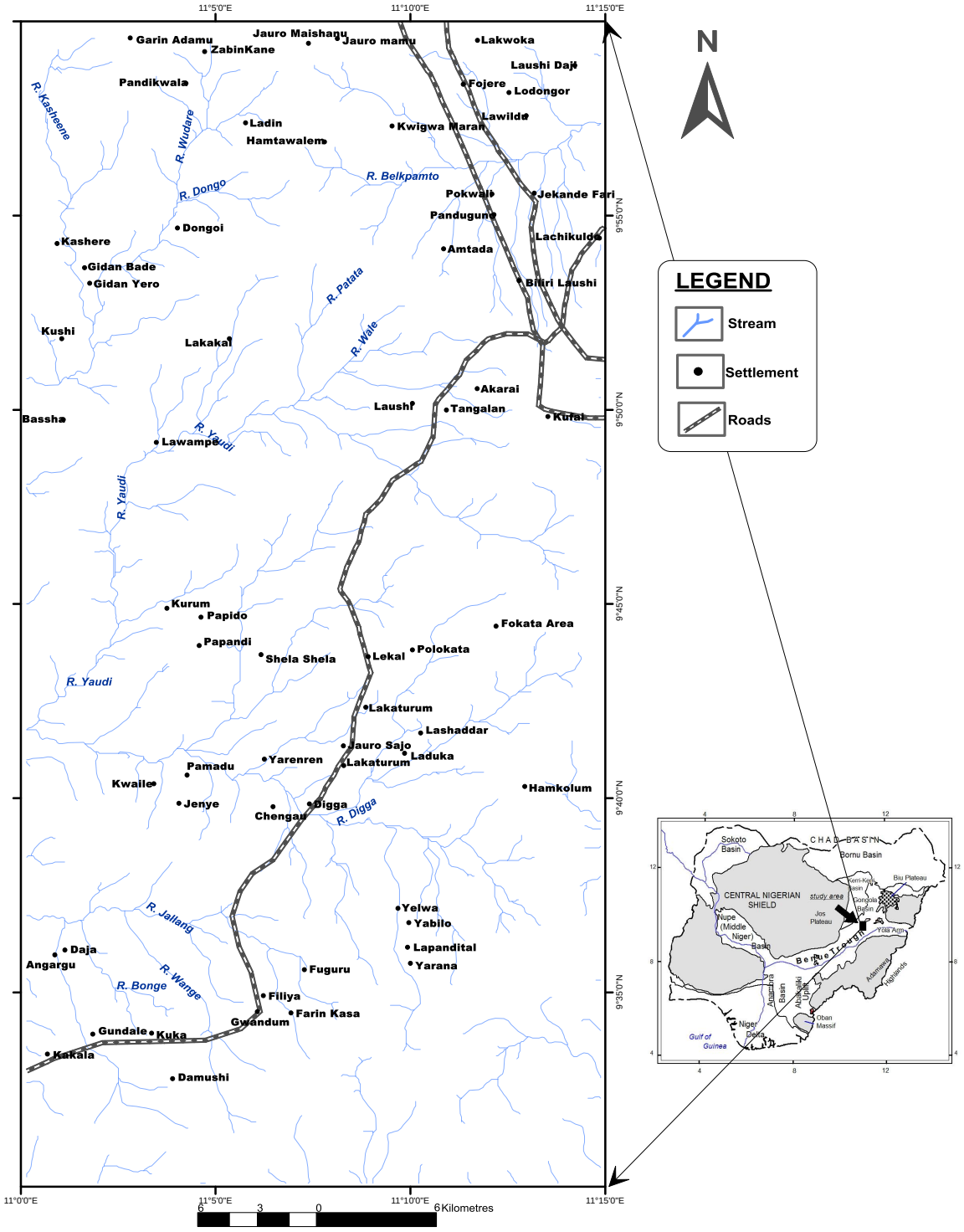



Figure 6: Drainage map of the surrounding area of onshore mud volcanoes.

## 2.5 Geological Background of the Area of Occurrence of Mud Volcanoes

### 2.5.1 History of the Benue Trough of Nigeria

The Benue Trough of Nigeria is a geographical and geological feature 1000 km long, extending from the Niger Delta to the Lake Chad Basin (Maurin *et al.*, 1986). The Benue Trough is a sediment filled NE-SW trending depression, about 1000 km long (Petters, 1978, Benkhelil, 1989). The Cretaceous structure lies within the Precambrian mobile belt of West Africa (Guiraud, 1990b). It is subdivided into lower, middle and upper regions. These three regions generally correspond to areas distinguished by characteristic stratigraphical and structural features (Benkhelil, 1989) (Figure 7).

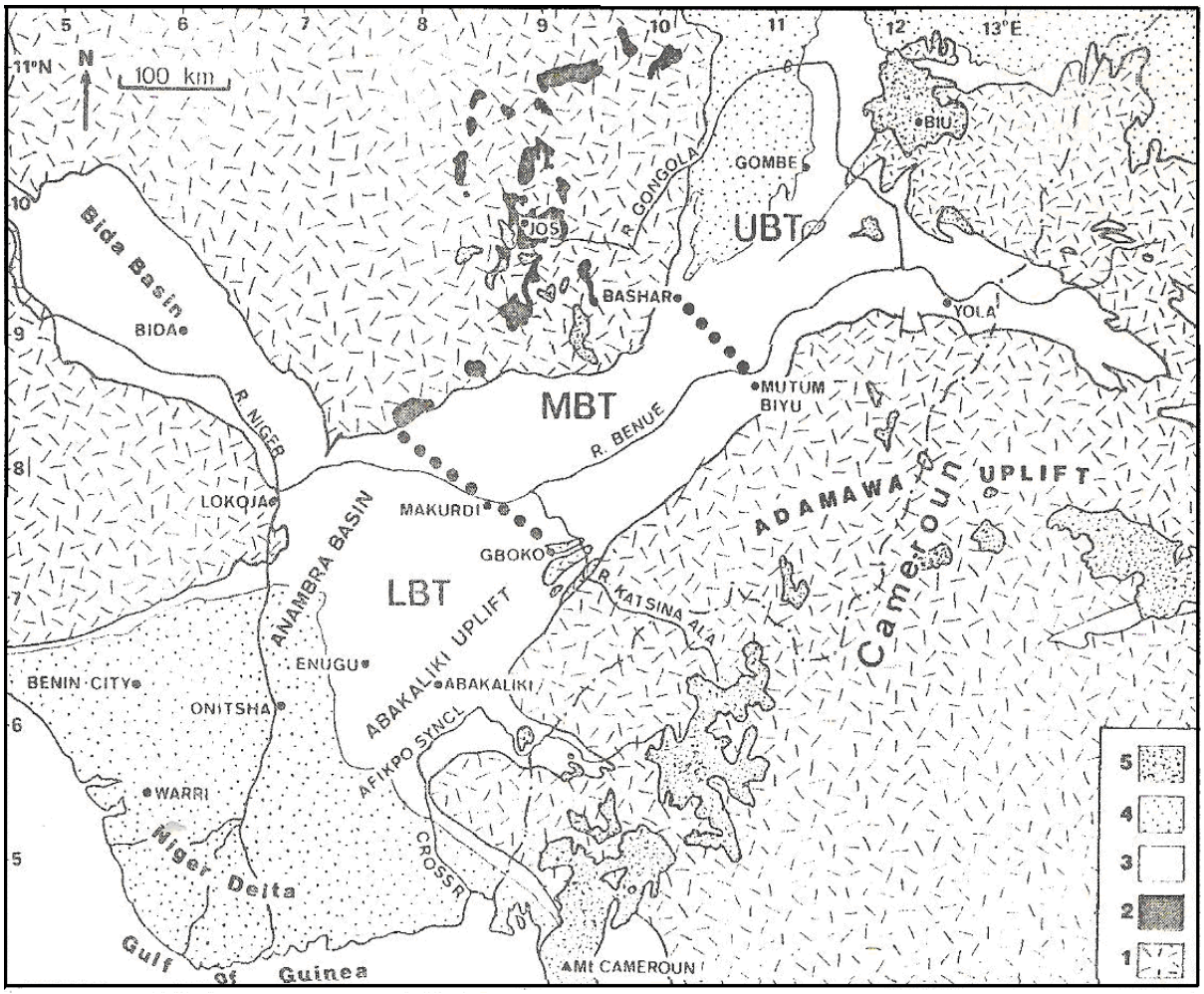



Figure 7: Outline geological map of the Benue Trough and adjacent areas. LBT- lower BenueTrough; MBT- middle Benue Trough; UBT- upper Benue Trough. 1- Precambrian; 2- Jurassic "Younger Granites"; 3- Cretaceous sediments; 5- Cenozoic-Recent basalts (including those of the Cameroun line) After Zaborski (1998)

### 2.5.2 Origin of the Benue Trough Nigeria

The mechanism responsible for the origin and evolution of the Benue Trough is still a subject of controversy. However, there are essentially two models; the rift and the pull-apart models. Majority of the early models were proposed based on a rifted origin beginning with King (1950), which proposed the first hypothesis on the origin of the Benue Trough, considering it as a rift opened in response to the breakup of Gondwanaland. After the development of the plate tectonics theory, Stoneley (1966) and Wright (1968) proposed a graben origin related to a readjustment of the African plate after the Cretaceous opening of the Gulf of Guinea. A sea floor spreading model was even put forward by Burke *et al.*, (1972) for the southern part of the Trough. Grant (1971) and Thiessen *et al.,* (1979) proposed a three-arm rift model in which the Benue Trough is an aulacogen. These models invoked stretching on a continental scale for the opening of the Benue Trough, comparable to that seen in the East African Rift system. More recently, an alternative model (Benkhelil 1982; Benkhelil & Robineau 1983) incorporates a transcurrent movement initiated on the continental extension of the Equatorial transform faults, the Benue Trough being the result of the juxtaposition of pull-apart basins along strike-slip faults. All of these models are based upon a fault framework with a NE-SW trend. The rift models assume that normal faults bound the structure while in the second hypothesis an axial network of strike-slip faults should act in a sinistral way. These interpretations are based on general features of the Trough and are commonly not supported by precise field data. Landsat and radar imageries (Popoff *et al.,* 1983) clearly show prominent NE-SW lineaments, mainly in the Upper Benue area. The major one which cuts across the Kaltungo Inlier affects both sediments and basement. They carried out structural and micro structural analyses on the fault rocks from this lineament. The aim was to define the mode of initial fracturing of the basement, the nature of deformations, the paleostress fields, as well as the chronology of

the tectonic events, based on the behaviour of the Kaltungo lineament fault rocks. Their main objective was to explain the role of these NE-SW lineaments within a model for the opening of the Benue Trough.

The pull-apart model which is the manifestation of strike-slip faulting can be integrated into a more regional view of the west and central African rift systems. According to Fairhead, (1988); Fairhead and Green (1989), the Equatorial Atlantic in the early Cretaceous was considered to be a transform boundary, and not a constructive plate boundary as proposed by Burke *et al*., (1971, 1972), Burke and Dewey (1973) and Burke and Dewey (1974), with Africa and South America sliding past one another. This assertion has been ascertained by proponents of the rift model e.g. Grant (1971) who proposed that the triple junction at the southern end of the Benue Trough was a rift-rift-fault triple junction, with the faulted segment represented by the Equatorial Atlantic. The Equatorial Atlantic subsequently opened into a true ocean, and the transform faults are presently active mainly between the segments of the mid-Atlantic ridge. In addition the transform faults in the Equatorial Atlantic extend up to the West African coast, and during the Cretaceous they also affected the continent itself. The two major strike-slip zones were the Benue Trough and the Central African Shear Zone which, according to Guiraud and Maurin (1991, 1992), are regarded as ancient shear zones reactivated during the Cretaceous. The Central African shear zone is the extension on the African plate of the Pernambuco fault in Brazil, exposed as the Foumban shear zone in Cameroon. Transform movements were transmitted into the African continent along these ancient shear zones (Benue Trough and Central African shear zone) as sinistral and dextral strike-slip movement respectively. Rift basins extend perpendicularly from these shear zones with the east Niger rifts extending from the line of the Benue Trough and the Sudanese and Kenyan rifts from the Central African shear zone

thereby constituting the West African Rift System and the greater part of the Central African Rift System respectively (Fairhead, 1988, Binks and Fairhead, 1992).

From all the models proposed above by several authors on the origin and history of the Benue Trough, this work agrees that the origin of the Benue Trough results from the combination of rifting and as well as sinistral strike-slips faulting.

## 2.6 Palaeogeographic History of the Benue Trough

There was almost a continuous deposition in the Benue Trough from Albian to Santonian Burke *et al*., (1971). Paleogeographic evolution of the Benue Trough was directly controlled by the opening of South Atlantic during the early Cretaceous and then the Late Cretaceous transgression Benkhelil, (1989). Sedimentation in the Benue Trough can therefore be traced as far back as Albian in the Cretaceous period through a series of transgression and regressions which persisted up till the Paleocene and Eocene and this can be partly or wholly linked to global sea level changes (Reyment and Tait, 1972).

### 2.6.1 Albian Transgression

The earliest record of marine transgression in the Upper Benue Trough was in Albian. According to Mascle *et al.*, (1988), final continental separation of Africa and South America occurred along the Ivory-Cost Guinea transform margin during the Late Albian to Early Cenomanian. The first marine penetration of the Benue Trough coincided with or immediately preceded the establishment of through-going seaway between the South and Equatorial Atlantic oceans (Zaborski, 2000). Recent evidence indicates that during the Late Albian, the sea shoaled in the poorly understood area south of Bashar (Zaborski 2000). There are suggestions that it extends further north, where it is represented by argillaceous beds in the lower parts of the Bima Group (Carter *et al.*, 1963; Cratchley

and Jones, 1965; Ayoola, 1981). However, Allix (1983) termed the shale dominated horizons to be of lacustrine origin with ages ranging between Late Aptian to Middle Albian. In the Upper Benue Trough, the Middle and Upper Albian is represented by the "Middle" and "Upper" "Bima Sandstone" (Guiraud 1990a; 1991b) which were deposited in fluvial systems discharging into the Benue sea (Jones, 1961; Ayoola, 1981; Allix, 1983, Guiraud, 1990a; 1991a).

### 2.6.2 Late Albian to Cenomanian Regression

A gradual regression from the interior of the Benue Trough started during the later part of Albian (Offodile, 1976). In the Upper Benue Trough, the greater part of the Cenomanian is represented by the Yolde Formation which contains dinoflagellates and arenaceous foraminifers at various stratigraphic levels (Lawal, 1982; Allix, 1983). At one locality, the upper part of the "Upper Bima Sandstone" has also yielded dinoflagellaes, from beds that were assigned a late Albian to early Cenomanian age (Allix, 1983).

The Yolde formation is precisely dated; its upper part is related genetically to the Late Cenomanian transgression. However, possible intermittent marginal marine conditions affected the Upper Benue Trough during the early and Middle Cenomanian, where the sea was advancing into the region from the north through the east Niger rifts (Zaborski, 2000).

### 2.6.3 Late Cenomanian to Early Turonian Transgression

According to Zaborski (2000), marine Upper Cenomanian to Lower Turonian sediments occur throughout the Benue Trough (but are unknown on the Calabar flank at least in outcrop). In the upper Benue Trough they are represented by the Dukul Formation in the Yola arm and the "Kanawa Member" of the Pindiga Formation in the

Gongola Arm (Carter *et al*., 1963; Zaborski *et al*., 1998). "The Kanawa Member" and Dukul Formation comprise of shales with limestones horizons (Zaborski, 2000).

### 2.6.4 Middle Turonian Regression

The uppermost Lower and Middle Turonian are represented by fluvial and littoral sandy facies, the Gulani, Dumbulwa and Deba Fulani Members of Pindiga Formation (Zaborski *et al*., 1998). Regressive conditions were less pronounced in the Yola Arm where the essentially argillaceous Jessu Formation is of Middle to Late Turonian age (Allix, 1983). The Gulani Formation includes a basal part comprising Kanawa Formation – type shales and thin sandstones with Thalassinoides burrows (Ayok, 2012).

### 2.6.5 Late Turonian to Coniacian Transgression

Marine Coniacian beds occur throughout the Benue Trough and in the Calabar Flank (Zaborski, 2000). The Sukuliye (Sekule) Formation and Numanha Shale represent open and more restricted marine Coniacian conditions respectively in the Yola arm, while Basin marine Coniacian sedments occur in the lower part of the Fika Member of the Pindiga Formation in the Gongola arm (Carter *et al*., 1963; Petters, 1978; Allix, 1983; Zaborski *et al*., 1998).

### 2.6.6 Santonian

The Benue Trough "proper" was inverted during the Late Santonian at about 85-83Ma as a result of global plate reorganization (Guiraud and Bosworth, 1997). This event also affected the East Niger rifts where folding took place and the Termit, Tefidet, Tenere Grein and Kafra rifts became isolated from one another as a discrete structure (Genik, 1993). The Santonian compression appears to have severed their link to the Gulf of

Guinea. An interval of erosion followed in the Benue Trough where Lower and Middle Campanian beds are unknown (Zaborski, 2000).

### 2.6.7 Late Campanian to Maastrichtian Transgression

During the Late Campanian, when a renewed phase of rifting took place, Sedimentation resumed in the Benue Trough (Popoff *et al*., 1988; Zaborski, 1998), and also in the east Niger rifts (Genik, 1993). In the Gongola Basin, the Fika Member contains Campanian beds with dinoflagellates and arenaceous foraminifers (Lawal, 1982; Allix, 1983). A juvenile *Libycoceras* was described from near Gombe in the Gongola Basin of the upper Benue Trough (Reyment, 1955; 1980).

The Campano-Maastrichtian cycle began with transgression which created a trans-Saharan migration route for *Libycoceras*, flooded the Benue Trough and allowed the genus to colonize southern Nigeria from the north (Zaborski, 2000). The available evidence suggests that prior to the mid – late Campanian, the East – Niger rifts had a marine connection to the North but a link with the Gulf of Guinea then developed; re – establishing the Trans – Saharan seaway ( Zaborski, 2000).

Late during the Campanian the Benue migration route was severed, initially perhaps by hypo saline conditions developing in the middle and upper Benue Trough and subsequently by the infilling of these areas by the Maastrictian fluvio - deltaic Lafia Formation and Gombe Formation respectively (Zaborski, 2000).

### 2.6.8 Palaeocene Transgression

According Zaborski (2000), the final transgression which affected Nigeria was of Late Paleocene age. The transgression affected part of the southern Nigeria where the Imo Shale was deposited in the Anambra Basin and eastern Benin Basin and to the west, is the

limestone of Ewekoro Formation which is a partial lateral equivalent of the Imo Shale (Zaborski, 2000). Also in the Iullemmeden Basin, Paleocene transgressive deposits occur as the Kalambaina Formation (Kogbe, 1979; 1981; Dikouma, 1994). In the Gongola Basin the continental Kerri-Kerri Formation represents the Paleocene, at least in part (Adegoke *et al*., 1978).

## 2.7 The Upper Benue Trough

### 2.7.1 Introduction

Earlier published works on the upper Benue Trough and southern Borno Basin were undertaken by Falconer (1911), Jones (1932), Raeburn and Jones (1934) and Barber *et al*. (1954). However, most of the later works were built upon that of Carter *et al.* (1963). Detailed information on the upper Benue Trough has been provided through the work of Allix (1983), Benkhelil (1985; 1986; 1988), Popoff (1988), Guiraud (1989, 1990a, 1991a, 1993) and Zaborski *et al*. (1998).

The review of the origin and evolution of the linear mega structure (Benue Trough) were provided by Benkhelil (1989). Carter *et al.,* (1963) produced the foundation work of the geology of the Upper Benue Trough. They referred to the area between the Yola arm and the Gongola arm as the "Zambuk ridge" a zone characterised by a number of important NE – SW trending sinitrial strike – slip faults. Maurin *et al.*, (1986) carried out structural and microstructural analyses on the fault rocks from the Kaltungo lineament with the aim of defining the mode of initial fracturing of the basement, the nature of deformations, the paleostress fields, as well as the chronology of the tectonic events, based on the behaviour of the Kaltungo lineament fault rocks. His main objective was to explain the role of these NE-SW lineaments within a model for the opening of the Benue Trough.

The basic lithostratigraphic successions for the Gongola Basin were established by Carter *et al.,* (1963) modified by Popoff *et al.,* (1986), Zaborski *et al.,* (1998) and Hamidu *et al.,* (2013). Carter *et al.,* (1963), Allix (1983), Popoff *et al.,* (1986) recognised and described a threefold subdivision of the Bima Group. Guiraud (1991a) provided the most detailed account of the Bima Group. The name Yolde Formation was proposed by Carter *et al.,* (1963) for the "transitional bed" between the Bima Formation and the Pindiga Formation. Carter *et al.,* (1963) described the Gombe Formation as been an estuarine deposit, Dike (1995) reported some coal horizon in the upper part of the Gombe Formation encountered in borehole penetrating the subcropping part of the unit. The Kerri – Kerri formation was described by Dike (1995). Figure 8 shows the the location of the onshore mud volcanoes on previous work done by Benkhelil (1985).

## 2.8 Stratigraphic Succession of the Upper Benue Trough

According to Zaborski (1998), the stratigraphic succession of the Upper Benue Trough, consists of Early Cretaceous continental clastics and a dominantly marine Late Cretaceous succession. The later sediments accumulated during a Late Cretaceous thermo-tectonic sag episode as a result of transgressive and regressive episodes and the youngest Cretaceous deposits accumulated during a renewed phase of rifting. The thickest sediments recorded in the Benue Trough were believed to have been deposited in rhomb grabens or pull-apart basins with sinistral strike-slip borders trending N40ºE to N70ºE ("Benue" trend) and normal borders striking N120º to N160ºE ("Chad" trend) (Guiraud, 1990b).

There was a "Pre rift" stage during the terminal Jurassic to earliest Cretaceous, when local depressions were thought to have developed in association with distension along NE-SW trending faults (Popoff, 1988). Subsequently, "basal conglomerates and

sandstones" of hundreds of metres thick, including boulders of very large size were deposited as a result of a N-S extensional phase and which may have produced the E-W Yola Arm and the small northern Cameroon basins during a Neocomain to Barremian "eo-rift" stage (Popoff, 1988). This stage was followed by magmatism in the Burashika area where lava flows have yielded ages close to the Jurassic – Cretaceous boundary (Popoff, 1988).

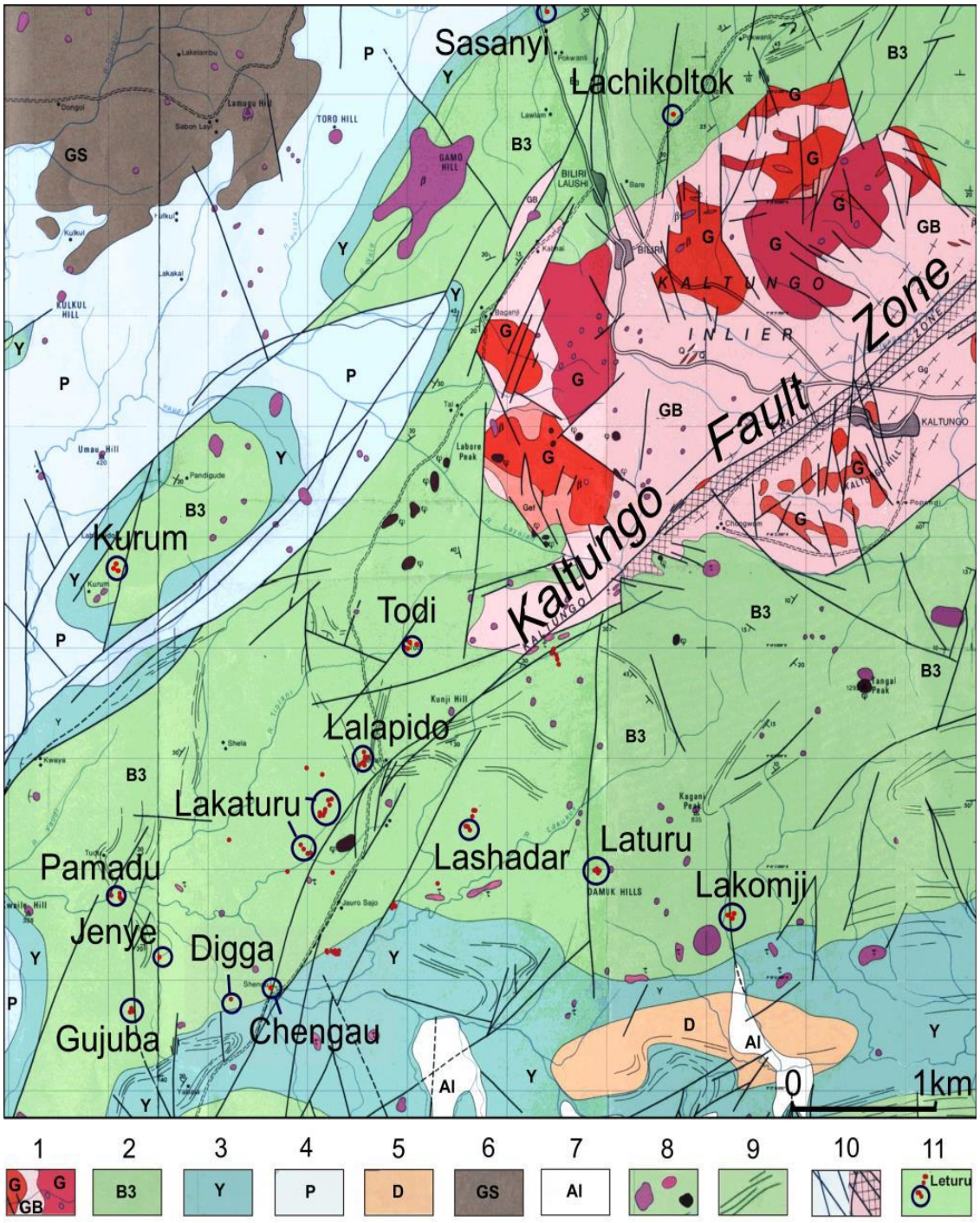
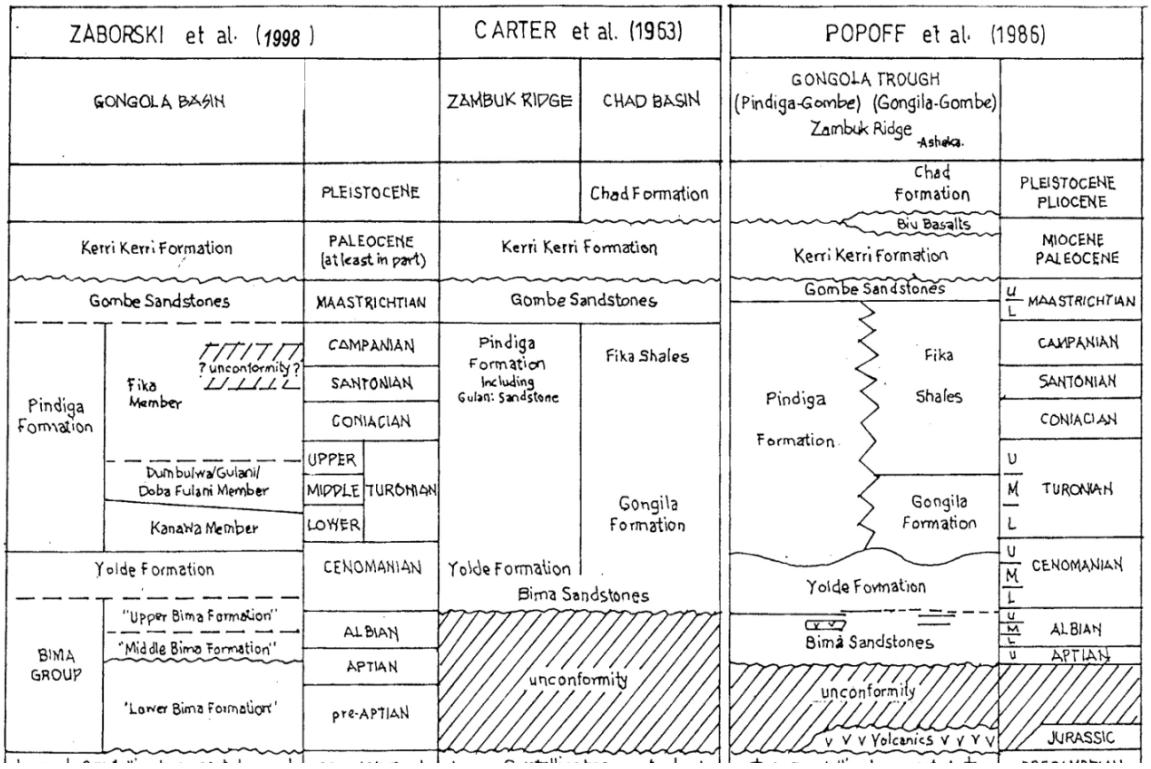



Figure 8: Geological map of the study area showing location of the mud volcanoes by the author (modified after Benkhelil, 1985). Explanation: 1 – Neogenic volcanics; 2 – Alluvium; 3 – Gombe Sandstone (Maastrichtian ); 4 – Dukul Formation (the lowest member of Pindiga Formation, Turonian; 5 – Pindiga Formation (Turonian-Senonian); 6 – Yolde Formation (Cenomanian); 7 – Upper Bima Sandstone (Albian); 8 – Precambrian basement rocks (mainly granites) of Kaltungo inlier; 9 – traces of bedding; 10 – faults and fault zones; 11 – location of mud volcanoe

"Syn-rift I" stage existed from Barremian to Middle Albian, when the rate of subsidence due to crustal extension increased giving rise to larger elongate basins (Popoff, 1988). These basins were believed to be the sites of lakes which temporarily merged to create a system of "great interior lakes" perhaps occupying the whole of the Benue Trough (Popoff, 1988).

According to Popoff (1988), a "Syn-rift II" phase took place during the later part of the Albian in response to further crustal stretching, giving way to a sag stage of basin development during the Cenomanian. The rates of subsidence were greatly reduced and crustal extension now ceased.

Table.1: Lithostratigraphic subdivision of the Gongola Basin as proposed by Zaborski *et al*., (1998), Popoff et al., (1986) and Carter et al., (1963).



The stratigraphic succession in the Yola and Gongola branches are slightly different. The details are explainedas propose by Carter *et al.*, (1963), later modified by Popoff *et al.*, (1986) and Zaborski *et al.*, (1998) (Table 1).

### 2.8.1 Bima Group

This Group consist of the Lower, Middle and Upper Bima Sandstone formations (Guiraud, 1990b) with a regional unconformity separating the Lower Sandstone from the younger beds (Figure 9). Lithostratigraphic sequence in the Gongola Basin begins with the thick lower Cretaceous Bima Group, a basically fining upwards continental succession reaching an overall thickness of several km.

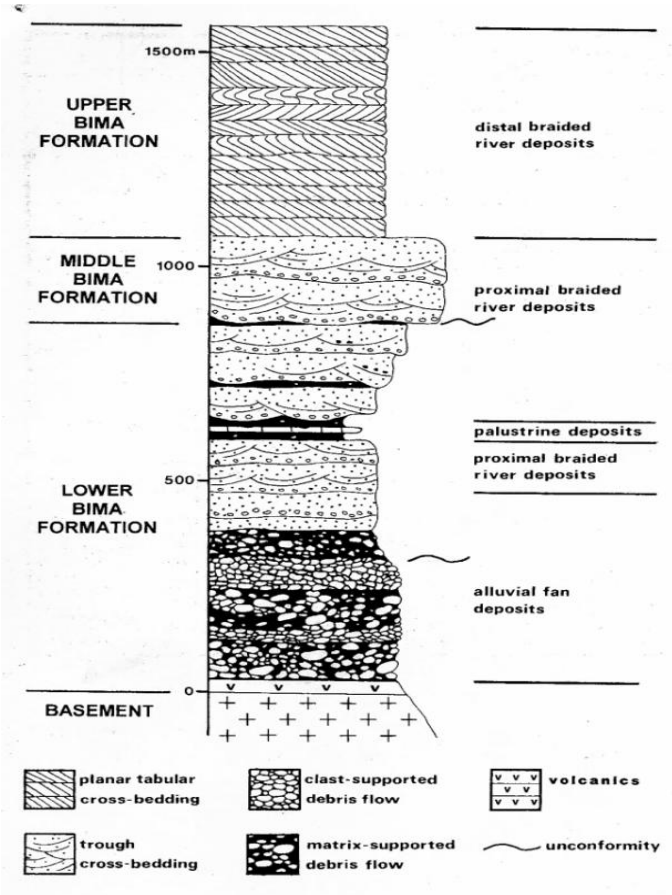



Figure 9: Generalized lithostratigraphic profile of Bima Group (Zaborski *et al.*, 1998, modified after Guiraud, 1991a).

According to Zaborski (2003), the entire unit represents active rifting to early thermotectonic sag stages of basin development. Carter *et al.*, (1963), Ojo and Pinna (1982), Allix (1983) and Guiraud (1990b, 1991a) have variously described the Bima Group. The description of the Bima group given by Guiraud (1990b; 1991a) (Figure 12) is accurate and comprehensive. Zaborski *et al.* (1998) also agrees with Guiraud (1990b; 1991a) informal subdivision of the Bima Group into "Lower", "Middle" and "Upper Bima formations".

**The "Lower Bima Formation"**

The Lower Bima Sandstone ("B1") is a highly variable unit ranging in thickness from 0 to over 1500 m and with age limits between terminal Jurassic and Early Albian. Lithofacies distributions were controlled by syn sedimentary tectonics which created a number of fault-bounded sub-basins within which marginal alluvial fan / distal debris flow deposits pass laterally into fining upwards fluvial cycles and in places into lacustrine deposits comprising of interbedded clays, fine – grained sandstone and calcareous beds (Zaborski *et al*., 1998).

**The "Middle Bima Sandstone"**

According to Zaborski *et al*., (1998), the Middle Bima Sandstone ("B1"), is a widely distributed, fairly uniform unit made up of fining – upward cycles each 5 – 10m thick. Trough and tabular cross – bedding characterises the sandstones in the lower part of each cycle, thin clays and palaeosols occur above. It marks the transition from the active rifting to thermotectonic stage of basin development with a thickness ranging between 100 to 500 m. These deposits were regarded as of proximal braided river origin. Guiraud (1991a) assigned a Late Aptian or Albian age.

**The "Upper Bima Sandstone"**

The Upper Bima Sandstone ("B3") is a fairly homogenous, relatively mature unit comprising of coarse to fine-grained sandstones characterised by tabular cross - bedding with laterally extensive sets a few tens of centimetres to few metres thick. Convolute bedding and overturned cross-bedding are also common. The average thickness is about 500m with maximum, in the Lamurde anticline, of 1200m. The Upper Bima Sandstone represents a distal braided river origin (Zaborski *et al.,* 1998).

### 2.8.2 Yolde Formation

The Yolde Formation has been described in the Yola arm by Carter et al (1963) and Allix (1983) and in the Gongola basin by Zaborski *et al* (1998). It consist largely of alternations of coarse to fine – grained, cross bedded or ripple bedded sandstone and grey to greenish shales. Thin limestones or calcareous sandstones occur especially in its upper part where oyster beds are common. The formation fines upward channel – filling coarse – grained sandstone with trough cross – bedding occurring in the lower part, thinly – bedded, medium to fine – grained often bioturbated sandstone appear higher up. Yolde formation gives rise to a subdued topography, often with sparse vegetation cover, and is poorly exposed in most part of the Gongola Basin though the unit occupies the core of a gentle anticlinorial structure between Kubtogana, Alhaji Ruhu and Ruwan Kuka and a good section occurs northwest of Ruwan Kuka (Zaborski *et al.,* 1998; Figure 10). The Yolde Formation reaches a maximum thickness of about 200 m but shows considerable lateral facies variation (Zaborski, 2003). It has age limits between Late Albian and Late Cenomanian (Lawal, 1982; Allix, 1983; Lawal and Moullade, 1986; Zaborski, 2003). Carter *et al.* (1963) defined it as the appearance of "marine" shales. Allix (1983) used the appearance of thick, laterally continuous siltstones or silty

shales or the base of a marker horizon comprising greenish fine – grained sands with disturbed cross bedding found in parts of the Yola arm.

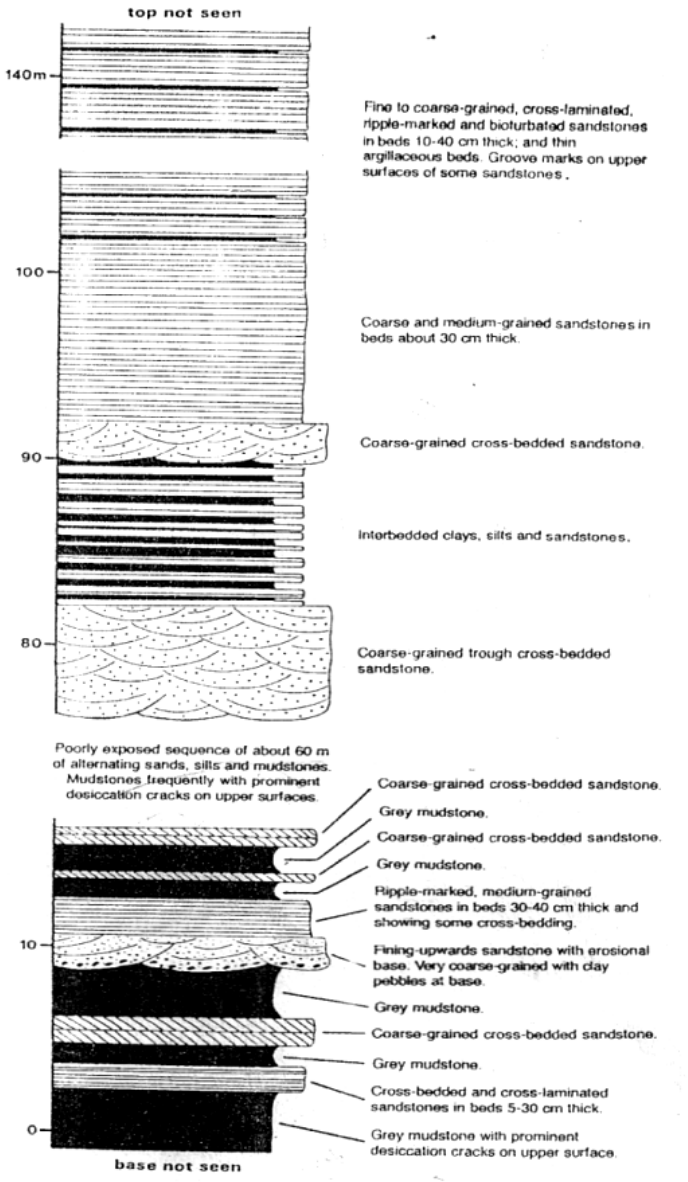



Figure 10: Section of Yolde Formation; exposed 750 m north of Ruwan Kuka (after Zaborski *et al*., 1998).

Zaborski (2003) described the argillaceous deposits in the lower portion of the formation as the upper parts of fining-upwards alluvial cycles and in most cases showing evidence of subaerial exposure represented by mud cracks and pedogenetic

features. According to him, going upward, the formation passes into a succession of more regularly bedded finer-grained sandstones (sometimes bioturbated), calcareous sandstones and shales, sometimes with lenticular bedding, and towards the top are fossiliferous calcareous sandstones the fauna being dominated by oysters. He interpreted the unit as representing a transition from fluvial to littoral to shallow sub littoral environments; with its upper part marking the beginning of the major Late Cenomanian transgression that affected the entire Benue Trough and large parts of the Saharan region, with more open marine the distal part of a southerly advancing seaway.

### 2.8.3 Pindiga Formation

The name "Pindiga Formation" was proposed by Carter *et al.,* (1963) for the "Calcareous Beds" and "Clay/Shales" previously described by Barber *et al.,* (1954). It makes up the greater part of the Upper Cretaceous deposits in the upper Benue Trough. In the Gongola Basin, the Gongila Formation and the Fika Shales of Carter *et al.,* (1963) are the equivalents of the Pindiga Formation while in the Yola Arm, the Dukul, Jessu and Sekuliye formations, the Numanha Shale and Lamja Sandstones of Carter *et al.,* (1963) are the lateral equivalents of the Pindiga Formation (Zaborski *et al.,* 1998).

Zarboski *et al.,* (1998) subdivided the Pindiga Formation into five members; the Kanawa Member (mainly shale and limestone), followed by lateral lithofacies equivalents, the Gulani, Deba Fulani and Dumbulwa members (mostly sand deposits) occurring in the middle part; and above, the Fika Member which is marine and mainly argillaceous. Detailed descriptions of each member by Zaborski *et al.,* (1998) are provided below.

**Kanawa Member**

According to Zaborski *et al.*, (1998) the Kanawa Member is the equivalent of the Kanawa Formation of Thompson (1958), a succession of shales and intercalated limestones outcropping around Kanawa to the east of Gombe. Thompson (1958) did not designate a type section for the unit but Zaborski *et al.*, (1998) reported numerous exposures in the Kanawa-Debe Habe area, for example the section (Figure 11). According to them the most complete sections occur along the Pindiga stream (the type section of Pindiga Formation of Carter *et al.*, 1963) and in the Ashaka Cement quarry.

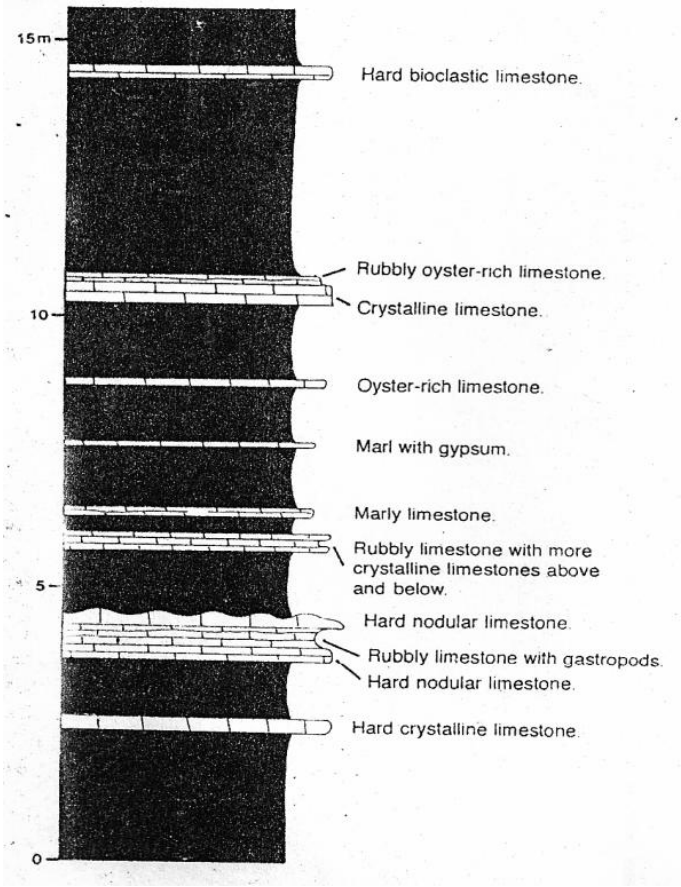



Figure 11: Pindiga Formation (Kanawa Member) Stream section at the base of the unit exposed 4km east of Kanawa (After Zaborski *et al.*, 1998)

This unit was deposited during the Late Cenomanian to Early Turonian transgression that affected the entire Benue Trough and also the Saharan region to the north (Busson,

1972; Reyment, 1980; Meister *et al.,* 1992). Its age-equivalent in the Yola Arm is the Dukul Formation which has a similar lithology of shaly mudstones with intercalated limestones (Carter *et al.,* 1963; Zaborski, 1990; Zaborski *et al.,* 1998).

The Kanawa Member provides an excellent stratigraphical marker horizon between the sandy units above and below, and in most places the shaly component weathers to distinctive black, cotton soil which is heavily cultivated (Zaborski *et al.,* 1998).

**Gulani Member**

Carter *et al.,* (1963) proposed the name "Gulani Sandstone" for a member within the Pindiga Formation. This is unit was treated in the same way by Zaborski *et al.,* (1998) who, identified a reference section west of Maliya comprising from top to bottom of 25 m of granule stones and very coarse to coarse-grained sandstones, showing cross-bedding with sets that are up to 4m thick. Also, 20m of poorly exposed intercalated pebbly sandstones with purple and white laminated mudstones, and 10m of very coarse-grained, pebbly cross-bedded sandstones with sets 50 – 60cm thick (Figure 12). Ayok *et al*., (2014) upgraded the Gulani Member to a formational status and proposed a lectostratotype north-east of Dogon-Zaga.

**Deba – Fulani Member**

Zaborski *et al.,* (1998) proposed the name "Deba-Fulani Member" for the sandy beds occurring in the middle part of Pindiga Formation over most of its outcrop. According to them the unit passes laterally into the Dumbulwa Member south of the Dumbulwa-Bage High and crops out over large parts of the plain west of Gongola River though its limits are difficult to determine due to extensive superficial alluvial cover. The outcrop of the Deba Fulani Member south of Deba Fulani is expressed by a low ridge of undulating topography where it weathers into a thin, red lateritic soil with regolith of

boulders and pebbly-sized fragments of dense and flaggy ironstone (Zaborski *et al.,* 1998). Zaborski *et al.,* (1998) proposed a type area west of Deba Fulani (in streams) with limited sections of interbedded 5-15 cm thick sandstones and siltstones; additional exposures that represent reference sections (Figure 13) occur in rivers that cut across the outcropping part of Deba Fulani to the south. The unit was estimated to be about 200 m thick between Sabon Gari and Batungo thinning to the south and wedging out south of Kumo. The unit is of coastal and shallow sublittoral origin though in places contains channel-filling sandstones of probably fluvial origin.

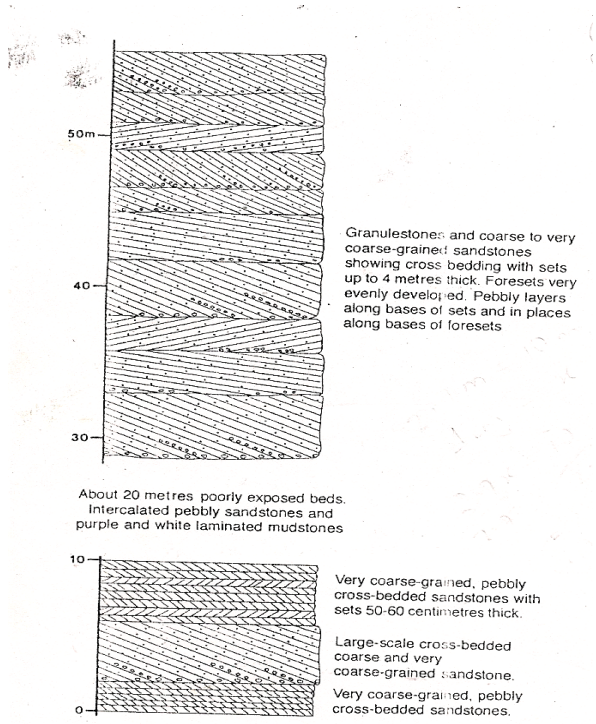



Figure 12: Pindiga Formations (Gulani Member).Section exposed 500 m west of Maliya in eastern limb of Jana syncline (After Zaborski *et al*., 1998).

**Dumbulwa Member**

The "Dumbulwa Member" is a name proposed by Zaborski *et al.,* (1998) for a unit which appears to be the same as the upper sandstone-shale portion of the "Gongila Formation" of Carter *et al*., (1963). At the foot of the Dumbulwa Hills, this unit has a

deeply erosional contact with the Kanawa Member (Zaborski *et al.*, 1998*)*. Numerous partial exposures of the Dumbulwa Member showing fining-upward cycles (Figure 14) occur in the Dumbulwa Hills which was proposed as the type area of the unit. Additionally, in the vicinity and to the south of Bage, the Dumbulwa Member contains coarse grained, feldspathic, tabular cross-bedded sandstones. Channel-filling sandstone bodies up to 3 m thick and 20 m across cutting though sequences of thinly bedded fine-grained sandstones and laminated silty sandstone also occur here (Zaborski *et al.*, 1998).

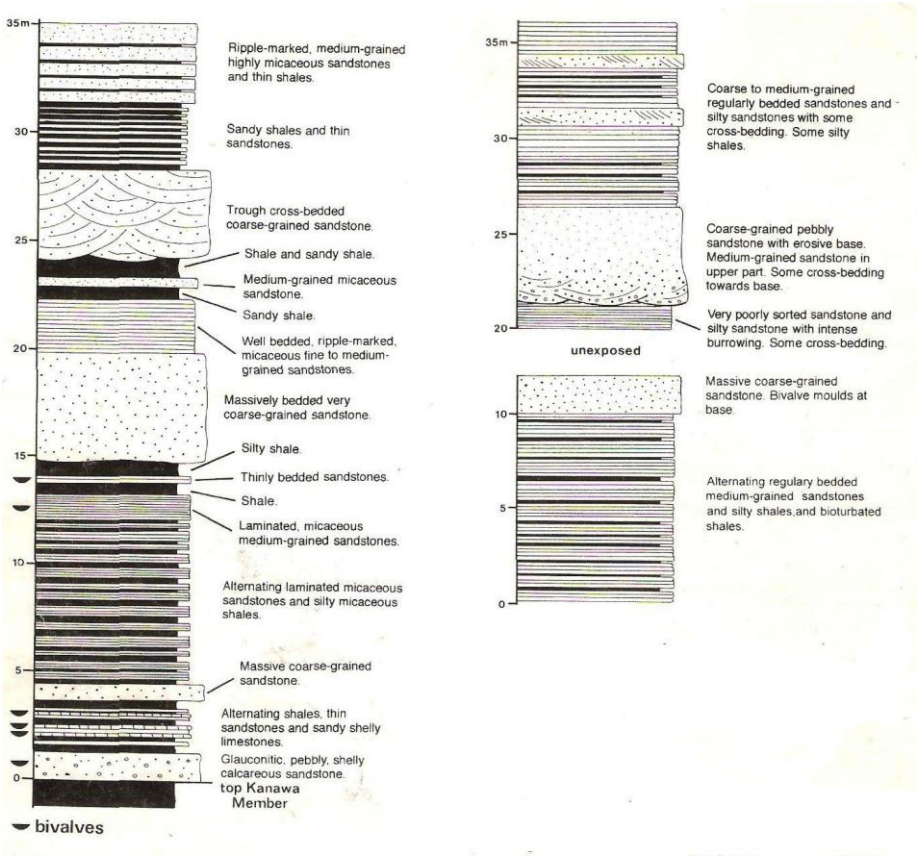



Figure 13: Pindiga Formation (Deba Fulani Member). Basal section exposed in Ashaka quarry (left), section exposed in the middle part of the unit, River Difa, Sabon Gari (right) (After Zaborski *et al*., 1998).

The Dumbulwa Member reaches its greatest thickness of about 200 metres in the Dumbulwa and Bage Hills. In the northeastern part of the Dumbulwa-Bage High, it

wedges out between Solare and Bularaba, while to the south and east of the Dumbulwa-Bage High, it apparently passes laterally into the Deba Fulani Member (Zaborski *et al.*, 1998).

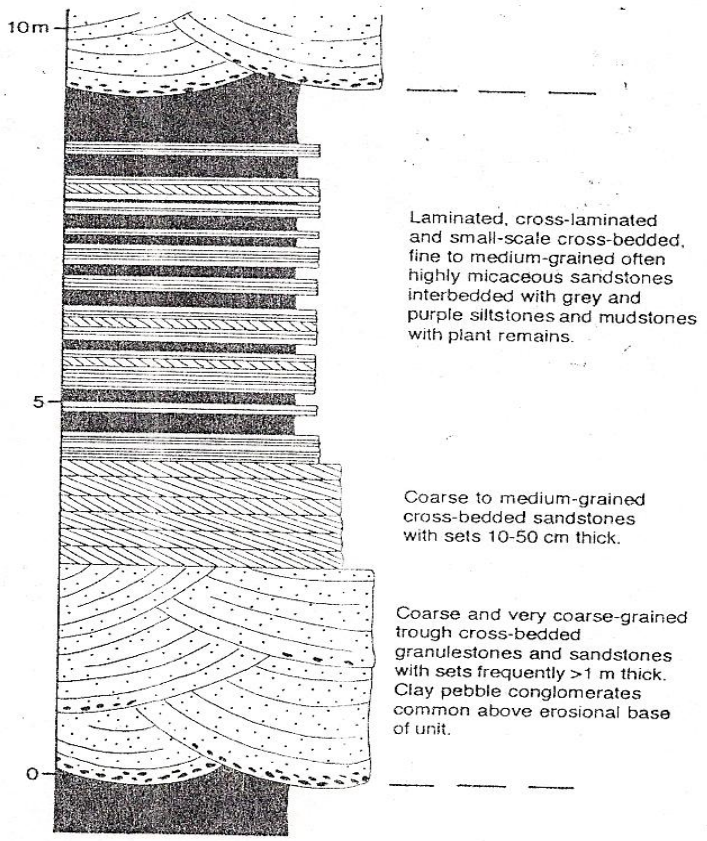



Figure 14: Pindiga Formation (Dumbuluwa Member). Complete fining-upward cycle, Doro Hill (after Zaborski *et al*., 1998).

**Fika Member**

Zaborski *et al.*, (1998) described the Fika Member as comprising the "Fika Shales" of Carter *et al.*, (1963) and being the equivalent of the upper, shale, member of the Pindiga Formation of the same authors.

The Fika Member reaches a thickness in excess of 460 m and comprises black shales, with silty and sandy shales, siltstones, fine-grained sandstones and carbonate beds at

various levels (Allix, 1983). The unit was believed to represent a period of continous deposition from Turonian to Maastrichtian by Carter *et al.,* (1963) and Lawal (1982). Simpson (1954) indicated that the Upper Campanian is separated from the Coniacian beds by an angular unconformity in the Lower Benue Trough. Zaborski *et al.,* (1998) were of the opinion that a Santonian-Campanian hiatus exists within the Fika Member. The lower part of the Fika Member was thought to be Upper Turonian to Coniacian, while the upper part has been dated using pollens and assigned a Late Campanian to Early Maastrichtian age (Lawal, 1982; Allix, 1983; Lawal and Moullade, 1986).

The Fika Member produces a low featureless topography, with its outcrop often recognized from the black shrinking clay soil to which it gives rise. Zaborski *et al.,* (1998) reported that the unit is often concealed by sandy alluvial deposits derived from the overlying Gombe Formation and Kerri-Kerri Formation. No exposure of any appreciable thickness was found for this unit and no type section so far has been designated for it. However, Thompson (1958) and Allix (1983) described the nature of this unit from borehole records around Gombe.

Zaborski *et al.,* (1998) described the unit to be made up of shaly mudstones; dark grey when fresh but weathering to lighter blue-green to grey colours. There is a general absence of macrofossils. Irregular bands and lenses of gypsum rarely thicker than a few centimetres occur.

### 2.8.4 Gombe Formation

The name "Gombe Formation" corresponds to the name "Gombe Formation" proposed by Carter *et al.,* (1963) for the "Gombe grits and clays" previously identified by Falconer (1911). Carter *et al*., (1963) interpreted the Gombe Formation as a deltaic and estuarine deposit. According to Allix (1983), the Gombe Formation has an average

thickness of 300 m. Lawal (1982) and Lawal and Moullade (1986) assigned a Maastrichtian age to the Gombe Formation based on pollens. Dike (1995) recognized the sub-cropping Gombe Formation beneath most of the Kerri-Kerri Formation towards the west of the Gongola Basin, and also identified coal horizons in the upper part of the Gombe Formation from boreholes that penetrated the unit. Zaborski e*t al.,* (1998) identified three major lithofacies within the Gombe Formation (Figure 15)

a) Basal transitional portion consisting of rapidly alternating thin beds of silty shales with plant remains, fine to medium-grained sandstones and thin flaggy ironstones. Bioturbation is common in this facies.

b) The "bedded facies" consisting of extremely regularly bedded, fine to medium-grained white and grey quartz arenites with interbedded silts, silty clays and both flaggy and vesicular ironstones; channel filling sandstones and convolute bedding are associated with this facies.

c) The "red sandstone facies", mainly composed of brick red coloured sandstones though they are sometimes grey or white. Within this facies there is a sporadic distribution of coarse to very coarse-grained, cross-bedded channel-filling sandstones.

The same authors deduced the palaeoenvironment of the basal transitional portion, "bedded facies" and "red sandstone facies" to be pro deltaic; shallow, hyposaline; and fluvial respectively.

### 2.8.5 Kerri-Kerri Formation

The Kerri Kerri Formation has a thickness of about 320 m and comprises sands, grits and clays deposited under a wide range of continental conditions (Adegoke *et al.,* 1986;

Dike 1995). A probable age of Paleocene has been assigned to the formation (Adegoke *et al.*, 1978).

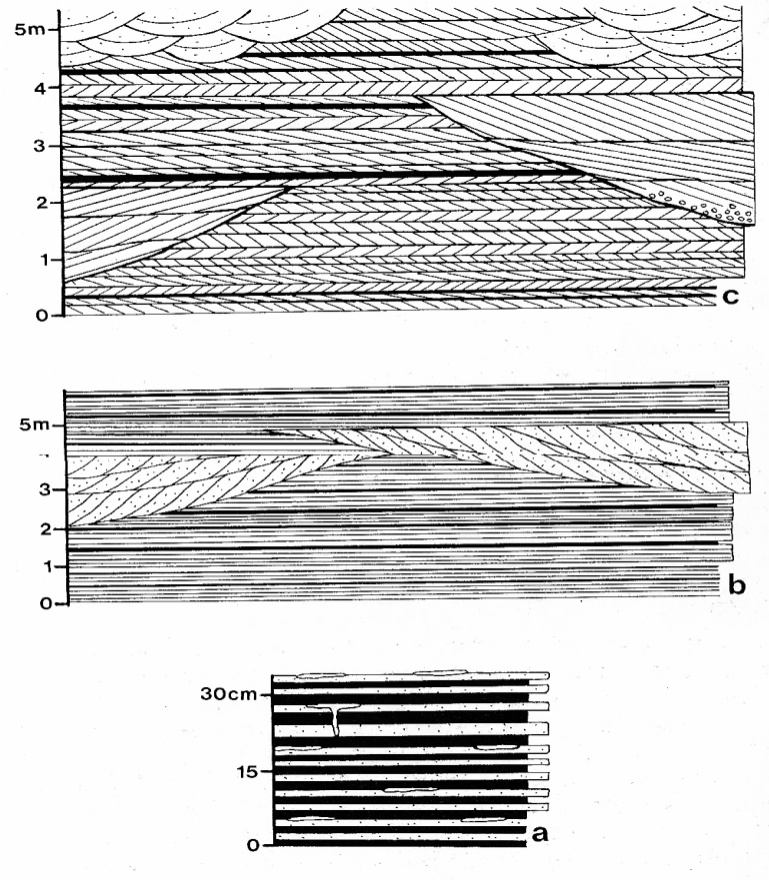



Figure 15: Gombe Formation, lithofacies recognizable within the Formation. a) Basal transitional portion, b) "bedded facies" c) "red sandstone facies" (After Zaborski *et al*., 1998)

### 2.8.6 Biu Basalt

Carter *et al.*, (1963) described the olivine basalts of the Biu Plateau as occuring as extensive lava flows. According to Turner (1978), the Biu Plateau basalts represent two major eruptive phases, with an intervening period of weathering and erosion. The Pliocene activity is characterized by an extensive lower group of thin flows covering the area south of Biu by a thick succession of more massive lavas which are deeply eroded

and therefore produces plateau that is highly dissected. The Quaternary activity is characterized by about 80 volcanoes concentrated along a NNW-SSE zone that is 50 m long. Benkhelil (1988) reported that the associated volcanic cones are arranged along N-S trending line in the western part of the plateau. According Wright (1989), the net thickness of the basalts is around 250 metres. Grant *et al.,* (1972) gave the radiometric ages of these rocks from 5.0 ± 0.2Ma to less than 0.8Ma.

### 2.8.7 Alluvium

Alluvium covers large parts of the Gongola and southern Bornu basins, notably the plain west of the Gongola River and to the north of the Dumbulwa-Bage High. The alluvium has largely been reworked by the present drainage (Ayok, 2012).

## 2.9 Structure of the Upper Benue Trough

Between the Yola arm and the Gongola arm, is an area structurally characterized by four major NE-SW trending sinistral strike-slip faults, namely, the Gombe, Bima-Teli, Kaltungo and Burashika faults (Zaborski *et al*., 1998). In addition to these faults are basement inliers, with the Kaltungo inlier being the most prominent (Zaborski, 1998). Other authors used other names e.g Carter *et al.,* (1963) termed it the "Zambuk Ridge", Guiraud (1993) called it the "Wuyo – Kaltungo basement high" and Zaborski (1998) termed it the "Wuyo - Kaltungo high" (Benkhelil 1982) said that Large-scale folds trending NE-SW, such as the Lamurde and Jarawa anticlines, affect the Cretaceous formations., major faults trending N30E to N60E such as the Kaltungo, Burashika and Zambuk faults, cut through the sediments and extend into the basement. Another one, the Gombe fault, sealed by the Upper Cretaceous Gombe formation, affects both the basement and Lower Cretaceous rocks. Generally, these faults are well marked on the

northeastern basin margins, whereas they disappear progressively southward in thicker sedimentary formations.

The overall trend of the Gongola arm is controlled by a series of N-S to NNE-SSW trending-faults (Zaborski *et al.*, 1998; Figure 16) while the Yola arm is characterized by deep seated E-W trending fractures (Benkhelil 1988; Maurin and Guiraud, 1989; 1990; Braide, 1992).

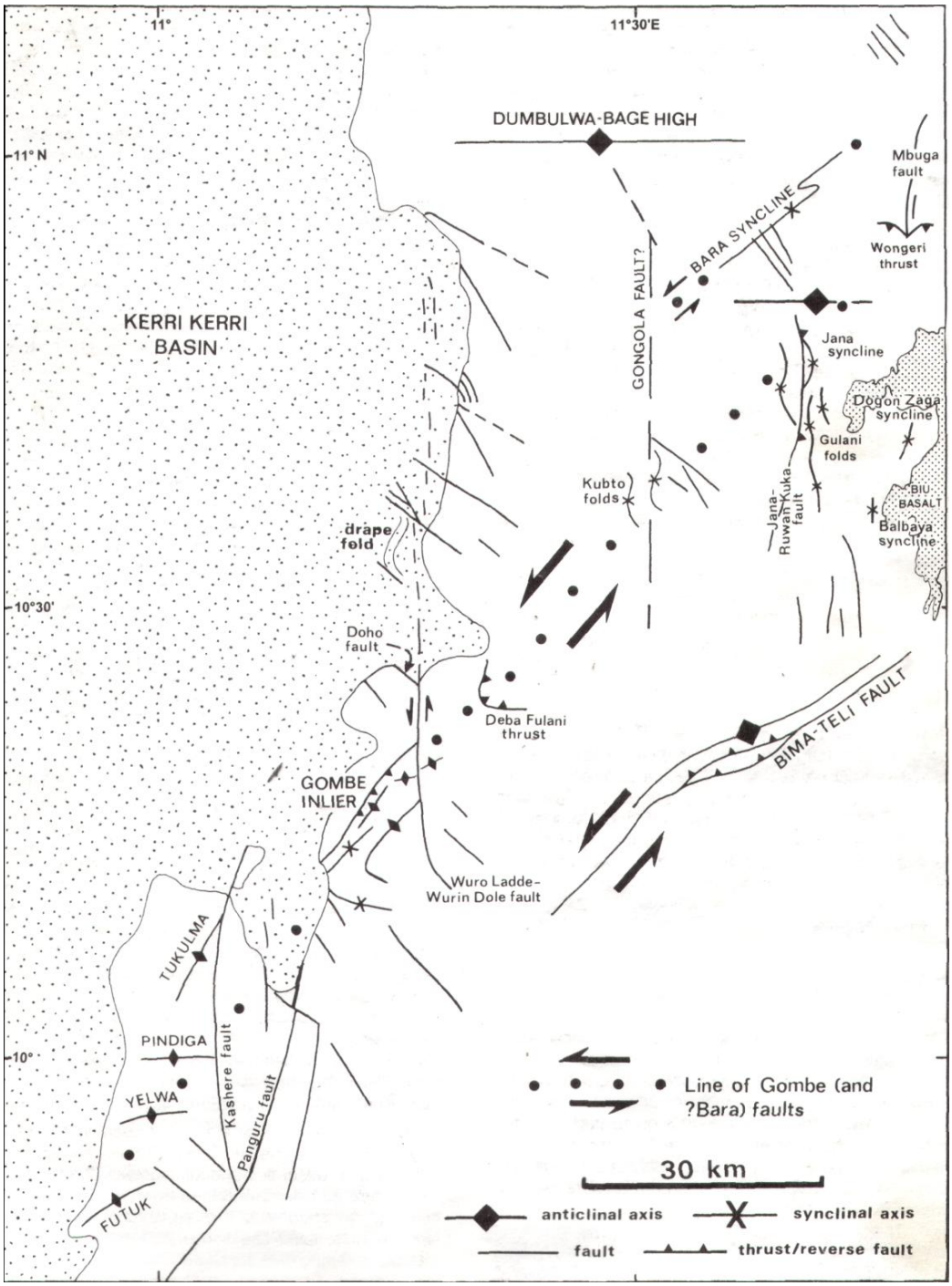



Figure 16: Map showing the main structural features of the outcropping Cretaceous Gongola Basin (after Zaborski *et al.*, 1998).

In Cameroun, the eastward extension of the Yola arm is the Garoua Basin which is bounded at its eastern extremity by NW-SE trending strike slip faults (Maurin and Guiraud, 1989; 1990).

According to Zaborski (1998), the major ENE-WSW trending folds of the Yola arm, including the Lamurde anticline and Dadiya syncline, have generally been attributed to terminal Maastrichtian compression but they may be Santonian, as suggested by Guiraud (1993) and more tentatively by Allix (1983). The folding episodes associated with the Middle Albian to Maastrichtian age generated the development of prominent anticlinal structures which dominated the Benue valley. These features genetically related, are separated into the Abakaliki, Keana and Lamurde anticlinoria in the lower, middle and upper parts of the Benue valley respectively (Offodile, 1984). The Gongola Basin is bounded to the north by the anticlinal feature of the Dumbulwa-Bage High, an area of positive structural inversion during the mid-Cretaceous (Zaborski *et al*., 1998). Folds axes in the Gongola arm show dominantly E-W and N-S trends. The former are in accordance with the regional pattern, while the latter folds are probably formed as a result of local deviations of the stress directions in the domain of the N-S transpressional faults (Zaborski, *et al*., 1998).

### 2.9.1 Faults

The Gongola basin has been suggested as a graben structures forming a relay zone between the Benue Trough and the Borno – Chad rift (Benkhelil and Robineau, 1983; Benkhelil *et al.*, 1988; Fairhead and Green, 1989; Guiraud and Maurin, 1991, 1992). Benkhelili (1982; 1987; 1989) consistently pointed out that the Gongola basin has been greatly influenced by sinistrial strike – slip movement along the basement faults. He believed that the Gongola basin was mainly controlled by $N15^0$ trending faults close to its western margin. The outcropping part of the Cretaceous Gongola basin naturally

exhibits faults with three main trends; NE – SW, NW – SE, and N – S, (Zaborski *et al.*, 1988).

The notable NE-SW trending fault is the Gombe fault which traverses the southern part of the Gongola Basin. This fault is the most northerly of the four major sinistral strike-slip basements that played a vital role in the Cretaceous history of the Upper Benue Trough; the others include the Bima-Teli, Kaltungo and Burashika faults. They role of these faults has been described in detail by Maurin *et al.*, (1986), Benkhelil (1988; 1989) and Guiraud (1990a; 1991a; 1991b; 1993). The group of NE-SW trending strike-slip faults was active from the earliest stages of Cretaceous sedimentation in the Upper Benue Trough. The deposition of the Bima Group was partly controlled by extensional or transtensional movement along these fractures (Guiraud, 1990b; 1993).

The faults trending N – S of the Gongola basin involve sets of in the Bage Hills and south of Balbaya. However, form a group of offset fractures including the Mbuga, Jana-Ruwan Kuka, Wuro Ladde-Wurin Dole, Panguru and Kashere faults (Guiraud, 1990b). Maurin *et al.,* (1986) described N-S trends within the basement rocks of the Kaltungo Inlier to the south of the Gongola Basin. They suggested that such pre-existing fractures may have played a role in controlling the shape of the pull-apart basins thought to have formed between the main NE-SW strike-slip faults of the Upper Benue Trough. The N-S group of faults are parallel to the general trend of the Gongola Basin (Zaborski *et al.*, 1998).

### 2.9.2 Folds

The directions of fold axes in the Gongola Basin show more variation than those in other parts of the Benue Trough according to Zaborski *et al.*, (1998). Guiraud (1990b,

1991b and 1993) described N –S to $20^0$ trending horizontal stresses trajectories for the Cretaceous.

Folding is wide spread in the Upper Benue Valley and affects the whole Cretaceous the whole Cretaceous sedimentary pile. The fold axes in the Gongola Basin are dominantly E-W and N-S trends; the E-W trend is in agreement with the regional stress pattern while the latter were probably products of local deviations of stress directions within the N-S transpressional fault zones (Zaborski *et al.*, 1998).

The major anticlinal structures of the Dumbulwa Bage hill and those between Titeba and Bara display east-west trending fold axes, consistent with N-S horizontal shortening (Zaborski *et al.*, 1998;). These structures mainly involve the Bima Group. The Dumbulwa-Bage High area was characterized by persistent uplift after the deposition of the Lower Bima Sandstone. This is evident from the wedging out of the the Middle Bima, Upper Bima and Yolde Formation, the attenuation of the Kanawa Member and the well preserved erosional surface at the base of the Dumbulwa Member.

Fold directions in the more argillaceous upper Cretaceous sediments in the Gongola Basin are much more variable according to Zaborski *et al.* (1998). Although the Bara syncline displays a NE-SW axis, its main fold trends are N-S and more or less at right angles to those typical in the upper Benue Trough. Some of these folds have linear axes and are clearly symmetrical. According to Zaborski *et al.* (1998), fold axes in the Gongola Basin display dominantly E-W and N-S trends; the former is in agreement with the regional stress pattern while the latter were probably products of local deviations of stress directions within the N-S transpressional fault zones (Zaborski *et al.*, 1998).

The folding episodes associated with the succession of marine, continental and transitional beds of middle albian to maastrichtian age have generated anticlinal

structures which dominate the Benue valley. The features, genetically are related, and are separated into the Abakaliki, Keana and Lamurde anticlinorial in the lower, middle and upper parts of the Benue valley respectively. Each anticlinorium is associated in almost the same geological setting, with hot and cold brines – springs, issuing from its flanks. The occurrences include the Abakaliki brine fields in the Lower Benue, Awe, Azara and Ribi brine fields of the middle Benue and the Ayaba and Todi salt springs of the upper Benue. In all the occurrences, the brines are known to issue from the geological formations deposited in environments transitional between predominantly marine and continental environments, invariably of about Albian to Cenomanian age (Offodile, 1984).

# CHAPTER THREE

# METHODOLOGY

## 3.0 Introduction

The methods used in the course of the study included; desk study, reconnaissance survey, interpretation of satellite images, fieldwork, laboratory studies and statistical data evaluation/processing.

## 3.1 Desk Study

Desk study: entails literature survey for previous work on mud volcanoes with emphasis on onshore mud volcanoes from the internet and libraries, collation of maps from geological survey agencies in Kaduna and Gombe and acquisition of satellite imageries.

## 3.2 Reconnaissance Survey

Reconnaissance field mapping of likely areas of occurrence of mud volcanoes in Nigeria lasted for one year (2012 to 2013), covering the Upper Benue Trough, the Middle Benue Trough, the Lower Benue Trough and the Niger Delta. Printed photographs of existing onshore mud volcanoes served as a guide while interacting with the natives and nomadic Fulani's during the course of the reconnaissance.

## 3.3 Interpretation of Satellite Image

The satellite image of the area was obtained from Google Earth using the coordinates of the study area. The images were interpreted directly on the computer screen in order to delineate geological structures as well as demarcate the lithological boundaries within the area of mud volcanoes occurrence.

## 3.4 Fieldwork

The fieldwork carried out in the study area is as follows:

**Field mapping**: The field mapping lasted for a period of four years (from 2012 to 2015). The mapping exercise covered Kaltungo sheet 173 (NW & SW). Geological mapping of the area of the mud volcanoes was done using traverses and the various lithologies were identified with their boundaries delineated. Using the satellite navigator, the position of each of the mud volcanoes was taken and annotated on the topographical map. About 200 onshore mud volcanoes were documented and their distribution in relation to the geology was examined during the fieldwork.

The physical characteristics of the mud volcanoes were observed in the field using the measuring tape to take their dimensions (i.e. the height of the cones ranging from half a metre to one metre and the diameter from half a metre to eight metres at their base). The observations were recorded and photographs were taken. Finally, ArcGIS 9 was used to produce an updated geological map using the acquired data.

The fieldwork was done in four dry and two rainy seasons with an average total of 108 days. River channels and footpaths served as routes for the mapping. The fieldwork work done around Todi, Lallapido, Kurum, Digga, Lakaturu, Gujuba, Jenye, Pamadu, Laturu, Lashadar, Lakomji Lachikoltok etc. Lallaipido and Billiri were used as base camps. Each phase of the fieldwork was carried out by the researcher and a field assistant who was fluent in Hausa and local languages of areas visited. During the fieldwork, it was discovered that the natives and nomadic Fulani were well aware of these mud volcanoes as they willingly offered assistance in locating them since they are dangerous phenomena that have, over the years, sank children, goats and cows. They call them “Nikki” in Tangale, “Gbom - Gbom” in Shongon and “Hurfare” in Hausa, all meaning “something that swallows”.

**Sampling activity:** A total of ten (10) samples from the Upper Bima sandstone and Yolde Formation were selected from different locations for sieve analysis. The aim of the sieve analysis was to determine particle size distribution and other grain size parameters i.e. mean, sorting, skewness and kurtosis. Ten (10) samples, one each from dry mud and from overburden material selected from 5 fields of onshore mud volcanoes were carefully sampled The aim of XRD analysis was to determine the mineralogical composition of the dried mud ejected from the mud volcanoes as well as the overburden materials within the area of the mud volcanoes occurrences with the view of comparing their mineralogy. Finally, Fourteen (14) water samples were collected, one from each of the fourteen fields of mud volcanoes. The water samples for cationic analysis were acidified to pH 2 with concentrated nitric acid at the point of collection.

## 3.5 Laboratory Sample Preparation and Analysis

### 3.5.1 Granulometric analysis (sieve analysis)

Sieve analysis was carried out on the sandstone sampled from the Upper Bima Sandstone and Yolde Formation in the Department of Geology Ahmadu Bello University, Zaria. Ten samples from the Upper Bima sandstone and Yolde Formation were selected from different locations for sieve analysis.

**Procedure**: The samples were soaked overnight in the laboratory, dried and carefully disaggregated with the help of pestle and mortar. The weight of the bottom pan, selected empty sieves (1.8 mm, 0.6 mm, 0.3 mm, 0.15 mm, 0.075 mm and <0.075 mm) and 100 g of each disaggregated samples were obtained using a weighing balance. The sieves and the bottom pan were fastened to a mechanical shaker, and the 100 g of the sample poured on the upper sieve. The machine was switched on and allowed to shake for ten (10) minutes. Sediment in each of the sieves and the bottom pan were weighed and

recorded. Precautions taken in the course of the sieve analysis including taking care in the separation of the sieves after shaking to avoid spill over of the retained sediments.

**Precaution**: During, the disaggregation of the samples, care was taken to avoid crushing and grinding in order not to distort the original shape of the grains. Results obtained from the sieve analysis are presented in a tabular form in chapter five.

### 3.5.2 X-Ray Diffractometer (XRD) Analysis

A total of ten (10) samples, one each from dry mud and from overburden material selected from 5 fields of onshore mud volcanoes were carefully sampled. They were labelled with identification shown in Table 2 and sent for laboratory analysis at the Faculty of Earth Sciences, University of Silesia, Poland.

**Table2: The XRD sample pairs with description taken from labels on sample containers**

| Location ID | Sample ID |
|---|---|
| Lakaturu saprolite | Sm 5 |
| Lakaturu mud slurry | Sm 6 |
| Lashadar saprolite | Sm 2 |
| Lashadar mud slurry | Sm 3 |
| Pamadu saprolite | Sm 7 |
| Pamadu mud slurry | Sm 10 |
| Jenye saprolite | Sm 9 |
| Jenye mud slurry | Sm 8 |
| Kurum saprolite | Sm 1 |
| Kurum mud slurry | Sm 4 |

The XRD data were obtained at room temperature for 5 samples of dry mud and 5 samples of the overburden. The XRD data were collected using a Panalytical X'Pert PRO MPD PW 3040/60 diffractometer with Theta-Theta geometry. Measurements conditions are provided in Table 3.

**Table 3: X-ray Diffractometer specification**

| Parameter | Settings |
|---|---|
| Radiation | Cu Kα1 radiation (λ=1,540598 Å)<br>Ni-Filter to reduce the Kβ radiation |
| Acceleration Voltage | 45 kV |
| Filament Current | 30 mA |
| Goniometer Settings | 2,5°- 65° 2Θ |
| Step Size | 0,008° 2Θ |
| Counting Time | 200 s |
| Detector | X'Celerator - using Real Time Multiple Strip detection technology |

X-ray diffraction is a method that provides detailed information about the atomic structure of crystalline substances. It is a powerful tool in the identification of inorganic phases such as metal sulfates. X-ray powder diffraction (XRPD), alternatively powder X-ray diffraction (PXRD), got its name from the technique of collecting X-ray diffraction patterns from packed powder samples. Generally, X-ray powder diffraction involves the characterization of the crystallographic structure, crystallite size, and orientation distribution in polycrystalline samples (Bob, 2009).

The penetration of X-ray beam is in the order of 100μm for CuKα, so the sample grain size should be between 5 and 10 μm. A careful grinding is important for the hydrated sulfate material. Heat produced by prolonged motorized grinding can introduce changes in the sample, so manual grinding in an agate mortar is preferred. Samples that are sensitive to air or humidity have to be prepared with the "Non-standard Sample Preparation" such as Kapton Foils with the Zero background Holder as a sample support. Sensitive substances can be also put into a glass capillary. A mixture of compounds gives a pattern that is made up of the patterns of all the individual compounds. This allows the identification of phases in the sample by the Rietveld method.

The principles of XRD phase quantification is sound theoretically: the limitations on accuracy are primarily experimental. Single-peak methods usually result in accuracies that are on the order of ±10%. Careful use of multiple peaks and reproducible procedures may reduce this figure to ±5%. Whole-pattern methods (including Rietveld) seem to produce accuracies that are ±2% [5]. Rietveld analysis is a mathematical method using analytical profile functions and least-squares algorithms to fit a theoretical to a measured pattern. In order to perform a Rietveld refinement structure data for all phases present in the sample are needed (e.g. ICSD – Inorganic Crystal Structure Data Base). The determination of amorphous content of a sample with Rietveld refinement is possible by addition of a crystalline standard phase. An internal standard is mixed with the sample after the grinding. The interpretation and quantitative analysis of the collected data were carried out by means of the High Score + Software using the ICDD PDF 4+ database version: 2013 and the ICSD database version: 2007. The quantitative content was calculated using the Rietveld method.

### 3.5.3 Water Analysis

Fourteen (14) water samples were collected, one from each of the fourteen fields of mud volcanoes. The water samples for cationic analysis were acidified to pH 2 with concentrated nitric acid at the point of collection. The samples were adequately labelled and refrigerated prior to analysis. The temperature, pH, total dissolved solids (TDS) and electrical conductivity (EC) were measured in the field and compared with the analysed physical parameters of the water sample. Analysis of collected samples was done at the Centre of Research and Supervision of Underground Mining, Department of Environmental and Natural Disaster Study Ltd, Poland using ICP – OES method.

### 3.6 Statistical Data Evaluation/ Processing

Results of the granulometric analysis carried out in the laboratory were interpreted using the cumulative frequency curves. From the cumulative frequency curves, critical percentiles (Φ5, Φ16, Φ25, Φ50, Φ75, Φ84 and Φ95) were obtained and used in the calculation of grain size parameters such as; graphic mean, sorting (graphic standard deviation), graphic skewness and graphic kurtosis; the results of these parameters for each of the samples were tabulated in chapter five. The formulae for calculating these parameters after Folk and Ward (1957) are shown below;

**Graphic Mean (M)**

$$\text{Mean } (\mu) = \frac{\phi 16 + \phi 50 + \phi 84}{3} \quad - - - \quad (1)$$

This is the measure of the average grain size diameter of the sediments. Table 3 below shows the values and corresponding interpretations of the graphic mean according to Folk and Ward (1957);

**Table 4: Interpretation scale of graphic mean (μ).**

| **ϕ scale** | **Interpretation** |
|---|---|
| - 1.0 to 0.0 | Very coarse sand |
| 0.0 to 1.0 | Coarse sand |
| 1.0 to 2.0 | Medium sand |
| 2.0 to 3.0 | Fine sand |
| 3.0 to 4.0 | Very fine sand |
| 4.0 to 5.0 | Coarse silt. |

**Graphic Standard Deviation (Sorting) (δ)**

$$\text{Standard Deviation } (\sigma) = \frac{\phi 84 - \phi 16}{4} + \frac{\phi 95 - \phi 5}{6.6} \quad - - - \quad (2)$$

This is a measure of degree spread of grain sizes about the mean and corresponds with the standard deviation. The values for sorting and their corresponding interpretations according to Fold and Ward (1957) are given in Table 5.

**Table 5: Interpretation scale for Graphic Sorting (δ)**

| ϕ scale | Interpretation |
|---|---|
| < 0.35 | Very well sorted (VWS) |
| 0.35 to 0.50 | Well sorted (WS) |
| 0.50 to 0.71 | Moderately well sorted (MWS) |
| 0.71 to 1.00 | Moderately sorted (MS) |
| 1.00 to 2.00 | Poorly sorted (PS) |
| 2.00 to 4.00 | Very poorly sorted (VPS) |
| >4.00 | Extremely poorly sorted (EPS) |

**Graphic Skewness (ski)**

$$\text{Skewness (Ski)} = \frac{\phi 84 + \phi 16 - 2\phi 50}{2(\phi 84 - \phi 16)} + \frac{\phi 95 + \phi 5 - 2\phi 50}{2(\phi 95 - \phi 5)} \quad (3)$$

This is a measure of bias in the grain size distribution either towards the coarser or finer grained end of the size range. Positively skewed samples have an excess of fine grains, negatively skewed samples have an excess of coarse grains. The values for skewness and their corresponding interpretations according to Folk and Ward (1957) are given in Table 6.

**Table 6: Interpretation scale of graphic skewness (Ski)**

| ϕ scale | Interpretation |
|---|---|
| > 0.30 | Strongly fine-skewed |
| 0.30 to 0.10 | Fine-skewed |
| 0.10 to - 0.10 | Near symmetrical |
| -0.10 to -0.30 | Coarse-skewed |
| > -0.30 | Strongly coarse-skewed |

**Graphic Kurtosis (Kr)**

$$\text{Kurtosis (Kr)} = \frac{\phi 95 - \phi 5}{2.44(\phi 75 - \phi 25)} \quad - \quad - \quad - \quad (3)$$

This is a measure of flatness of the grain size distribution as it would appear on a simple frequency curve. Flat distributions are platykurtic and peak distributions are leptokurtic. The values for kurtosis and their corresponding interpretations according to Folk and Ward (1957) are shown in Table 7.

**Table 7: Interpretation scale of graphic kurtosis (KG)**

| **ϕ scale** | **Interpretation** |
|---|---|
| <0.67 | Very platykurtic |
| 0.6 to 0.9 | Platykurtic |
| 0.9 to 1.11 | Mesokurtic |
| 1.11 to 1.50 | Leptokurtic |
| 1.50 to 3.00 | Very leptokurtic |
| > 3.00 | Extremely leptokurtic |

Piper diagram and Schoeller diagram are graphical presentation of hydrochemical date with resulting interpretation. The major ions concentration in milligrams per litre was converted to mili – equivalent per litre (meq/l) and used in plotting the Piper trilinear diagram (Piper, 1944) and Schoeller diagram (Schoeller, 1964). Statistical correlation analysis was used to show the correlation between these parameters; Na, K, Ca, Mg, Fe, Cl, $HCO_3$, $CO_3$, $SO_4$ and $SiO_2$

# CHAPTER FOUR

# RESULTS

## 4.1 Geology of the Sorrounding Area of Mud Volcanoes

The geological map of the area is shown in Figure 17 and is composed dominantly of the Late Cretaceous Succession comprising of the Upper Bima Formation, the Yolde Formation, the Kanawa Member of Pindiga Formation and volcanic basalt. The geological map produced for the study area is an integration of those previous ones of Benkhelil, (1986), Guiraud, (1989) and Zaborski *et al.*, (1998).

### 4.1.1 Stratigraphy of the study area

**Upper Bima Formation:** The Upper Bima Formation outcrops in about 25% of the area of occurrence of mud volcanoes and covers the central, north-eastern and the southern parts. This unit is characterised by gently undulating and flat plains in topography. Towards the south of Todi, the Upper Bima Formation is characterized by tabular cross-bedded sandstone with sets that are a few tens of centimetres to a few metres thick (Plate 3). In hand specimen, the sandstone is fairly homogeneous, relatively mature, greyish in colour, medium to coarse grained quartz arenite, having angular to sub - angular grains. The sandstone is predominantly quartz with little feldspars and iron oxide resulting from weathering activities.

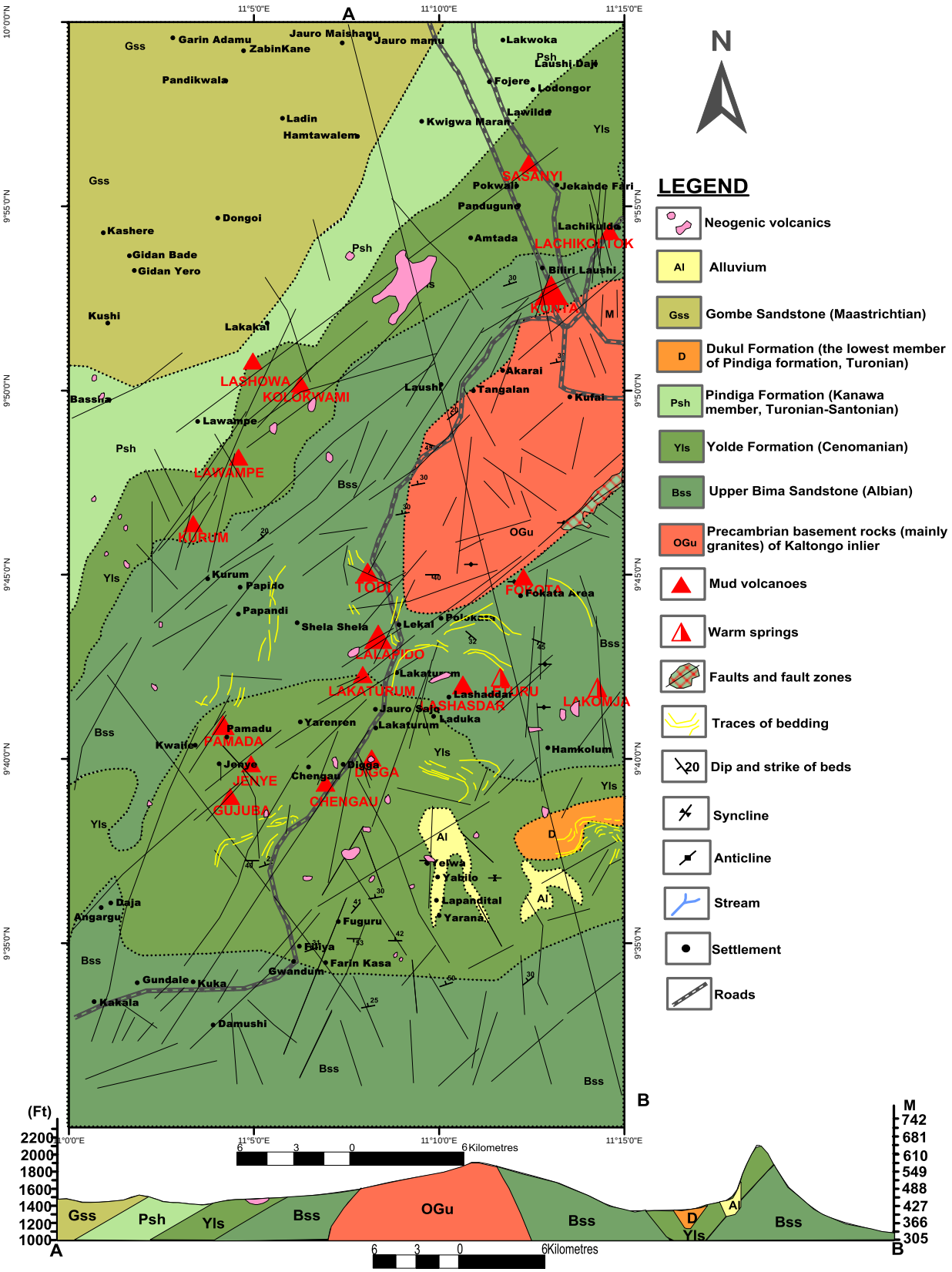



Figure 17: The geological map of the area of occurrence of mud volcanoes (modified after Benkhelil, (1985) with the boundaries adjusted and mud volcanoes located on the map by the present author.



Plate 2: An outcrop of Upper Bima Sandstone (B 3) at south of Todi village (N09$^0$44’ 58.1” and E11$^0$ 07’54.5”).




Plate 3: An outcrop of Upper Bima Sandstone (B 3) at south of Todi village showing tabular cross-bedding (N09$^0$44’ 58.6” and E11$^0$ 07’50.9”).

**Yolde Formation:** The Yolde Formation constitutes more than half of the area of occurrence of mud volcanoes and its outcropping in the central, north eastern and southern portions. This unit is generally characterised by gently undulating topography often with sparse vegetation. They are poorly consolidated, fine to medium - grained, moderately sorted, sub-rounded feldspartic sandstone (Plate 4). The Yolde Formation shows convolute bedding (Plate 5) formed by tectonic activity on soft sediments deposited prior to lithification.

**Pindiga Formation (Kanawa Member):** The Kanawa Member of the Pindiga Foramtion constitutes less than 25% of the area of occurrence of mud volcanoes and is outcropping in the north-western portion. This unit usually forms flat topography, characterized by outcrops of dark clay with beds of fossiliferous limestone (Plate 6). Most often, the upper surfaces of the limestone shows Thalassinoides burrows (Plate 7).

**Volcanic Basalts:** There are dark coloured, fine crystalline igneous rocks (basalts) that intruded into the Bima Formation and Yolde Formation in most cases. In topography, they form prominent hills in the study area and are of Neogene to Quaternary age (Plate 8).



Plate 4: Yolde Formation at Kurum showing flat lying outcrop of fine grained sandstone ($N9^0$46' 09.4" and $E11^0$ 04'04.1")




Plate 5: Yolde Formation at Lakaturu showing convolute bedding ($N9^0$42' 12.0" and $11^0$07'42.7")



Plate 6: Kanawa Member of the Pindiga Formation at Kurum showing regoliths of fossiliferous limestones with ammonites very evident ($N09^{0}46^{'}15^{''}$ and $E011^{0}03^{'}4$')



Plate 7: Kanawa Member of the Pindiga Formation at Kurum showing intense bioturbation of *thalassinoids* ($N09^{0}46^{'}15^{''}$ and $E011^{0}03^{'}4$')




Plate 8: Olivine basalt at Pokata showing fine grained crystalline texture and dark colour

### 4.1.2 Geological Structures in the Study Area

The structures in the study area are shown in figure 18 and correspond to those of Benkhelil, (1986) and Guiraud (1989). The structures include faults and folds.

**Faults:** The prominent fault zone in the study area includes the major NE – SW trending Kaltungo lineament and other minor ones with similar trend. Additionally, other minor faults with different trend include N – S and NW –SE (Figures 18, 19 and 20) directions.

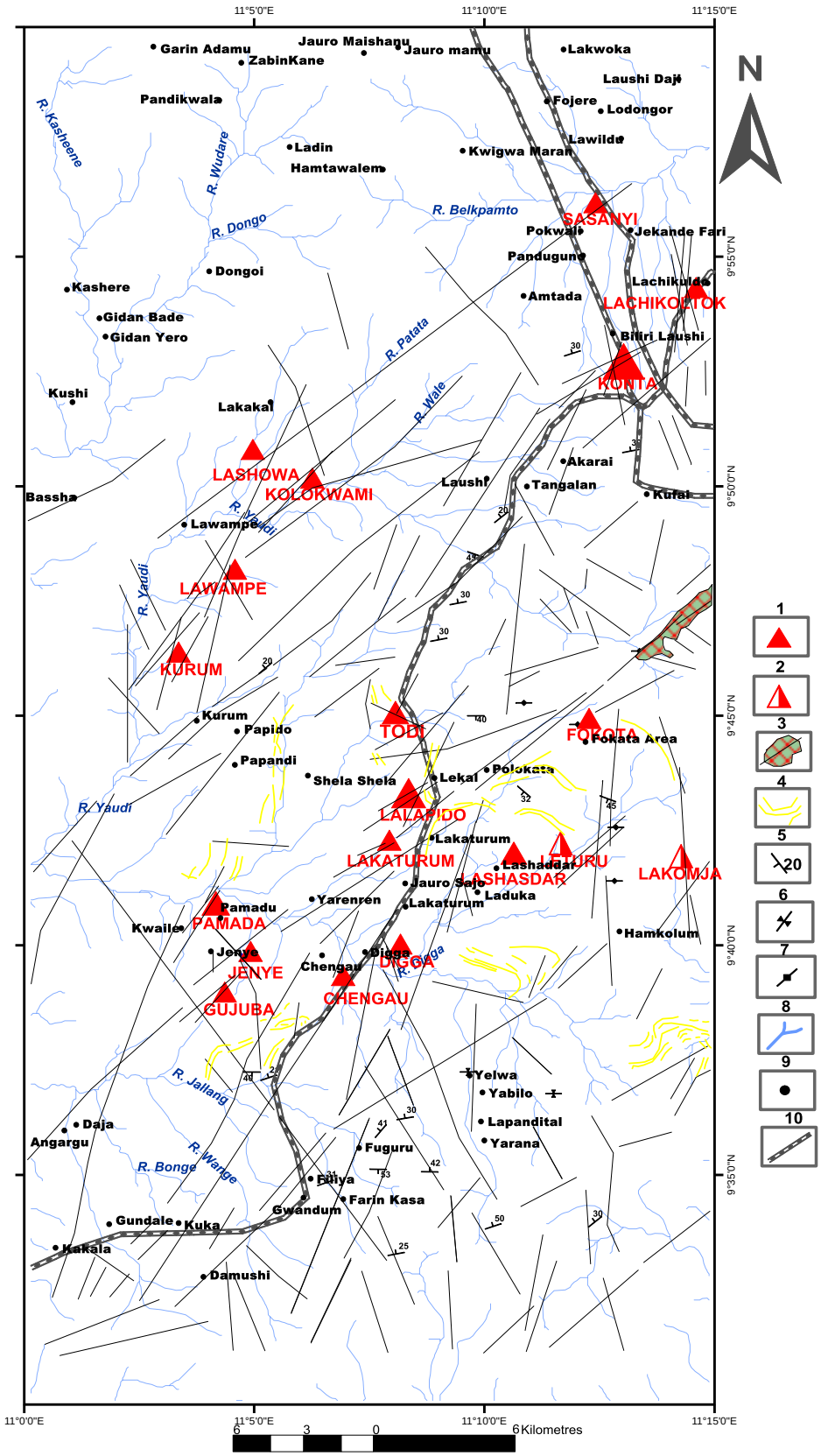



Figure 18: The structural map of the area of occurrence of mud volcanoes showing the location of mud volcanoes on faults (modified after Benkhelil, (1985) with mud volcanoes located on the map by the present author. Explanations: 1 - Mud volcanoes; 2 – Warm springs; 3 - faults and fault zones ; 4 - traces of beddings; 5 - Dip and Strike of beds; 6 – Syncline; 7 – Anticline; 8 – Stream; 9 - Settlements ;10 – Roads.

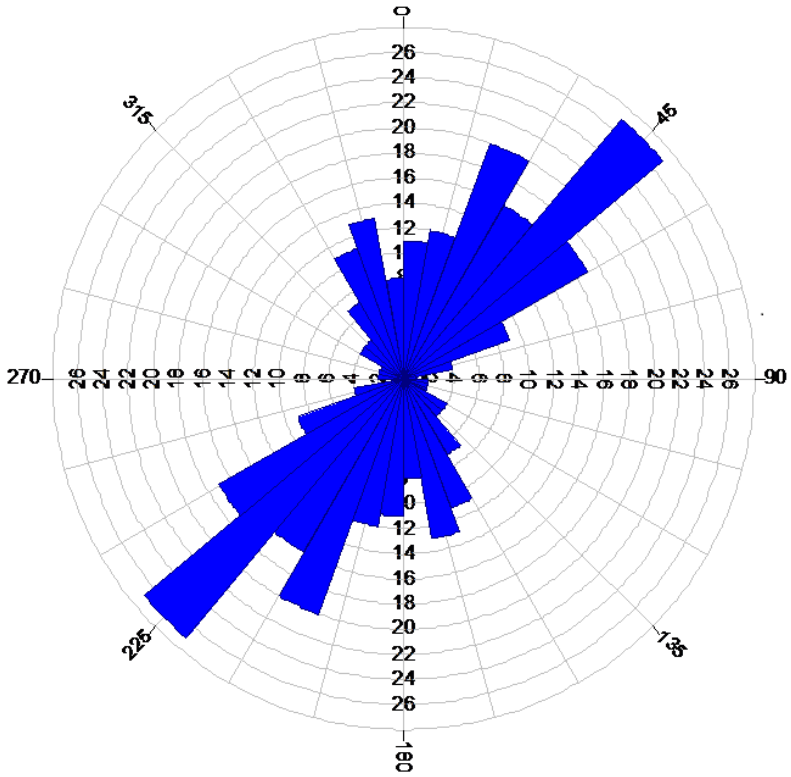



Figure 19: Rose diagram showing the trends of faults in the study area




Figure 20: Satellite image of the area showing mud volcanoes and the trends of some of the faults ($N9^{0}37^{'}13.5^{''}$ - $N9^{0}44^{'}20^{''}$ and $E11^{0}03^{'}35.5''$ - $E11^{0}14^{'}40''$) (modified from Google Earth, (N.A.S.A)). 1 – field of mud volcanoes, 2 – minor faults, 3 – Major faults 4 – dip of bedding

**NE – SW Faults:** The group of NE – SW faults is the dominant type with the Kaltungo lineament being the most prominent. At Lallapido and Todi the fault is marked by a 2 metres shear zone, where bedding dips gently northeast, with the dip reoriented of up to 30° (Plates 9 and 10)**.**

**N – S Faults:** N – S faults occur as minor faults within the area of occurrence of mud volcanoes, with only a few of them clearly manifesting at Gujuba, Jenye and Pamadu within the Yolde Formation. These faults occur alongside the major NE – SW Kaltungo lineament in the study area. At Gujuba, within the Dadiya syncline, N – S trending fault terminates at an outcrop of a basaltic rock that occurs at the south of the syncline.

**NW – SW Faults:** These faults are noticeable mostly around Chengau, Lashadar and Lakaturu areas (Figures 18, 19 and 20) and also occur together with NE – SW faults.

**Folds:** Notable major fold in the area of occurrence of mud volcanoes is the Dadiya syncline having an axial trend of NE – SW with beds on both limbs dipping at $40^0$. At Gujuba, beds of the Yolde Formation within the dadiya syncline are strongly asymmetric and their steep dipping limbs are highly sheared, suggesting a control by a deep-seated fault trending N – S and NW - SE passing through the middle of the syncline (Figure 21).



Plate 9: A fault zone within the Upper Bima Formation at Lallapido Showing NE – SW trend ($N09^{0}43^{'}13^{''}$ and $E011^{0}08^{'}58^{''}$).



Plate 10: A fault zone within the Upper Bima Formation at Todi Showing NE – SW trend ($N09^{0}43^{'}13^{''}$ and $E011^{0}08^{'}58^{''}$).




Figure 21: Dadiya Syncline from satellite image (N9$^0$37$'$13.9$''$ - N9$^0$38$'$49$''$ and E11$^0$03$'$ 43.3$''$ - E11$^0$06$'$ 28.6$''$) (Google Earth image modified from NASA). 1 – Field of mud volcanoes 2 - fault, 3 – trough of the syncline, 4 – orientation of bed

## 4.2 Physical Characteristics of Onshore Mud Volcanoes in the Study Area

Physical characteristics of individual mud volcanoes in each of the field were studies and measurements were taken during the fieldwork as shown in appendix A. However, summary description of the physical characteristics of various mud volcanoes field putting into cosiderations the ranges was also done and presented in Table 8 below.

**Table 8: A description of the field of occurrences of the mud volcanoes and their associated geological formation in the study area**

| Field of mud volcanoes | Range of elevation (m.a.s.l) | Range of Temperature | Range of base diameter of cone (metres) | Range of height of cone (metres) | Ejected materials from the volcanoes | Geological formation |
|---|---|---|---|---|---|---|
| Lallapido | 348 to 404 | 24.3 to 26.7 | 0.4 to 3.5 | 0.0 to 0.9 | Mud slurry and water | Upper Bima Sandstone |
| Gujuba | 322 to 362 | 20.7 to 22.9 | 1.0 to 3.0 | 0.0 to 0.1 | Mud slurry and water | Yolde Formation |
| Jenye | 322 to 331 | 23.5 to 25.5 | 1.8 to 4.5 | 0.6 to 0.8 | Mud slurry and water | Yolde Formation |
| Pamadu | 305 to 336 | 21.1 to 25.6 | 2.0 to 8.0 | 0.2 to 0.6 | Mud slurry and water | Yolde Formation |
| Lashadar | 339 to 396 | 24.6 to 26.4 | 0.1 to 3.5 | 0.0 to 0.1 | Muddy water | Upper Bima Sandstone |
| Lakaturu | 339 to 350 | 23.0 to 26.9 | 0.5 to 2.5 | 0.2 to 0.4 | Mud slurry and water | Yolde Formation |
| Digga | 324 to 337 | 25.8 to 26.6 | 0.5 to 3.5 | 0.0 to 0.1 | reddish – brownish water | Yolde Formation |
| Kurum | 331 to 340 | 24.3 to 26.4 | 0.8 to 1.0 | 0.4 to 1.2 | Mud slurry and water | Yolde Formation |
| Lawampe | 343 to 345 | 24.5 to 24.9 | 5.0 to 4.0 | 0.0 to 0.1 | reddish – brownish water | Pindiga Formation |
| Kolokwami | 343 to 384 | 24.0 to 24.9 | 5.5 to 4.5 | 0.0 to 0.1 | Muddy water | Yolde Formation |
| Lashuwo | 356 to 375 | 23.3 to 23.8 | 0.5 to 1.0 | 0.0 to 0.0 | reddish – brownish water | Pindiga |
| Todi | 365 to 387 | 22.2 to 24.6 | 5.0 to 8.0 | 0.2 to 0.6 | Mud slurry and water | Upper Bima Sandstone |
| Konta | 492 to 496 | 23.4 to 23.7 | 6.0 to 8.0 | 0.0 to 0.0 | Water | Upper Bima Sandstone |
| Lachikoltok | 438 to 444 | 21.8 to 22.4 | 2.5 to 4.0 | 0.1 to 0.3 | Mud slurryand water | Yolde Formation |

The slurry of mud and water seeping from craters of the mud volcanoes was tasteless, consisting of clayey and sandy particles suspended in fresh or saline water. Their diameter at base varies from 0.1 m to 8 .0 m while their height varies from 0.0 m to 1.2 m. The temperature of atmospheric air, one metre above ground surface, at time of measurement varied from 27 $^{o}$C to 29$^{o}$C. The temperature of slurry 10 cm deep in the volcano neck varied from 20.7 $^{o}$C to 26.7 $^{o}$C (Table 8), most of the temperature measured within the neck of the volcano fell below local mean annual temperature ranges from 26$^{o}$C to 27$^{o}$C (Schoeneich and Garba, 2010) except to the two thermal warm springs with temperatures of 41.9 and 41.2 $^{0}$c. The prevailing form of ejection was a very slow continuous seepage of slurry, sometimes water. Some of the mud volcanoes were perennial, seeping out tasteless, fresh water and gritty clay slurry sometimes containing pebbles of host sandstones, at a rate of fraction of cubic centimetre per second.

Most of the mud volcanoes are concentrated along the NE – SW; NW – SE and N – S faults and are mostly situated on the Yolde Formation and Upper Bima Sandstone (Table 8). The mud volcanoes documented occurred in groups, further referred to as ‘’fields’’ with each field consisting of several individual mud volcanoes. There are about 14 fields of volcanoes. However, most of the mud volcanoes in fields 1 to 14 were seeping out mud slurry and very few were seeping out only water while some of them were dormant with dry crater. Descriptions of the characteristics of each of these fields are as follow:

## Lallapido Mud Volcanoes

In Lallapido, the mud volcanoes were confined to a small area of about 4.5 km². The field consists of 29 mud volcanoes out of which 19 were seeping out slurry of mud and water slowly from craters or having the slurry stagnant in the crater. The mud volcanoes are concentrated along the NE – SW trending fault situated on the Upper Bima Sandstone (Figure 22). The range of temperature at the neck of mud volcanoes at Lallapido was 24.3 to 26.7°C. In most of the mud volcanoes, the cones are of mud (clay and sand) and their diameter at base varies from 0.4 to 3.5 metres while their heights are less than 0.9 metres (Table 8). Typical examples of the mud volcanoes found at Lallapido are shown in Plate 11 to 14.

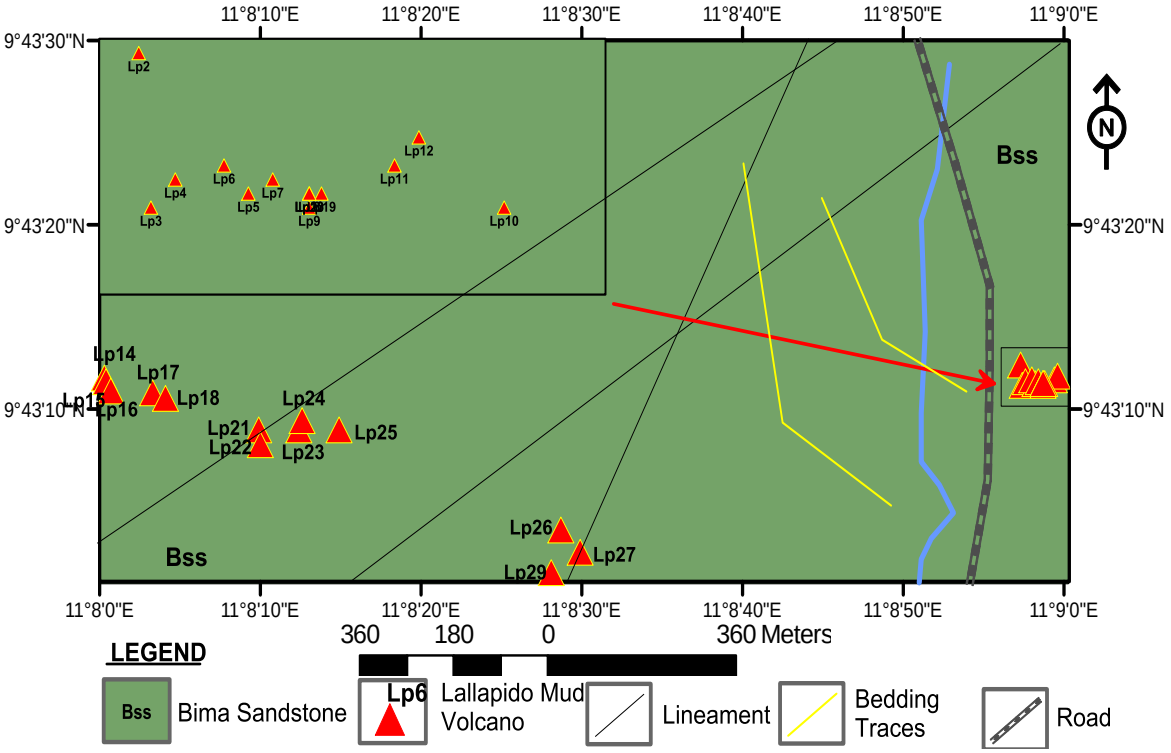



Figure 22: Lallapido mud volcanoes located by the author on the background of geological map by Benkhelil, (1985) with the mud volcanoes being located on or close to the NE – SW trending faults within the Bima Formation



Plate 11: A mud volcano occurrence at Lallapido, showing the angle of slope, fresh mud flowing from the crater and dry mud seen around the cone with precipitated salt ($N09^0$ 43' 11.4" and $E011^0$ 08' 58.9; photo taken: 16/02/12)



Plate 12: A mud volcano occurrence at Lallapido, small cone with fresh mud flowing from the crater ($N09^0$ 43' 12.4" and $E011^0$ 08' 57.4; photo taken: 16/02/12)



Plate 13: A mud volcano occurrence at Lallapido, showing the angle of slope, dry mud and fresh mud flowing from the crater (N09$^0$ 43’ 11.3” and E011$^0$ 08’ 57.5; photo taken: 16/02/12)



Plate 14: A mud volcano occurrence at Lallapido, showing the angle of slope, with fresh mud flowing from the crater and dry mud with precipitated salt seen around the crater and temperature being measured at the neck of the volcanoe (N09$^0$ 43’ 11.5” and E011$^0$ 08’ 57.7; photo taken: 16/02/12)

**Gujuba Mud Volcanoes**

The field at Gujuba consists of twelve (12) mud volcanoes. The Gujuba field covers an area of about 3 km². All the mud volcanoes documented at Gujuba were seeping out water slowly from craters. Slurry seeping from craters was tasteless, consisting of clayey particles and sand suspended in fresh water with precipitated salt noticed on the cone. The Gujuba mud volcanoes are concentrated along the NE – SW; NW – SE and N – S faults and are situated on the Yolde Formation (Figure 23). The range of temperature at the neck of mud volcanoes at Gujuba was 24.3 to 26.7°C. Their diameter at base of the mud volcanoes varies from 1.0 m to 3.0 m while their heights are less than 0.1 m (Table 8). Typical examples of the mud volcanoes found at Gujuba are shown in Plate 15 to 18.

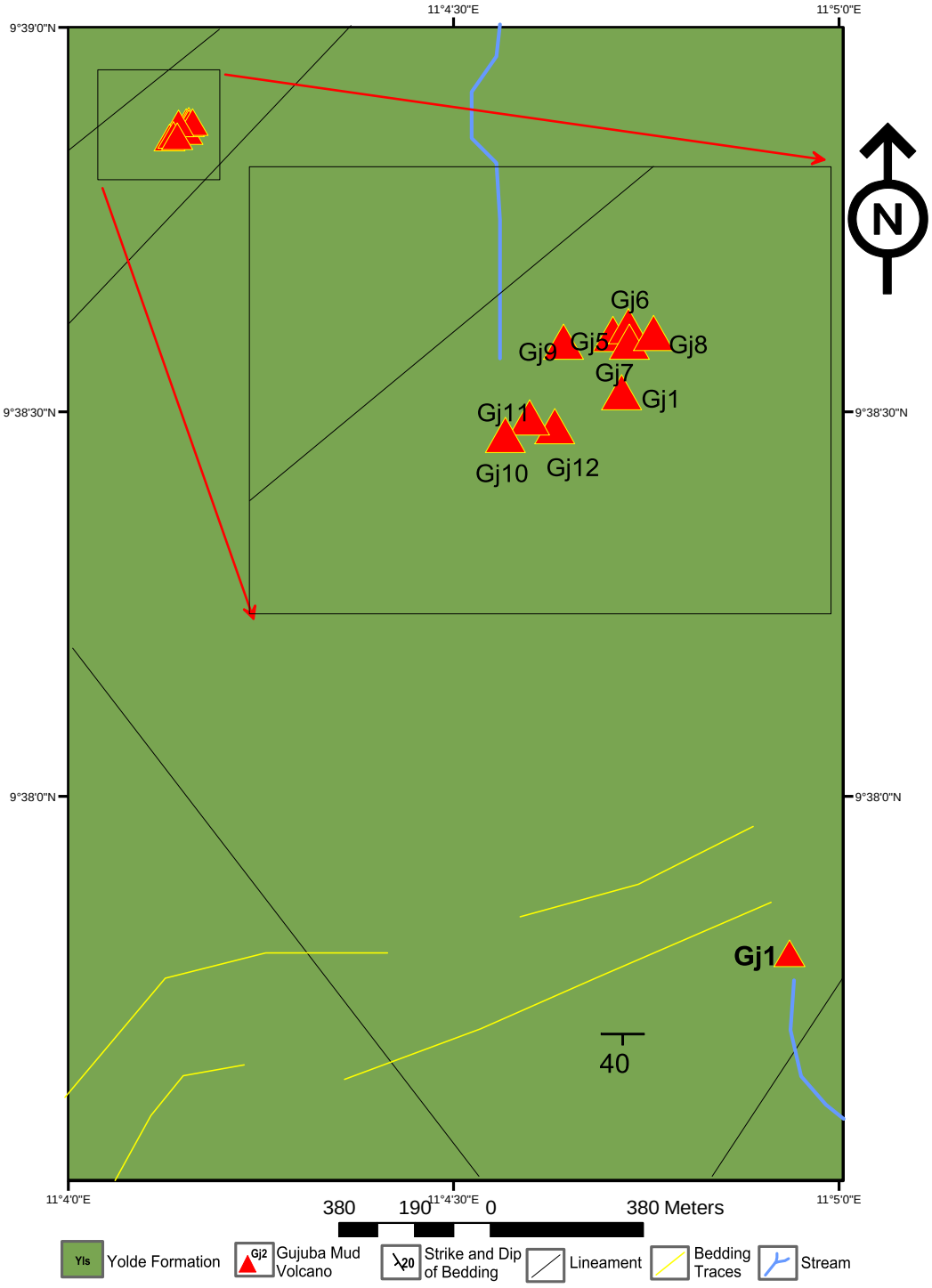



Figure 23: Gujuba mud volcanoes located by the author on the background of geological map by Benkhelil, (1985) with the mud volcanoes being located on or close to the NE – SW and NW – SE trending faults within the Yolde Formation



Plate 15: A mud volcano at Gujuba with slurry of mud and water seeping from the crater with whitish precipitates seen around the crater at Gujuba (N09$^0$37’47.9”, E011004’56.3”; photo taken: 17/02/12)



Plate 16: A mud volcano at Gujuba with slurry of mud and water seeping from the crater with whitish precipitates seen around the crater at Gujuba (N09$^0$38’51.9” E011$^0$04’09.3”; photo taken: 17/02/12)



Plate 17: A mud volcano at Gujuba with slurry of mud and water seeping from the crater with whitish precipitates seen around the crater at Gujuba (N09$^0$42’52.1” E011$^0$07’09.3”; photo taken: 17/02/12)



Plate 18: A mud volcano at Gujuba with slurry of mud and water seeping from the crater with whitish precipitates seen around the crater (N09$^0$42’52.2” E011$^0$07’09.2”; photo taken: 17/02/12)

**Jenye Mud Volcanoes**

The Jenye field covers an area of about 3 km². Overall, it comprises of 11 mud volcanoes in which, all of them were seeping out slurry of mud and water from the crater. The Jenye mud volcanoes are concentrated along NE – SW and NW – SE faults, and are situated on the Yolde Formation (Figure 24). In most of the volcanoes, the cones are of mud (clay, and sandy). The range of temperature at the neck of mud volcanoes at Jenye was 23.5 to 25.5°C. Their diameter at base varies from 1.8 to 4.5 metres while their height varies from 0.6 to 0.8 metres (Table 8). Typical examples of the mud volcanoes found at Jenye are shown in Plate 19 to 22.

Also, very intriguing during the course of the fieldwork was a cow that came to lick the precipitated salt from the mud volcanoes at Jenye which got stuck, and was rescued by the research team as shown in Plate 22.

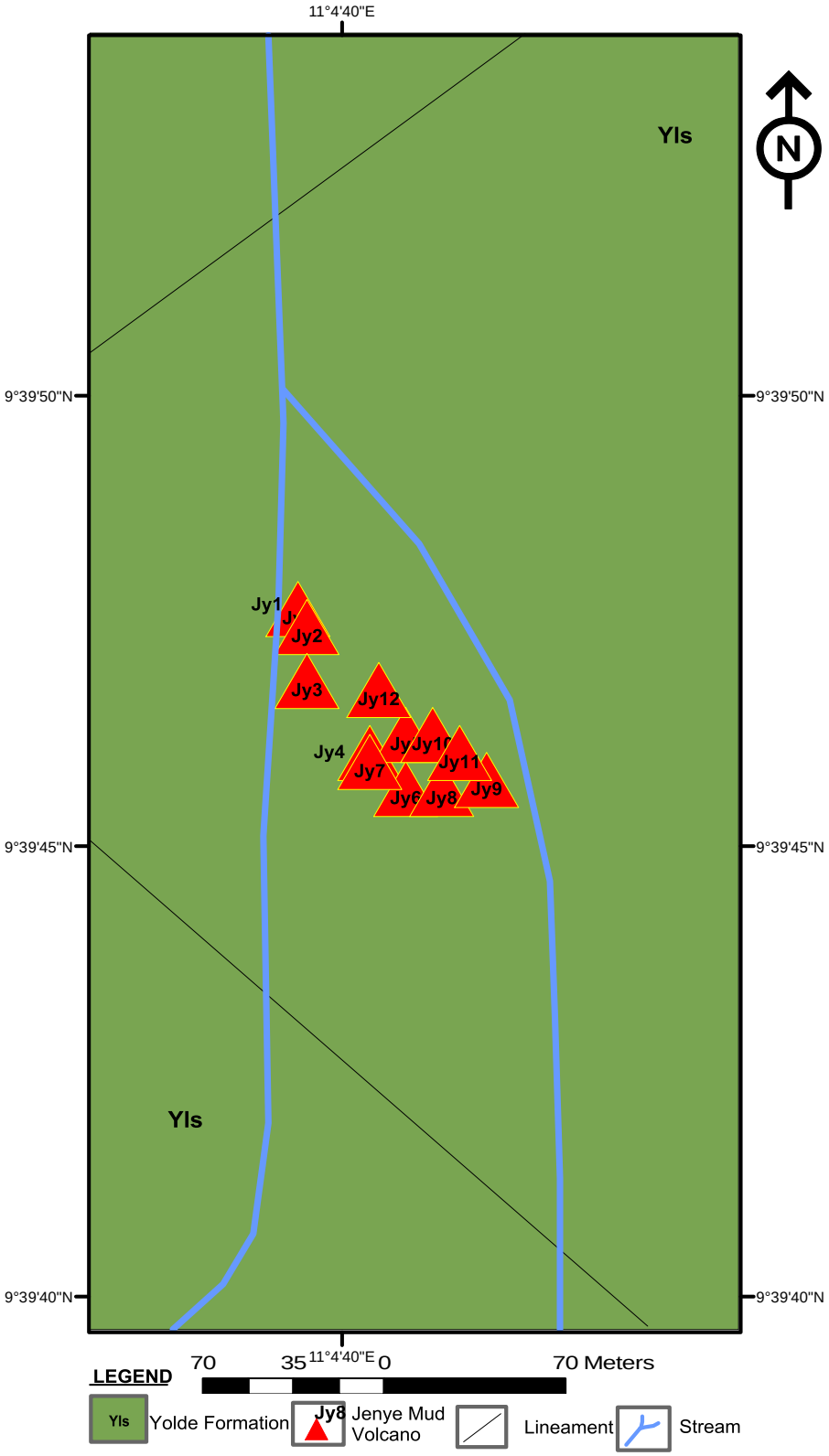



Figure 24: Jenye mud volcanoes located by the author on the background of geological map by Benkhelil, (1985) with the mud volcanoes being located between the NE – SW and NW – SE trending faults within the Yolde Formation



Plate 19: A mud volcano at Jenye with slurry of mud and water seeping from the crater with whitish precipitates and grasses seen around the crater (N09$^0$39’47.6” E011$^0$04’39.5”; photo taken: 17/02/12)



Plate 20: A mud volcano at Jenye with slurry of mud and water seeping from the crater with whitish precipitates and grasses seen around the crater (N09$^0$39’47.4” E011$^0$04’39.6”; photo taken: 17/02/12)



Plate 21: A mud volcano at Jenye with slurry of mud and water seeping from the crater with grasses and precipitated salt seen around the crater (N09$^0$39’46.8” E011$^0$04’39.6”; photo taken: 17/02/12)



Plate 22: A Cow being rescued from a mud volcano at Jenye, The cow came to the mud volcano to lick the salt (N09$^0$39’46.2” and E011$^0$04’41.0”; photo taken: 17/02/12)

**Pamadu Mud Volcanoes**

The Pamadu mud volcanoes field covers an area of about 4.5 km². There are 27 mud volcanoes at Pamadu, out of which 23 of the mud volcanoes at the time of measurement were seeping out mud slurry from their crater; one volcano was seeping out only water from its crater while one of the mud volcanoes was dormant and inactive. The Pamadu mud volcanoes are concentrated along faults trending NE – SW situated on the Yolde Formation (Figure 25). The range of temperature at the neck of mud volcanoes at Pamadu was 21.1 to 25.6°C while the mud volcanoes cone is of height 0.2 to 0.6 metres and diameter at base 2.0 to 8.0 metres (Table 8 and 9). Typical examples of the mud volcanoes found at Pamadu are shown in Plate 23 to 26.

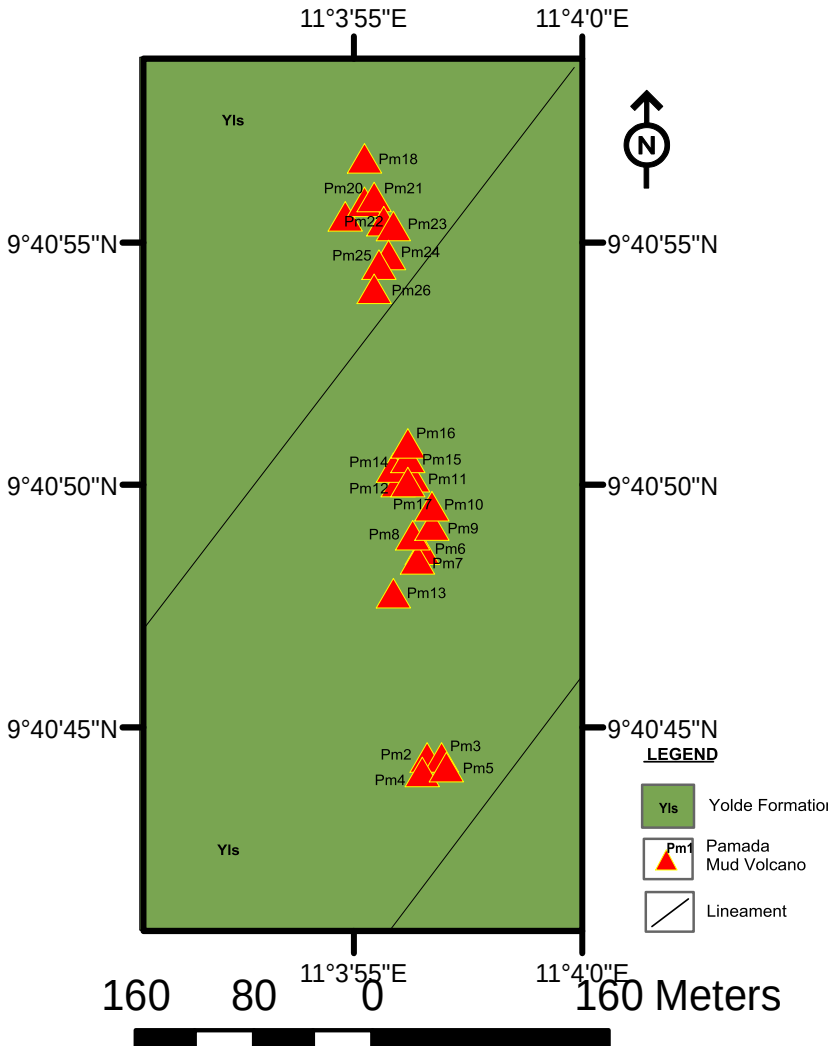



Figure 25: Pamadu mud volcanoes located by the author on the background of geological map by Benkhelil, (1985) with the mud volcanoes being located on or close to the NE – SW trending faults within the Yolde Formation



Plate 23: A mud volcano at Pamadu with slurry of mud and water seeping from the crater with whitish precipitates seen around the crater (N09$^0$39’46.7” E011$^0$04’40.4”; photo taken: 18/02/ 2012)



Plate 24: A mud volcano at Pamadu with slurry of mud and water seeping from the crater with whitish precipitates seen around the crater (N09$^0$40’44.4” E011$^0$04’56.5”; photo taken: 18/02/ 2012)



Plate 25: A mud volcano at Pamadu with slurry of mud and water seeping from the crater with whitish precipitates seen around the crater (N09$^0$40’44.2” E011$^0$03’56.6”; photo taken: 18/02/ 2012)



Plate 26: A mud volcano at Pamadu with slurry of mud and water seeping from the crater with whitish precipitates seen around the crater (N09$^0$40’49.0” E011$^0$03’55.9”; photo taken: 18/02/ 2012)

## Lashadar Mud Volcanoes

The Lashadar field covers an area of about 3 km². There are eleven (11) mud volcanoes that were observed during the course fieldwork out of which, ten were seeping out little slurry of mud and water. The Lashadar mud volcanoes are concentrated along NE – SW trending fault within the Upper Bima Sandstone (Figure 26). The range of temperature at the neck of mud volcanoes at Lashadar was 24.6 to 26.4°C. As shown in Plate 66, the mud volcanoes are mostly of height 0.1 meters and diameter at base ranges from 0.1 to 3.5 meters (Table 8). Typical examples of the mud volcanoes found at Lashadar are shown in Plate 27 to 30.

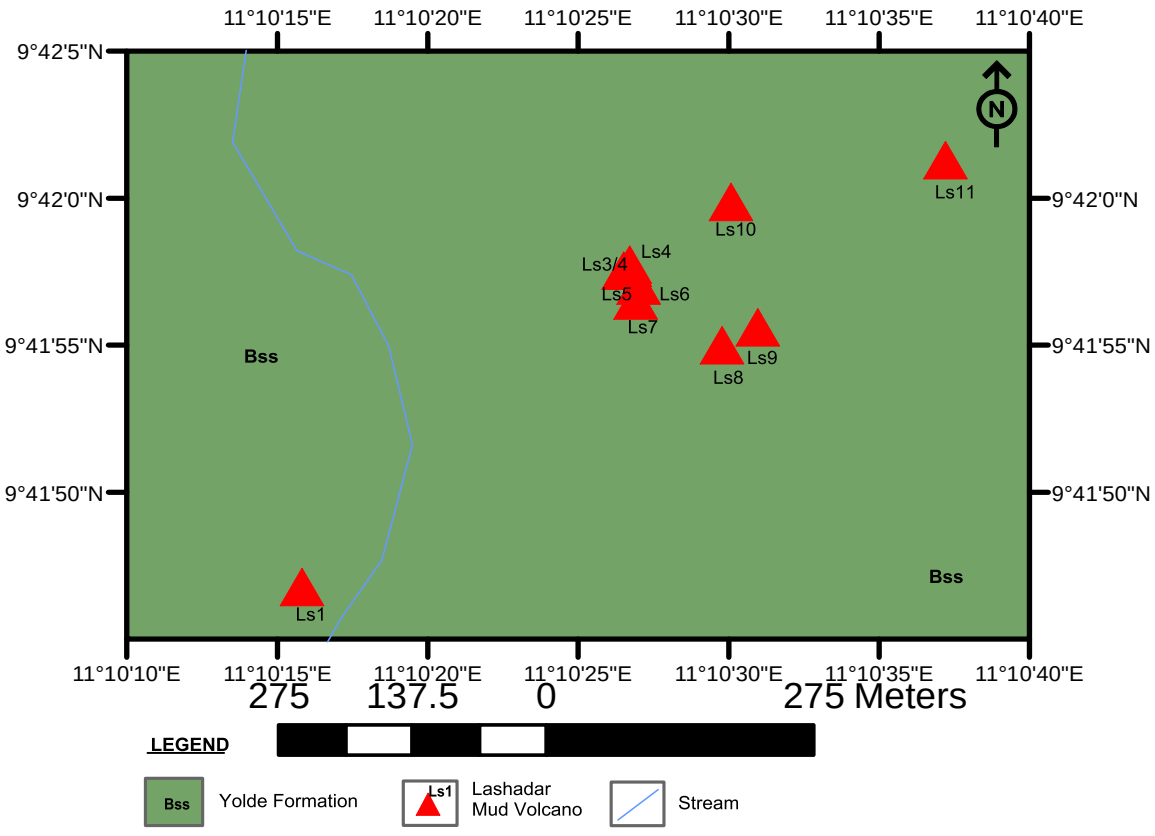



Figure 26: Lashadar mud volcanoes located by the author on the background of geological map by Benkhelil, (1985) with the mud volcanoes being located close to s stream trending N –S the Upper Bima Sandstone



Plate 27: A mud volcano at Lashadar with slurry of mud and water seeping from the very tiny crater with precipitated salt seen around the crater (N09$^0$41’47.5” EO11$^0$10’15.6”; photo taken: 19/02/2012)



Plate 28: A mudvolcano at Lashadar with slurry of mud and water seeping from the tiny crater and whitish precipitates seen around the crater (N09$^0$41’58.1” EO11$^0$10’26.6”; photo taken: 19/02/2012)



Plate 29: A mud volcano at Lashadar with little dry slurry of mud around the crater and water seeping in the crater (N09$^0$41’58.1” EO11$^0$10’26.4”; photo taken: 19/02/2012)



Plate 30: A mud volcano at Lashadar with slurry of mud and water seeping from the crater with whitish precipitates seen around the crater (N09$^0$41’58.3” EO11$^0$10’26.6”; photo taken: 19/02/2012)

## Lakaturu Mud Volcanoes

The Lakaturu field covers an area of about 3 $km^2$, having a total of 15 mud volcanoes, out of which 13 were seeping out mud slurry from their craters, one volcano was seeping out water while one was dormant in the course of the fieldwork. As shown Figure 27, the Lakaturu mud volcanoes are concentrated along NE – SW, situated on the Yolde Formation and the range of temperature at the neck of mud volcanoes at Lakaturu was 23.0 to 26.9 °C, the mud volcanoes cone are of height 0.2 to 0.4 meters and diameter at base 0.5 to 2.5 meters (Table 8). Typical examples of the mud volcanoes found at Lakaturu are shown in Plate 31 to 34. Mud volcanoes can be dangerous as it only takes few seconds for animals (including humans) to be sunk. Plate 34 shows undergraduate student who was rescued from a mud volcano during the course of the fieldwork.

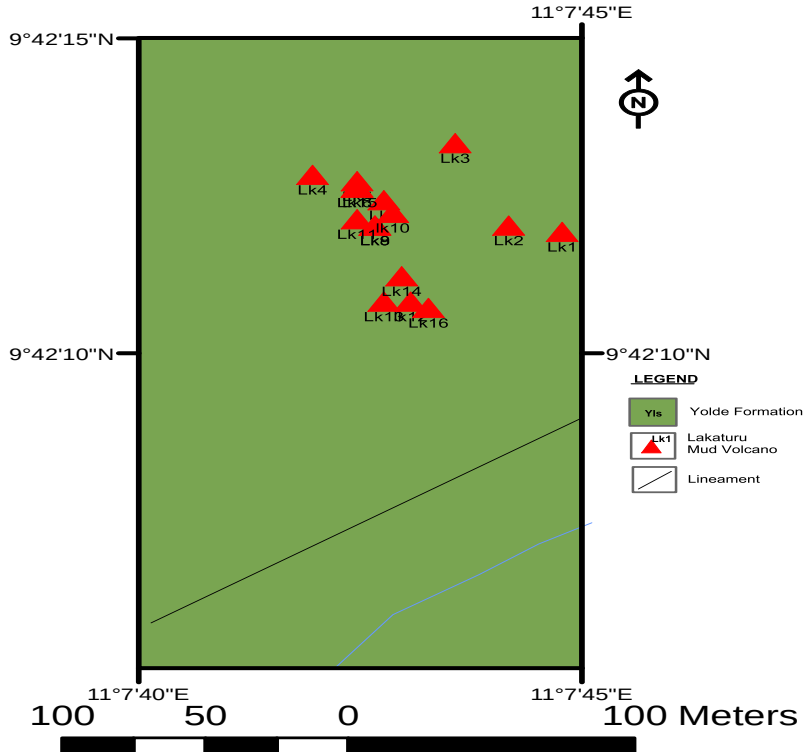



Figure 27: Lakaturu mud volcanoes located by the author on the background of geological map by Benkhelil,(1985) with the mud volcanoes being located on or close to the NE – SW trending faults within the Yolde Formation



Plate 31: A mud volcano at Lakaturu with slurry of mud and water seeping from the crater with precipitated salt seen around the crater (N09$^0$42’11.9” EO11$^0$07’44.8”; photo taken: 20/02/2012)



Plate 32: A mud volcano at Lakaturu with slurry of mud and water seeping from the crater with precipitated salt seen around the crater (N09$^0$42’11.9” EO11$^0$07’44.8”; photo taken: 20/02/2012)



Plate 33: A mud volcano at Lakaturu with slurry of mud and water seeping from the crater with precipitated salt seen around the crater(N09$^0$42’11.9” EO11$^0$07’44.8” ; photo taken: 20/02/2012**)**




Plate 34: The result of mistakenly stepping into the edge of a mud volcano at Lakaturu in Upper Benue Trough of Nigeria (Dry twigs are kept on the mud volcano by locals to prevent sinking of animals) (N09$^0$42’12.7” and E011$^0$07’42.5”; photo taken: 20/02/2012)

**Chengau Mud Volcano**

The Chengau occurrence has only one volcano of water variety (Plate 35). The range of temperature at the neck of mud volcanoes at Chengau was 26.4 to 26.4 °C. The diameter at the base of mud volcano cone varies from 1.0 m to 1.2 metres, height of the cones from 0.0 m. The cones, which is water saturated are so soft that it is not possible to stand on it.



Plate 35: Photograph of water volcano with the craters is seeping out brownish – reddish water and grasses are sparsely found on top of the cone with precipitated salt seen around the cone at Chengau (N09$^0$39'17.8" E011$^0$06'40.3" ; photo taken: 20/02/2012)

**Digga Mud Volcanoes**

The Digga field covers an area of about 3.6 km², having 6 mud volcanoes, out of which five were seeping out reddish – brownish water from the crater. Only one of the mud volcanoes was seeping out slurry of mud and water from the crater. As shown in Figure 28, the Digga mud volcanoes are concentrated along faults trending NW – SE within the Yolde Formation and The range of temperature at the neck of mud volcanoes at Digga

was 24.6 to 26.4°C. The diameter at the base of cone varies from 0.5 to 3.5 metres; heights are less than 0.1 meters (Table 8). Typical examples of the mud volcanoes found at Digga are shown in Plate 36 to 37.

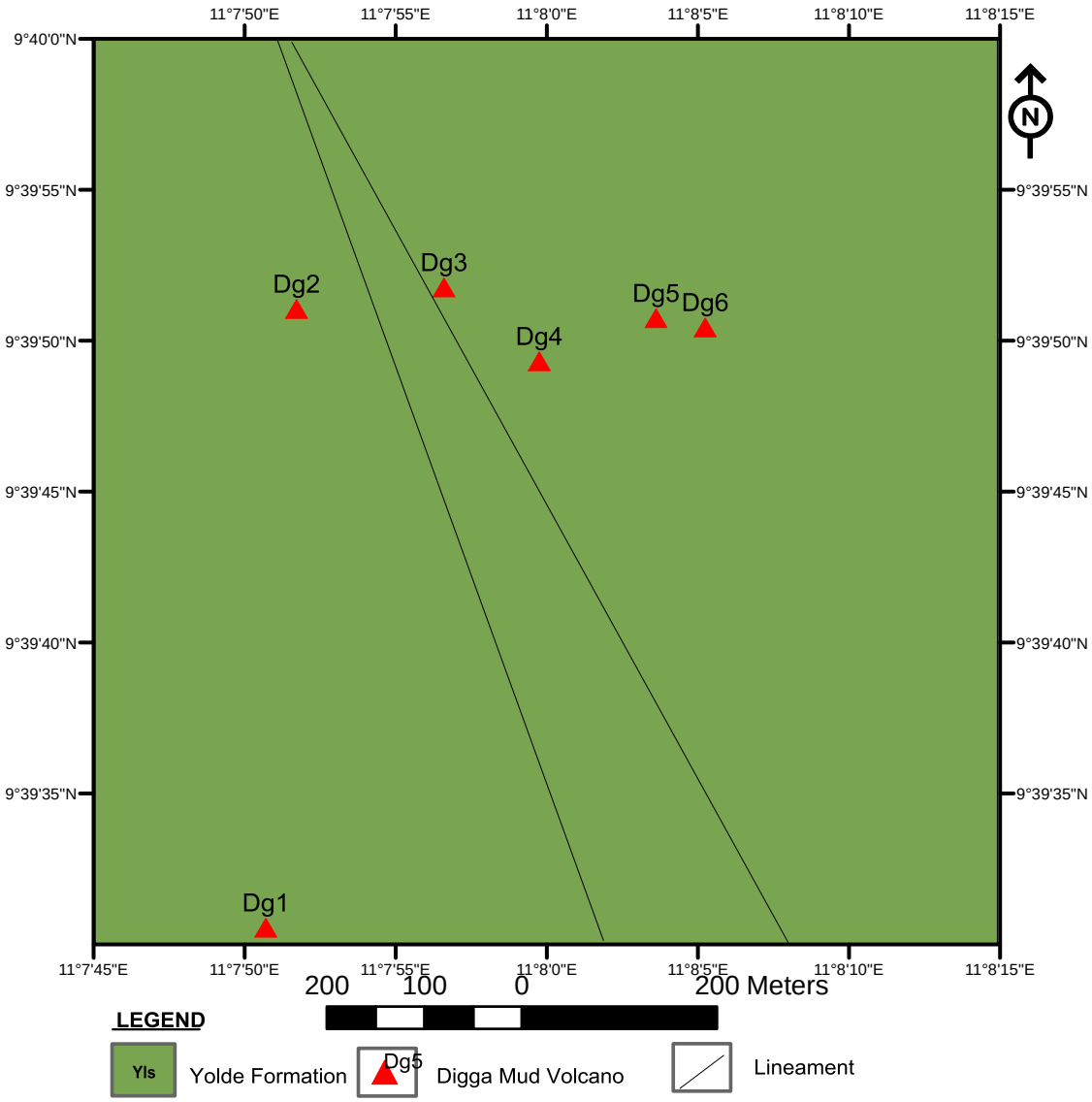



Figure 28: Digga mud volcanoes located by the author on the background of geological map by Benkhelil, (1985) with the mud volcanoes being located on or close to the NW – SE trending faults within the Yolde Formation



Plate 36: A volcano of water variety seeping out water of brownish – reddish colour from the crater with grasses and precipitated salt seen around the crater at Digga (N09$^0$39’31.2” E011$^0$07’50.6” ; photo taken: 20/02/2012)



Plate 37: A volcano of water variety seeping out water of brownish – reddish colour from the crater with grasses and precipitated salt seen around the crater at Digga(N09$^0$39’51.3” E011$^0$07’51.6” ; photo taken: 20/02/2012)

## Kurum Mud Volcanoes

The Kurum field were confined to a small area of about 4500 m². Twenty mud volcanoes were observed in the course of the fieldwork. All of them were seeping out slurry of mud from their craters. The Kurum mud volcanoes are concentrated along faults trending NE – SW situated on the Yolde Formation (Figure 29). The range of temperature at the neck of mud volcanoes at Kurum was 24.3 to 26.4°C and mud cone of height 1.2 metres and diameter at base 0.8 to 1.0 metres (Table 8). Typical examples of the mud volcanoes found at Kurum are shown in Plate 38 to 41. Villagers make what they call "potash" after filtering the precipitated salt from the mud volcanoe at Kurum as shown in Appendix B.

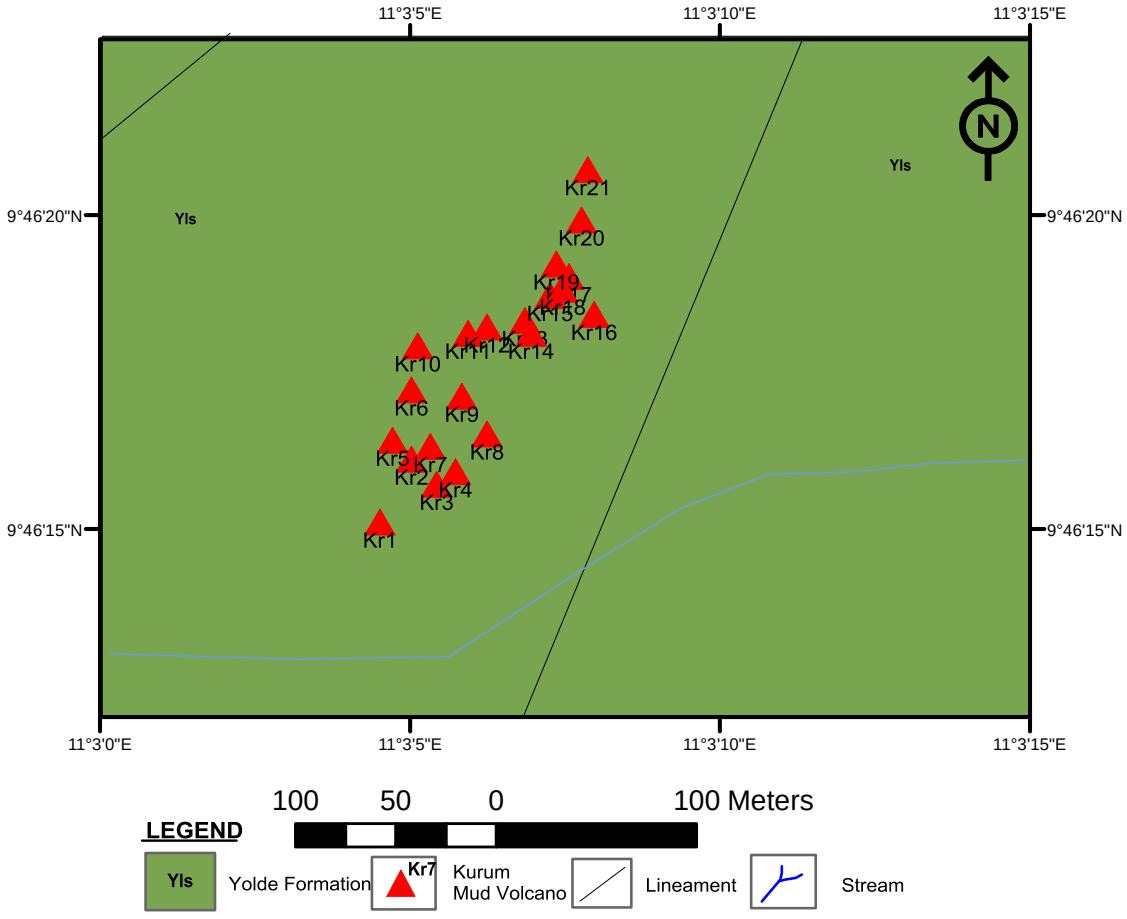



Figure 29: Kurum mud volcanoes located by the author on the background of geological map by Benkhelil, (1985) with the mud volcanoes being located on or close to the NE – SW trending faults within the Yolde Formation



Plate 38: A mud volcano at Kurum with slurry of mud and water seeping from the crater with cracks of dry mud and precipitated salt seen around the crater (N09$^0$46’15.1” E011$^0$03’04.4”; photo taken: 21/02/2012)



Plate 39: A mud volcano of two craters at Kurum with slurry of mud and water seeping from the craters and precipitated salt seen around the crater (N09$^0$46’16.1” E011$^0$03’04.9”; photo taken: 21/02/2012)



Plate 40: A volcano of water variety at Kurum with water seeping from the crater (N09$^0$46'15.7" E011$^0$03'05.3"; photo taken: 21/02/2012)



Plate 41: A mud volcano at Kurum with slurry of mud and water seeping from the crater with precipitated salt seen around the crater (N09$^0$46'15.9" E011$^0$03'05.6"; photo taken: 21/02/2012)

## Lawampe Mud Volcanoes

The Lawampe field is confined to a small area of about 1 km², having 3 mud volcanoes which are found arranged along a stream trending NW – SE situated at the boundary between Yolde Formation and the Pindiga Formation (Figure 30). In the course of the fieldwork, the mud volcanoes were active with slurry of mud and water seeping out of the crater, however, in some of them, activity of the seepage of slurry was overtaken by the seeping out of only reddish water on which grasses have grown on the mud (Plate 42). The range of temperature at the neck of mud volcanoes at Lawampe was 24.5 to 24.9°C, and the cone is of heights are less than 0.1 metres and diameter at base 5.0 - 4.0 metres as shown on (Table 8).

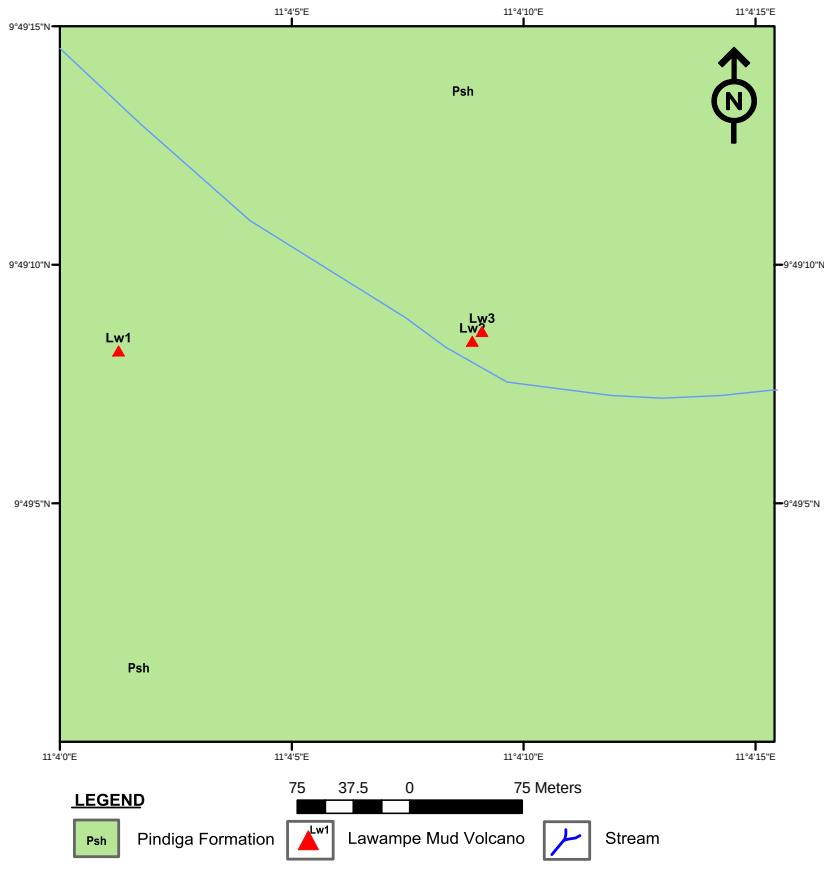



Figure 30: The Lawampe mud volcanoes located by the author on the background of geological map by Benkhelil, (1985) with the volcanoes of water variety being located close to a stream within the Pindiga Formation



Plate 42: A mud volcano at Lawampe with slurry of mud and water seeping from the crater with grasses and precipitated salt seen around the crater (N09$^0$49'08.3" E011$^0$04'01.2"; photo taken: 21/02/2012)

**Kolokwami Mud Volcanoes**

The Kolokwami field are confined to a small area of about 1.5 km². There are four (4) individual mud volcanoes. The Kolokwani mud volcanoes are concentrated along faults trending NW – SE situated on Yolde Formation (Figure 31). The range of temperature at the neck of mud volcanoes at Kolokwami was 24.0 to 24.9°C, and the cone is of height less than 0.1 metres and diameter at base 5.5 to 4.5 metres (Table 8). They were active with slurry of mud and water seeping out of the crater and in one, the activity of the seepage of slurry was overtaken by the seeping out of only reddish water on which grasses have grown on the volcano (Plate 43).

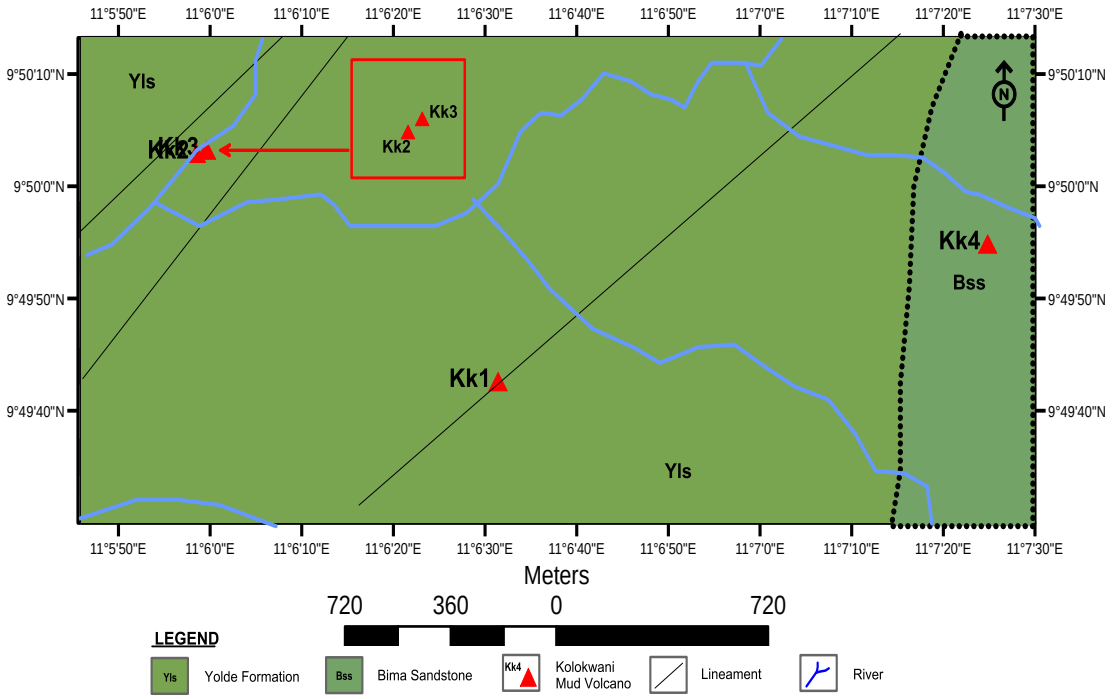



Figure 31: Kolokwani mud volcanoes located by the author on the background of geological map by Benkhelil, (1985) with the mud volcanoes being located on or close to the NE – SW trending faults within the Yolde Formation



Plate 43: A mud volcano at Kolokwami with slurry of mud and water seeping from the crater with grasses and precipitated salt seen around the crater (N09$^0$49'42.8" E011$^0$06'30.4"; photo taken: 21/02/2012)

## Lashuwo Mud Volcanoes

The Lashuwo field are confined to a small area of about 1.5 km². There are 2 volcanoes. The Lashuwo volcanoes are found along a stream trending NE - SW situated on the Pindiga Formation (Figure 32). The range of temperature at the neck of mud volcanoes at Lashuwo was 23.3 to 23.8°C, which was below the atmospheric temperature of the surrounding (Plate 44).

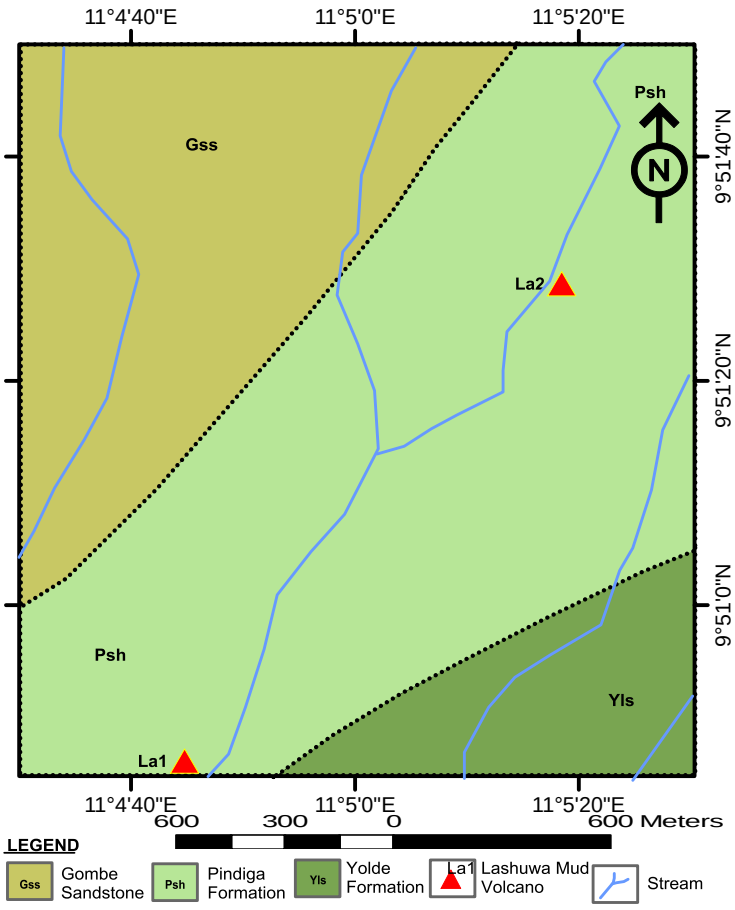



Figure 32: Lashuwa volcanoes of variety located by the author on the background of geological map by Benkhelil, (1985) with the volcanoes of water being located close to a stream NE – SW trending faults within the Pindiga Formation.



Plate 44: A volcano of water variety at Lashuwo with slurry of mud and water seeping from the crater with grasses and precipitated salt seen around the crater (N09$^0$50'46.0" E011$^0$04'44.7"; photo taken: 21/02/2012)

## Todi Mud Volcanoes

The Todi mud volcanoes field covers an area of about 3 km² and the volcano fields at Todi consist of 12 mud volcanoes. The mud volcanoes were seeping out slurry of mud from their crater and were all active at the time of fieldwork. The Todi mud volcanoes are concentrated along faults trending NE – SW and NW - SE situated on the Upper Bima Sandstone (Figure 33). The range of temperature at the neck of mud volcanoes at Todi was 22.2 to 24.6°C, and mud volcanoes cone range in height from 0.2 to 0.6 metres and diameter at base 5.0 to 8.0 metres as shown in Table 8 and 9. Typical examples of the mud volcanoes found at Todi are shown in Plate 45 to 48.

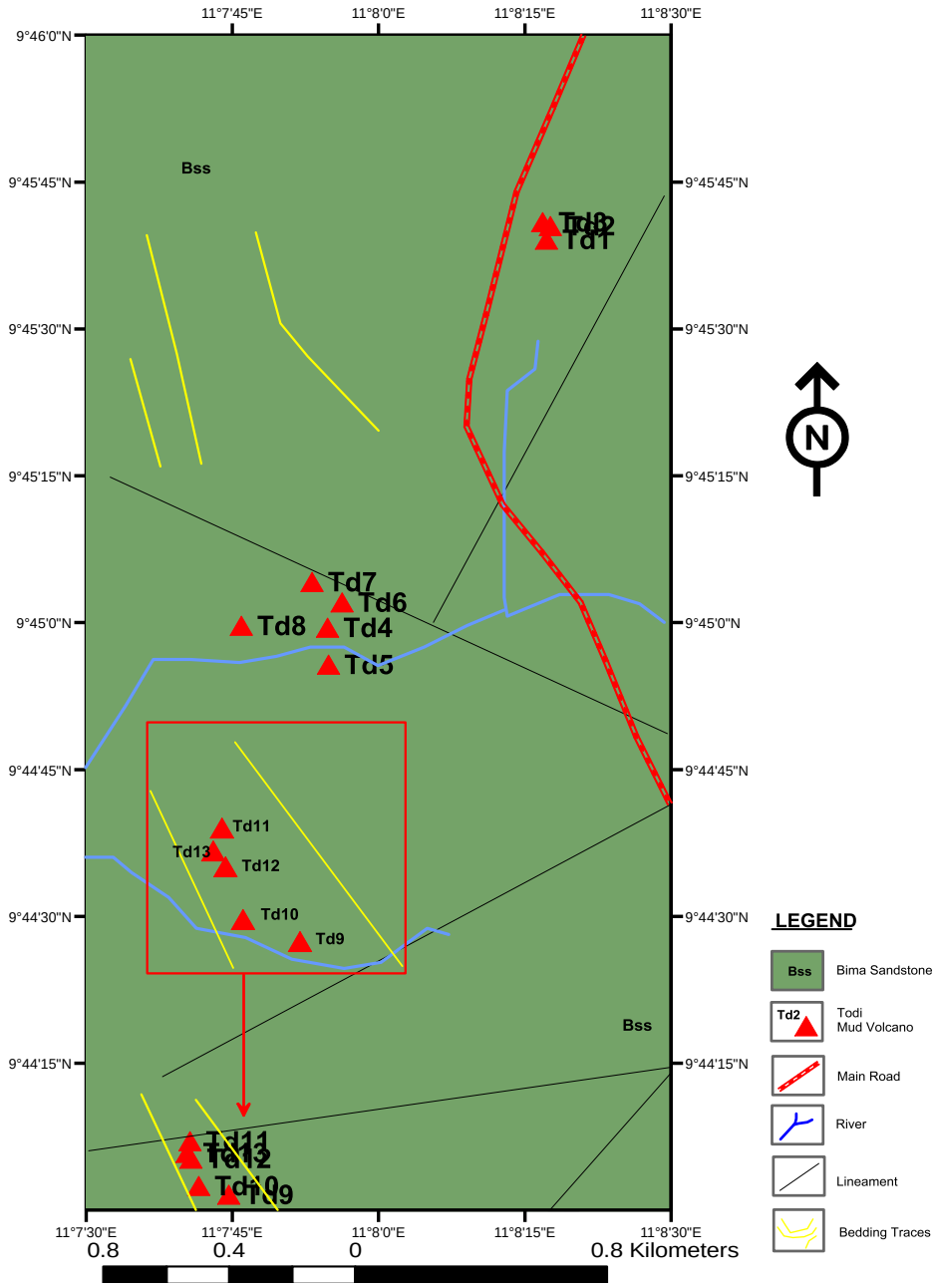



Figure 33: Todi mud volcanoes located by the author on the background of geological map by Benkhelil, (1985) with the mud volcanoes being located on or close to the NE – SW and NW - SE trending faults within the Bima Formation



Plate 45: A mud volcano showing multi crater at Todi with slurry of mud and water seeping from the crater with precipitated salt seen around the crater (N09$^0$45'38.9" E011$^0$08'17.7"; photo taken: 22/02/2012)



Plate 46: A mud volcano at Todi with slurry of mud and water seeping from the crater with whitish precipitates seen around the crater (N09$^0$45'40.3" E011$^0$08'18.8"; photo taken: 22/02/2012)



Plate 47: A mud volcano at Todi with slurry of mud and water seeping from the crater with whitish precipitates seen around the crater (N09$^0$45’40.7” E011$^0$08’17.3”; photo taken: 22/02/2012)



Plate 48: A mud volcano at Todi with slurry of mud and water seeping from the crater with whitish precipitates seen around the crater (N09$^0$44’59.0” E011$^0$07’55.1”; photo taken: 22/02/2012)

## Konta Mud Volcanoes

The Konta field covers an area of about 1.6 km² consisting of 3 volcanoes, seeping out water from their craters as observed during the fieldwork. As shown in Figure 34, the Konta volcanoes occur along faults trending NE – SW and N - S situated on the Upper Bima Sandstone and the range of temperature at the neck of mud volcanoes at Konta was 23.4 to 23.7°C (Plate 49).

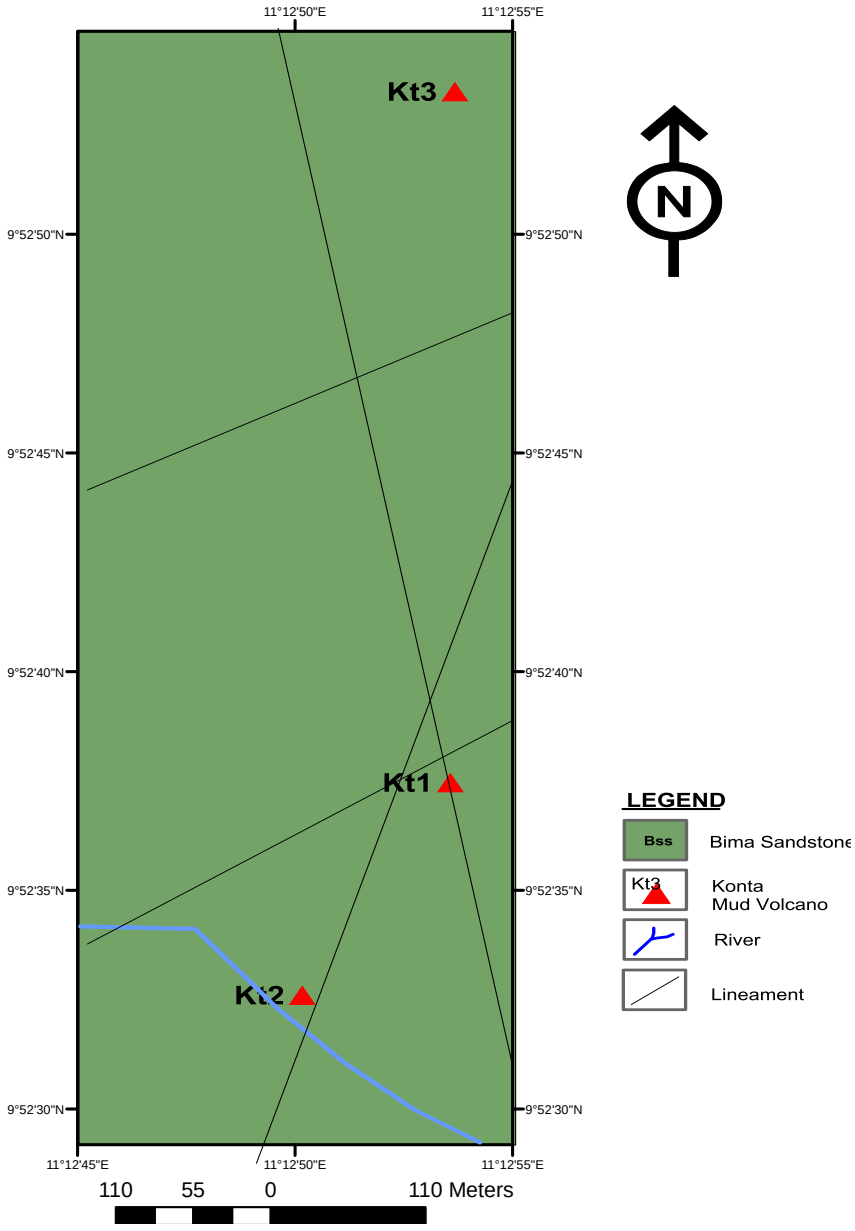



Figure 34: Konta mud volcanoes located by the author on the background of geological map by Benkhelil, (1985) with the mud volcanoes being located on or close to the NE – SW and N – S trending faults within the Bima Formation



Plate 49: A volcano of water variety at Konta with water seeping from the crater and grasses seen around the crater (N09$^0$46’18.3” E011$^0$03’06.7”)

**Lachikoltok Mud Volcanoes**

The Lachikoltok field covers a small area of about 2.5 km² consisting of 7 mud volcanoes of both mud and water variety, seeping out slurry of mud and water from their crater, the volcanoes were all active at the time of fieldwork. As shown in Figure 35, the Lachikoltok mud volcanoes are concentrated along faults trending NW – SE and N - S within the Yolde Formation and the range of temperature at the neck of mud volcanoes at lachikoltok was 21.8 to 22.4°C. The mud volcanoes cone ranges in height from 0.1 to 0.3 meters and diameter at base 2.5 to 4.0 meters (Table 8). Typical examples of the mud volcanoes found at Lachikoltok are shown in Plate 50 and 51.

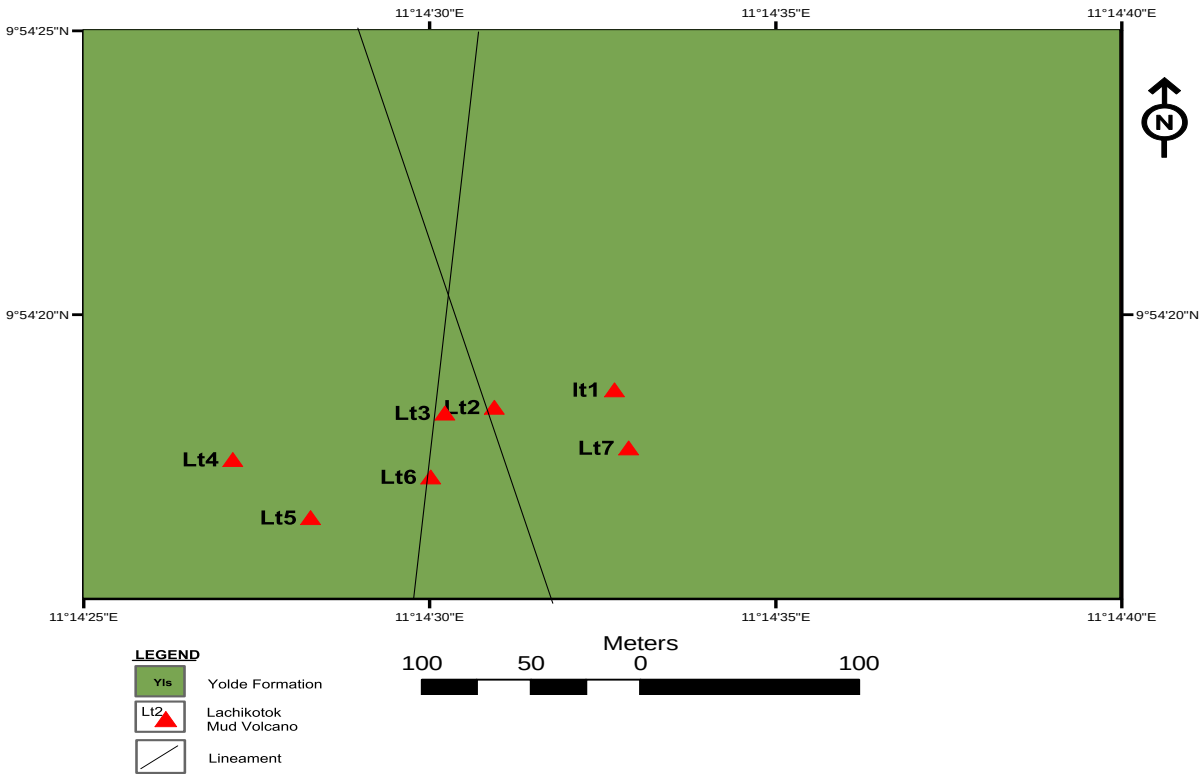



Figure 35: Lachikoltok mud volcanoes located by the author on the background of geological map by Benkhelil, (1985) with the mud volcanoes being located on or close to the N – S and NW - SE trending faults within the Yolde Formation



Plate 50: A mud volcano at Lachikoltok with slurry of mud and water seeping from the crater with grasses and precipitated salt seen around the crater (N09$^0$54'18.8" E011$^0$14'32.5" ; photo taken: 22/02/2012)



Plate 51: A volcano of water variety at Lachikoltok with water seeping from the crater with grasses and precipitated salt seen around the crater (N09$^0$54'18.5" E011$^0$14'30.8"; photo taken: 22/02/2012)

## Sasanyi Mud Volcanoes

The Sasanyi mud volcanoes field covers a small area consisting of five (5) individual volcanoes of water variety, seeping out mud and water from their crater, the volcanoes were all active at the time of fieldwork. The Sasanyi volcanoes which is of water variety are arranged around a stream trending NE – SW within the Bima Formation as shown in Figure 36. The range of temperature at the neck of mud volcanoes at Sasanyi was 24.0 to 25.4°C, which is a below the atmospheric temperature of the surrounding (Plates 52 and 53).

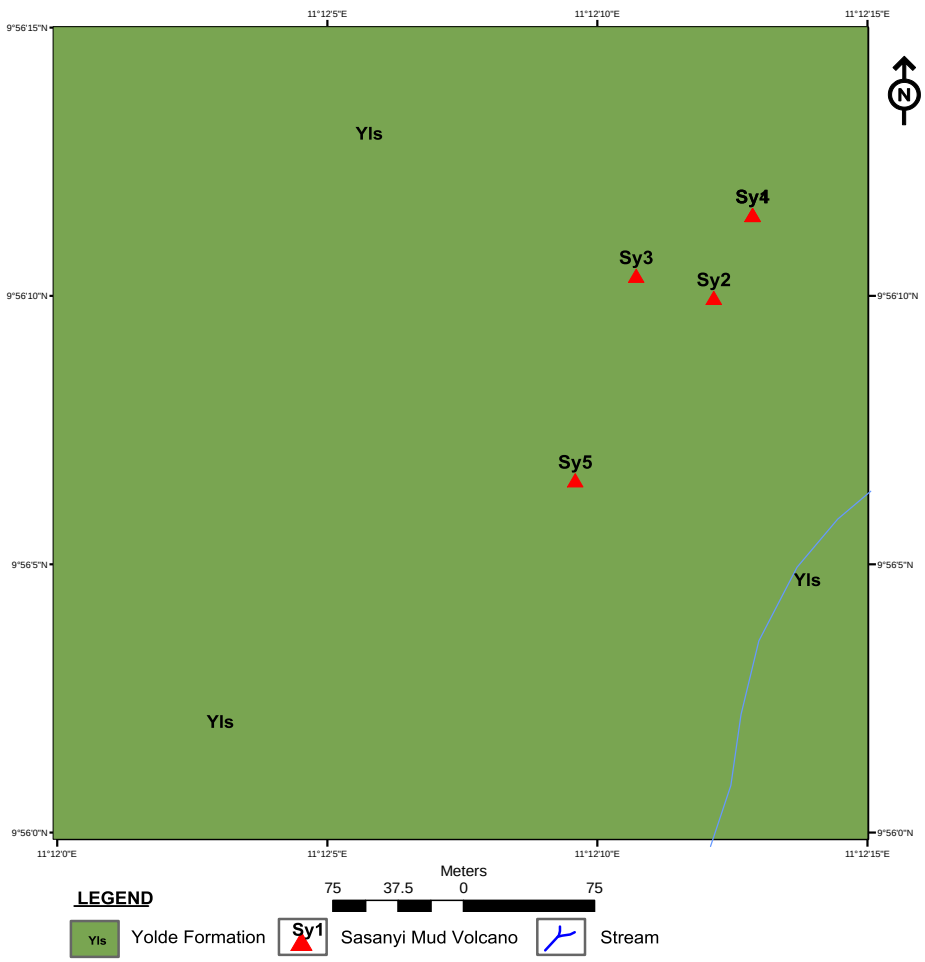



Figure 36: Sasanyi volcanoes of water variety located by the author on the background of geological map by Benkhelil, (1985) with the volcanoes being located close to a stream trending NE within the Yolde Formation



Plate 52: A volcano of water variety at Sasanyi with water seeping from the crater and grasses are seen around the crater (N09$^0$56'11.6" E011$^0$12'12.6"; photo taken: 23/02/2012)



Plate 53: A volcano of water variety at Sasanyi with water seeping from the crater and grasses are seen around the crater (N09$^0$56'10.1" E011$^0$12'11.9"; photo taken: 23/02/2012)

## Fokata Mud Volcanoes

The Fokata volcanoes are of water variety and the field covers a small area consisting of twenty one (21) individual volcanoes of water variety, seeping out water from their crater, while in some cases, wet ground surfaces were noticed with precipitated salt seen on these wet surfaces. The volcanoes were all active at the time of fieldwork. The Fokata volcanoes of water variety are arranged in N – S and NW – SE trend but no fault or stream was visible within the Bima Formation as shown in Figure 37. The range of temperature at the neck of mud volcanoes at Fokota was 22.4 to 22.4°C, which is a below the atmospheric temperature of the surrounding (Plates 54).

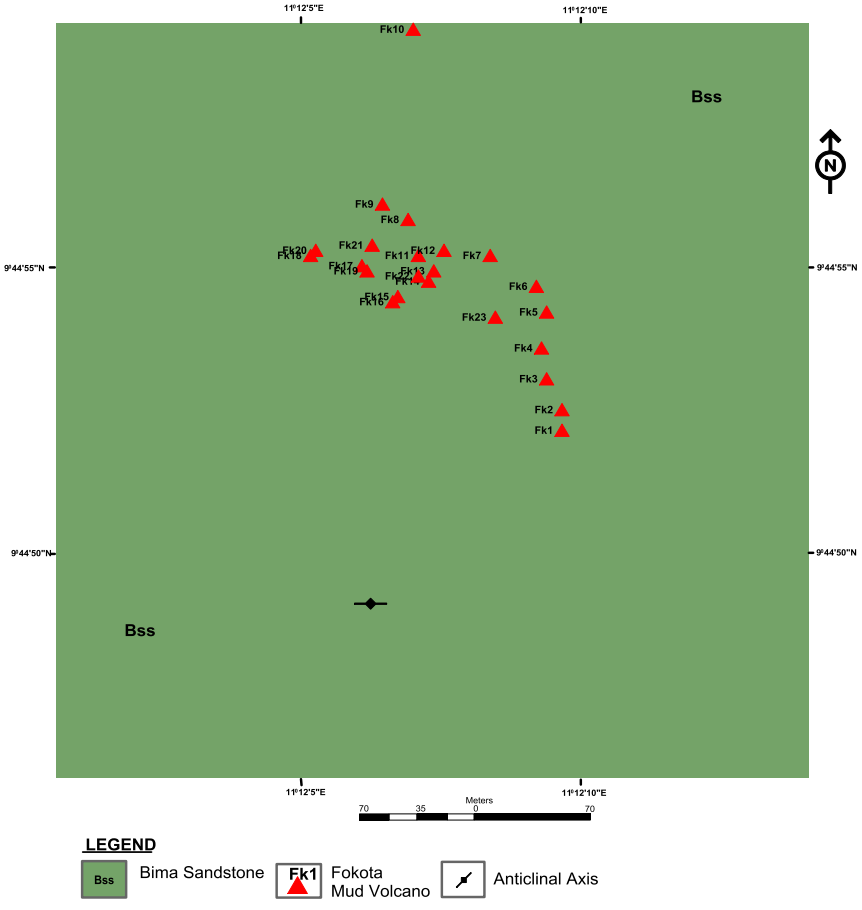



Figure 37: The Geological map showing the Fokata volcanoes being located on or close to the NE – SW trending faults within the Bima Formation



Plate 54: A volcano of water variety at Fokata with water seeping from the crater and grasses are seen around the crater (N09$^0$44'52.1" E011$^0$12'09.9"; photo taken: 09/02/2013)

**Warm Springs at Leturu and Lakomji**

Two warm springs were discovered in the course of the field work. They are the Leturu warm springs (N09$^0$42'10.1" E011$^0$11'31.8") and the Lakomji warm spring (N09$^0$41'05.9" E011$^0$14'09.0") (Plate 55 and 56). The springs are both of the same dimension with diameter of three (3) meters to two and half (2.5) meters for the Leturu warm spring and three and half (3.5) meters to two and half (2.5) meters for the Lakomji warm spring. They are warm with the temperatures of 41.9$^0$ for the Leturu warm spring and 41.2$^0$ for the Lakomji warm spring. It is also interesting to know that inhabitants close to the areas where these warm springs are located confirm to me that they rely on water for bathing during the dry season when the weather is so cold.



Plate 55: A warm spring at Leturu with warm water seeping from the crater (N09$^0$42'10.1" E011$^0$11'31.8"; photo taken: 19/02/2012)



Plate 56: A warm spring at Lakomji with warm water seeping from the crater (N09$^0$41'05.9" E011$^0$14'09.0"; photo taken: 19/02/2012)

## 4.3 Distribution of onshore mud volcanoes in the studu area

Most of the onshore mud volcanoes found in Nigeria were located in groups referred to as fields, and are shown on the geological map of the area produced in Figure 19. The map shows that the mud volcanoes are located mostly towards the south western end of the Kaltungo fault, where the major fault line begins to disappear within other minor faults. The Kaltungo fault generally trends NE – SW. Using the interpreted satellite image of the study area obtained from Google Earth, the faults were delineated and the various fields of onshore mud volcanoes were located parallel to the fault zones (Figure 38).

At Lalapido, a field of mud volcanoes was observed parallel to a faulted Upper Bima Sandstone beds. The mud volcanoes are occurring in a NE – SW trend at a distance of about 20 metres parallel to the fault zone. At Lakaturu, mud volcanoes occur parallel (NE – SW) faulted Yolde Formation. The width of the fault zone is five meters and the bedding dips gently northeast, with a dip angle of 30° (Plate 57). The Gujuba mud volcanoes occur parallel to the N – S trending faulted sandstone of Yolde Formation located within the Dadinya syncline.

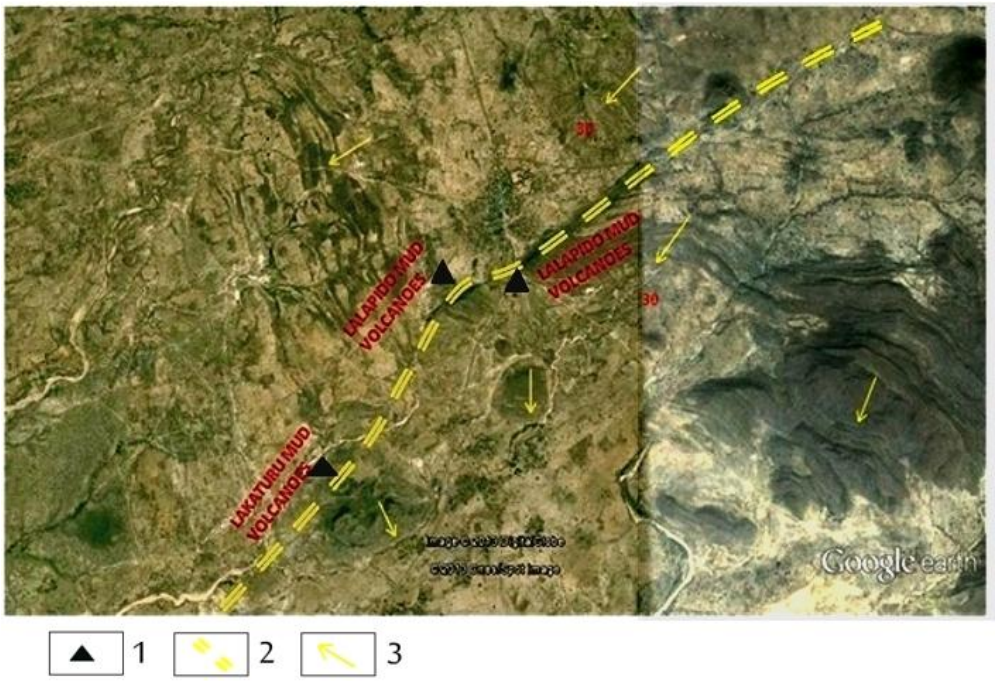



Figure 38: A faulted zone from satellite image showing trend of NE – SW. 1 – Field of mud volcanoes, 2 - Fault 3 - Orientation of beds (Base map is image from Google Earth)



Plate 57: Faulted Yolde Formation at Lakaturu showing trend of NE – SW with mud volcanoes around it, pointed with red arrows, at $N9^{0}42^{'}11.5^{''}$ and $E11^{0}07^{'}42.1''$.

## 4.4 Granulometric analysis from rocks around the surrounding area of mud volcanoes

Granulometric analysis was employed to determine the grain size distribution of the clastic sediments within the area of occurrence of the mud volcanoes. Fresh samples were obtained from various locations as shown in Table 9. From the granulometric analysis, statistical parameters such as graphic mean, graphic standard deviation, graphic skewness and graphic kurtosis were determined. This gives a strong clue to the origin and the depositional history of the sediments.

**Table 9: Tabulated result for sieve size analysis by the Author in the sedimentology laboratory, department of Geology, A.B.U Zaria**

| Aperture (mm) | Aperture (ϕ) | Weight % | Cumulative weight % | Sample ID | Location ID |
|---|---|---|---|---|---|
| 1.8 | -0.84 | 2.00 | 2.00 | | |
| 0.6 | 0.73 | 7.00 | 9.00 | Lap 1 | Lalapido |
| 0.3 | 1.73 | 38.66 | 47.66 | | |
| 0.15 | 2.73 | 37.65 | 85.31 | | |
| 0.075 | 3.73 | 5.28 | 90.59 | | |
| <0.075 | 4.73 | 8.98 | 99.57 | | |
| | | | | | |
| 1.8 | -0.84 | 3.00 | 3.00 | | |
| 0.6 | 0.73 | 8.67 | 11.67 | Tod 1 | Todi |
| 0.3 | 1.73 | 27.78 | 49.45 | | |
| 0.15 | 2.73 | 38.11 | 77.56 | | |
| 0.075 | 3.73 | 5.72 | 83.28 | | |
| <0.075 | 4.73 | 16.37 | 99.65 | | |
| | | | | | |
| 1.8 | -0.84 | 0.68 | 0.68 | | |
| 0.6 | 0.73 | 3.43 | 4.11 | Tod 2 | Todi |
| 0.3 | 1.73 | 26.48 | 30.59 | | |
| 0.15 | 2.73 | 41.99 | 72.58 | | |
| 0.075 | 3.73 | 9.85 | 82.43 | | |
| <0.075 | 4.73 | 17.09 | 99.52 | | |
| | | | | | |
| 1.8 | -0.84 | 1.53 | 1.53 | | |
| 0.6 | 0.73 | 3.99 | 5.52 | | |
| 0.3 | 1.73 | 12.64 | 18.16 | Lak 1 | Lakaturu |
| 0.15 | 2.73 | 44.86 | 63.02 | | |
| 0.075 | 3.73 | 22.63 | 85.65 | | |
| <0.075 | 4.73 | 12.47 | 98.12 | | |
| | | | | | |
| 1.8 | -0.84 | 1.41 | 1.41 | | |
| 0.6 | 0.73 | 2.34 | 3.75 | Kur 1 | Kurum |
| 0.3 | 1.73 | 13.55 | 17.30 | | |
| 0.15 | 2.73 | 26.63 | 43.93 | | |
| 0.075 | 3.73 | 43.31 | 87.24 | | |
| <0.075 | 4.73 | 11.95 | 99.19 | | |

| Aperture (mm) | Aperture (ϕ) | Weight % | Cumulative weight % | Sample ID | Location Id |
|---|---|---|---|---|---|
| 1.8 | -0.84 | 1.33 | 1.33 | | |
| 0.6 | 0.73 | 13.16 | 14.49 | LaP 2 | Lallapido |
| 0.3 | 1.73 | 46.31 | 60.80 | | |
| 0.15 | 2.73 | 30.28 | 91.08 | | |
| 0.075 | 3.73 | 4.61 | 95.69 | | |
| <0.075 | 4.73 | 3.67 | 99.36 | | |
| | | | | | |
| 1.8 | -0.84 | 0.34 | 0.34 | | |
| 0.6 | 0.73 | 1.33 | 1.67 | | |
| 0.3 | 1.73 | 17.96 | 19.63 | Lash 1 | Lashadar |
| 0.15 | 2.73 | 57.56 | 77.19 | | |
| 0.075 | 3.73 | 16.84 | 94.03 | | |
| <0.075 | 4.73 | 5.23 | 99.26 | | |
| | | | | | |
| 1.8 | -0.84 | 1.15 | 1.15 | | |
| 0.6 | 0.73 | 4.00 | 5.15 | | |
| 0.3 | 1.73 | 52.66 | 57.81 | | |
| 0.15 | 2.73 | 25.65 | 83.46 | Pam 1 | Pamadu |
| 0.075 | 3.73 | 10.99 | 94.45 | | |
| <0.075 | 4.73 | 3.47 | 97.92 | | |
| | | | | | |
| 1.8 | -0.84 | 12.75 | 12.75 | | |
| 0.6 | 0.73 | 9.88 | 22.63 | | |
| 0.3 | 1.73 | 14.94 | 37.57 | | |
| 0.15 | 2.73 | 38.27 | 75.84 | Kur 2 | Kurum |
| 0.075 | 3.73 | 11.50 | 87.34 | | |
| <0.075 | 4.73 | 10.72 | 98.06 | | |
| | | | | | |
| 1.8 | -0.84 | 0.69 | 0.69 | | |
| 0.6 | 0.73 | 0.89 | 1.58 | | |
| 0.3 | 1.73 | 20.93 | 22.51 | Jen 1 | Jenye |
| 0.15 | 2.73 | 45.96 | 68.47 | | |
| 0.075 | 3.73 | 24.74 | 93.21 | | |
| <0.075 | 4.73 | 4.58 | 97.79 | | |

## Cumulative Frequency Curves

From the cumulative frequency curves plotted in Figures 39 to 48, the parameters needed for the calculation of the graphical mean, graphic standard deviation, graphic skewness and graphic kurtosis were determined.

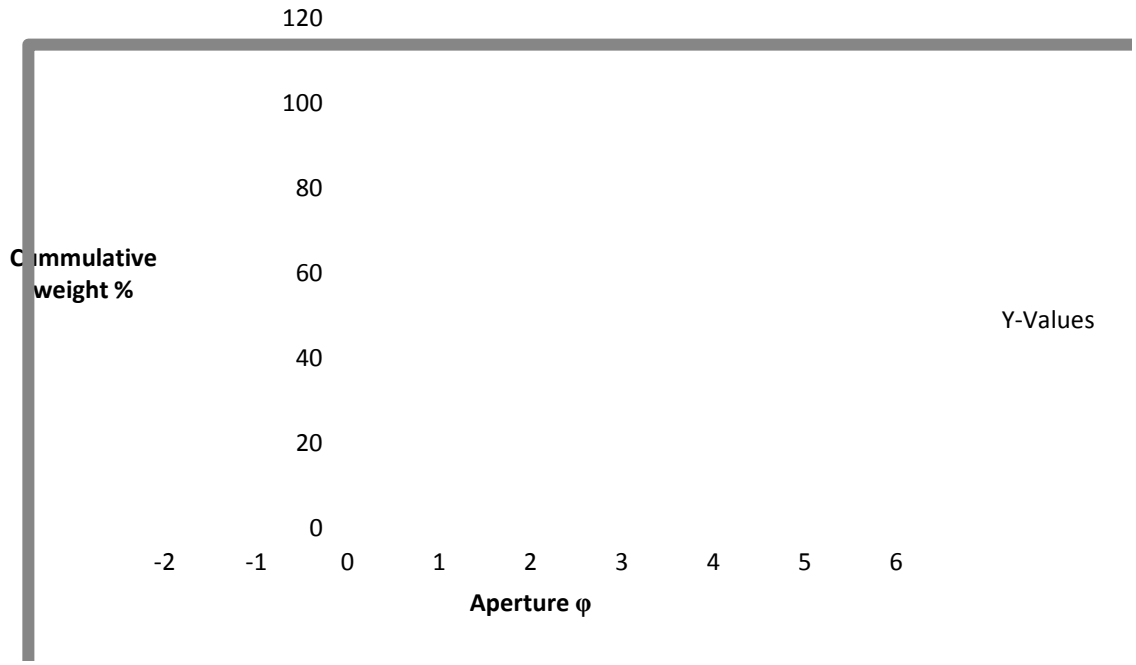



Figure 39: Cumulative frequency curve for Lallapido (Lap 1)

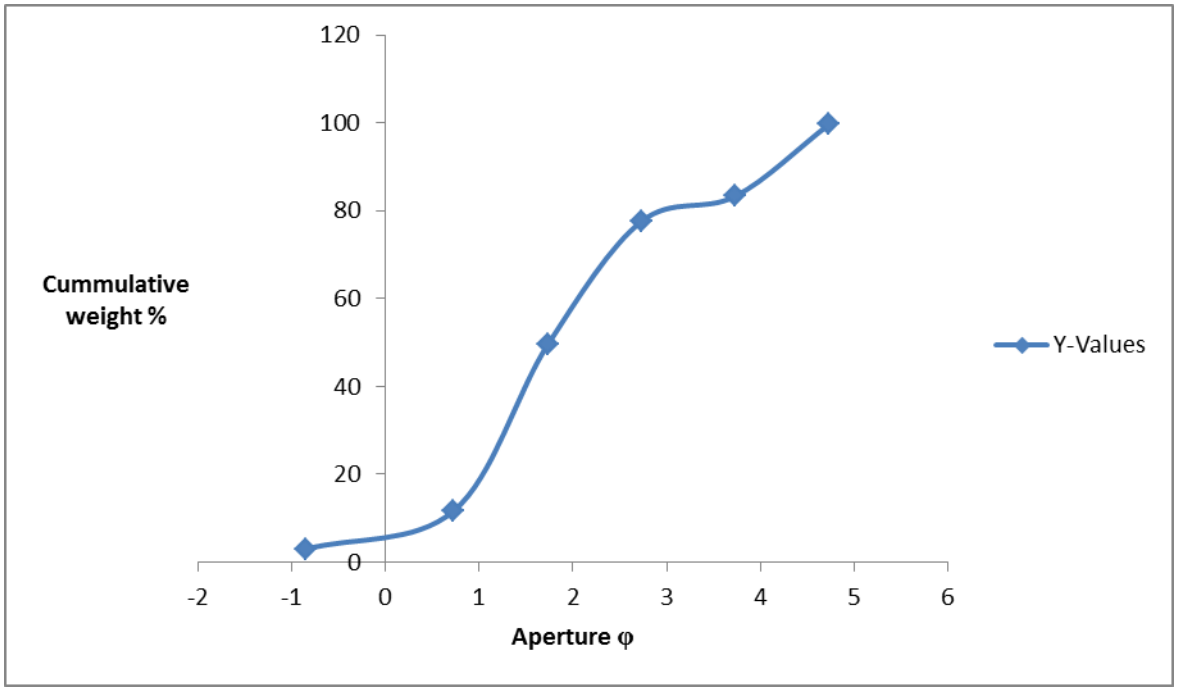



Figure 40: Cumulative frequency curves for Todi (Tod 1)

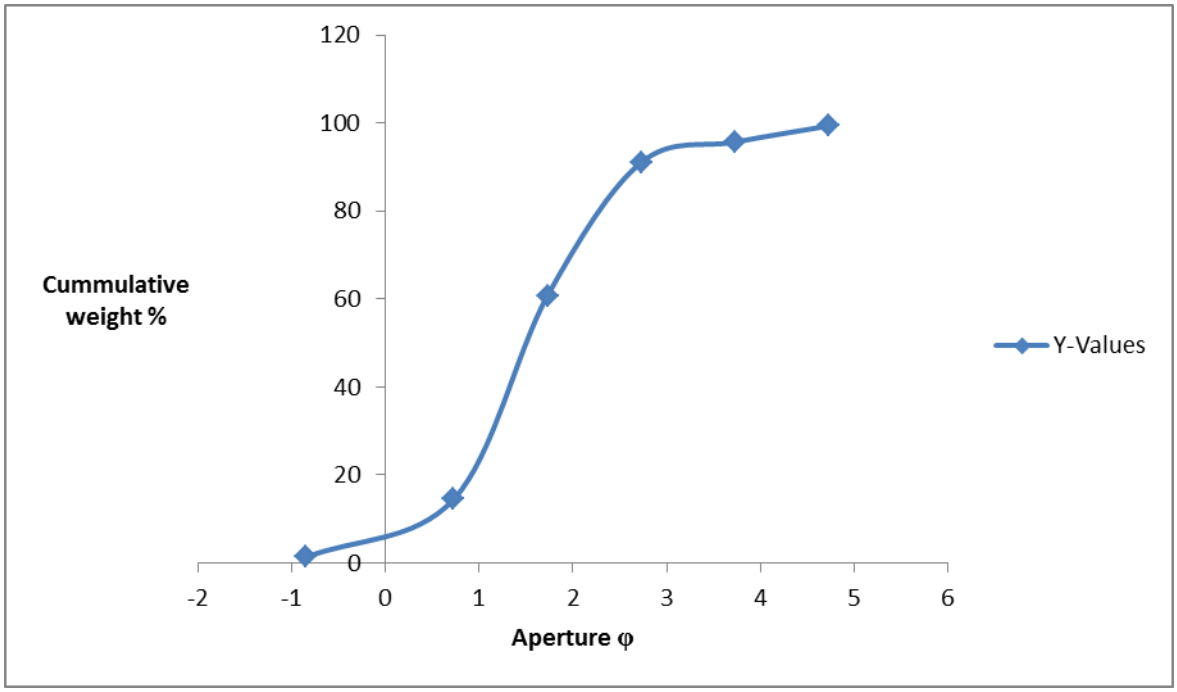



Figure 41: Cumulative frequency curve for Todi (Tod 2)

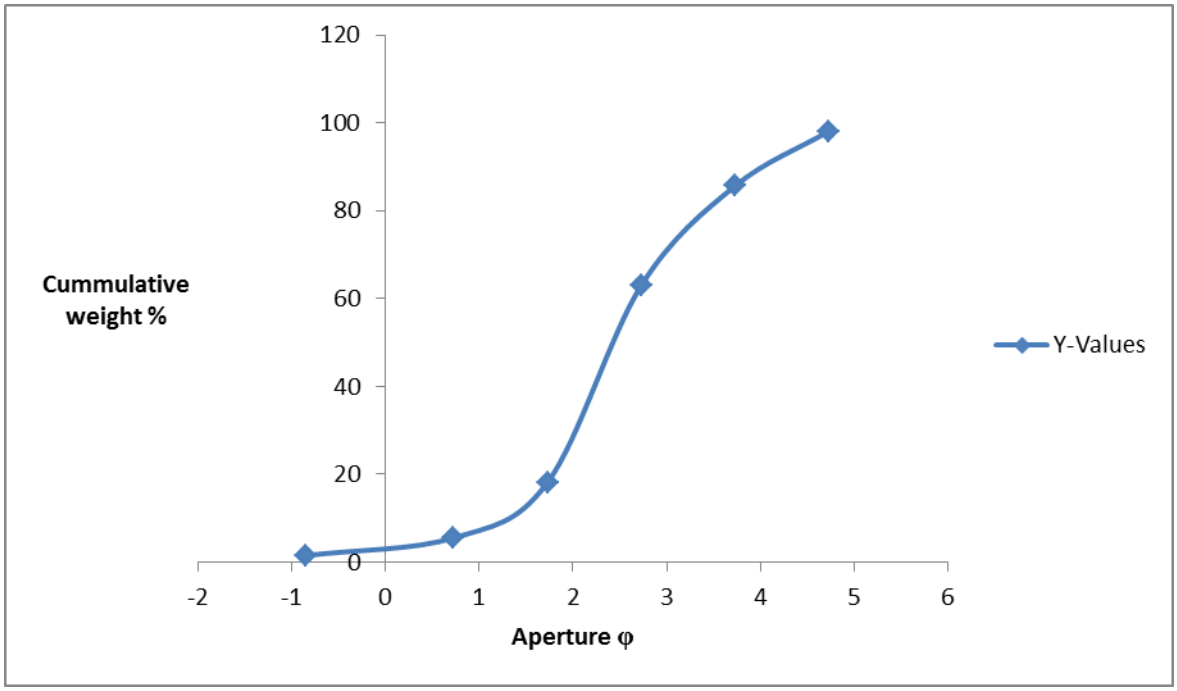



Figure 42: Cumulative frequency curve for Lakaturu (Lak 1)

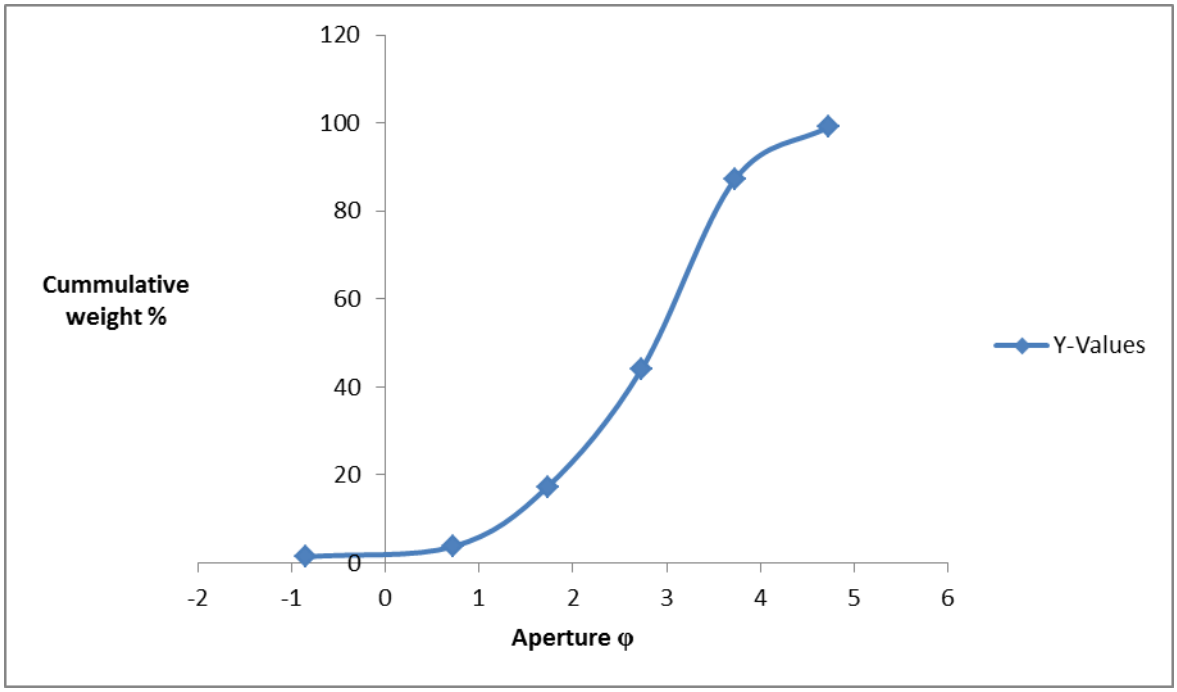



Figure 43: Cumulative frequency curve for Kurum (Kur 1)

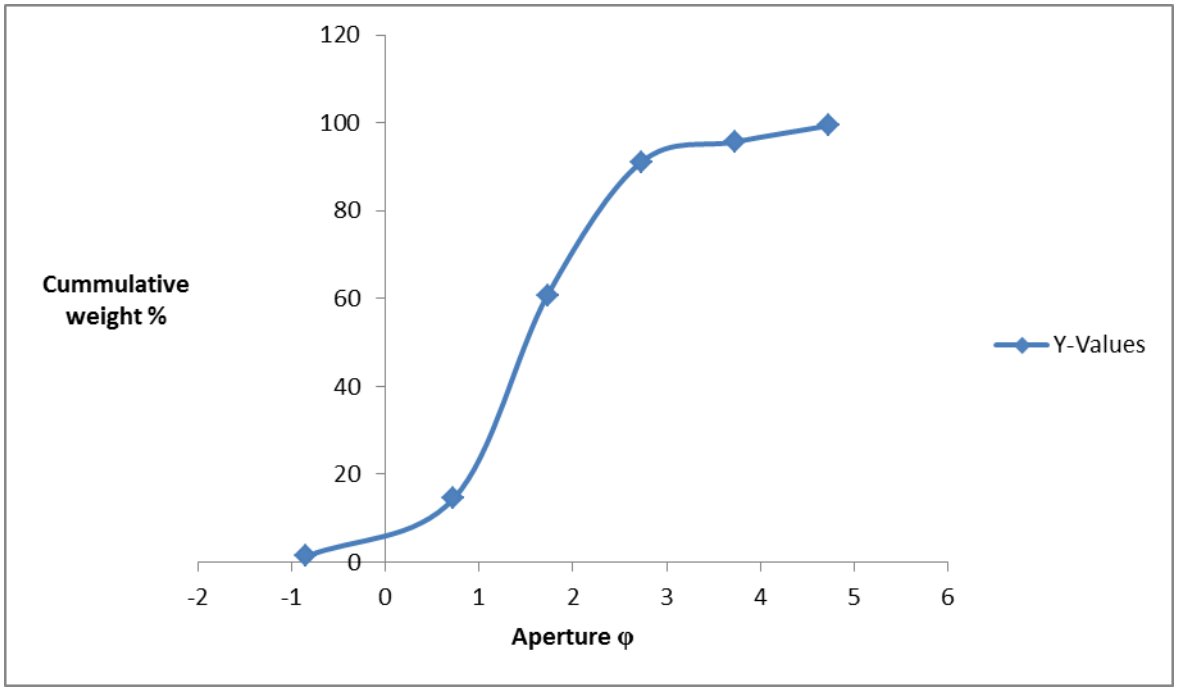



Figure 44: Cumulative frequency curve for Lallapido (Lap 2)

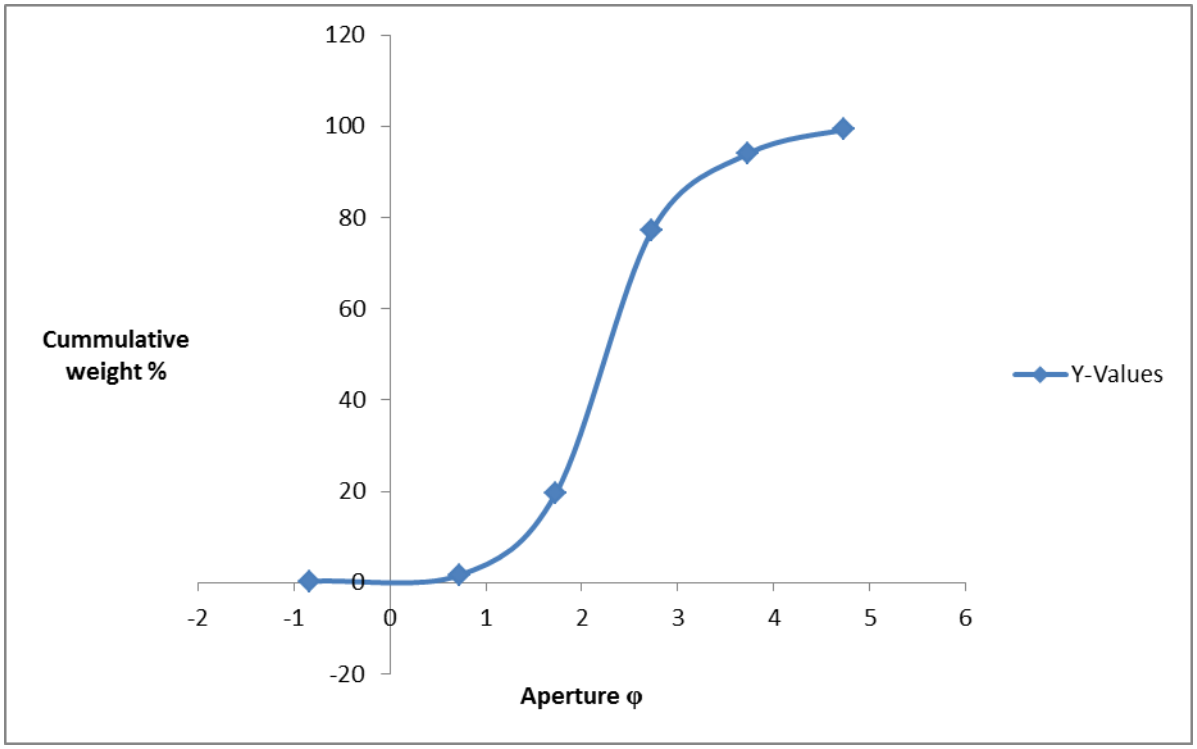



Figure 45: Cumulative frequency curve for Lashadar (Lash 1)

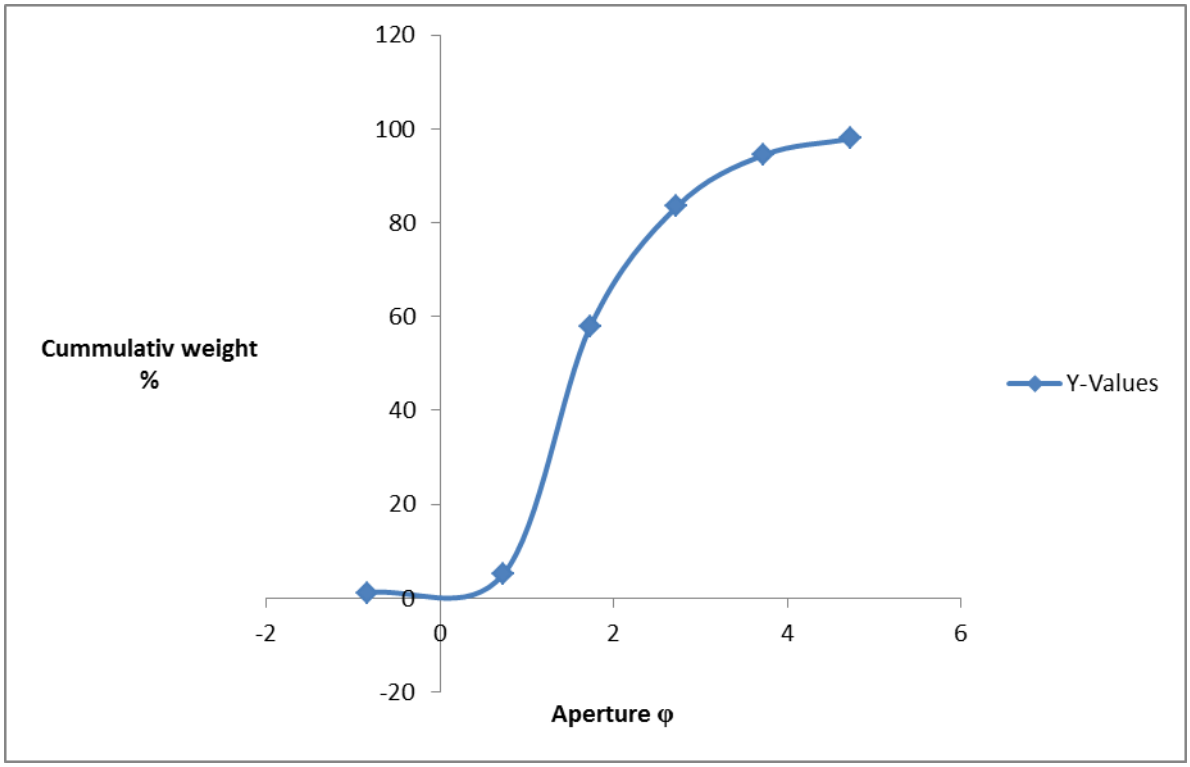



Figure 46: Cumulative frequency curve for Pamadu (Pam 1)

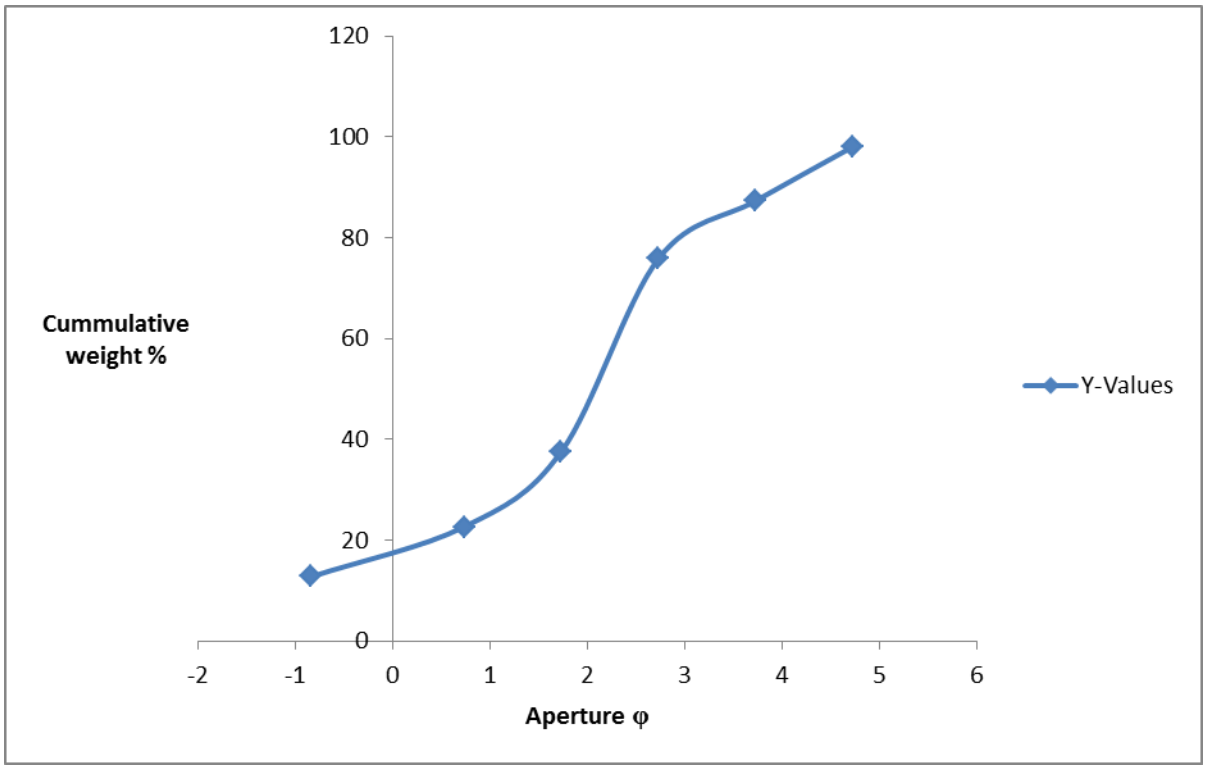



Figure 47: Cumulative frequency curve for Kurum (Kur 2)

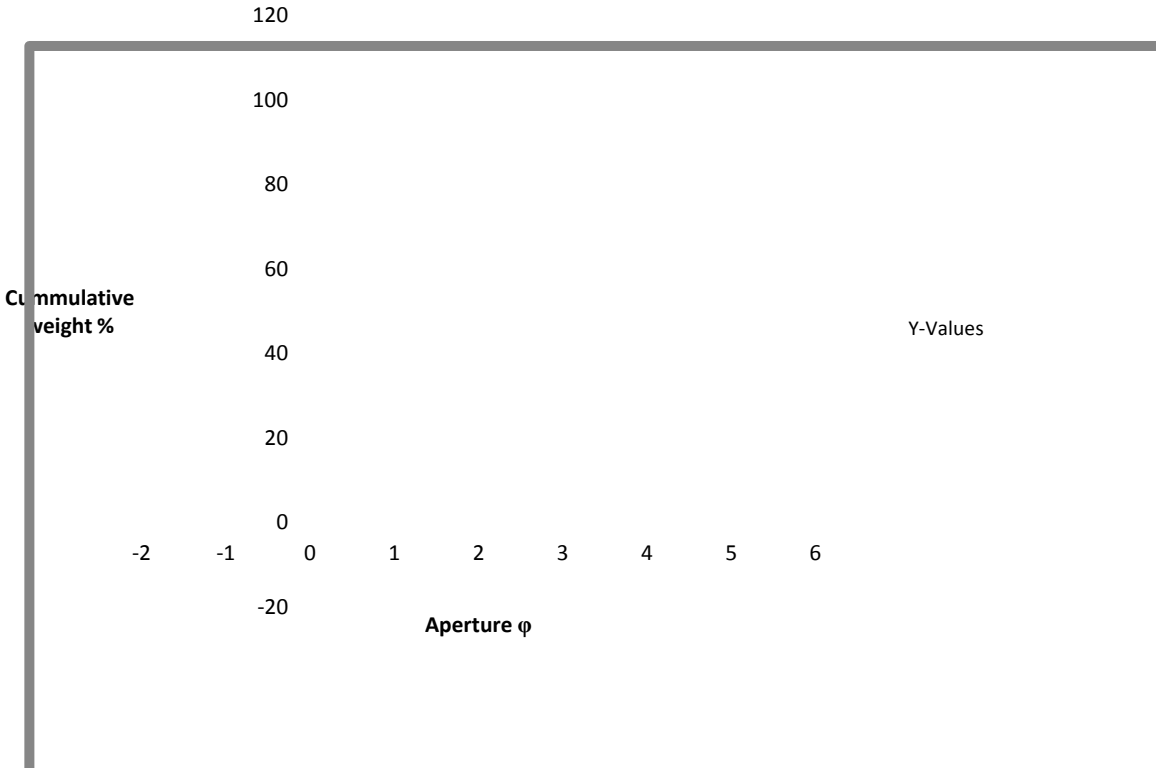



Figure 48: Cumulative frequency curve for Jenye (Jen 1)

**Table 10: Calculated values for grain size parameters of sandstone samples within the areas of occurrence of mud volcanoes and their interpretations.**

| Sample ID | Location ID | ϕ5 | ϕ16 | ϕ25 | ϕ50 | ϕ75 | ϕ84 | ϕ95 | Mean ϕ | Sorting ϕ | Skweness ϕ | Kurtosis ϕ |
|---|---|---|---|---|---|---|---|---|---|---|---|---|
| Lap1 | Lallapido | 0.8 | 1.1 | 1.3 | 1.9 | 2.2 | 2.5 | 3.1 | 1.8<br>Medium sand | 0.69<br>Moderately well sorted | -0.05<br>Nearly symmetrical | 1.05<br>Mesokurtic |
| Tod 1 | Todi | -0.1 | 0.9 | 1.2 | 1.6 | 2.7 | 2.8 | 4.3 | 1.7<br>Medium sand | 1.14<br>Poorly sorted | 0.35<br>Strongly fine skewed | 1.20<br>Leptokurtic |
| Tod 2 | Todi | -0.2 | 0.8 | 1.1 | 1.5 | 2.2 | 2.5 | 3.2 | 1.6<br>Medium sand | 0.94<br>Moderately sorted | 0.08<br>Nearly symmetrical | 1.27<br>Leptokurtic |
| Lak 1 | Lakaturu | 0.1 | 1.8 | 2.0 | 2.5 | 3.4 | 3.8 | 4.5 | 2.7<br>Fine sand | 1.16<br>Poorly sorted | 0.10<br>Fine skewed | 1.64<br>Very leptokurtic |
| Kur 1 | Kurum | 1.0 | 1.7 | 2.6 | 3.0 | 3.4 | 3.8 | 4.3 | 2.8<br>Fine sand | 1.03<br>Poorly sorted | -0.23<br>Coarse skewed | 1.64<br>Very leptokurtic |
| Lap 2 | Lallapido | -0.1 | 0.8 | 1.2 | 1.6 | 2.3 | 2.5 | 4.4 | 1.6<br>Medium sand | 1.11<br>Poorly sorted | 0.27<br>Fine skewed | 1.67<br>Very leptokurtic |
| Lash 1 | Lashadar | 1.3 | 1.7 | 2.1 | 2.4 | 2.8 | 3.2 | 4.2 | 2.4<br>Fine sand | 0.82<br>Moderately sorted | 0.15<br>Fine skewed | 1.69<br>Very leptokurtic |
| Pam 1 | Pamadu | 0.3 | 1.0 | 1.3 | 1.8 | 2.3 | 2.8 | 3.9 | 1.9<br>Medium sand | 0.99<br>Moderately sorted | 0.14<br>Fine skewed | 1.47<br>Leptokurtic |
| Kur 2 | Kurum | -1.3 | 0.1 | 1.3 | 2.4 | 2.8 | 3.4 | 4.5 | 2.0<br>Medium sand | 1.52<br>Poorly sorted | -0.14<br>Coarse skewed | 1.58<br>Very leptokurtic |
| Jen 1 | Jenye | 1.2 | 1.6 | 2.1 | 2.5 | 3.1 | 3.3 | 3.8 | 2.5<br>Fine sand | 0.82<br>Moderately sorted | -0.03<br>Coarse skewed | 1.07<br>Mesokurtic |

Grain size parameters such as the graphic mean, graphic sorting, graphic skewness and graphic kurtosis were obtained from the graphs in the cumulative frequency curves in Figures 30 to 39 for the various locations are shown in Table 10. The graphic mean indicates that at Lap 1, Lap 2, Tod 1, Tod 2, and Pam 1, the sediments are medium sand while at Lak1, Kur 1, Lash 1 and Jen 1, the sediments are fine grained. The graphic sorting indicates that at Lap 1, Lash, Tod 2, Pam 1 and Jen 1, the sediments are moderately sorted while at Lap 2, Kur 1, Kur 2 and Tod 1, the sediments are poorly sorted. From the graphic skewness determined, in lak 1, Lap 2, Lash 1, Pam 1 the sediments are fine skewed, the sediments at Kur 1, Kur 2, and Jen 1 are coarse skewed, and the sediments at Lap 1 and Tod 2 are nearly symmetrical. At Tod 1 the sediments are strongly fine skewed. The graphic kurtosis indicates that at Lak 1, Kur 1, Lap 2, Lash 1 and Kur 2, the sediments are very leptokurtic; the sediments are leptokurtic at Tod 1, Tod 2 and Kur 2.While the sediments at Lap 1 and Jen 1 is mesokurtic.

In summary, the sediments around the mud volcanoes at Lallapido shows that at Lallapido, Todi and Pamadu were medium sands, moderately sorted to poorly sorted, fine skewed to nearly symmetrical skewed and mesokurtic to very leptokurtic. While the sediments surrounding the mud volcanoes at Lakaturu, Kurum, Lashadar were medium to fine sands, moderately sorted to poorly sorted, fine skewed to coarse skewed and mesokurtic to very leptokurtic. The textural properties of the sediments that was analysed for grain size parameters suggest that sampled sediments from the sorrunding of mud volcanoes at Lallapido, Todi and Lashadar are occuring within the continental Upper Bima Sandstone while the sediments sourrounding mud volcanoes at Lakaturu, Kurum and Pamadu are within the Yolde Formation which is of a transitional environment between continental Upper Bima Sandstone and marine Pindiga Fomations. In summary, the sediments surrounding the areas of occurrences of the mud

volcanoes are deposited in environments transitional between marine and non marine environments of about Albian to Cenomanian in age.

## 4.5 X –Ray Diffractogram (XRD) analysis on extruded clays from the mud volcanoes

The mineralogy of the dry mud from the mud volcanoes and the saprolite indicates that they have mineralogical compositions ranging from quartz, kaolinite and Microcline. Also, little of smectite and benthonite were noticed at Kurum and Lashadar. Other accessory minerals like goethite, hematite, feldspars and probably Fe oxides are noticed. The qualitative mineral content of the mud volcano and saprolite content are shown on Figures 49 – 53.

**<u>Kurum saprolite and mud slurry (Sm 1and 4)</u>**

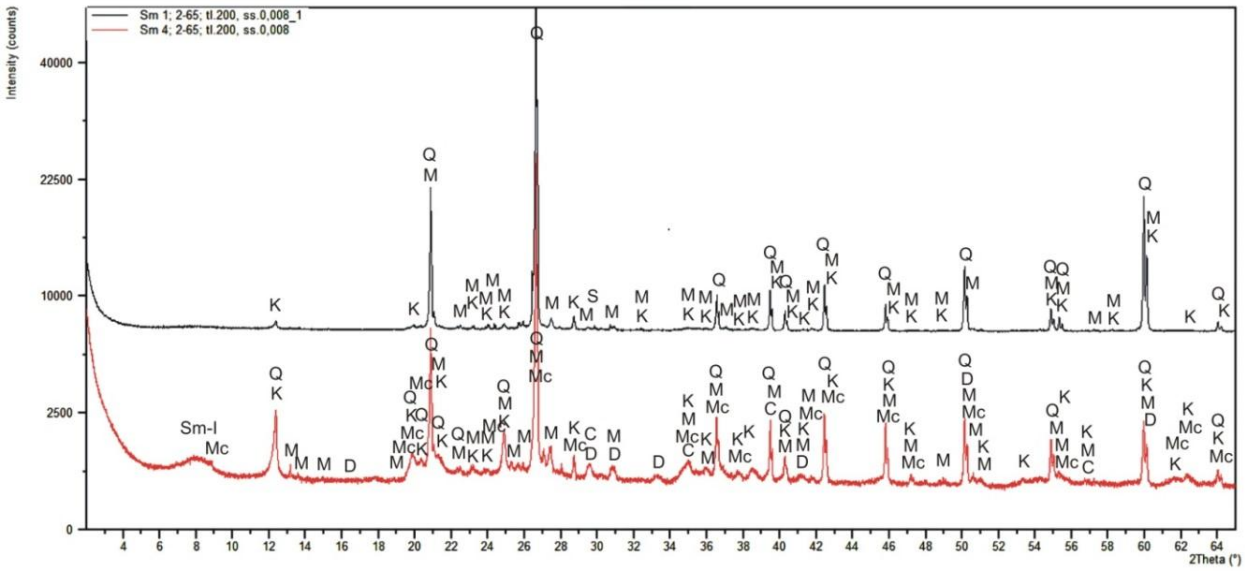



Figure 49: Measured XRD pattern (diffractogram) showing clay and other accessory minerals from mud volcano and saprolite at Kurum (Sm 4 and 1) (The red line at the bottom is for the extruded mud, while the red line is for the saprolite).

From the Kurum saprolite sampled analysed (Sm 1, (Figure 49), the quartz content is 87%, feldspars is 8% while kaolinite is 4%. There are very small amount of other minerals such as traces of evaporite minerals (probably sylvite). While clay minerals

composition of the mud slurry (Sm 4, (Figure 49) are the quartz content 62%. There is large amount of kaolinite (18%) and muscovite (1-3%) or illite, and a lot of mixed-layered clay minerals (probably illite-smectite) and high content of microcline (16%). A dolomite (1.6%) has been detected and trace amounts of calcite (max. 1%), and a very small amount of sodium feldspar (albite or plagioclase).

The high value of quartz in both the saprolite and the mud slurry suggest the ability of the quartz to be resistant to weathering. While feldspar and the mica usually weathers to clay minerals like kaolinite, smectitite and illite as shown in Sm 4 (Figure 49). The presence of traces of calcite and dolomite could suggest the presence of marine organisms which further gives a clue of a transitional unit which is the Yolde Formation for the extruded mud from the mud volcanoes because of the quantity of the evaporates noticed.

**Lashadar saprolite and mud slurry (Sm 2 and 3)**

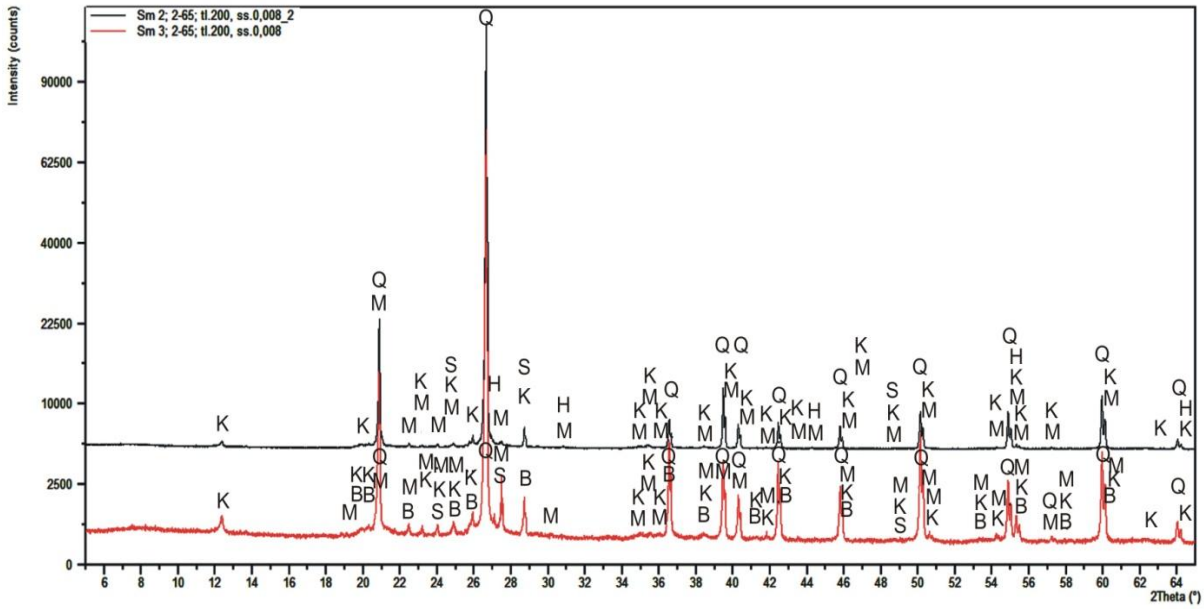



Figure 50: Measured XRD pattern (diffractogram) showing clay and other accessory minerals from mud volcanoes and saprolite at Lashadar (Sm 3 and 2) (The red line at the bottom is for the extruded mud, while the red line is for the saprolite).

The Lashadar saprolite (Sm 2, Figure 50) is dominated by quartz in the amount of 90% ± 3%. Also there are the other minerals: microcline (5 ± 1%) and kaolinite 3-4 ± 1%. The rest of the composition constitutes trace evaporite minerals (less than 1%). There are probably trace amounts of smectites; very small amount of sodium feldspar (plagioclase or albite - 3.19 - 3.2 Å) but they are on the detection limit. While the mineral compositions in the Lashadar mud slurry (Sm 3) is quartz content: 90.6%. Moreover, there are: microcline (5%) and kaolinite (3.5%). In addition, there is less than 1% - probably sylvite (KCl - 3,107 Å), with possibly traces of barite (3.44 Å) or perhaps pyrolusite ($MnO_2$). Kaolinite and microcline are relatively constant, bentonite is only found in the mud slurry in low concentration. The clay mineral association in the overburden material shows difference to that from the mud volcano (Figure 50), it contain hematite and does not have bentonite in it. Hematite is weathered mineral from Fe – Mg minerals. Also, the high value of quartz in both the saprolite and the mud slurry suggest the granite was the basement rock within this area.

**Lakaturu saprolite and mud slurry (Sm 5 and 6)**

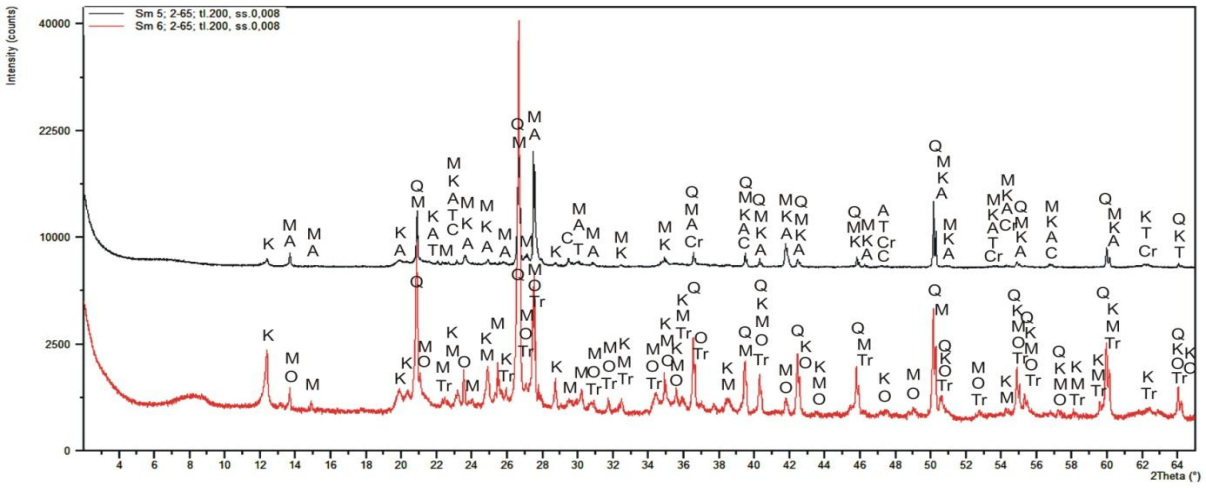



Figure 51: Measured XRD pattern (diffractogram) showing clay and other accessory minerals from mud volcano and saprolite at Lakaturu (Sm 6 and 5) (The red line at the bottom is for the extruded mud, while the red line is for the saprolite)

The Lakaturu saprolite (Sm 5, Figure 51) has the content of quartz be than in other samples - approx. 40% ± 3% and there is a relatively large amount of feldspars: microcline 27% ± 3%, plagioclase 24%. Furthermore, the kaolinite in the amount of 8% has been detected. A different silica type was found: cristobalite and tridymite (4,034 Å) - approx. 2%. On the diffractograms this type of silica is represented by clear but much lower than ordinary quartz peaks. In the sample the traces of evaporite minerals (3,107 Å) and kaolinite occur, there may also be a trace amount of calcite. Flat bulge on the beginning of the diffractogram (Figure 51) shows the range of 11-15 Å and it may indicate the presence of disordered clay minerals, arranged in a mixed-layered structures, probably of smectite –illite type. While in the Lakaturu mud slurry (Sm 6, Figure 51), quartz content is approximately 65%, a large content of feldspars (25%) including microcline (17%) and orthoclase (8%); there is also a large amount of kaolinite (11%). Just as in the sample 5 at the beginning of the diffractogram there is the bulge observed in the range of 10-12 Å that indicates the presence of mixed-layered clay minerals, probably illite-smectite. Reflection 3.07 Å is an evidence of sylvite admixture and/or barite. In addition, 3.07 Å and 2.64 Å reflections occur that indicates the presence of trona mineral ($Na_3H$ ($CO_3$) 2 ($H_2O$)$_2$ – approximately, 1% by weight. The presence of traces of cristobalite and tridymite in Sm5 (Figure 51) which are high temperature polymorph of quartz and usually occurs in cavities of felsic volcanic rocks in marine sedimentary rocks derived from biogenic sediments. The traces of trona minerals in Sm 6 (Figure 51) are of non-marine evaporate minerals and it is primary source of sodium carbonate. The presence of the cristobalite, tridymite and tronal minerals together further suggests a transitional unit for the extruded mud from the mud volcanoes.

**Pamadu mud slurry and saprolite (Sm 7 and 10)**

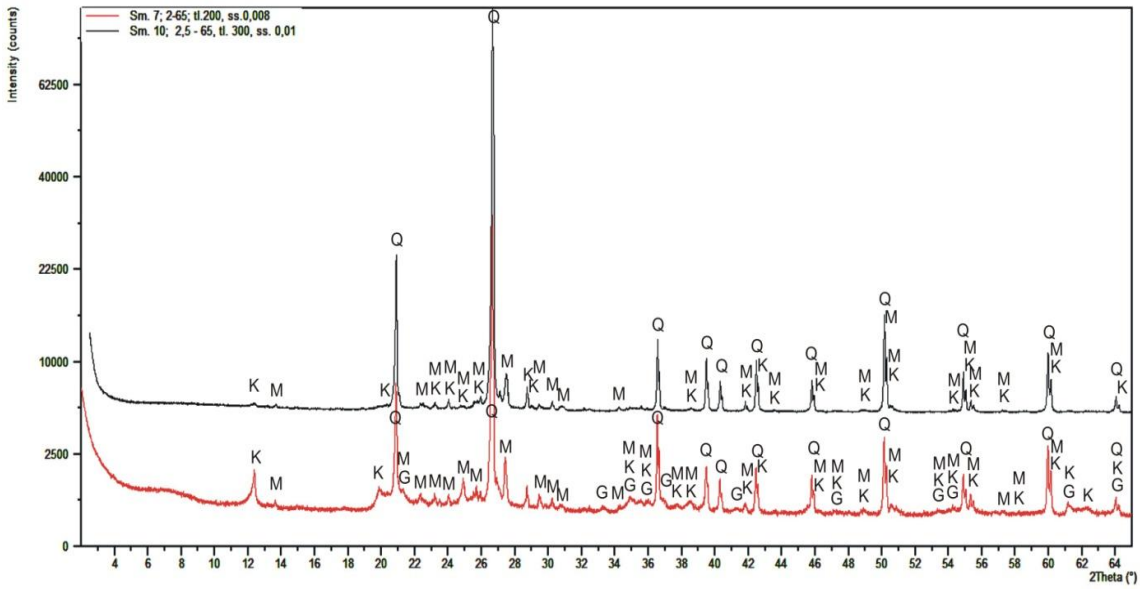



Figure 52: Measured XRD pattern (diffractogram) showing clay and other accessory minerals from mud volcanoes and saprolite at Pamadu (Sm 7 and 10) (The red line at the bottom is for the extruded mud, while the red line is for the saprolite)

In the Pamadu mud slurry (Sm 7, Figure 52), the mineral composition is dominated by quartz (approximately, 72%), orthoclase feldspar (approximately, 16%), clay minerals which include kaolinite (11%) and possibly disordered clay minerals (mixed-layered). There are also reflections of goethite (1-2%). While for the Pamadu saprolite (Sm 10, Figure 52), the mineral composition is dominated by quartz content - 87%; feldspars are mainly microcline (11%), low content of clay minerals (approximately, 1.5%), reappears reflection 3,108 Å (probably sylvite and/or barite). Kaolinite and microcline are relatively constant while the geothite is present in low concentration. The clay mineral association in the overburden material is also similar to that from the mud volcano, but it does not contain the goethite. The high value of quartz in both the saprolite and the mud slurry suggests the high quartz resistance to weathering. While feldspar and the mica usually weathers to clay minerals like kaolinite, as shown in Sm 8

and 9 (Figure 52). The presence of traces of goethite suggests weathering from Fe – Mg mineral.

**Jenye mud slurry and saprolite (Sm 8 and 9)**

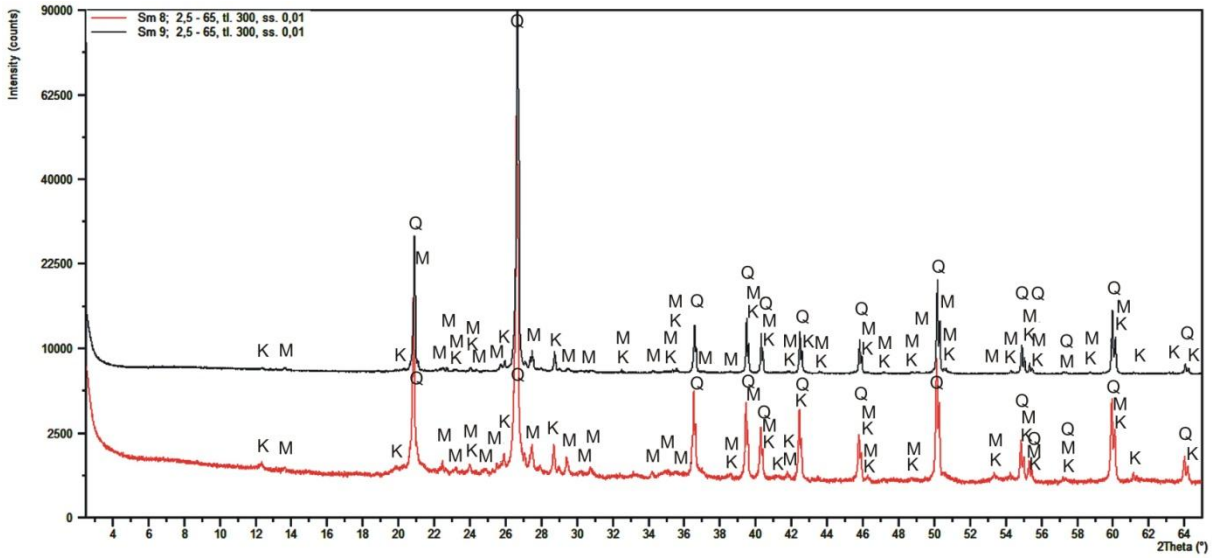



Figure 53: Measured XRD pattern (diffractogram) showing clay and other accessory minerals from mud volcanoes and saprolite at Jenye (Sm 8 and 9) (The red line at the bottom is for the extruded mud, while the red line is for the saprolite).

In the Jenye mud slurry (Sm 8, Figure 53); it was dominated by quartz with an average of 89%. There is also microcline (6-8%) and kaolinite (2-3%). Kaolinite and microcline are relatively constant. While in the Jenye saprolite (Sm 9, Figure 53), there is a lot of quartz in the amount of approximately 91%; the other ingredients are: microcline (8%), as well as small amounts of kaolinite and mixed-layered clay minerals. The clay mineral association in the overburden material is also similar to that from the mud volcano. The high value of quartz in both the saprolite and the mud slurry suggest the ability of the quartz resistance to weathering. While feldspar and the mica usually weathers to clay minerals like kaolinite as shown in Sm 8 and 9 (Figure 53). The presence of traces of goethite suggests weathering from Fe – Mg mineral.

## 4.6 Hydrochemistry of water from onshore mud volcanoes in the study area

The results of analysed physico – chemical parametrs, cationic and anionic concentration are shown in Table 11 and 12.

**Table 11: Physico - chemical parameters of water from onshore mud volcanoes in Nigeria**

| Location ID | Sample ID | pH | Temp °C | TDS mg/l | EC uS/cm | TH mg/l $Caco_3$ |
|---|---|---|---|---|---|---|
| Lakaturu | K 1 | 8.62 | 24.9 | 2729 | 2100 | 829 |
| Chengau | K 2 | - | 26.4 | 2717 | - | - |
| Jenye | K 3 | - | 25.8 | 4208 | - | - |
| Gujuba | K 4 | 8.73 | 22.1 | 3637 | 2400 | 1110 |
| Laturu | K 5 | 7.94 | 41.9 | 448 | 324 | 155 |
| Pamadu | K 6 | 8.01 | 22.8 | 776 | 256 | 108 |
| Kurum | K 7 | 8.58 | 25.6 | 2280 | 2430 | 979 |
| Todi | K 8 | 8.99 | 22.5 | 12757 | 2670 | 1180 |
| Sasanyi | K 9 | - | 22.0 | 653 | - | - |
| Lachikoltok | K 10 | 7.99 | 22.1 | 456 | 222 | 102 |
| Digga | K 11 | - | 26.2 | 2078 | - | - |
| Lashadar | K 12 | 8.53 | 25.5 | 1132 | 1150 | 478 |
| Lakomji | K 13 | - | 41.2 | 249 | | |
| Lallapido | K 14 | 8.70 | 26.1 | 1126 | 1770 | 713 |

**Table 12: Hydrochemical parameters analysed in water from onshore mud volcanoes in Nigeria**

| Location ID | Sample ID | $Ca^{2+}$ mg/l | $Mg^{2+}$ mg/l | $Na^{+}$ | $K^{+}$ mg/l | $HCO_{3-}$ mg/l | $CO_3^{2-}$ mg/l | $Cl^{-}$ mg/l | $SO_4^{2-}$ mg/l | Fe mg/l | $SiO_2$ mg/l |
|---|---|---|---|---|---|---|---|---|---|---|---|
| Lakaturu | K 1 | 32 | 2.75 | 781 | 29 | 1235 | 88.8 | 325 | 12.6 | 0.22 | 23.2 |
| Chengau | K 2 | 15 | 2.45 | 852 | 23 | 1501 | 168 | 123 | 13.9 | 4.56 | 14.4 |
| Jenye | K 3 | 10 | 1.19 | 1058 | 13 | 1747 | 137 | 202 | 12.6 | 0.26 | 9.49 |
| Gujuba | K 4 | 21 | 2.72 | 1178 | 18 | 1903 | 240 | 246 | 16.9 | 4.55 | 7 |
| Laturu | K 5 | 17 | 3.07 | 50 | 31 | 293 | 3 | 6 | 12.9 | 0.24 | 32 |
| Pamadu | K 6 | 22 | 7.82 | 188 | 20 | 495 | 3 | 5 | 12.5 | 0.67 | 22.2 |
| Kurum | K 7 | 35 | 10.4 | 688 | 41 | 1171 | 72 | 228 | 12.7 | 0.02 | 22.3 |
| Todi | K 8 | 17 | 20 | 4789 | 134 | 3111 | 2040 | 2625 | 13.2 | 0.13 | 8.12 |
| Sasanyi | K 9 | 46 | 4.67 | 84 | 9 | 415 | 3 | 48 | 13.2 | 2.23 | 28.4 |
| Lachikoltok | K 10 | 41 | 6.9 | 41 | 32 | 262 | 3 | 6 | 12.9 | 5.74 | 45.6 |
| Digga | K 11 | 8 | 1.16 | 600 | 14 | 1196 | 84 | 141 | 12.9 | 0.73 | 20.4 |
| Lashadar | K 12 | 13 | 1.43 | 310 | 17 | 647 | 3 | 98 | 13.4 | 0.22 | 30.2 |
| Lakomji | K 13 | 29 | 4.46 | 19 | 20 | 126 | 3 | 5 | 13.9 | 0.02 | 29.4 |
| Lallapido | K 14 | 15 | 3.66 | 327 | 21 | 561 | 72 | 100 | 14.4 | 0.07 | 12.4 |

From the results of the physic – chemical parameters as presented in Table 11 above, the temperature ranges from 22.9 to 25.1$^0$C in all the sampled locations except for Laturu and Lakomji with high temperature of 41.9$^0$C and 41.2$^0$C. The pH is highest at Todi with a value of 8.99, 8.73 at Gujuba, 8.70 at Lallapido, 8.62 at Lakaturu and 8.58 at Kurum. The lowest value of pH is at Lashikoltok with value of 7.89 and 7.94 at Laturu. The TDS is highest at Todi with a value of 12,757 mg/l, 2280 mg/l at Kurum, 3637 mg/l at Gujuba, 1126 mg/l at Lallapido and 2729 mg/l at Lakaturu. The lowest values are found in Lachikoltok, Pamadu and Laturu with concentration of 456 mg/l, 776 mg/l and 448 mg/l. The EC is highest at Todi with a value of 2670 uS/cm, 2430 uS/cm at Kurum, 2400 uS/cm at Gujuba, 2100 uS/cm at Lakaturu, 1770 uS/cm at lallapido and 1150 uS/cm at Lashadar. The lowest EC are found in Lashikoltok, Pamadu and Laturu with values of 222 uS/cm, 256 uS/cm and 324 uS/cm respectively. The TH is highest at Todi with a value of 1180 mg/l, 1110mg/l at Gujuba, 979 mg/l at Kurum,

829 mg/l at Lakaturu and 713 mg/l at Lallapido. The lowest TH is found in Pamadu, Lashikoltok and Laturu with values of 105 mg/l, 140 mg/l and 155 mg/l respectively.

Table 12 shows the concentration of Na is highest at Todi with a value of 4789 mg/l, 1178 mg/l at Gujuba, 1058 mg/l at Jenye, 852 mg/l at Chengau, 781 mg/l at Lakaturu, 688 mg/l at Kurum and 600 mg/l at Digga. The lowest concentration is found in Lakomji, Lashikoltok and Laturu with concentration of 19 mg/l, 41 mg/l and 50 mg/l. The concentration of K is highest at Todi with a value of 134 mg/l, 41 mg/l at Kurum, 32mg/l and 31 mg/l at Lachikoltok and Laturu. The lowest concentration of K is found in Sasanyi, Jenye and Digga with concentration of 9 mg/l, 13 mg/l and 14 mg/l respectively. The concentration of Ca is highest at Sasanyi with a value of 46 mg/l, 41mg/l at Lachikoltok, 35mg/l at Kurum, and 32mg/l at Lakaturu. The lowest concentration of Ca is found in Digga, Jenye, Lashadar and Lallapido with 8 mg/l, 10 mg/l, 13 mg/l and 15 mg/l respectively.

The concentration of Mg is highest at Todi with a value of 20 mg/l, 10.4 mg/l at Kurum, 7.82 mg/l at Pamadu 6.9 mg/l at Lachikoltok, 4.46 mg/l and 3.07 mg/l for Lakomji and Laturu. The lowest concentration of Mg is found in Digga and Jenye with 1.16 mg/l and 1.19 mg/l. The concentration of Fe is highest at Lachiukoltok with a value of 5.74 mg/l, 4.56 at Chengau, 4.55 mg/l at Gujuba and 2.23 mg/l at Sasanyi. The lowest concentration of Fe is found in Lakaturu, Lashadar, and Lakomji with 0.02 mg/l. O.02 mg/l at Kurum, 0.07 mg/l at Lallapido and 0.13 mg/l at Todi. The concentration of $HC0_3$ is highest at Todi with a value of 3111 mg/l, 1903 mg/l at Gujuba, 1747 mg/l at Jenye, 1501mg/l at Chengau, 1235mg/l at Lakaturu, 1196 mg/l at Digga and 1171 mg/l at Kurum. The lowest concentration of $HC0_3$ is found in Lakomji with values of 126 mg/l and 293 mg/l at Laturu. The concentration of Cl is highest at Todi with a value of 2625 mg/l, 325 mg/l at Lakaturu, 246 mg/l at Gujuba and 228 mg/l at Kurum. The

lowest concentration of Cl is found in Lakomji, Pamadu and Laturu with values of 6 mg/l, 5 mg/l and 6 mg/l respectively. The concentration of $C0_3$ is highest at Todi with a value of 2040 mg/l, 240 mg/l at Gujuba, 168 mg/l at Chengau and 137 mg/l at Jenye. The lowest concentration of $C0_3$ is found in Lakomji, Laturu, Lachikoltok and Pamadu with values of 3 mg/l each. The concentration of $S0_4$ is highest at Lallapido with a value of 2040 mg/l, 240 mg/l at Gujuba, 168 mg/l at Chengau and 137mg/l at Jenye. The lowest concentration of $S0_4$ is found in Pamadu, Lakaturu and Jenye with values of 12.5 mg/l for Pamadu and 12.6 mg/l for Lakaturu and Jenye.

### 4.5.1 The summary of hydrochemical parameters of water from mud volcanoes

The summary description of hydrochemical parameters of the physico – chemical parameters, cationic and anionic concentration in comparison with the W.H.O (2011) and N.I.S (2007) standards are shown in Table 13. Table 14 shows the ranges of the hydrochemial parameters in mud volcanoes within the Yolde Formation and Upper Bima Formation.

**Table 13: Comparison of the hydrochemical data analysed in water from all mud volcanoes in the study area (for Laboratory records, see Appendix A, see also Table 9) and NIS, (2007) and WHO, (2011) standards for drinking water**

| Parameter | Mud Volcanoes water | | | (WHO, 2011) recommended | (WHO, 2011) max permissible | NIS (2007) |
|---|---|---|---|---|---|---|
| | Min | Max | Average | | | |
| pH | 7.9 | 8.9 | 8.5 | 6.5 | 8.5 | 6.5 – 8.5 |
| TDS (mg/l) | 249 | 12757 | 2517.57 | 500 | 1000 | 500 |
| EC (uS/cm) | 222 | 2670 | 1480.22 | 250 | 1480 | 1000 |
| Temp (°C) | 22.9 | 40.7 | 25.97 | Variable | Variable | variable |
| TH (mg/l CacO3) | 102 | 1180 | 641.00 | 100 | 500 | 150 |
| $Ca^{2+}$ (mg/l) | 8.26 | 46.4 | 22.86 | 75 | 200 | - |
| $Mg^{2+}$(mg/l) | 1.16 | 20 | 5.19 | 50 | 150 | 0.2 |
| $Na^{+}$ (mg/l) | 18.6 | 4789 | 783.17 | | 200 | 200 |
| $K^{+}$ (mg/l) | 9.4 | 134 | 30.13 | 10 | 15 | - |
| $HCO_3^{-}$ (mg/l) | 126 | 3111 | 1047.35 | Variable | Variable | Variable |
| $CO_3^{2-}$ (mg/l) | 3 | 2040 | 224.36 | - | - | - |
| $Cl^{-}$ (mg/l) | 5 | 2625 | 297 | 250 | 600 | 250 |
| $SO_4^{2-}$ (mg/l) | 12.5 | 16.9 | 13.42 | 250 | 500 | 100 |
| Fe (mg/l) | 0.02 | 5.74 | 1.40 | 0.3 | 1.0 | 0.3 |
| SiO2 (mg/l | 7 | 45.6 | 21.794 | - | - | - |

**Table 14: Comparison of the physico–chemical characteristics of water from the mud volcanoes and the various geological formations excluding the warm springs**

| Parameters | Mud Volcanoes Water | | | Geological Formations |
|---|---|---|---|---|
| | Min | Average | Max | |
| pH | 7.99 | 8.73 | 8.4 | Yolde Formation |
| | 8.53 | 8.99 | 8.7 | Upper Bima Sandstone |
| TDS (mg/l) | 456 | 2729 | 1975 | Yolde Formation |
| | 1126 | 12757 | 5005 | Upper Bima Sandstone |
| EC (µS/cm) | 222 | 2430 | 1061 | Yolde Formation |
| | 1150 | 2670 | 1863 | Upper Bima Sandstone |
| Temp (°C) | 22.1 | 25.6 | 23.5 | Yolde Formation |
| | 22.5 | 26.1 | 24.7 | Upper Bima Sandstone |
| TH (mg/l $CaCO_3$) | 102 | 1110 | 626 | Yolde Formation |
| | 478 | 1180 | 790 | Upper Bima Sandstone |
| $Na^+$ (mg/l) | 188 | 1178 | 708 | Yolde Formation |
| | 310 | 4789 | 1808 | Upper Bima Sandstone |
| $K^+$ (mg/l) | 18 | 41 | 28 | Yolde Formation |
| | 17 | 134 | 57 | Upper Bima Sandstone |
| $Ca^{2+}$ (mg/l) | 8.26 | 46.40 | 22.86 | Yolde Formation |
| | 13 | 46 | 24.60 | Upper Bima Sandstone |
| $Mg^{2+}$(mg/l) | 2.72 | 7.82 | 6.10 | Yolde Formation |
| | 1.43 | 20 | 8.36 | Upper Bima Sandstone |
| ∑Fe (mg/l) | 0.02 | 5.74 | 2.24 | Yolde Formation |
| | 0.07 | 0.22 | 0.14 | Upper Bima Sandstone |
| $Cl^-$ (mg/l) | 5 | 325 | 162 | Yolde Formation |
| | 98 | 2625 | 941 | Upper Bima Sandstone |
| $HCO_3^-$ (mg/l) | 262 | 1903 | 1013 | Yolde Formation |
| | 561 | 3111 | 1439 | Upper Bima Sandstone |
| $CO_3^{2-}$ (mg/l) | 3 | 240 | 81.40 | Yolde Formation |
| | 3 | 2040 | 705 | Upper Bima Sandstone |
| $SO_4^{2-}$ (mg/l) | 12.5 | 16.9 | 13.5 | Yolde Formation |
| | 13.2 | 14.4 | 13.7 | Upper Bima Sandstone |
| $SiO_2$ (mg/l | 7.0 | 45.6 | 24.1 | Yolde Formation |
| | 8.12 | 30.2 | 16.9 | Upper Bima Sandstone |

**Table 15: Percentage of hardness of the water from the mud volcanoes in Upper Benue Trough and classification according to WHO (2011).**

| Hardness $CaCO_3$ (mg/l) | Water classification | Result of study | |
|---|---|---|---|
| | | % | Site and value of $CaCO_3$ (mg/l) |
| 0 – 60 | Soft | | |
| 61 – 120 | Moderately | 15% | Pamadu (108); Lachikoltok (102) |
| 121 – 180 | Hard | 5% | Laturu (155) |
| >180 | Very hard | 80% | Lakaturu (829); Gujuba (1110); Kurum (979); Todi (1180); Lashadar (478); Lallapido (713) |

The summary of their characteristics and average values in comparison with the NIS (2007) and WHO (2011) standards for drinking water are shown in Table 13. The total dissolved solids (TDS) ranged from 249 to 12757 mg/l; the high TDS are indications of high mineralized water with free migration history and water – rock reactions. pH ranged from 7.94 to 8.99 and indicate mineralised water because its alkaline has greatly influenced the dissolution and precipitation of minerals in the water from the mud volcanoes. Electrical conductivity (EC) ranged from 222 to 2670 µS/cm; total hardness ranged from 102 mg/l to 1180 mg/l. The W.H.O guideline for classification of hard water as shown in Table 15, shows that the water from the mud volcanoes are mainly very hard (80%), moderately hard 15 % and 5% hard.

Major and minor elements such as $Na^+$, $HCO_3^-$, $\Sigma Fe$ and $Cl^-$ were noticed to be higher than both the NIS (2007) and WHO (2011) recommended standards. The dominant cation in the water from the mud volcanoes is the $Na^+$ with values ranging from 18.6 mg/l to 4789 mg/l. This suggest the water from the craters of the mud volcanoes are issuing out from a zone of mineralised water because the concentration of $Na^+$ is far above the maximum permissible limit of W.H.O (2011). Also, the possible source of the high sodium in this water from the

mud volcanoes could be from weathered plagioclase feldspars and clays whereas the high value of bicarbonate might be due to atmospheric carbon dioxide and existing pH range of 8.00 to 8.90.

From the results in Table 14, the average value of the total dissolved solids (TDS) of water from mud volcanoes within the Yolde Formation is 1975 mg/l while that in the Upper Bima Sandstone is 5005 mg/l; pH average value of water from within the Yolde Formation is 8.4 while that in the Upper Bima Sandstone is 8.7; electrical conductivity (EC) average value of water from within the Yolde Formation is 1061 mg/l while that in the Upper Bima Sandstone is 1863 mg/l; total hardness (TH) average value of water from within the Yolde Formation is 626 mg/l while that in the Upper Bima Sandstone is 790 mg/l. The average value of the major and minor elements such as $Na^{+}$, $K^{+}$, $Ca^{2+}$, $Mg^{2+}$, $Cl^{-}$, $HCO_3^{-}$, $CO_3^{2-}$ and $SO_4^{2-}$ were noticed to be higher in the water from within the Upper Bima Sandstone while Fe and $SiO_2$ were noticed to be higher in the water from within the Yolde Formation.

The very high values of pH, TDS, TH, Sodium, Bicarbonate and Cloride from water sampled and analysed from mud volcanoes occurring in areas surrounded by Upper Bima Sandstone and high values in water from mud volcanoes occurring in areas surrounded by Yolde Formations as shown in Table 14, indicates that onshore mud volcanoes in the study area located within a transitional environment of marine and non – marine (Albian to Cenomanian). This could suggest that the waters are seeping out from the transition zone between the connate water of the stagnant belt and meteoric water of the dynamic belt and are mineralised with high alkalinity, hardness and salinity.

### 4.5.2 Water Type

The Major ions concentration in milli – equivalent per litre (meq/l) were calculated and useful in plotting the Piper (1944) trilinear diagram where the ions in milli – equivalent per litre are expressed in percentages of cations and anions (Figure 54). However, the Schoeller diagram (Figure 55) was plotted using the major ion concentrations in milli – equivalent per litre (meq/l).

The Piper (1944) trilinear diagram is used to infer hydrogeological facies. These plots include two triangles, one for plotting the concentration of major cations and the other for plotting the concentration of anions. The trilinear diagram is useful in bringing out chemical relationships among groundwater samples in more definite terms compared to other conventional plotting methods. It reveals the analogies, dissimilarities and different types of water in the area. Plots of hydrochemical parameters of the groundwater the Piper (1944) trilinear diagrams, shows that eighty percent (90%) of water samples from the area falls within the high alkaline proportion type predominantly bicarbonate and sodium. And ten percent (10%) belongs to the normal earth alkaline water proportion. The water characterisation shown by the Piper diagram, shows five (5) main water facies types namely; Na-$HCO_3$, $_{Na}$-$HCO_3$-Cl, Na-Ca-$HCO_3$, Na-Cl-$CO_3$--$HCO_3$ $_{and}$ Ca-Na-$HCO_3$ (Table 13). The Na-$HCO_3$, water facie type are about 75% , Na-$HCO_3$-Cl and Ca-Na-$HCO_3$ water facie types are about 10% each and the remaining Na-Ca-$HCO_3$ and Na-Cl-$CO_3$--$HCO_3$ water facie type together are about 5%. This water from the mud volcanoes was classified into Na – $HCO_3$ (dominant) and Ca-Na-$HCO_3$ (minor) waters.

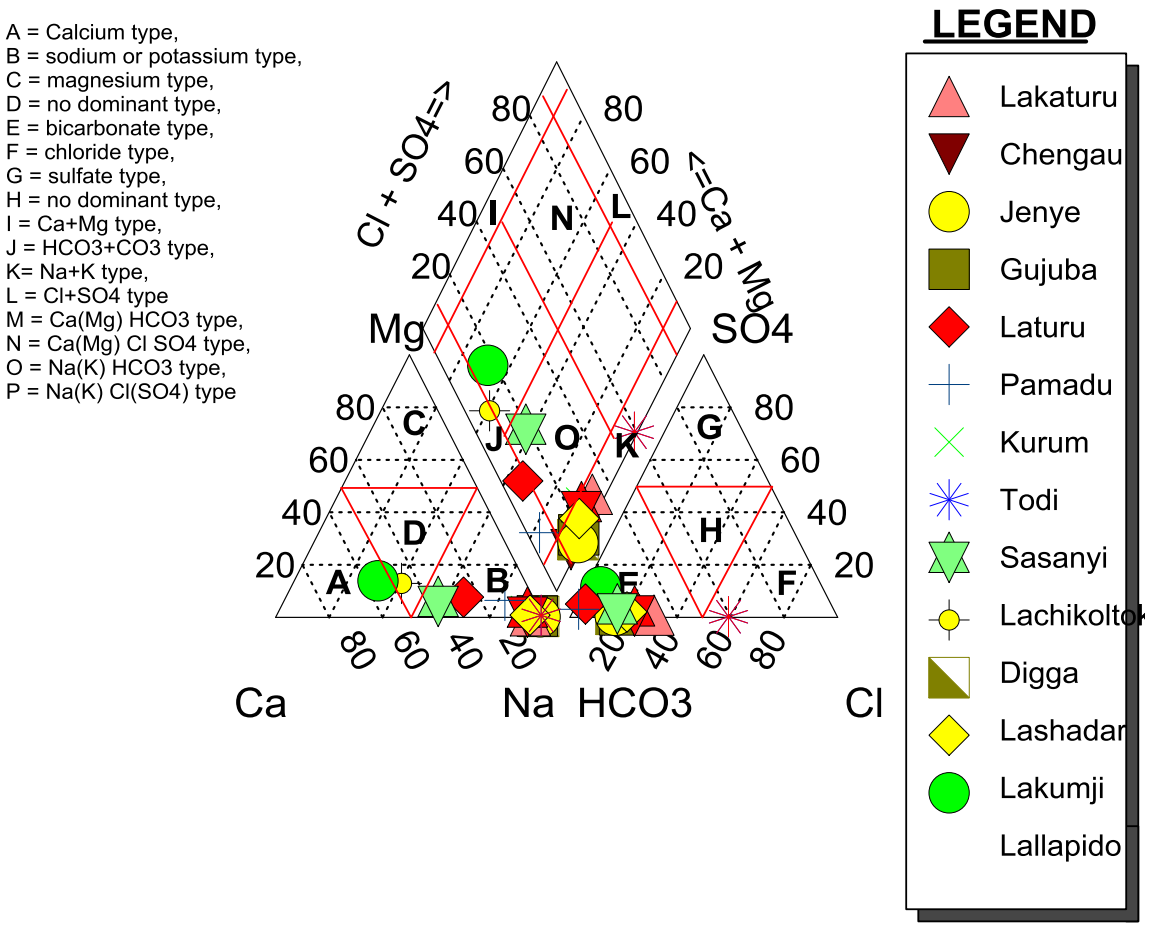



Figure 54: Piper trilinear diagram showing the hydrochemical facies (used for water classification based on the percentage of major ions in equivalents per million (Piper, 1964)

The Schoeller diagram represents the combination of major and minor constituents of groundwater in the study area. This is achieved using Schoeller's semi – logarithmic diagram from which water types are derived based on ionic concentration. The results obtained, also indicates five (5) main water facies types namely; Na-$HCO_3$, Na-$HCO_3$-Cl, Na-Ca-$HCO_3$, Na-Cl-$CO_3$--$HCO_3$ and Ca-Na-$HCO_3$ (Table 13).

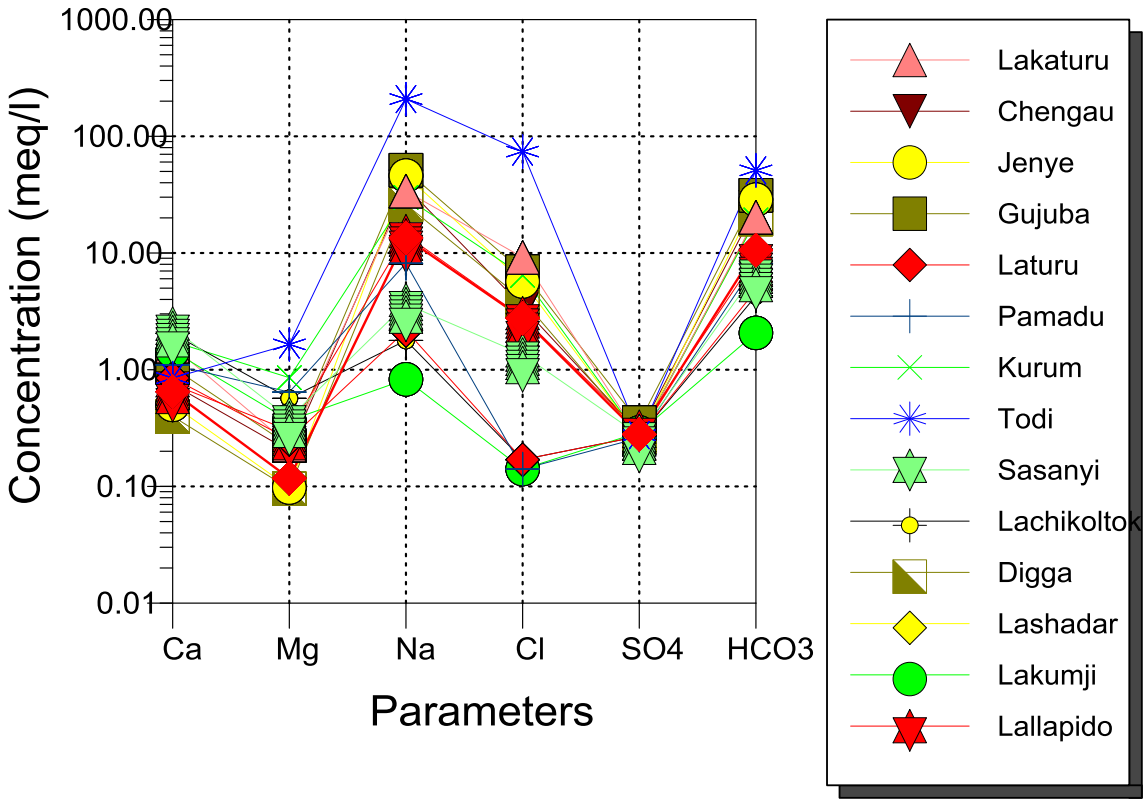



Figure 55: Schoeller diagram for water samples from the study area (Schoeller, 1964)

The Na-$HCO_3$, water type is the dominant water type. The $HCO_3$ is the most dominant among anions, followed by Cl and $SO_4$. On the side of the cations, prevailing cation is Na, followed by Ca and Mg. This plot again buttresses the composition of major cations and anions present from water samples in the study area, and shows that they are in consonance with results from the Piper diagram. The Schoeller diagram was plotted using the major ions concentration in milli – equivalent per litre (meq/l).

**Table 16: Classification of water type from the mud volcanoes in the study area**

| Location ID | Dominant cations | Dominant anions | Water type |
|---|---|---|---|
| Lakaturu | $Na^+$ | $HCO_3^-$, $Cl^-$ | Na- $HCO_3^-$- $Cl^-$ |
| Chengau | $Na^+$ | $HCO_3^-$ | Na- $HCO_3^-$ |
| Jenye | $Na^+$ | $HCO_3^-$ | Na- $HCO_3^-$ |
| Gujuba | $Na^+$ | $HCO_3^-$ | Na- $HCO_3^-$ |
| Laturu | $Na^+$ | $HCO_3^-$ | Na- $HCO_3^-$ |
| Pamadu | $Na^+$ | $HCO_3^-$ | Na- $HCO_3^-$ |
| Kurum | $Na^+$ | $HCO_3^-$, $Cl^-$ | Na- $HCO_3^-$- $Cl^-$ |
| Todi | $Na^+$ | $Cl^-$, $CO_3^{2-}$, $HCO_3^-$ | Na-Cl- $CO_3^{2-}$-$HCO_3^-$ |
| Sasanyi | $Na^+$, Ca | $HCO_3^-$ | Na-Ca- $HCO_3^-$ |
| Lachikoltok | Ca, $Na^+$ | $HCO_3^-$ | Ca-Na- $HCO_3^-$ |
| Digga | $Na^+$ | $HCO_3^-$ | Na- $HCO_3^-$ |
| Lashadar | $Na^+$ | $HCO_3^-$ | Na- $HCO_3^-$ |
| Lakomji | Ca, Na | $HCO_3^-$ | Ca-Na- $HCO_3^-$ |
| Lallapido | $Na^+$ | $HCO_3^-$ | Na- $HCO_3^-$ |

### 4.5.3 Correlation Analysis

**Table 17: Correlation matrix of hydrochemical data in the study area**

| | $Na^+$ | $K^+$ | $Ca^{2+}$ | $Mg^{2+}$ | ∑Fe | $Cl^-$ | $HCO_3^-$ | $CO_3^{2-}$ | $SO_4^{2-}$ | $SiO_2$ |
|---|---|---|---|---|---|---|---|---|---|---|
| **$Na^+$** | 1.00 | 0.90 | -0.26 | 0.75 | -0.13 | 0.98 | 0.90 | 0.96 | 0.06 | -0.58 |
| **$K^+$** | | 1.00 | -0.06 | 0.90 | -0.16 | 0.96 | 0.67 | 0.95 | -0.11 | -0.26 |
| **$Ca^{2+}$** | | | 1.00 | 0.20 | 0.30 | -0.17 | -0.37 | -0.22 | -0.13 | 0.55 |
| **$Mg^{2+}$** | | | | 1.00 | -0.13 | 0.82 | 0.48 | 0.80 | -0.18 | -0.14 |
| **∑Fe** | | | | | 1.00 | -0.19 | 0.00 | -0.16 | 0.43 | 0.17 |
| **$Cl^-$** | | | | | | 1.00 | 0.80 | 0.98 | -0.03 | -0.44 |
| **$HCO_3^-$** | | | | | | | 1.00 | 0.80 | 0.19 | -0.76 |
| **$CO_3^{2-}$** | | | | | | | | 1.00 | 0.01 | -0.43 |
| **$SO_4^{2-}$** | | | | | | | | | 1.00 | -0.42 |
| **$SiO_2$** | | | | | | | | | | 1.00 |

Statistical correlation analysis between the following parameters: $HCO_3^-$, K, $Ca^{2+}$, $Mg^{2+}$, ∑Fe, $Cl^-$, $CO_3^{2-}$, $SO_4^{2-}$ and $SiO_2$ (Table 14) was done to determine their sources. The statistical analysis done indicates positive correlation between $Na^+$– $K^+$ (0.9), $Na^+$– $Mg^{2+}$ (0.75), $Na^+$– $Cl^-$ (0.98), $Na^+$– $HCO_3^-$ (0.90), $Na^+$– $CO_3^{2-}$ (0.96), $K^+$– $Mg^{2+}$ (0.9), $K^+$– $Cl^-$ (0.96), $K^+$– $HCO_3^-$ (0.67), $K^+$– $CO_3^{2-}$ (0.95), $Mg^{2+}$– $Cl^-$ (0.82), $Mg^{2+}$– $CO_3^{2-}$ (0.80), $Cl^-$– $HCO_3^-$ (0.8), $Cl^-$– $CO_3^{2-}$ (0.98) and $HCO_3^-$– $CO_3^{2-}$ (0.8). On the other hand, there are negative relationships between $Na^+$– $Ca^{2+}$, K– $Ca^{2+}$, ∑Fe –Na, ∑Fe– $K^+$, $Ca^{2+}$– $Cl^-$, $Ca^{2+}$– $HCO_3^-$, $CO_3^{2-}$– $HCO_3^-$, $CO_3^{2-}$– $Ca^{2+}$ and $HCO_3^-$– $SiO_2$. Parameters with positive correlation suggest that the ions in the water are derived from the same source. On the other hand, those with the negative correlation have separate source from the previous ones.

Table 14, seems to indicate that the water from the mud volcanoes is of connate water from the stagnant belt, judging from high correlation coefficient between Na, K and Cl. Fluctuating coefficient of magnesium with other elements may result from admixture of meteoric water from the dynamic belt. The abundance of chemical concentrations in water from the mud volcanoes within the study area is in order of Na > K > Ca > Mg for the major cations and $HCO_3$ > Cl > $SO_4$ for the major anions. The water extruding from the mud volcanoes is classified into Na – $HCO_3$ (dominant) and Ca-Na-HCO3 (minor) waters. The Na – $HCO_3$ water type represents about 80% of the total water sample from the area with high alkaline proportion predominantly bicarbonate and Sodium.

As shown in Table 9, the temperature of water discharging from mud volcanoes in study area varies in range from 22.9 to 40.7 °C. However most of the measurements do not exceed the mean annual air temperature in the area, which is 26.5°C. Only at Laturu and Lakomji warm springs were high temperatures (41.9 and 41.2°C) noticed and these indicate thermal water flowing from the crater.

### 4.5.4 Classification of water from mud volcanoes as mineral water

The criteria for the chemical composition of mineral water based on the European Union water directive are shown in Table 18. The basis of classification is the total dissolved solids (TDS).

**Table18. Criteria for mineral waters in accordance with the EU mineral water Directive (Source: Van der Aa, 2003)**

| Mineral water type | Criterion |
|---|---|
| Very low mineral concentration mineral content | (TDS) < 50 mg/l |
| Low mineral concentration | TDS 50 - 500 mg/l |
| intermediate mineral concentration | TDS 500 - 1500 mg/l |
| High mineral concentration | TDS > 1500 mg/l |

**Table 19: Classification of water from mud volcanoes in the study area in accordance with the EU mineral water directive**

| Location ID | Sample ID | TDS mg/l | Mineral water type |
|---|---|---|---|
| Lakaturu | K 1 | 2729 | High mineral concentration |
| Chengau | K 2 | 2717 | High mineral concentration |
| Jenye | K 3 | 4208 | High mineral concentration |
| Gujuba | K 4 | 3637 | High mineral concentration |
| Laturu | K 5 | 448 | Low mineral concentration |
| Pamadu | K 6 | 776 | Intermediate mineral concentration |
| Kurum | K 7 | 2280 | High mineral concentration |
| Todi | K 8 | 12757 | High mineral concentration |
| Sasanyi | K 9 | 653 | Intermediate mineral concentration |
| Lachikoltok | K 10 | 456 | Low mineral concentration |
| Digga | K 11 | 2078 | High mineral concentration |
| Lashadar | K 12 | 1132 | Intermediate mineral concentration |
| Lakomji | K 13 | 249 | Low mineral concentration |
| Lallapido | K 14 | 1126 | Intermediate mineral concentration |

**Table 20: Classification system for mineral waters based on concentration of chloride (mg/l) (Source: Van der Aa, 2003)**

| Fresh-salt class | Chloride (mg/l) |
|---|---|
| Very oligohaline | < 5 |
| Oligohaline | 5-30 |
| Fresh | 30-150 |
| Fresh-brackish | 150-300 |
| Brackish | 300-1000 |
| Brackish-salt | 1000 – 10,000 |

**Table 21: Classification of mineral waters from mud volcanoes in the study area based on concentration of chloride (mg/l)**

| Location ID | Sample ID | Concentration of $HCO_{3-}$ mg/l | Concentration of $Cl^-$ mg/l | Fresh – Salt water class |
|---|---|---|---|---|
| Lakaturu | K 1 | 1235 | 325 | Brackish |
| Chengau | K 2 | 1501 | 123 | Fresh |
| Jenye | K 3 | 1747 | 202 | Fresh-brackish |
| Gujuba | K 4 | 1903 | 246 | Fresh-brackish |
| Laturu | K 5 | 293 | 6 | Oligohaline |
| Pamadu | K 6 | 495 | 5 | Oligohaline |
| Kurum | K 7 | 1171 | 228 | Fresh-brackish |
| Todi | K 8 | 3111 | 2625 | Brackish-salt |
| Sasanyi | K 9 | 415 | 48 | Fresh |
| Lachikoltok | K 10 | 262 | 6 | Oligohaline |
| Digga | K 11 | 1196 | 141 | Fresh |
| Lashadar | K 12 | 647 | 98 | Fresh |
| Lakomji | K 13 | 126 | 5 | Oligohaline |
| Lallapido | K 14 | 561 | 100 | Fresh |

According to the European Union water directive, the TDS in the range of 50 to 500 mg/l are classified as low mineral water while the TDS in the range of 500 to 1500 mg/l are classified as intermediate mineral waters. The water having TDS greater than 1500 mg/l is classified in most cases as highly mineralised water (Van der Aa, 2003). The World Health Organisation also gave a recommended value of TDS to be 500 mg/l and maximum permissible limit to be 1000 mg/l.

The content of TDS in the water from Todi, Jenye, Gujuba, Lakaturu, Kurum, Chengau and Digga, is greater than 1500 mg/l., so the mud volcano waters from these places can be classified as high mineral concentration (Table 19) (Figure 56). The waters from Pamadu, Sasanyi, Lashadar and Lalaipido can be classified as intermediate mineral concentration while the water from Lachikoltok, Laturu and Lakomji are classified as low mineral concentration.

The classification of mineral water can also be based on the chloride concentration which will also aid the classification based on the TDS (Table 20). Water with less than 5 mg/l chloride concentration is classified as very oligohaline water, water with 5 to 30 mg/l chloride concentration are classified as oligohaline water, water with 30 to 150 mg/l are classified as fresh water, water with 150 to 300 mg/l chloride concentration are classified as fresh – brackish water, water with 300 to1000 mg/l chloride concentration are classified as brackish water while water with 1000 to 10,000 mg/l chloride concentration are classified as brackish – salt water (Van der Aa, 2003).

Waters from mud volcanoes field at Todi and Kurum are highly mineralized mineral waters, containing chloride (greater than 200 mg/l). At Todi, the water is brackish salt, as the concentration of Cl is very high and is in the highest category within the fresh - salt water classes while Kurum water is of fresh -brackish type (Table 21) (Figure 57). The waters from

Laturu, Lachikoltok, Lakomji, Pamadu and Sasanyi have much lower mineralization. Waters from mud volcanoes field at Gujuba water is very/extremely hard, fresh-brackish mineral water containing bicarbonate, chloride and sodium. Waters from mud volcanoes field at Lakaturu water contains 325 mg/l of chloride, so it is brackish mineral water, containing bicarbonate, chloride and sodium. At Chengau and Jenye mud volcanoes field, the mineral waters are of type containing bicarbonate and sodium; Waters from mud volcanoes field at Jenye contains also more than 200 mg/l of chloride, so Jenye is fresh-brackish water and Chengau represents fresh type. Water from mud volcanoes at Lalapido field is very, or even extremely hard mineral water, containing sodium, classified as fresh water due to moderate concentration of Cl in range of 30 to150 mg/l. Water from mud volcanoes at Lashadar field is very hard, fresh water which contains bicarbonate and sodium. Comparison of the concentration of the chloride with the bicarbonate is shown in Figure 58.

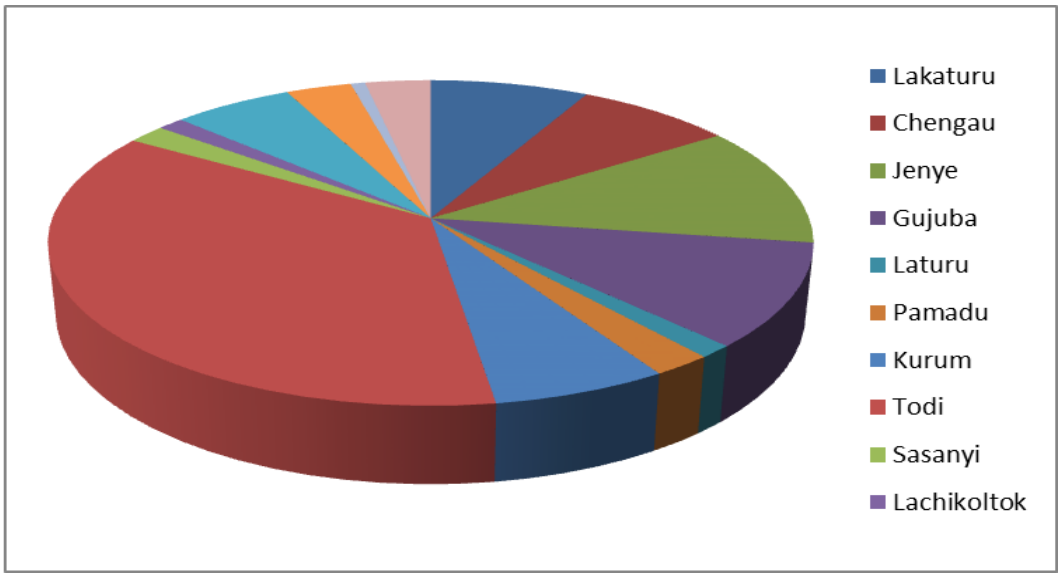



Figure 56: Pie chart showing classification of mineral water based on TDS for water samples from the study area

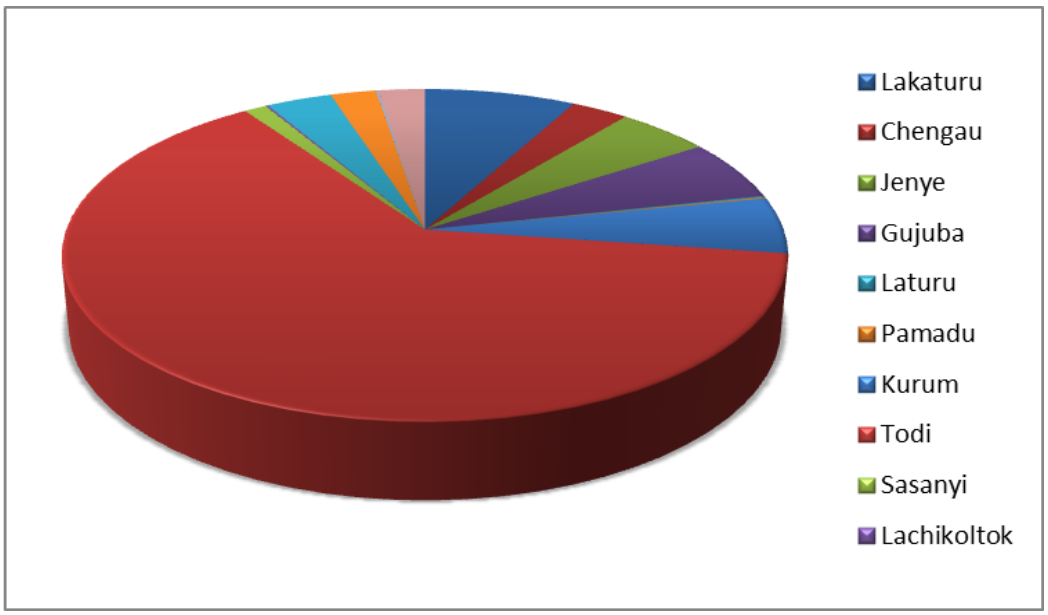



Figure 57: Pie chart showing the classification of mineral water based on Cloride for water samples from the study area

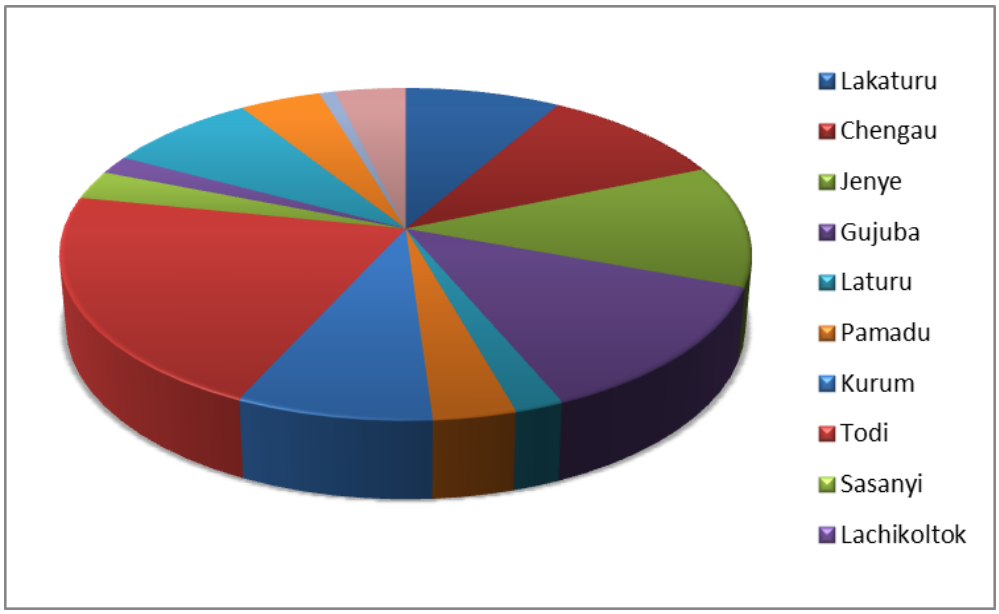



Figure 58: Pie chart showing the classification of mineral water based on Bicarbonate for water samples from the study area

# CHAPTER FIVE

# SYNTHESIS AND EVOLUTIONAL MODEL OF MUD VOLCANOES

## 5.1 Mud volcano morphology in the study area

Basic structure of the onshore mud volcano is formed by the escaping water through strike slip faults to the surface and carries along mud with lower density than the surrounding Cretaceous sedimentary succession. Slurry of water and mud are ejected in a cone feature to form volcanoes. Mud volcanoes form as fluidized argillaceous sediments of predominantly Yolde Formation, and water that are extruded along structural weaknesses (conduits) within the Upper Bima Sandstone.

The onshore mud volcanoes in the study area comprises of two morphological features as follows:

a) An external cone – like feature: Extruded slurry of mud and water from the crater of onshore mud volcanoes in the study area brought to the surface cones of varying sizes usually fractions of metres. The external morphology and expression of a mud volcano may vary almost indefinitely (Figure 59).

b) The internal feeder or conduit: The internal feeder or conduit is the major feature that brings extruded slurry of mud and water to the surface. The diameters of volcanic conduits may have a profound impact on mud volcanic activity (Figure 60).

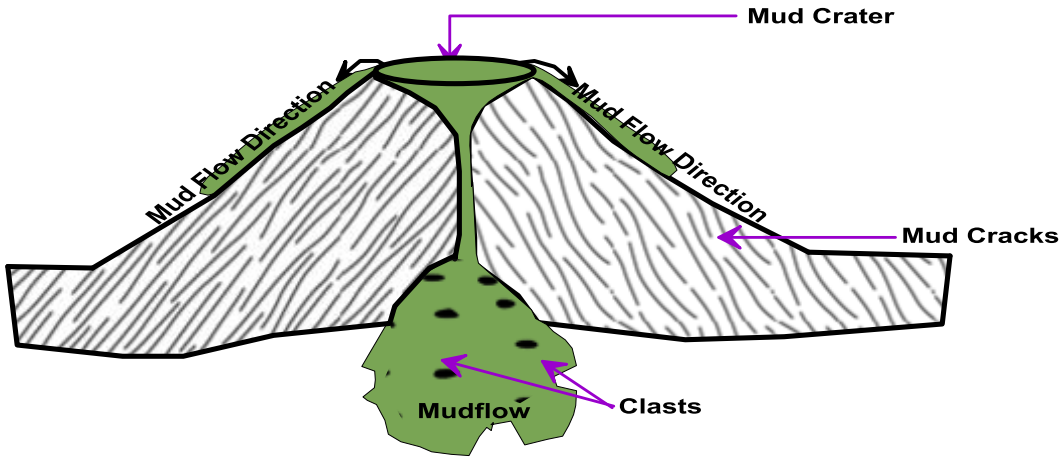



Figure 59: Schematic diagram showing the external morphology of a mud volcano in the study area

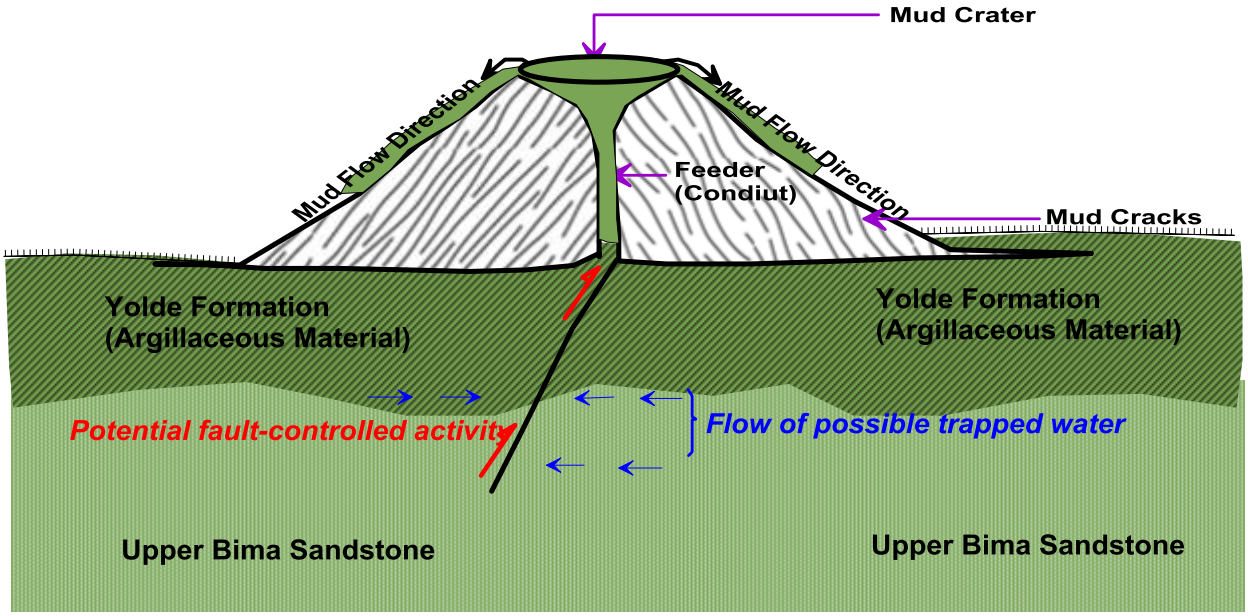



Figure 60: Schematic diagram showing the process of volcanic mud formation in the study area

## 5.2 Mechanisms of volcanic mud formation in the study area

The primary criterion for mud volcanism is the existence of traped water within the Cretaceous sediments of the Upper Benue Trough. The Yolde Formation is the argillaceous carrier beds that are being washed to the surface. The Yolde Formation reaches a maximum thickness of about 200 m but shows considerable lateral facies variation and has age limits between Late Albian and Late Cenomanian (Zaborski, 2003). Mud volcanic processes are initiated by the endogenetic events which triggers the extrusion of the mud slurry from the subsurface. The NE – SW trending Kaltungo serves as the main fault through which extrusion of slurry of mud and water from the onshore mud volcanoes in the study area is carried out. Offodile (1974) reported that the succession of marine, continental and transitional beds of Middle Albian to Maastrichtian age in the Benue valley, from all indications have undergone, at least three phases tectonic activity reported in Cenomanian, Santonianand post Maatrichtian times. When the subsurface overpressure reaches a threshold depth where the overburden weight is exceeded, fracturing and breaching of the uppermost units occur, sometimes facilitated by external factors such as earthquakes. The upward movement of the mud to surface is due to buoyancy and differential pressure (Mazzini *et al.*, 2009).

Though there has never been a reported case of earthquakes, however there are endogenetic events within the Upper Benue Trough. Earlier authors have reported the reactivation of major faults during the evolutionary history of the basin (Benkhelil, 1986; Maurin *et al.*, 1986 and Zaborski *et al*., 1998). Therefore, the occurrences of mud volcanoes around fault zones could possibly suggest manifestation of neotectonism in the study area. Eruption of mud volcanoes along the fault zones could also suggest a possible subsurface hydrogeological response to regional tectonic stress caused by abnormal pore pressure within the shallow aquifers around the study area.

Texturally, the sediments are fine to medium sands, moderately sorted to poorly sorted, fine skewed to coarse skewed and mesokurtic to very leptokurtic. The grain sizes suggest that the mud volcanoes in the study area are located on the Yolde Formation and the Upper Bima Sandstone.

Mineralogy of the sediments shows the presence of smectite and bentonite clay mineral in some samples of clay from the onshore mud volcanoes from in the study area. It indicates that the depositional environments for the mud volcanoes are transitional between non – marine Upper Bima Sandstone and marine Yolde Formation (albian to Cenomanian). The average temperature of the mud volcanoes is $24^0$C suggests that the ejected argillaceous materials are of predominantly clays from the Yolde Formation from shallow depth (tens of meters).

Hydrochemical composition of water from mud volcanoes in study area further shows that the groundwater seeping from the crater of the mud volcanoes can be interpreted as being mineralised with high alkalinity, hardness and salinity water ranges from fresh to brackish water which suggests the mixing of connate water from the Upper Bima Sandstone with meteoric water that infiltrates into the groundwater and seeps to the ground surface through the fault zones.

The origin of mud volcanoes is globally categorised as follows: (a) mud volcanoes *sensu stricto* linked with hydrocarbon gas release (Dimitrov, 2002; *fide:* Rukavičková and Hanžl, 2008); (b) hydrothermal mud volcanoes (Pitt and Hutchinson, 1982; *fide:* Rukavičková and Hanžl, 2008); (c) mud volcanoes as a manifestation of an earthquake or a sudden endogenetic event (Rogozhin *et al*., 2007; *fide:* Rukavičková and Hanžl, (2008).

Following after the classification of mud volcanoes by Rogozhin *et al.* (2007), onshore mud volcanoes found in the Upper Benue Trough, based on their sizes, heights, and nature, fall

within the origin of mud volcanoes resulting from the manifestation of earthquake or sudden endogenetic events. They observed that the argillaceous material ejected to the surface is derived from shallow depths, the height of this type of mud volcanoes reaches generally several decimetres, rarely above one metre; their diameter may attain several metres. This description is similar to the description of the mud volcanoes found in the study area. Furthermore, groups of small mud volcanoes found in NW Gobi and Altay, Mongolia as reported by Rukavičková and Hanžl (2008) are similar in size to the onshore mud volcanoes found in the study area. According to them, the origin of the mud volcanoes in NW Gobi and Altay is closely associated with the recent seismic activity in the area.

### 5.3 Similarities between onshore mud volcanoes in Nigeria and those in other parts of the world.

There are similarities between onshore mud volcanoes discovered on land in Nigeria and those on land in other countries such as India, Venezuela, Trinidad and Tobago, Mongolia and California in terms of their height, shape, size, precipitated salt, mud flow from the crater and dry mud. Obvious similarities exist between onshore mud volcanoes from Lakaturu and that of Trinidad and Tobago (Plates 33 and 58), Kurum and Baratang, Andaman Islands in India (Plates 38 and 59), Lallaipido and Monagas in Venezuela (Plates 11 and 60).



Plate 33: Photo of typical mud volcano in Lakaturu showing precipitated salt (0.5 m high, 1.4m of diameter)



Plate 58: The photo of similar mud volcano in Trinidad and Tobago showing precipitated salt (0.7 m high, 0.8m of diameter)(*https://en.wikipedia.org/wiki/File:Devil%27s_Woodyard*, *,2007*)



Plate 38: Photo of typical mud volcano in Kurum (0.9m high, 1.2 cm of diameter)



Plate 59: Photo of similar mud volcano in Baratang Andaman Islands and India (0.8m high, 1.2 of diameter)(*http://commons.wikimedia.org/wiki/File:Baratang_mud_volcano.jpg)*



Plate 11: Photo of typical mud volcano in Lallapido (0.8 high, 1.2 of diameter)



Plate 60: Photo of similar mud volcano in Monagas, Venezuela showing mud flow from the crater (0.4m high, 0.9 of diameter) (Source: *https://en.wikipedia.org/wiki/File:Volcan_de_lodo.jpg)*

# CHAPTER SIX

# SUMMARY, CONCLUSION AND RECOMMENDATION

## 6.1 Summary and Conclusion

The mud volcanoes are geological phenomena yet to be completely understood. Little has been published on mud volcanoes in Nigeria. They occur offshore of Nigeria, in the Niger Delta according to Graue (2000) and Heggeland (2001). This dissertation is the first information on the documentation of onshore mud volcanoes in Nigeria. The following results and conclusions are drawn from the present study:

a) Onshore mud volcanoes are being documented for the first time in this study in Nigeria and will hopefully be integrated into the world distribution and occurrence map of mud volcanoes.

b) Mud volcanoes found on land in Nigeria are located as fields and are structurally controlled. They occur along the NE – SW trending Kaltungo fault and other minor N – S and NW –SE trending faults. They also occur on N –S fault along the Dadiya syncline.

c) Granulometric analysis of the Cretacceous Bima and Yolde outcrop of sandstone around the mud volcanoes indicates that they are mostly fine to medium grained, poorly to moderately sorted, dominantly fine skewed to coarse skewed with strongly fine skewed, symmetrical skewed, dominantly very leptokurtic to leptokurtic with few mesokurtic.

d) About 57% of the onshore mud volcanoes documented in the study area are located on the Yolde formation, 29% of them are located on Upper Bima Sandstone while about 14% are located on the Pindiga Formation. The Yolde Formation is the transitional unit between the underlain continental Bima Sandstone and the overlain marine Pindiga Formation.

e) In Lashadar and Lakaturu, similarities of clays minerals from the mud volcanoes and the overburden saprolite, probably suggest that the argillaceous material that is been extruded out is at shallow depth, because it seems to be the same sediment (material); as deep as the depth of the soft overburden which was only extruded from tens of meters.

f) This study reveals the general hydrochemistry and quality of water issuing from the craters of the mud volcanoes found in the study area are highly alkaline (pH ranges from 7.94 to 8.99), saline (TDS ranges from140 to1620 mg/L), very hard (TH ranges from 102 to 1180 mg/L), and belong to five main hydrochemical types: Na-HCO3, Na-HCO3-Cl, Na-Ca-HCO3, Na-Cl-CO3- HCO3 and Ca-Na-HCO3. The Na-HCO3 hydrochemical type is dominant, representing about 80% of the total volcanic water from the area.

g) Most of the waters can be classified as mineral waters. Chemical content of the majority of mud volcano waters show that they may be transported to the surface from significant depths as the mineralization is high in most of them. These waters range from fresh to brackish water which suggests the mixing of connate water with meteoric water.

h) The Laturu and Lakomji warm springs have higher temperature of 41.9°C and 41.2°C. In this case we can say for sure that there is thermal water flowing from the crater There are volcanic remains (volcanic plugs) in the study area formed during Cenozoic volcanic and tectonic activity which suggests a possibility of deep magmatic body existence still subjecting to cooling and generating geothermal anomalies and could also suggest the possibility of the mud volcanoes having their origin from hydrothermal mud volcanoes.

i) These groups of mud volcanoes found onshore Nigeria, are characterised, as small mud or often sand volcanoes from which material ejected to the surface is derived from shallow depths, usually only a few tens of metres. The height of this type of mud volcanoes reaches generally several decimetres, rarely above one meter; their diameter may attain

several metres. These descriptions above are similar to mud volcanoes as a manifestation of an earthquake or a sudden endogenetic event as reported by Rogozhin *et al*., (2007).

j) Similarities exist between mud volcanoes discovered on land in Nigeria and those on land in India, Venezuela, Trinidad and Tobago, Mongolia and California in terms of their height, shape, size, precipitated salt, mud flow from the crater and dry mud.

k) Also, eruption of mud volcanoes along the fault line is one of several possible subsurface hydrogeological responses to regional tectonic stress as the dense fluid up flow is caused by abnormal hydrogeological pressure. Also, the ground water pressure increases in response to the increasing weight of the overburden and this is likely to have resulted in the emergence of mud volcanoes along areas of weaknesses such as faults and folds within the study area.

## 6.2 Recommendations

a) Encouragement of more research into the area of mud volcanoes both offshore and onshore in Nigeria.

b) Continuous awareness of the public through seminars and conferences on mud volcanism as most people are still not conversant with mud volcanoes

c) More detailed investigation on the documented mud volcanoes using seismic methods to determine their exact depth.

d) Further investigation is required to determine how active is the areas of occurrences of these mud volcanoes since they are mostly associated with faults using geophysics and other methods.

e) It is necessary to provide for most of these communities where the mud volcanoes are occurring, potable water to prevent them from using the water that seeps from the mud volcanoes for domestic purposes.

f) The problem of possible medicinal values of the mud volcano mineralized water should be recognized and this study suggests further balneogeological research to determine their most suited therapeutic use.

## References


Adegoke, O. S., Jan Du Chene, R. E., Agumanu, A. E. and Ajayi, P. O. (1978): Palynology and age of the Kerri Kerri Formation, Nigeria. *Revista Espanola Micropalaeontologia.* 10, 267-283.

Adegoke, O. S., Agumanu, A. E., Benkhelil, M. J. and Ajayi, P. O. (1986): New Stratigraphic, sedimentologic and structural data on the Kerri-Kerri Formation, Bauchi and Borno States, Nigeria. *Journal of African Earth Science,* 5(3), 249 – 277.

Akesson, M. (2008): Mud volcanoes – a review. Bachelor Thesis, Department of Geology, University of Lund, Sölvegatan 12, SE-223 62 Lund, Sweden

Allix, P. (1983): Environments mésozoïques de la partenord – orientale du fossé de la Bénoué (Nigéria). Stratigraphie, sédimentologie, évolution géodynamique – *Travanx laboratoire. Sciences Terre, Marseille St. Jérôme*, (B), 21, 1 – 200.

Ayok, J. (2012): Stratigraphy of the eastern Gongola Basin, north – eastern Nigeria, with special emphasis on the Turonian Gulani Formation. Unpublished Ph.D thesis submitted to the Department of Geology, Ahamadu Bello University Zaria.

Ayok, J., Zaborski, P.M., Hamza, H. and Danbatta, U.A., (2014): The Gulani Formation (Turonian) in the eastern Gongola Basin, north – eastern Nigeria: a re – evaluation of the lithostratigraphic status, *Journal of Mining and Geology*, 36(2), 153 – 173.

Ayoola, E. O. (1981): Paleocurrent and sedimentological studies in the Benue Trough, Nigeria. *Sedimentary Geology* 28, 153–162.

Arkhangelski, A. (1932): Some words about genesis of mud volcanoes on the Apsheron Peninsula and Kerch–Taman area, Bull. MOIP, Ser. Geol. 3 (3), 269–285 (in Russian).

Audley - Charles, M. (1968): The geology of Portuguese Timor, *Mem. Geol. Soc. London*, *4*, 1– 76.

Barber, W., Tait, E. A. and Thompson, J. D. (1954): The geology of the lower Gongola. *Annual Report Geological Survey Nigeria* 1952-1953, 18-20.

Benkhelil, J. (1982): Benue Trough and Benue Chain. *Geological Magazine*, 11, 155 – 198.

Benkhelil, J. (1985): Geological map of part of the Upper Benue Valley, on scale 1:100,000, with explanatory note. Elf Nigeria Ltd., Lagos. Nigeria.

Benkhelil, J. (1986): Structure et évolution géodymaique du basin intracontinental de la Bénoué (Nigéria). *Thèse doctorat, Université de Nice*, 230 p.

Benkhelil, J. (1987): Cretaceous deformation, magmatism and metamorphism in the Lower Benue Trough, Nigeria. *Geological Journal*, **22**: 467-493.

Benkhelil, J. (1988): Structure et évolution géodynamique du basin intracontinental de la Bénoué Nigria). *Bulletin Centres Recherches exploration-Production Elf-Aquitaine* 12, 29-128.

Benkhelil, J. (1989): The origin and evolution of the Cretaceous Benue Trough, Nigeria. *Journal of African Earth Science*, 8, 251 – 282.

Benkhelil, J. and Robineau, B. (1983): La fossé de la Bénoué est-il un rift? *Bulletin centres Recherches Exploration-Production Elf-Aquitaine* 7, 315-321.

Benkhelil, J. Dainelli, P., Pensard, J. F., Popoff, M. and Saugy, L. (1988): The Benue Trough: Wrench fault related basin on the border of the equatorial Atlantic. *In Triassic-Jurassic rifting, continental break and the origin of the Atlantic Ocean and Passive margins*, part B (Edited by Manspeizer, W) 787-819. Elsevier, Amsterdam.

Binks, R. M. and Fairhead, J. D. (1992): A Plate Tectonic Setting for Mesozoic rifts of West and Central Africa. *Tectonophysics* **213**, 141-151.

Birchwood, K. M. (1965): Mud volcanoes in Trinidad, *Inst. Pet. Rev., 19*, 164–167.

Blumer, E. (1922): *Die Erdöllagerstätten*, pp. 63–68, Enke Verlag, Stuttgart, Germany.

Bob, B. (2009): He, Two-dimensional x-ray diffraction, John Wiley and Sons, 2009 – 426.

Braide, S. (1992): Tectonic origin of preconsolidation deformation, Bima Sandstone, Yola Basin, Benue Trough. *Bulletin Nigerian Association Petroleum Explorationists* 7, 39-45.

Brown, K.M. (1990): The nature and hydrogeologic significance of mud diapirs and diatremes for accretionary systems. J. Geophys. Res. 95, 8969–8982.

Bryan, K. (1919): Classification of springs. Journal of Geology 27: 552-561.

Burke, K., Dessauvagie, T. F. J. and Whiteman, A. J. (1971): Opening of the Gulf of Guinea and geological history of the Benue depression and Niger Delta. *Nature* 233, 51-55.

Burke, K. C., Dessauvagie, T. F. J. and Whiteman, A. J. (1972): Geological history of the Benue valley and adjacent areas. In: African Geology (Edited by Dessauvagie, T.F.J. and Whiteman, A. J.), pp. 187-205. Ibadan University Press, Ibadan, Nigeria.

Burke, K. and Dewey, J. F. (1973): Plume-generated triple junctions: key indicators in applying plate tectonics to old rocks. *Journal Geology* 81, 406-433.

Burke, K. and Dewey, J. F. (1974): Two plates in Africa during the Cretaceous? *Nature* 249, 313-316.

Busson, G. (1972): Principes, méthods et résultants d'une étude stratigraphique du Mésozoïque saharien. *Mém. Mus. Natl. Hist. nat.* (Paris) (n.s.), 26, 1-441.

Carter, J. D., Barber, W., Tait, E. A. and Jones, G. P. (1963): The Geology of Parts of Adamawa, Bauchi and Borno Provinces in north-eastern Nigeria. *Bulletin of the Geological Survey of Nigeria,* 30, 1 – 108.

Chhibber, H. L. (1934): The Geology of Burma. Macmillan, NY, 528 pp.

Chiodini, G., D'Alessandro, W. and Parello, F. (1996): Geochemistry of gases and waters discharged by the mud volcanoes at Paterno, Mt. Etna (Italy), *Bull. Volcanol., 58*, 51–58.

Cratchley, C. R. and Jones, G.P. (1965): An interpretation of the geology and gravity anomalies of the Benue Valley, Nigeria. *Overseas Geological Surveys Geophysical Paper* 1, 1-26.

Deecke, W. (1897): Ober die Sicilianischen Schlammvu1kane. Globus LXXI/5.

Dike, E. F. C. (1995): Stratigraphy and structure of Kerri–Kerri Basin, north-eastern Nigeria. *Journal of Mining and Geology*, 29(2), 77 – 92.

Dikouma, M. S. (1994): Fluctuations du niveau marin au Maastrichtien et au Paléocène dans le basin intracratonique des Iullemmeden (Niger occidental). Biochronologie et dynamique des corps sédimentaires. *Africa Geoscience Review* 1, 283-417.

Dimitrov, L. I. (2002): Mud volcanoes – the most important pathway for degassing deeply buried sediments. *Earth-Science Reviews 59*, 49-76.

Dimitrov, L. I. (2003): Mud volcanoes – a significant source of atmospheric methane. *Geo-Marine Letters* 23, 155-161.

Fairhead, J. D. (1988): Mesozoic Plate Tectonics reconstructions of the central South Atlantic Ocean: the role of the West and Central African rift system. *Tectonophysics* 155, 181-192.

Fairhead, J. D. and Green, C. M. (1989): Controls on rifting in Africa and the regional tectonic model for Nigeria and Niger rift basins. *Journal of African Earth Sciences* 8, 231-249.

Falconer, J. D. (1911): *The Geology and Geography of northern Nigeria*. Macmillan, London, 295pp.

Federal Survey of Nigeria (1975): *Topographic maps, 1: 50,000, Sheet 173, Kaltungo N.W. and S.W.* First edition, Printed by Federal Surveys, Lagos, Nigeria.

Folk, R. L. and Ward, W. (1957): Brazos River bay: a study in the significance of grain size parameter. *Journal of Sedimentary Petrology*, **27**: 3-26.

Fowler, S. R., Mildenhall, J., Zalova, S., Riley, G., Elsley, G., Desplanques, A. and Guliyev, F. (2000): Mud volcanoes and structural development on Shah Deniz. J Petrol Sci Eng 28:189–206.

Gansser, A. (1960): Ueber Schlamvulkane und Salzdome (On mud volcanoes and salt domes). Mitt. Geol. Inst. Eidg. Tech. Hochsch. Univ. Zurich, Ser. B, 15, 46 pp.

Garàcia, E., Danobeitia, J. and Verges, J. (2003): Mapping active faults offshore Portugal (36°N – 38°N): implications for seismic hazard assessment along the southwest Iberian margin. Geol. 31(1): 83–86.

Gardner, J. M. (2000): Gulf of Cadiz /Moroccan margin, mud diapirism and mud volcanism study, introduction and geological setting. In Kenyon NH, Ivanov MK, Akhmetzhanov AM and Akhmanov GC: Multidisciplinary Study of the Geological Processes on the North East Atlantic and Western Mediterranean Margins. IOC Technical Series 56, UNESCO, p. 101.

Genik, G. J. (1993): Petroleum Geology of Cretaceous–Tertiary rift basins in Niger, Chad and Central African Republic. *Bulletin of the American Association of Petroleum Geologists*, 77, 1405 – 1434.

Goubkin, I. and Federov, S. (1940): Mud volcanoes of the USSR in connection with oil and gas prospects. Proc. 27th Int. Geol. Congr., Moscow 4, 33– 67 (in Russian).

Guiraud, M. (1989): Geological map of part of the Upper Benue Valley (scale 1:150,000) (with explanatory note). Elf Nigeria Ltd, Lagos, Nigeria.

Guiraud, M. (1990a): Mécanisme deformation du basin sur décrochements multiples de la Haute-Bénoué (Nigéria); facies et géometrie des corps sédimentataires, microtectonique et déformations synsédimenaires. *Mémoir d'Habilitation, Université de Montpellier, France*.

Guiraud, M. (1990b): Tectono-sedimentary framework of the Early Cretaceous continental Bima Formation (Upper Benue Trough, (NE) Nigeria). *Journal of African Earth Science*, 10, 341 – 353.

Guiraud, M. (1991a): Mécanisme de formation du basin crétacé su decrochements multiples de la Haute-Bénoué (Nigéria). *Bulletin Centres Recherches Exploration-Production Elf-Aquitaine* 15, 11-67.

Guiraud, M. (1991b): Reorientation de la contrainte horizontal $\sigma 1$ sur decrochements. Un exemple ; les decrochements senestres NE-SW du bassin de la Haute-Bénoué (NE Nigéria). *Comptes Rendus Academié Sciences Paris* (II) 313, 929-936.

Guiraud, M. (1993): Late Jurassic rifting-Early Cretaceous rifting and Late Cretaceous transpressional inversion in the Upper Benue Basin (NE Nigeria). *Bulletin Centres Recherches Exploration-Production Elf-Aquitaine* 17, 371-383.

Guiraud, R. and Bosworth, W. (1997): Senonian basin inversion and rejuvenation of rifting in Africa and Arabia: synthesis and implications to plate – scale tectonies. *Tectonophysics*, 282, 39 – 82.

Guiraud, R. and Maurin, J. C. (1991): Le rifting en Afrique au Crétacé inférieur : synthèse structurale, mise en évidence de deux étapes dans la genèse des bassins, relations avec les ouvertures océaniques péri-africaines. *Bulletin Société Géologique France* 162, 811-823.

Guiraud, R. and Maurin, J. C. (1992): Early Cretaceous Rifts of Western Central Africa: an Overview. *Tectonophysics*, 213; 153-168.

Gutscher, M. A., Dominguez, S., Westbrook, G., Gente, P., Babonneau, N., Miranda, T., Mulder, E., Gonthier, R., Bartolome, Luis, J. and Rosas, F. (2007): Tectonic shortening and gravitational spreading in the Gulf of Cadiz accretionary wedge: results from bathymetric swath mapping and seismic surveys Geophysical Research, vol. 9.

Grant, N. K. (1971): The South Atlantic, Benue Trough and Gulf of Guinea Cretaceous triple junction. *Bulletin of the Geological Society of America*, 82, 2295 – 2298.

Grant, N. K., Rex, D. C. and Freeth, S. J. (1972): Potassium – argon ages and strontium isotope ratio measurements from volcanic rocks in northeastern Nigeria. *Contributions Mineralogy Petrolog*y 35, 277 – 292.

Graue, K. (2000): Mud volcanoes in deep water Nigeria. *Marine and Petroleum Geology 17*, 959-974.

Hamidu, I., Zaborski, P.M., and Hamza, H. (2013): A review of the Campanian to Maastrichtian lithostratigraphic succession in the Cretaceous Gongola Basin of North – East Nigeria. *Journal of Mining and Geology*, 49(2), 145 – 160.

Harrison, 1.V. (1944): Mud volcanoes on the Makran coast. Geogr. 103 (4), 180-181.

Hedberg, H. D. (1974): Relation of methane generation to undercompacted shales, sale diapirs, and mud volcanoes. AAPG Bull. 58 (4), 661–673.

Hedberg, H. D. (1980): Methane generation and petroleum migration. In: Roberts III, W.H., Cordell, P.J. (Eds.), Problems of Petroleum Migration. AAPG Stud. Geol., vol. 10, pp. 179– 206.

Heggland, R., Nygaard, E., Gallagher, J. W. (2001): Techniques and experiences using exploration 3D seismic data to map drilling hazards, *Offshore Technology Conference, OTC 7968*, 119–127.

Hem, J. D. (1970): Study and investigation of the chemical characteristics of natural water. 2nd edition, U.S. Geological Survey Water Supply Paper 1473, 363p.

Hem, J. D. (1991): Study and interpretation of chemical characteristics of natural water: Book 2254, 3rd edition. Scientific publishers, Jodhpur India, 263p.

Higgins, G. E. and Saunders, J. B. (1973): Mud volcanoes—their nature and origin; contribution to the geology and paleobiology of the Caribbean and adjacent areas. Verh. Naturforsch. Ges., Basel 84,101– 152.

Hovland, M., Gallagher, J.W., Clennell, M. B. and Lekvam, K. (1997): Gas hydrate and free volumes in marine sediments: example from Niger Delta front. Mar. Pet. Geol. 14 (3), 245– 255.

*https://en.wikipedia.org/wiki/File*:Baratang_mud_volcano.jpg (14/07/2013): Mud volcanoe in Barang Island.

*https://en.wikipedia.org/wiki/File*:Devil%27s_*Woodyard_Dec,2007.jpg* (14/07/2013): Mud volcano in Trinidad and Tobago .

*https://en.wikipedia.org/wiki/File:Volcan_de_lodo.jpg* (14/07/2013): Yagrumito mud volcano in Monagas, Venezuela.

Ivanov, M. K., Limonov, A. F. and Van Weering, T. C. E. (1996): Comparative characteristics of the Black Sea and Mediterranean Ridge mud volcanoes. Mar. Geol. 132, 253– 271

Jakubov, A. A., Ali-Zade, A. A. and Zeinalov, M. M. (1971): Mud volcanoes of the Azerbaijan SSR: atlas (in Russian). Azerbaijan Academy of Sciences, Baku, 258 pp

Jones, B. (1932): The geology of southern Bornu. *Annual Report Geological Survey Nigeria 1931*, 9-14.

Jones, G. P. (1961): Sedimentary structures in the Bima Sandstone. *Records Geological Survey Nigeria,* 1959, 5-14.

Judd, A. (2005): Gas emissions from mud volcanoes; In: *Mud volcanoes, geodynamics and seismicity.* Proceedings of the NATO Advanced Research Workshop on Mud Volcanism, Geodynamics and Seismicity. Baku, Azerbaijan 20-22 May 2003. The Springer Verlag, Amsterdam.

Kalinko, M. (1964): Mud volcanoes, reasons of their origin, development and fading. VNIGRI 40, 30–54 (in Russian).

Keilhack, K. (1912): Lehrbuch der Grundwasser und Quellenkunde, Berlin.

Kholodov, V. N. (2002): Mud volcanoes, their distribution regularities and genesis; communication 1. Mud volcanic provinces and morphology of mud volcanoes. Lithol Miner Res 37: 197–209.

King, L. C. (1950): Speculation on the outline and the mode of distruption of Gondwanaland. *Geological Magazine* 87, 353-359.

Kirk, B. (1919): Clasification of springs. *The Journal of Geology, vol. 27, No. 7, pp. 522 – 561.*

Kogbe, C. A. (1979): Geology of the south-eastern (Sokoto) sector of the Iullemmeden Basin. Bulletin, Department of Geology, Ahmadu Bello University, Zaria, Nigeria 2(1), xv+ 420 pp

Kogbe, C. A. (1981): Attempt to correlate the stratigraphic sequence in the Middle Benue Basin with those of the Anambra and Upper Benue Basins. *Earth Evolution Sciences* 2, 139-143.

Kopf, A. J. (2002): Significance of mud volcanism. *Reviews of Geophysics 40 (2).*

Kugler, H. G. (1933): Contribution to the knowledge of sedimentary volcanism in Trinidad. Journal of the Institute of Petroleum Technology 19, 743–760.

Kugler, H.G. (1939): Visit to Russian oil districts. J. Inst. Pet. 25 (184), 68-88.

Lawal, O. (1982): Biostratigraphie, palynologie et paléo-environments des formations crétacées de la Haute – Bénoué, Nigéria north-Oriental. Thèse de Doctorat de Specialité, Université de Nice, 198pp.

Lawal, O. and Moullade, M. (1986): Palynological biostratigraphy of Cretaceous sediments in the Upper Benue Basin. *Revista de Micropalaeontology*; 29, 61 – 83.

Mhammedi N. A., El Moumni B., El Hmaidi A., Raissouni A. and El Arrim, A. (2008): Mineralogical and geochemical study of mud volcanoes in north Moroccan Atlantic margin, *African Journal of Environmental Science and Technology* 2 (11), 387-396.

Maurin, J. C., Benkhelil, J. and Robineau, B. (1986): Fault rocks of the Kaltungo lineament, north – eastern Nigeria, and their relationship with Benue Trough tectonics. *Journal of Geological Society of London*, 143, 587 – 599.

Maurin, J. C. and Guiraud, M. (1989): Relations entre tectonique et sédimentation dans les basins barrémo-aptiens du Nord Cameroun. *Comptes Rendus Académie Sciences Paris* (II) 308, 787-792.

Maurin, J. C. and Guiraud, R. (1990): Relationships between tectonics and sedimentations in the Barremo - Aptian intracontinental basins of northern Cameroon. *Journal African Earth Sciences* 10, 331-340.

Mascle, J., Blarez, E. and Mariho, M. (1988): The shallow structures of the Guinea and Ivory-Coast – Ghana transform margins: their bearing on the Equatorial Atlantic Mesozoic evolution. *Tectonophysics* 155, 193-209.

Mazzini, A., Nermoen, A., Krotkiewski, M., Podladchikov, Y.Y., Planke, S., Svensen, H., 2009. Strike-slip faulting as a trigger mechanism for overpressure release through piercement structures. Implications for the LUSI mud volcano, Indonesia. Marine and Petroleum Geology 26, 1751–1765.

Meister, C., Alzouma, K., Lang, J. and Mathey, B. (1992): Les ammonites du Niger (Afrique occidentale) et la transgression transsaharienne au cours du Cénomanian-Turonien. Geobios 25, 55-100.

Milkov, A. V. (2000): Worldwide distribution of submarine mud volcanoes and associated gas hydrates. *Marine Geology 167*, 29-42.

Mrazec, M. L. (1915): Les plis diapirs et le diapirisme en ge´ne´ral. Comptes Rendus des Se´ances, Institut Ge´ologique de Roumanie, 4, 226–270.

N.I.S, (2007): Nigerian Standard for Drinking Water Quality, Nigerian Industrial Standard NIS 554:2007. Approved by Standard Organization of Nigeria, ICS 13.060.20, 30p

Obaje, N.G. (2009): *Geology and Mineral Resources of Nigeria*, Lecture Notes in Earth Sciences 120, DOI 10.1007/978-3-540-92685-6 1, Springer-Verlag Berlin Heidelberg

Offodile, M. E. (1976): The geology of the Middle Benue, Nigeria. *Special Volume Palaeontological Institution University Uppsala*, 4: 1-166.

Offodile M. E. (1984): The geology and tectonics of Awe brine field. Journal of African Earth Sciences, Vol. 2, No. 3, pp. 191 – 202.

Ojo, O. M. and Pinna, P. (1982): Palaeogeographical and structural evolution of the Benue Trough of Nigeria. *Cretaceous Research* 3, 195-207.

Paine, W. R. (1968): Recent peat diapirs in the Netherlands: A comparison with Gulf Coast salt structures, in *Diapirism and Diapirs*, edited by G. Braunstein and G. D. O'Brien, *AAPG Mem., 8*, 271–274.

Panahi B. (2005): Mud volcanism, geodynamics and seismicity of Azerbaijan and the Caspian Sea region, In; Martinelli G, Panahi B (eds) Mud Volcanoes, Geodynamics and Seismicity.NATO Sci Ser 51, Springer, Amsterdam, pp 89–104.

Pascoe, E.H. (1912): The oilfields of Burma. Mem. Geol. Surv. India, Miner. 8, 251-256.

Petters, S. W. (1978): Mid-Cretaceous paleoenvironments and biostratigraphy of the Benue Trough, Nigeria. *Bulletin Geological Society America* 89, 151-154.

Pitt, A.M. and Hutchinson, R.A. (1982): Hydrothermal changes related to earthquake activity at Mud Volcano, Yellowstone National Park Wyoming, Journal of Geophysical Research, 87(B4): 2762–2766.

Pitt M. W. and Alfaro C. (2001): Geologic / hydrogeological setting and classification of springs in Springs and Bottled Waters of the World: Ancient History, Source, Occurrence edited by Philip E. LaMoreaux, Judy T. Tanner (Eds) ISBN 3 – 540 – 61841-4 Springer- Verlag Berlin Heidelberg New York.

Piper, A. M. (1944): A graphic procedure in the geochemical interpretation of water analysis. Trans. American Geophysical Union, Vol. 25, pp.914 – 923.

Popoff, M. (1988): Du Gondwana à l'Atlantique sud: connexions du fossé de la Bénoué avec les bassins.

Popoff, M., Benkhelil, J., Simon, B. and Motte, J. J. (1983): Approche Geodinamique du Fossé de la Bénué (NE Nigeria): á Partit des Données de Terrain et de Teledetection. In: Benkhelil J., Guiraud, M., Posard, J.F. and Sangy, L. (1989) The Bornu-Benue Trough, the Niger Delta and its Offshore: Tectono-sedimentary reconstruction during

the Creataceous and Tertiary from Geophysical data and Geology. Geology of Nigeria, Nigeria, pp. 277-309.

Popoff, M., Wiedmann, J. and Wasz, I. (1986): The Upper Cretaceous Gongila and Pindiga Formations, northern Nigeria. Subdivisions, age, stratigraphic correlations and paleogeographic implications, *Eclogae geologica Helv*; 79, 343 – 363

Popoff, M., Doucet, J. F. and Latil-Brun, M. V. (1988): Analyse de la subsidence au Crétacé supérieur-Paléocène dans le basin d'Anambra, SW du fossé de la Bénoué. Apports à la géodynamique de la plaque Afrique. *Competes Rendus Académie Sciences Paris* (II) 1271 – 1276.

Raeburn, C. and Jones, B. (1934): The Chad Basin: Geology and water supply. *Bulletin Geological Survey of Nigeria*, 15: 1 – 61.

Reed, D. L., Silver, E. A., Tagudin, J. E., Shipley, T. H. and Vrolijk, P. (1990): Relations between mud volcanoes, thrust deformation, slope sedimentation, and gas hydrate, Offshore North Panama. Mar. Pet. Geol. 7, 44–54.

Reinhard, M. and Wenk, E. (1951): Geology of North Borneo. H. M. Stationery Office, London.

Reyment R. A. (1955): The Cretaceous Ammonoidea of southern Nigeria and the southern Cameroons. *Bulletin Geological Survey Nigeria* 25, 1-112.

Reyment, R. A. (1980): Biogeography of the Saharan Cretaceous and Paleocene epicontinental transgressions. *Cretaceous Research* 1, 299-327.

Reyment, R. A. and Tait, E.A. (1972): Biostratigraphy dating of the early history of the South Atlantic Ocean. Phil. Trans. Roy. Soc. London (B) 224, 55 – 95.

Rogozhin, E. A., Ovsyuchenko, A. N., Marakhov, A.V. and Ushan ova, E.A. (2007): Tectonic setting and geological manifestations of the 2003 Altai Earthquake, Geotectonics 41: 87–104.

Rukavičková Lenka and Hanžl Pavel (2008): Mud volcanoes in the Khar Argalantyn Nuruu, NW Gobi Altay, Mongolia as manifestation of recent seismic activity, *Journal of Geosciences, 53, pp. 181 – 191.*

Schoeller, H. (1964): La classificatiob geochimique des eaux. I.A.S.H. Publication no.64, Gen. Assembly of Berkeley 1963 V. 4, pp. 16 – 24

Schoeneich, K. and Garba, L. (2010): Hydrogeology (Geol.405), Unpublished Lecture Notes, Department of Geology, Ahmadu Bello University, Zaria

Simpson, A. (1954): The Nigerian coalfield. The geology of parts of Onitsha, Owerri an Benue provinces, *Bulletin Geological Survey Nigeria* 24, viii + 85pp

Snead, R .E. (1964): Active mud volcanoes of Baluchistan, West Pakistan. Geogr. Rev. 4, 546- 560

Stoneley, R. (1966): The Niger Delta region in the light of the theory of continental drift. *Geological Magazine* 103, 385-397.

Thiessen, R., Burke, K. C. and Kidd, W. S. F (1979): African Hotspots and their relation to the underlying mantle. Geol., 997:263 – 266

Thompson, J. H. (1958): The geology and hydrology of Gombe, Bauchi Province. *Records Geological Survey of Nigeria* 1956, 46 – 65.

Turner, D. C. (1978): Volcanoes of Biu basalt plateau, north - eastern Nigeria. *Journal Mining and Geology* 15, 49 – 63.

Umaru, A. (2000): The Geology of the area in and around Todi, parts of Kaltungo Sheet 173 NW, Gombe State. Unpublished B.Sc. project submitted to the Department of Geology, Ahamadu Bello University Zaria.

Van der Aa M., 2003. Classification of mineral water types and comparison with drinking water standards. Environmental Geology, 44, 554–563.

Vogt, P. R., Cherkashev, G., Ginsburg, G., Ivanov, G., Milkov, A., Crane, K., Lein, A., Sundvor, E., Pimenov, N. and Egorov, A. (1997): Haakon Mosby mud volcano provides unusual example of venting. *Eos, Transactions, American Geophysical Union 78 (48)*, 549; 556-557.

Wegmann, C. E. (1930): Ueber Diapirismus, *Bull. Comm. Geol. Finn.*, *92*, 58–76.

Whitten, D. G. A. and Brooks, J. R. V. (1972): Pengium dictionary of geology, Pengium books Ltd, Harmondsworth Middlesex, England.

World Health Orgaisation (WHO) (2011): Guidelines for drinking water quality, International Standards for Drinking Water. Vol.1. Geneva, 130pp

Wright, J. B. (1968): South Atlantic continental drift and the Benue Trough. *Tectonophysics* 6, 301-310.

Wright, J. B. (1989): Volcanic rocks in Nigeria. In: Geology of Nigeria (*2nd revised edition*) (Edited by Kogbe, C.A.), pp.125 – 173, Rock View (Nigeria) Ltd., Jos, Nigeria

Zaborski, P. M. (1990): The Cenomanian and Turonian (mid-Cretaceous) ammonite biostratigraphy of north - eastern Nigeria. *Bulletin British Museum Natural History* (Geology) 46, 1-18

Zaborski, P. M. (1998): A review of the Cretaceous System in Nigeria. *Africa Geoscience Review,* 5, 385 – 483.

Zaborski, P. M. (2000): The Cretaceous and Paleocene transgressions in Nigeria and Niger. *Journal of Mining and Geology*, 36(2), 153 – 173.

Zaborski, P. M. (2003): Guide to the Cretaceous System in the Upper Part of the Upper Benue Trough, north - eastern Nigeria. *Africa Geoscience Review*, Vol. 10, Nos. 1 and 2, pp. 13 – 32.

Zaborski, P. M., Ugodulunwa, F., Idornigie, A., Nnabo, P. and Ibe, K. (1998): Stratigraphy and structure of the Cretaceous Gongola Basin, north - eastern Nigeria. *Bulletin de Centre des Recherches Exploration Production Elf-Aquitaine*, 21, 153 – 186.

# APPENDIX A

**Location and physical description of the onshore mud volcanoes in the study area**

| /o | Location ID | Geographical Coordinates | Dates of measurement | Elevation m.a.s.l | Temp of the slurry $^0$C | Cone diametre (m) | Cone height (m) | Remark |
|---|---|---|---|---|---|---|---|---|
| 1 | **(Lallapido)** Lp1 | N09$^0$ 43' 11.4" E11$^0$ 08' 58.9" | 16-02-12 | 394 | - | 2.8 - 2.2 | 0.9 | Active with mud seeping out of the crater |
| 2 | Lp2 | N09$^0$ 43' 12.4" E11$^0$ 08' 57.4" | 16-02-12 | 391 | 25.1 | 0.7. - 0.5 | 0.2 | Active with mud seeping out of the crater |
| 3 | Lp3 | N09$^0$ 43' 11.3" E11$^0$ 08' 57.5" | 16-02-12 | 400 | 26.7 | 0.5 - 0.4 | 0.5 | Active with mud seeping out of the crater |
| 4 | Lp4 | N09$^0$ 43' 11.5" E11$^0$ 08 57.7" | 16-02-12 | 400 | 26.3 | 0.4 - 0.3 | 0.3 | Active with mud seeping out of the crater |
| 5 | Lp5 | N09$^0$ 43' 11.4" E11$^0$ 08' 58.3" | 16-02-12 | 399 | 25.3 | 1.8 -1.1 | 0.3 | Active with mud and water seeping out of the crater, grasses are grown around the cone. |
| 6 | Lp6 | N09$^0$ 43' 11.6" E11$^0$ 08' 58.1" | 16-02-12 | 399 | 25.7 | 1.5 - 0.8 | 0.3 | Active with mud seeping out of the crater |
| 7 | Lp7 | N09$^0$ 43' 11.5" E11$^0$ 08' 58.5" | 16-02-12 | 400 | - | 0.5 - 0.4 | 0.4 | Active with mud seeping out of the crater. |
| 8 | Lp8 | N09$^0$ 43' 11.4" E11$^0$ 08' 58.8" | 16-02-12 | 403 | - | 0.5 - 0.4 | 0.4 | Active with mud seeping out of the crater. |
| 9 | Lp9 | N09$^0$ 43' 12.1" E11$^0$ 08' 58.4" | 16-02-12 | 402 | 26.7 | 0.5 - 0.3 | 0.6 | Active with mud seeping out of the crater |
| 10 | Lp10 | N09$^0$ 43' 11.3" E11$^0$ 09' 00.4" | 16-02-12 | 397 | - | 1.0 – 1.0 | 0.5 | Active with mud seeping out of the crater |
| 11 | Lp11 | N09$^0$ 43' 11.6" E11$^0$ 08' 59.5" | 16-02-12 | 396 | 26.1 | 1.0 - 1.1 | 0.5 | Active with mud seeping out of the crater |
| 12 | Lp12 | N09$^0$ 43' 11.8" E11$^0$ 08' 59.7" | 16-02-12 | 392 | 25.9 | 1.0 - 0.8 | 0.5 | Active with mud seeping out of the crater |

| | | | | | | | | |
|---|---|---|---|---|---|---|---|---|
| 13 | Lp13 | N09$^0$ 43’ 11.4”<br>E11$^0$ 08’ 58.8” | 16-02-12 | 398 | 26.3 | 0.9 - 0.8 | 0.5 | Inactive. |
| 14 | Lp14 | N09$^0$ 43’ 11.7”<br>E11$^0$ 08’ 00.4” | 16-02-12 | 400 | 26.0 | 1.0 - 0.8 | 0.2 | Active with mud seeping out of the crater |
| 15 | Lp15 | N09$^0$ 43’ 11.5”<br>E11$^0$ 08’ 00.5” | 16-02-12 | 399 | 25.9 | 0.9 - 0.8 | 0.2 | Active with mud seeping out of the crater |
| 16 | Lp16 | N09$^0$ 43’ 11.0”<br>E11$^0$ 08’ 00.8” | 16-02-12 | 404 | 25.3 | 0.9 - 0.7 | 0.5 | Active with mud seeping out of the crater |
| 17 | Lp17 | N09$^0$ 43’ 10.9”<br>E11$^0$ 08’ 03.4” | 16-02-12 | 401 | - | 0.9 - 0.8 | 0.2 | Inactive. |
| 18 | Lp18 | N09$^0$ 43’ 10.6”<br>E11$^0$ 08’ 04.2” | 16-02-12 | 398 | - | 2.5- 2.0 | 0.0 | Wet surface with whitish powder and grasses. |
| 19 | Lp19 | N09$^0$43$^I$12.4$^{II}$<br>E11$^0$08’57.2” | 16-02-12 | 392 | 24.7 | 2.0 – 2.5 | 0.0 | Active with water seeping from the crater. |
| 20 | Lp20 | N09$^0$ 43’ 11.4”<br>E11$^0$ 08’ 58.8” | 16-02-12 | 401 | 26.5 | 2.5 - 2.5 | 0.0 | Water seeping out of the crater, grasses seen grown around the water |
| 21 | Lp21 | N09$^0$ 43’ 08.9”<br>E11$^0$ 08’ 10.0” | 16-02-12 | 395 | - | 0.9 - 0.8 | 0.2 | Active with water seeping out of the crater, grasses seen grown around the water |
| 22 | Lp22 | N09$^0$ 43’ 08.1”<br>E11$^0$ 08’ 10.1” | 16-02-12 | 396 | - | 0.9 - 0.8 | 0.2 | Inactive. |
| 23 | Lp23 | N09$^0$ 43’ 08.9”<br>E11$^0$ 08’ 12.5” | 16-02-12 | 396 | 24.3 | 1.2 – 1.0 | 0.7 | Active with mud seeping out of the crater |
| 24 | Lp 24 | N09$^0$ 43’ 0.9.4”<br>E11$^0$ 08’ 12.7” | 16-02-12 | 392 | 27.8 | 0.9 - 0.7 | 0.5 | Inactive. |
| 25 | Lp25 | N09$^0$ 43’ 08.9”<br>E11$^0$ 08’ 15.0” | 16-02-12 | 393 | - | 0.9 - 0.7 | 0.5 | Inactive. |
| 26 | Lap26 | N09$^0$43’03.5”<br>E11$^0$08’28.8” | 16-02-12 | 348 | 24.5 | 3.5 - 2.5 | 0.2 | Active with mud and water seeping out of the crater. |
| 27 | Lap27 | N09$^0$43’02.3”<br>E11$^0$08’30.0” | 16-02-12 | 361 | 24.3 | 3.5 - 2.5 | 0.2 | Active with mud and water seeping out of the crater. |
| 28 | Lap28 | N09$^0$43’01.2”<br>E11$^0$08’28.2” | 16-02-12 | 362 | 24.6 | 3.5 - 2.5 | 0.2 | Active with mud and water seeping out of the crater. |

| | | | | | | | | |
|---|---|---|---|---|---|---|---|---|
| 29 | **(Gujuba)** Gj1 | N09$^0$37’47.9” E11$^0$04’56.3” | 17-02-12 | 355 | 22.5 | 1.0 – 1.0 | 0.1 | Active with mud and seeping out of the crater |
| 30 | Gj2 | N09$^0$38’51.9” E11$^0$04’09.3” | 17-02-12 | 362 | 22.9 | 2.5 – 2.0 | 0.1 | Active with mud seeping out of the crater |
| 31 | Gj3 | N09$^0$38’52.1” E11$^0$04’09.3” | 17-02-12 | 351 | 20.8 | 1.5 – 1.0 | 0.1 | Active with mud and water seeping out of the crater |
| 32 | Gj4 | N09$^0$38’52.2” E11$^0$04’09.2” | 17-02-12 | 347 | 22.1 | 2.5 – 2.0 | 0.1 | Active with mud seeping out of the crater |
| 33 | Gj5 | N09$^0$38’52.6” E11$^0$04’09.4” | 17-02-12 | 351 | 22.7 | 2.0- 1.5 | 0.1 | Active with mud seeping out of the crater |
| 34 | Gj6 | N09$^0$38’52.7” E11$^0$04’09.4” | 17-02-12 | 347 | 21.8 | 2.0 - 1.6 | 0.1 | Active with mud seeping out of the crater |
| 35 | Gj7 | N09$^0$38’52.5” E11$^0$04’09.4” | 17-02-12 | 356 | 22.1 | 2.1 - 1.7 | 0.1 | Active with mud seeping out of the crater |
| 36 | Gj8 | N09$^0$38’52.6” E11$^0$04’09.7” | 17-02-12 | 350 | 20.7 | 1.0 - 0.6 | 0.1 | Active with mud seeping out of the crater |
| 37 | Gj9 | N09$^0$38’52.5” E11$^0$04’08.6” | 17-02-12 | 346 | 21.3 | 3.0 – 2.0 | 0.2 | Active with mud seeping out of the crater |
| 38 | Gj10 | N09$^0$38’51.4” E11$^0$04’07.9” | 17-02-12 | 352 | 23.1 | 1.5 - 1.0 | 0.2 | Active with mud seeping out of the crater |
| 39 | Gj11 | N09$^0$38’51.6” E11$^0$04’08.2” | 17-02-12 | 352 | 22.9 | 2.0 - 1.8 | 0.2 | Active with mud seeping out of the crater |
| 40 | Gj12 | N09$^0$38’51.5” E11$^0$04’08.5” | 17-02-12 | 350 | 21.8 | 3.0 – 2.0 | 0.2 | Active with mud seeping out of the crater |
| 41 | **(Jenye)** Jy1 | N09$^0$39’47.6” E11$^0$04’39.5” | 17-02-12 | 324 | 24.5 | 3.0 – 2.0 | 0.7 | Active with mud seeping out of the crater |
| 42 | Jy2 | N09$^0$39’47.4” E11$^0$04’39.6” | 17-02-12 | 322 | 25.8 | 4.0 – 3.5 | 0.7 | Active with mud seeping out of the crater |
| 43 | Jy3 | N09$^0$39’46.8” E11$^0$04’39.6” | 17-02-12 | 326 | 24.6 | 4.5 – 3.0 | 0.8 | Active with mud seeping out of the crater |
| 44 | Jy4 | N09$^0$39’46.0” E11$^0$04’40.3” | 17-02-12 | 325 | 24.4 | 3.5- 3.0 | 0.7 | Active with mud seeping out of the crater |
| 45 | Jy5 | N09$^0$39’46.2” E11$^0$04’40.6” | 17-02-12 | 325 | 24.1 | 2.0 - 1.8 | 0.8 | Active with mud seeping out of the crater |

| | | | | | | | | |
|---|---|---|---|---|---|---|---|---|
| 46 | Jy6 | N09$^0$39’45.6” E11$^0$04’40.7” | 17-02-12 | 323 | 23.9 | 2.5 – 2.0 | 0.7 | Active with mud seeping out of the crater |
| 47 | Jy7 | N09$^0$39’45.9” E11$^0$04’40.3” | 17-02-12 | 323 | 24.6 | 3.0 - 2.8 | 0.7 | Active with mud seeping out of the crater |
| 48 | Jy8 | N09$^0$39’45.6” E11$^0$04’41.1” | 17-02-12 | 323 | 23.9 | 2.8 - 2.2 | 0.6 | Active with mud seeping out of the crater |
| 49 | Jy9 | N09$^0$39’45.7” E11$^0$04’41.6” | 17-02-12 | 324 | 23.6 | 4.0 - 3.5 | 0.5 | Active with mud seeping out of the crater |
| 50 | Jy10 | N09$^0$39’46.2” E11$^0$04’41.0” | 17-02-12 | 325 | 23.5 | 3.5 - 2.5 | 0.7 | Active with mud seeping out of the crater |
| 51 | Jy11 | N09$^0$39’46.0” E11$^0$04’41.3” | 17-02-12 | 331 | 24.6 | 2.3 - 2.2 | 0.6 | Active with mud seeping out of the crater |
| 52 | **(Pamadu)** Pm1 | N09$^0$39’46.7” E11$^0$04’40.4” | 18-02-12 | 328 | 24.2 | 2.0 - 1.9 | 0.4 | Active with mud seeping out of the crater |
| 53 | Pm2 | N09$^0$40’44.4” E11$^0$03’56.2” | 18-02-12 | 336 | 21.9 | 2.5 - 2.0 | 0.3 | Active with mud seeping out of the crater |
| 54 | Pm3 | N09$^0$40’44.4” E11$^0$03’56.5” | 18-02-12 | 320 | 22.3 | 2.0 - 1.5 | 0.4 | Active with mud seeping out of the crater |
| 55 | Pm4 | N09$^0$40’44.1” E11$^0$03’56.1” | 18-02-12 | 317 | 22.8 | 3.0 - 2.5 | 0.3 | Active with mud seeping out of the crater |
| 56 | Pm5 | N09$^0$40’44.2” E11$^0$03’56.6” | 18-02-12 | 320 | 21.1 | 3.0 - 2.1 | 0.3 | Active with mud and water seeping out of the crater. |
| 57 | Pm6 | N09$^0$40’48.7” E11$^0$03’56.1” | 18-02-12 | 322 | 25.6 | 2.0 - 1.7 | 0.5 | Active with mud seeping out of the crater |
| 58 | Pm7 | N09$^0$40’48.5” E11$^0$03’56.0” | 18-02-12 | 310 | - | 2.8 - 2.1 | 0.3 | Inactive. |
| 59 | Pm8 | N09$^0$40’49.0” E11$^0$03’55.9” | 18-02-12 | 309 | 24.5 | 0.8 - 0.5 | 0.2 | Active with mud seeping out of the crater |
| 60 | Pm9 | N09$^0$40’49.0” E11$^0$03’55.9” | 18-02-12 | 308 | 23.8 | 2.0 - 1.5 | 0.5 | Active with mud seeping out of the crater |
| 61 | Pm10 | N09$^0$40’49.2” E11$^0$03’56.3” | 18-02-12 | 309 | 24.0 | 2.0 - 1.5 | 0.2 | Active with mud and water seeping out of the crater. Grasses also grows around the cone. |
| 62 | Pm11 | N09$^0$40’49.6” E11$^0$03’56.3” | 18-02-12 | 312 | 23.8 | 2.0 - 1.5 | 0.2 | Active with mud seeping out of the crater |

| | | | | | | | | |
|---|---|---|---|---|---|---|---|---|
| 63 | Pm12 | N09$^0$40’50.2”<br>E11$^0$03’55.9” | 18-02-12 | 313 | 23.4 | 2.0 - 1.7 | 0.3 | Active with mud seeping out of the crater |
| 64 | Pm13 | N09$^0$40’50.1”<br>E11$^0$03’55.6” | 18-02-12 | 310 | 24.3 | 3.0 - 2.5 | 0.4 | Active with mud seeping out of the crater |
| 65 | Pm14 | N09$^0$40’47.8”<br>E11$^0$03’55.5” | 18-02-12 | 313 | 24.6 | 3.5 - 2.7 | 0.4 | Active with mud seeping out of the crater |
| 66 | Pm15 | N09$^0$40’50.4”<br>E11$^0$03’55.5” | 18-02-12 | 311 | 24.0 | 2.2 - 1.7 | 0.3 | Active with mud seeping out of the crater |
| 67 | Pm16 | N09$^0$40’50.6”<br>E11$^0$03’55.8” | 18-02-12 | 309 | 24.8 | 2.0 - 1.8 | 0.3 | Active with mud seeping out of the crater |
| 68 | Pm17 | N09$^0$40’50.9”<br>E11$^0$03’55.8” | 18-02-12 | 307 | 24.1 | 2.0 - 5.2 | 0.3 | Active with mud seeping out of the crater. |
| 69 | Pm18 | N09$^0$40’50.1”<br>E11$^0$03’55.8” | 18-02-12 | 309 | 23.6 | 1.8 - 1.5 | 0.2 | Active with mud seeping out of the crater. |
| 70 | Pm19 | N09$^0$40’56.8”<br>E11$^0$03’54.9” | 18-02-12 | 308 | 24.6 | 2.7 - 1.5 | 0.2 | Active with mud seeping out of the crater. |
| 71 | Pm20 | N09$^0$40’55.6”<br>E11$^0$03’54.5” | 18-02-12 | 306 | 23.5 | 0.8 - 0.5 | 0.2 | Active with mud seeping out of the crater. |
| 72 | Pm21 | N09$^0$40’55.9”<br>E11$^0$03’54.9” | 18-02-12 | 306 | 23.6 | 0.8 - 0.4 | 0.5 | Active with mud seeping out of the crater. |
| 73 | Pm22 | N09$^0$40’56.0”<br>E11$^0$03’55.1” | 18-02-12 | 305 | 23.5 | 2.0 - 0.8 | 0.1 | Active with mud seeping out of the crater. |
| 74 | Pm23 | N09$^0$40’55.5”<br>E11$^0$03’55.3” | 18-02-12 | 307 | 23.8 | 2.0 - 1.5 | 0.2 | Active with mud seeping out of the crater. |
| 75 | Pm24 | N09$^0$40’55.4”<br>E11$^0$03’55.5” | 18-02-12 | 307 | 24.1 | 2.0 - 1.5 | 0.2 | Active with mud seeping out of the crater. |
| 76 | Pm25 | N09$^0$40’54.8”<br>E11$^0$03’55.4” | 18-02-12 | 307 | 24.1 | 2.5 - 1.5 | 0.2 | Active with mud seeping out of the crater. |
| 77 | Pm26 | N09$^0$40’54.6”<br>E11$^0$03’55.2” | 18-02-12 | 308 | 24.8 | 2.8 - 2.5 | 0.2 | Active with mud seeping out of the crater. |
| 78 | Pm27 | N09$^0$40’54.1”<br>E11$^0$03’55.1” | 18-02-12 | 308 | 24.5 | 3.8 - 2.5 | 0.2 | Active with mud seeping out of the crater. |
| 79 | **(Lashadar)**<br>Ls1 | N09$^0$41’47.5”<br>E11$^0$10’15.6” | 19-02-12 | 339 | 25.5 | 0.3 – 0.2 | 0.1 | Active with mud seeping out of the crater. |
| 80 | Ls2 | N09$^0$41’58.1”<br>E11$^0$10’26.6” | 19-02-12 | 365 | 26.1 | 0.2 - 0.1 | 0.1 | Active with mud seeping out of the crater. |

| | | | | | | | | |
|---|---|---|---|---|---|---|---|---|
| 81 | Ls3 | N09$^0$41’58.1” E11$^0$10’26.4” | 19-02-12 | 378 | 24.7 | 0.2 - 0.1 | 0.1 | Active with mud seeping out of the crater. |
| 82 | Ls4 | N09$^0$41’58.3” E11$^0$10’26.6” | 19-02-12 | 376 | 24.6 | 0.2 - 0.1 | 0.1 | Active with mud seeping out of the crater. |
| 83 | Ls5 | N09$^0$41’58.2” E11$^0$10’26.6” | 19-02-12 | 376 | 25.0 | 0.2 - 0.1 | 0.1 | Active with mud seeping out of the crater. |
| 84 | Ls6 | N09$^0$41’57.6” E11$^0$10’26.9” | 19-02-12 | 378 | 25.4 | 0.8 - 0.5 | 0.1 | Active with mud seeping out of the crater. |
| 85 | Ls7 | N09$^0$41’57.1” E11$^0$10’26.8” | 19-02-12 | 376 | 25.2 | 0.4 - 0.3 | 0.1 | Active with mud seeping out of the crater. |
| 86 | Ls8 | N09$^0$41’55.6” EO11$^0$10’29.7” | 19-02-12 | 377 | 25.8 | 0.2 - 0.3 | 0.1 | Active with mud seeping out of the crater. |
| 87 | Ls9 | N09$^0$41’56.2” E11$^0$10’30.9” | 19-02-12 | 380 | 26.4 | 0.4- 0.3 | 0.1 | Active with mud seeping out of the crater. |
| 88 | Ls10 | N09$^0$42’00.4” E11$^0$10’30.0” | 19-02-12 | 375 | 25.1 | 0.3 - 0.5 | 0.1 | Active with mud seeping out of the crater. |
| 89 | Ls11 | N09$^0$42’01.8” E11$^0$10’37.2” | 19-02-12 | 396 | 25.2 | 3.5 - 2.5 | 0.0 | Active with water seeping out of the crater. |
| 90 | **(Leturu)** Le | N09$^0$42’10.1” E11$^0$11’31.8” | 19-02-12 | 400 | 41.9 | 3 - 2.5 | 0.0 | Very active thermal warm spring with warm water. |
| 91 | **(Lakomji)** Lj | N09$^0$41’05.9” E11$^0$14’09.0” | 19-02-12 | 433 | 41.2 | 3.5 - 2.5 | 0.0 | Very active thermal warm spring with warm water. |
| 92 | **(Lakaturu)** Lk1 | N09$^0$42’11.9” E11$^0$07’44.8” | 19-02-12 | 339 | 25.5 | 2.0 - 1.5 | 0.4 | Active with mud seeping out of the crater. |
| 93 | Lk2 | N09$^0$42’12.0” E11$^0$07’44.2” | 19-02-12 | 342 | 24.9 | 2.0 - 0.5 | 0.2 | Active with mud seeping out of the crater. |
| 94 | Lk3 | N09$^0$42’13.3” E11$^0$07’43.6” | 19-02-12 | 341 | 24.8 | 1.8 - 0.5 | 0.2 | Active with mud seeping out of the crater. |
| 95 | Lk4 | N09$^0$42’12.8” E11$^0$07’42.0” | 19-02-12 | 342 | 24.2 | 2.0 - 1.1 | 0.2 | Active with mud seeping out of the crater. |
| 96 | Lk5 | N09$^0$42’12.7” E11$^0$07’42.5” | 19-02-12 | 347 | 28.3 | 1.5 - 0.5 | 0.4 | Active with mud seeping out of the crater. |
| 97 | Lk6 | N09$^0$42’12.6” E11$^0$07’42.5” | 19-02-12 | 346 | 24.9 | 2.0 - 0.5 | 0.4 | Active with mud seeping out of the crater. |

| | | | | | | | | |
|---|---|---|---|---|---|---|---|---|
| 98 | Lk7 | N09$^0$42’12.4” E11$^0$07’42.8” | 19-02-12 | 345 | 23.1 | 2.0 - 1.8 | 0.2 | Active with mud seeping out of the crater. |
| 99 | Lk8 | N09$^0$42’12.0” E11$^0$07’42.7” | 19-02-12 | 347 | 24.2 | 2.0 - 1.5 | 0.4 | Active with mud seeping out of the crater. |
| 100 | Lk9 | N09$^0$42’12.0” E11$^0$07’42.7”E | 19-02-12 | 343 | 24.5 | 2.0 - 1.5 | 0.2 | Active with mud seeping out of the crater. |
| 101 | Lk10 | N09$^0$42’12.2” E11$^0$07’42.9” | 19-02-12 | 345 | 23.0 | 0.5 - 0.5 | 0.4 | Active with mud seeping out of the crater. |
| 102 | Lk11 | N09$^0$42’12.1” E11$^0$07’42.5” | 19-02-12 | 347 | 24.O | 1.0 - 0.8 | 0.2 | Active with mud seeping out of the crater. |
| 103 | Lk12 | N09$^0$42’10.8” E11$^0$07’43.1” | 19-02-12 | 345 | 25.3 | 2.0 - 1.0 | 0.2 | Active with mud seeping out of the crater. |
| 104 | Lk13 | N09$^0$42’10.8” E11$^0$07’42.8” | 19-02-12 | 347 | 26.9 | 1.5 - 0.5 | 0.2 | Cone m, m high, active with mud seeping out of the crater. |
| 105 | Lk14 | N09$^0$42’11.2” E11$^0$07’43.0” | 19-02-12 | 346 | 27.3 | 2.0 - 1.5 | 0.2 | Cone m, 0.2 m high, active with mud seeping out of the crater. |
| 106 | Lk15 | N09$^0$42’12.6” E11$^0$07’42.5” | 19-02-12 | 350 | 26.9 | 2.5 - 1.5 | 0.3 | Active with mud seeping out of the crater. |
| 107 | Lk16 | N09$^0$42’10.7” E11$^0$07’43.3” | 19-02-12 | 346 | 25.1 | 2.5 - 1.5 | 0.3 | Active with mud seeping out of the crater. |
| 108 | **(Chengau)** Cg1 | N09$^0$39’17.8” E11$^0$06’40.3” | 19-02-12 | 332 | 26.4 | 0. 5 - 0.5 | 0.0 | Active with water seeping from the crater and precipitated salt seen around the crater. |
| 109 | **(Digga)** Dg1 | N09$^0$39’31.2” E11$^0$07’50.6” | 19-02-12 | 337 | 25.9 | 0.5 - 0.5 | 0.0 | Active with water seeping from the crater and precipitated salt seen around the crater. |
| 110 | Dg2 | N09$^0$39’51.3” E11$^0$07’51.6” | 19-02-12 | 337 | 26.1 | 0.5 - 0.5 | 0.0 | Active with water seeping from the crater and precipitated salt seen around the crater. |
| 111 | Dg3 | N09$^0$39’52.0” E11$^0$07’56.4” | 19-02-12 | 324 | 26.6 | 2.5 -1.5 | 0.0 | Active with water seeping from the crater and precipitated salt seen around the crater. |
| 112 | Dg4 | N09$^0$39’49.6” E11$^0$07’59.5” | 19-02-12 | 326 | 26.2 | 3.5 - 1.5 | 0.0 | Active with water seeping from the crater and precipitated salt seen around the crater. |

| | | | | | | | | |
|---|---|---|---|---|---|---|---|---|
| 113 | Dg5 | N09$^0$39’51.0”<br>E11$^0$08’03.3” | 19-02-12 | 326 | 26.0 | 1.5 - 0.5 | 0.1 | Active with mud and water seeping from the crater and precipitated salt seen around the crater. |
| 114 | Dg6 | N09$^0$39’50.7”<br>E11$^0$08’04.9” | 19-02-12 | 330 | 25.8 | 1.5 - 0.5 | 0.0 | Active with water seeping from the crater and precipitated salt seen around the crater. |
| 115 | **(Kurum)**<br>Kr1 | N09$^0$46’15.1”<br>E11$^0$03’04.4” | 20-02-12 | 336 | 25.5 | 1.5 - 1.0 | 1.1 | Active with water seeping from the crater and precipitated salt seen around the crater. |
| 116 | Kr2 | N09$^0$46’16.1”<br>E11$^0$03’04.9” | 20-02-12 | 339 | 25.6 | 0.5 -1.0 | 0.3 | Active with water seeping from the crater and precipitated salt seen around the crater. |
| 117 | Kr3 | N09$^0$46’15.7”<br>E11$^0$03’05.3” | 20-02-12 | 340 | 25.1 | 0.5 – 1.0 | 0.3 | Active with water seeping from the crater and precipitated salt seen around the crater. |
| 118 | Kr4 | N09$^0$46’15.9”<br>E11$^0$03’05.6” | 20-02-12 | 331 | 25.2 | 0.5 – 1.0 | 0.3 | Active with water seeping from the crater and precipitated salt seen around the crater. |
| 119 | Kr5 | N09$^0$46’16.4”<br>E11$^0$03’04.6” | 20-02-12 | 333 | 26.7 | 0.5 -1.0 | 0.4 | Active with water seeping from the crater and precipitated salt seen around the crater. |
| 120 | Kr6 | N09$^0$46’17.2”<br>E11$^0$03’04.9” | 20-02-12 | 333 | 24.9 | 0.5 -1.0 | 0.4 | Active with water seeping from the crater and precipitated salt seen around the crater. |
| 121 | Kr7 | N09$^0$46’16.3”<br>E11$^0$03’05.2” | 20-02-12 | 333 | 24.9 | 0.5 -1.0 | 0.3 | Active with water seeping from the crater and precipitated salt seen around the crater. |
| 122 | Kr8 | N09$^0$46’16.5”<br>E11$^0$03’06.1” | 20-02-12 | 334 | 24.7 | 0.5 -1.0 | 0.4 | Active with mud seeping from the crater with precipitated salt seen around the crater. |
| 123 | Kr9 | N09$^0$46’17.1”<br>E11$^0$03’05.7” | 20-02-12 | 334 | 26.2 | 0.5 -1.0 | 0.4 | Active with mud seeping from the crater with precipitated salt seen around the crater. |
| 124 | Kr10 | N09$^0$46’17.9”<br>E11$^0$03’05.0” | 20-02-12 | 334 | 26.4 | 0.5 -1.0 | 0.4 | Active with mud seeping from the crater with precipitated salt seen around the crater. |

| | | | | | | | | |
|---|---|---|---|---|---|---|---|---|
| 125 | Kr11 | N09$^0$46’18.1”<br>E11$^0$03’05.8” | 20-02-12 | 335 | 24.9 | 0.5 -1.0 | 0.5 | Active with mud seeping from the crater with precipitated salt seen around the crater. |
| 126 | Kr12 | N09$^0$46’18.2”<br>E11$^0$03’06.1” | 20-02-12 | 335 | 24.6 | 0.5 -1.0 | 0.4 | Active with mud seeping from the crater with precipitated salt seen around the crater. |
| 127 | Kr13 | N09$^0$46’18.3”<br>E11$^0$03’06.7” | 20-02-12 | 333 | 25.1 | 0.5 -1.0 | 0.4 | Active with mud seeping from the crater with precipitated salt seen around the crater. |
| 128 | Kr14 | N09$^0$46’18.1”<br>E11$^0$03’06.8” | 20-02-12 | 334 | 25.2 | 0.5 – 1.0 | 0.5 | Active with mud seeping from the crater with precipitated salt seen around the crater. |
| 129 | Kr15 | N09$^0$46’18.7”<br>E11$^0$03’07.1” | 20-02-12 | 334 | 24.7 | 0.5 – 1.0 | 0.4 | Active with mud seeping from the crater with precipitated salt seen around the crater. |
| 130 | Kr16 | N09$^0$46’18.4”<br>E11$^0$03’07.8” | 20-02-12 | 334 | 25.4 | 0.5 – 1.0 | 0.5 | Active with mud seeping from the crater with precipitated salt seen around the crater. |
| 131 | Kr17 | N09$^0$46’19.0”<br>E11$^0$03’07.4” | 20-02-12 | 335 | 24.7 | 0.5 – 1.0 | 0.6 | Active with mud seeping from the crater with precipitated salt seen around the crater. |
| 132 | Kr18 | N09$^0$46’18.8”<br>E11$^0$03’07.3” | 20-02-12 | 338 | 25.2 | 0.5 – 2.0 | 0.5 | Cone, 0.5m - 1 m, 0.5m high, with mud seeping from the crater with precipitated salt seen around the crater. |
| 133 | Kr19 | N09$^0$46’19.2”<br>E11$^0$03’07.2” | 20-02-12 | 332 | 25.1 | 0.5 – 2.0 | 0.4 | Active with mud seeping from the crater with precipitated salt seen around the crater. |
| 134 | Kr20 | N09$^0$46’19.9”<br>E11$^0$03’07.6” | 20-02-12 | 335 | 24.3 | 0.5 – 1.0 | 0.5 | Active with mud seeping from the crater with precipitated salt seen around the crater. |
| 135 | Kr21 | N09$^0$46’20.7”<br>E11$^0$03’07.7” | 20-02-12 | 336 | 26.2 | 0.5 – 1.5 | 0.2 | Active with mud seeping from the crater with precipitated salt seen around the crater. |
| 136 | **(Lawampe)** Lw1 | N09$^0$49’08.3”<br>E11$^0$04’01.2” | 21-02-12 | 343 | 24.6 | 0.5 – 2.0 | 0.1 | Active with mud seeping from the crater with precipitated salt seen around the crater. |
| 137 | Lw2 | N09$^0$49’08.5” | 21-02-12 | 345 | 24.5 | 0.5 – 1.5 | 0.2 | Active with mud seeping from the crater with |

| | | | | | | | | |
|---|---|---|---|---|---|---|---|---|
| | | E11$^0$04’01.5” | | | | | | precipitated salt seen around the crater. |
| 138 | Lw3 | N09$^0$49’08.7” E11$^0$04’01.7” | 21-02-12 | 345 | 24.9 | 0.5 – 1.5 | 0.2 | Active with mud seeping from the crater with precipitated salt seen around the crater. |
| 139 | **(Kolokwami)** Kk1 | N09$^0$49’42.8” E11$^0$06’30.4” | 21-02-12 | 343 | 24.2 | 0.5 – 1.5 | 0.2 | Active with mud seeping from the crater with precipitated salt seen around the crater. |
| 140 | Kk2 | N09$^0$50’04.2” E11$^0$05’57.5” | 21-02-12 | 366 | 24.7 | 0.5 – 1.5 | 0.2 | Active with mud seeping from the crater with precipitated salt seen around the crater. |
| 141 | Kk3 | N09$^0$50’04.5” E11$^0$05’58.6” | 21-02-12 | 366 | 24.7 | 0.5 – 1.8 | 0.4 | Active, with mud seeping from the crater with precipitated salt seen around the crater. |
| 142 | Kk4 | N09$^0$49’55.7” E11$^0$07’23.8” | 21-02-12 | 384 | 24.0 | 0.5 – 1.8 | 0.4 | Active, with mud seeping from the crater with precipitated salt seen around the crater. |
| 143 | **(Lashuwo)** Lo1 | N09$^0$50’46.0” E11$^0$04’44.7” | 21-02-12 | 356 | 23.8 | 0.5 – 1.0 | 0.2 | Active, with mud seeping from the crater with precipitated salt seen around the crater. |
| 144 | Lo2 | N09$^0$51’28.6” E11$^0$05’18.4” | 21-02-12 | 375 | 23.8 | 0.5 – 1.0 | 0.2 | Active, with mud seeping from the crater with precipitated salt seen around the crater. |
| 145 | **(Todi)** Td1 | N09$^0$45’38.9” E11$^0$08’17.7” | 22-02-12 | 383 | 24.3 | 8.0 – 5.0 | 0.6 | Active, with mud seeping from the crater with precipitated salt seen around the crater. |
| 146 | Td2 | N09$^0$45’40.3” E11$^0$08’18.1” | 22-02-12 | 381 | 24.6 | 0.5 – 1.0 | 0.4 | Active, with mud seeping from the crater with precipitated salt seen around the crater. |
| 147 | Td3 | N09$^0$45’40.7” E11$^0$08’17.3” | 22-02-12 | 387 | 24.0 | 0.5 – 1.5 | 0.2 | Active, with mud seeping from the crater with precipitated salt seen around the crater. |
| 148 | Td4 | N09$^0$44’59.0” E11$^0$07’55.1” | 22-02-12 | 365 | 22.5 | 0.5 – 1.5 | 0.4 | Active, with mud seeping from the crater with precipitated salt seen around the crater. |
| 149 | Td5 | N09$^0$44’55.2” E11$^0$07’55.2 | 22-02-12 | 371 | 22.2 | 0.5 – 1.0 | 0.4 | Inactive but the cone remains intact. |

| | | | | | | | | |
|---|---|---|---|---|---|---|---|---|
| 150 | Td6 | N09$^0$45’01.6” E11$^0$07’56.6” | 22-02-12 | 378 | 23.2 | 0.5 – 1.0 | 0.2 | Active, with mud seeping from the crater with precipitated salt seen around the crater. |
| 151 | Td7 | N09$^0$45’03.7” E11$^0$07’53.5” | 22-02-12 | 377 | 22.9 | 1.0 -1.0 | 0.2 | Active, with mud seeping from the crater with precipitated salt seen around the crater. |
| 152 | Td8 | N09$^0$44’59.2” E11$^0$07’46.2” | 22-02-12 | 369 | 23.1 | 1.5 – 1.0 | 0.2 | Active, with mud seeping from the crater with precipitated salt seen around the crater. |
| 153 | Td9 | N09$^0$44’00.7” E11$^0$07’44.9” | 22-02-12 | 375 | 22.8 | 3.5 - 2.5 | 0.1 | Active, with mud seeping from the crater with precipitated salt seen around the crater. |
| 154 | Td10 | N09$^0$44’01.6” E11$^0$07’41.8” | 22-02-12 | 370 | 22.8 | 5.0 - 4.0 | 0.0 | Active, with mud seeping from the crater with precipitated salt seen around the crater. |
| 155 | Td11 | N09$^0$44’06.2” E11$^0$07’40.9” | 22-02-12 | 376 | 23.1 | 8.0 -7.0 | 0.1 | Active, with mud seeping from the crater with precipitated salt seen around the crater. |
| 156 | Td12 | N09$^0$44’04.4” E11$^0$07’41.0” | 22-02-12 | 375 | 23.4 | 0.5 -1.0 | 0.2 | Active, with mud seeping from the crater with precipitated salt seen around the crater. |
| 157 | Td13 | N09$^0$44’05.0” E11$^0$07’40.6” | 22-02-12 | 376 | - | 0.7 -1 .0 | 0.3 | Active, with mud seeping from the crater with precipitated salt seen around the crater. |
| 158 | **(Konta)** Kt1 | N09$^0$52’35.2” E11$^0$12’53.3” | 22-02-12 | 496 | 23.4 | 5.5 -3.5 | 0.0 | Active, with water seeping from the crater and grasses grown around the crater. |
| 159 | Kt2 | N09$^0$52’29.6” E11$^0$12’50.0” | 22-02-12 | 492 | 23.7 | 3.8 -3.5 | 0.0 | Active, with water seeping from the crater and grasses grown around the crater. |
| 160 | Kt3 | N09$^0$52’26.4” E11$^0$12’53.4” | 22-02-12 | 496 | 23.5 | 3.5 -3.0 | 0.0 | Active, with water seeping from the crater and grasses grown around the crater. |
| 161 | **(Lachikoltok)** Lt1 | N09$^0$54’18.8” E11$^0$14’32.5” | 22-02-12 | 442 | 22.1 | 1.8 - 1.5 | 0.3 | Active, with mud and water seeping from the crater with precipitated salt seen around the crater. |
| 162 | Lt2 | N09$^0$54’18.5” | 22-02-12 | 438 | 21.9 | 5.5 – 5.0 | 0.2 | Active, with mud and water seeping from the |

| | | | | | | | | |
|---|---|---|---|---|---|---|---|---|
| | | E11$^0$14’30.8” | | | | | | crater with precipitated salt seen around the crater. |
| 163 | Lt3 | N09$^0$54’18.4” E11$^0$14’30.1” | 22-02-12 | 441 | 21.8 | 2.8 - 2.5 | 0.2 | Active, with mud and water seeping from the crater with precipitated salt seen around the crater. |
| 164 | Lt4 | N09$^0$54’17.6” E11$^0$14’27.1” | 22-02-12 | 440 | 22.0 | 1.8 - 1.0 | 0.2 | Active, with mud and water seeping from the crater with precipitated salt seen around the crater. |
| 165 | Lt5 | N09$^0$54’16.6” E11$^0$14’28.2” | 22-02-12 | 442 | 22.3 | 1.0 – 0.9 | 0.2 | Active, with mud and water seeping from the crater with precipitated salt seen around the crater. |
| 166 | Lt6 | N09$^0$54’17.3” E11$^0$14’29.9” | 22-02-12 | 444 | 22.3 | 1.8 – 1.0 | 0.2 | Active, with mud and water seeping from the crater with precipitated salt seen around the crater. |
| 167 | Lt7 | N09$^0$54’17.8” E11$^0$14’32.7” | 22-02-12 | 443 | 22.4 | 1.5 – 1.0 | 0.0 | Active, with mud and water seeping from the crater with precipitated salt seen around the crater. |
| 168 | **(Sasanyi)** Sy1 | N09$^0$56’11.6” E11$^0$12’12.6” | 23-02-12 | 395 | 22.0 | 7.5 – 7.0 | 0.0 | Active, with water seeping from the crater with precipitated salt seen around the crater. |
| 169 | Sy2 | N09$^0$56’10.1” E11$^0$12’11.9” | 23-02-12 | 397 | 22.3 | 5.5 – 4.5 | 0.0 | Active, with water seeping from the crater with precipitated salt seen around the crater. |
| 170 | Sy3 | N09$^0$56’08.8” E11$^0$12’10.5” | 23-02-12 | 398 | 22.1 | 6.5 – 5.0 | 0.0 | Active, with water seeping from the crater with precipitated salt seen around the crater. |
| 171 | Sy4 | N09$^0$56’11.6” E11$^0$12’12.6” | 23-02-12 | 404 | 20.8 | 4.5 – 4.0 | 0.0 | Active, with water seeping from the crater with precipitated salt seen around the crater. |
| 172 | Sy5 | N09$^0$56’06.8” E11$^0$12’09.4” | 23-02-12 | 407 | - | 5.5 – 5.2 | 0.0 | Active, with water seeping from the crater with precipitated salt seen around the crater. |

| | | | | | | | | |
|---|---|---|---|---|---|---|---|---|
| 173 | **(Fokata)** Fk1 | N09$^0$44’52.1” E11$^0$12’09.9” | 09-02-13 | 343 | 22.6 | 5.0 – 4.0 | 0.0 | Active, with reddish water seeping from the crater with grasses and precipitated salt seen around the crater. |
| 174 | Fk2 | N09$^0$44’52.5” E11$^0$12’09.9” | 09-02-13 | 345 | 22.1 | 4.0 – 4.2 | 0.0 | Active, with reddish water seeping from the crater with grasses and precipitated salt seen around the crater. |
| 175 | Fk3 | N9$^0$44’53.1” E11$^0$12’09.6” | 09-02-13 | 345 | 22.9 | 5.5m – 4.8 | 0.0 | Active, with reddish water seeping from the crater with grasses and precipitated salt seen around the crater. |
| 176 | Fk4 | N09$^0$44’53.7” E11$^0$12’09.5” | 09-02-13 | 343 | 22.1 | 5.5m – 4.0 | 0.0 | Active, with reddish water seeping from the crater with grasses and precipitated salt seen around the crater. |
| 177 | Fk5 | N09$^0$44’54.4” E11$^0$12’09.6” | 09-02-13 | 366 | 22.7 | 5.0m – 4.2 | 0.0 | Active, with reddish water seeping from the crater with grasses and precipitated salt seen around the crater. |
| 178 | Fk6 | N09$^0$44’54.9” E11$^0$12’09.4” | 09-02-13 | 366 | 22.1 | 5.0m – 4.5 | 0.0 | Active, with reddish water seeping from the crater with grasses and precipitated salt seen around the crater. |
| 179 | Fk7 | N09$^0$44’55.5” E11$^0$12’08.5” | 09-02-13 | 384 | 22.0 | 5.0m – 5.0 | 0.0 | Active, with reddish water seeping from the crater with grasses and precipitated salt seen around the crater. |
| 180 | Fk8 | N09$^0$44’56.2” E11$^0$12’06.9” | 09-02-13 | 356 | 22.8 | 4.5m – 4.5 | 0.0 | Active, with reddish water seeping from the crater with grasses and precipitated salt seen around the crater. |
| 181 | Fk9 | N09$^0$44’56.5” E11$^0$12’06.4” | 09-02-13 | 375 | 22.1 | 4.5 – 3.5 | 0.0 | Active, with reddish water seeping from the crater with grasses and precipitated salt seen around the crater. |
| 182 | Fk10 | N09$^0$44’59.9” | 09-02-13 | 383 | 22.1 | 5.0 – 4.8 | 0.0 | Active, with reddish water seeping from the crater with grasses and precipitated salt seen |

| | | | | | | | | |
|---|---|---|---|---|---|---|---|---|
| | | E11$^0$12’07.0” | | | | | | around the crater. |
| 183 | Fk11 | N09$^0$44’55.5”<br>E11$^0$12’07.1” | 09-02-13 | 381 | 22.6 | 5.3 – 4.5 | 0.0 | Active, with reddish water seeping from the crater with grasses and precipitated salt seen around the crater. |
| 184 | Fk12 | N09$^0$44’55.6”<br>E11$^0$12’07.6” | 09-02-13 | 387 | 22.1 | - | - | Ground surface wet with water |
| 185 | Fk13 | N09$^0$44’55.2”<br>E11$^0$12’07.4” | 10-02-13 | 365 | 22.5 | - | - | Ground surface wet with water |
| 186 | Fk14 | N09$^0$44’55.0”<br>E11$^0$12’07.3” | 10-02-13 | 371 | 22.2 | - | - | Ground surface wet with water |
| 187 | Fk15 | N09$^0$44’54.7”<br>E11$^0$12’06.7” | 10-02-13 | 378 | 22.1 | - | - | Ground surface wet with water |
| 188 | Fk16 | N09$^0$44’54.6”<br>E11$^0$12’06.6” | 10-02-13 | | 22.1 | - | - | Ground surface wet with water |
| 189 | Fk17 | N09$^0$44’55.3”<br>E11$^0$12’06.0” | 10-02-13 | | 22.4 | - | - | Ground surface wet with water |
| 190 | Fk18 | N09$^0$44’55.5”<br>E11$^0$12’05.0” | 10-02-13 | | 22.4 | - | - | Ground surface wet with water |
| 191 | Fk19 | N09$^0$44’55.2”<br>E11$^0$12’06.1” | 10-02-13 | | 22.4 | - | - | Ground surface wet with water |

| | | | | | | | | |
|---|---|---|---|---|---|---|---|---|
| 192 | Fk20 | N09$^0$44’55.6”<br>E11$^0$12’05.1” | 10-02-13 | | 22.7 | - | - | Ground surface wet with water |
| 193 | Fk21 | N09$^0$44’55.7”<br>E11$^0$12’06.2” | 10-02-13 | | 22.1 | - | - | Ground surface wet with water |
| 194 | Fk22 | N09$^0$44’55.1”<br>E11$^0$12’07.1” | 10-02-13 | | 22.7 | - | - | Ground surface wet with water |
| 195 | Fk23 | N09$^0$44’54.3”<br>E11$^0$12’08.6” | 10-02-13 | | 22.7 | - | - | Ground surface wet with water |

# APPENDIX B



A mud volcano occurrence at Lallapido, showing fresh mud flowing from the crater and shattered Bima Sandstone forming part of the cones (N09$^0$ 43' 11.4" and E011$^0$ 08' 58.8; photo taken: 16/02/12)



A mud volcano occurrence at Lallapido, showing the angle of slope, fresh mud flowing from the crater with dry mud and precipitated salt seen around the crater (N09$^0$ 43' 12.1" and E011$^0$ 08' 58.4; photo taken: 16/02/12)



A mud volcano occurrence at Lallapido, showing the angle of slope, dry mud and fresh mud flowing from the crater (N09$^0$ 43' 11.3" and E011$^0$ 09' 00.4; photo taken: 16/02/12)



A mud volcano occurrence at Lallapido, showing the angle of slope, dry mud and fresh mud flowing from the crater (N09$^0$ 43' 11.6" and E011$^0$ 08' 59.5; photo taken: 16/02/12)



A mud volcano occurrence at Lallapido, showing the angle of slope, dry mud and fresh mud flowing from the crater (N09$^0$ 43' 11.8" and E011$^0$ 08' 59.7; photo taken: 16/02/12)



A dormant mud volcano at Lallapido, showing the angle of slope, with cone still intact but no mud is flowing out of the crater (N09$^0$ 43' 11.4" and E011$^0$ 08' 58.8; photo taken: 16/02/12)



A mud volcano occurrence at Lallapido, showing the angle of slope, dry mud and whitish precipitates seen around the cone and fresh mud flowing from the crater (N09$^0$ 43' 11.7" and E011$^0$ 09' 00.4; photo taken: 16/02/12)



A mud volcano occurrence at Lallapido, showing the angle of slope, dry mud and fresh mud flowing from the crater (N09$^0$ 43' 11.5" and E011$^0$ 09' 00.5; photo taken: 16/02/12)



A mud volcano occurrence at Lallapido, showing the angle of slope, dry mud and very few fresh mud around the crater (N09$^0$ 43' 11.0" and E011$^0$ 09' 00.8; photo taken: 16/02/12)



A mud volcano occurrence at Lallapido, showing fresh mud flowing from the crater and whitish precipitates seen around the crater (N09$^0$ 43' 10.9" and E011$^0$ 09' 03.4; photo taken: 16/02/12)



A mud volcano occurrence at Lallapido, showing the angle of slope, fresh mud flowing from the crater, grasses grown on the volcano and precipitated salt seen aroun the cone (N09$^0$ 43' 10.6" and E011$^0$ 09' 04.2; photo taken: 16/02/12)



A volcano of water variety at Lallapido, showing no cone, with water, grasses and white precipitates seen around it (N09$^0$ 43' 12.4" and E011$^0$ 08' 57.2; photo taken: 16/02/12)



A mud volcano occurrence at Lallapido, showing the angle of slope, dry mud and whitish precipitates seen around the crater and fresh mud flowing from the crater (N09$^0$ 43' 11.4" and E011$^0$ 08' 58.3; photo taken: 16/02/12))



A mud volcano occurrence at Lallapido, showing the angle of slope, fresh mud flowing from the crater with dry mud and precipitated salt seen around the crater (N09$^0$ 43' 11.6" and E011$^0$ 08' 58.1; photo taken: 16/02/12)



A mud volcano occurrence at Lallapido, showing the angle of slope, dry mud and fresh mud flowing from the crater (N09$^0$ 43' 11.5" and E011$^0$ 08' 58.5; photo taken: 16/02/12)



A mud volcano at Gujuba with slurry of mud and water seeping from the crater with whitish precipitates seen around the crater (N09$^0$38'52.6" E011$^0$04'09.4"; photo taken: 17/02/12)



A water volcano at Lallapido, the crater of the volcano has being dug by the Fulani's to enable them access water for their cows (N09$^0$ 43' 08.9" and E011$^0$ 08' 10.0; photo taken: 16/02/12)



A water volcano at Lallapido, the crater of the volcano has being dug by the Fulani's to enable them access water for their cows (N09$^0$ 43' 08.9" and E011$^0$ 08' 10.0; photo taken: 16/02/12)



A mud volcano at Gujuba with slurry of mud and water seeping from the crater with precipitated salt seen around the crater (N09$^0$38'52.7" E011$^0$04'09.4"; photo taken: 17/02/12)



A mud volcano at Gujuba with slurry of mud and water seeping from the crater with precipitated salt seen around the crater (N09$^0$38'52.5" E011$^0$04'09.4"; photo taken: 17/02/12)



A mud volcano at Gujuba with slurry of mud and water seeping from the crater with precipitated salt seen around the crater (N09$^0$38’52.6” E011$^0$04’09.7”; photo taken: 17/02/12)



A mud volcano at Gujuba with slurry of mud and water seeping from the crater with precipitated salt seen around the crater (N09$^0$38’52.5” E011$^0$04’08.6”; photo taken: 17/02/12)



A mud volcano at Gujuba with slurry of mud and water seeping from the crater with precipitated salt seen around the crater (N09$^0$38’51.4” E011$^0$04’07.9”; photo taken: 17/02/12)



A mud volcano at Jenye with slurry of mud and water seeping from the crater with whitish precipitates and grasses seen around the crater (N09$^0$39’46.0” E011$^0$04’40.3”; photo taken: 17/02/12)



Plate 46: A mud volcano at Jenye with slurry of mud and water seeping from the crater with whitish precipitates and grasses seen around the crater (N09$^0$39’46.2” E011$^0$04’40.6”; photo taken: 17/02/12)



A mud volcano at Jenye with slurry of mud and water seeping from the crater with whitish precipitates and grasses seen around the crater (N09$^0$39’45.6” E011$^0$04’40.7”; photo taken: 17/02/12)



A mud volcano at Jenye with slurry of mud and water seeping from the crater with whitish precipitates and grasses seen around the crater (N09$^0$39’45.9” E011$^0$04’40.3”; photo taken: 17/02/12)



A mud volcano at Jenye with slurry of mud and water seeping from the crater with whitish precipitates and grasses seen around the crater (N09$^0$39’45.6” E011$^0$04’41.1”; photo taken: 17/02/12)



A mud volcano at Jenye with slurry of mud and water seeping from the crater with whitish precipitates and grasses seen around the crater (N09$^0$39’45.7” E011$^0$04’41.6”; photo taken: 17/02/12)



A mud volcano at Pamadu with water seeping from the crater with grasses and precipitated salt seen around the crater (N09$^0$40’44.4” E011$^0$04’56.2”; photo taken: 18/02/ 2012)



A mud volcano at Pamadu, massive with slurry of mud and water seeping from the crater with precipitated salt seen around the crater (N09$^0$40’44.1” E011$^0$04’56.1”; photo taken: 18/02/ 2



A mud volcano at Pamadu with slurry of mud and water seeping from the crater with whitish precipitates seen around the crater (N09$^0$40’48.7” E011$^0$03’56.1”; photo taken: 18/02/ 2012)



A mud volcano at Pamadu with slurry of mud and water seeping from the crater with whitish precipitates seen around the crater (N09$^0$40’49.0” E011$^0$03’55.9”; photo taken: 18/02/ 2012)



Plate 60: A mud volcano at Pamadu with slurry of mud and water seeping from the crater with whitish precipitates seen around the crater (N09$^0$40’49.2” E011$^0$03’56.3”; photo taken: 18/02/ 2012)



A mud volcano at Pamadu with slurry of mud and water seeping from the crater with whitish precipitates seen around the crater (N09$^0$40’49.6” E011$^0$03’56.3”; photo taken: 18/02/ 2012)



A volcano of water variety at Pamadu, water seeps from the crater with grasses and whitish precipitates seen around the crater (N09$^0$40’50.2” E011$^0$03’55.9”; photo taken: 18/02/ 2012)



A mud volcano at Pamadu with slurry of mud and water seeping from the crater with whitish precipitates seen around the crater (N09$^0$50'.1" E011$^0$03'55.6"; photo taken: 18/02/ 2012)



A mud volcano at Pamadu with slurry of mud and water seeping from the crater with whitish precipitates seen around the crater (N09$^0$40'47.8" E011$^0$03'55.5"; photo taken: 18/02/ 2012)



A Mud volcano at Pamadu with slurry of mud and water seeping from the crater with whitish precipitates seen around the crater (N09$^0$40'54.1" EO11$^0$03'55.1"; photo taken: 18/02/ 2012)



A mud volcano at Lashadar with slurry of mud and water seeping from the crater (N09$^0$41'58.2" EO11$^0$10'26.6"; photo taken: 19/02/2012)



A mud volcano at Lashadar with tiny slurry of mud and water seeping from the crater (N09$^0$41’57.6” EO11$^0$10’26.9”; photo taken: 19/02/2012)



A mud volcano at Lashadar with slurry of mud and water seeping from the crater with whitish precipitates seen around the crater (N09$^0$41’57.1” EO11$^0$10’26.8”; photo taken: 19/02/2012)



A mud volcano at Lashadar with slurry of mud and water seeping from the crater with whitish precipitates seen around the crater (N09$^0$41’55.6” EO11$^0$10’29.7”; photo taken: 19/02/2012)



A Mud volcano at Lashadar with slurry of mud and water seeping from the crater with precipitated salt seen around the crater (N09$^0$41’56.2” EO11$^0$10’30.9”; photo taken: 19/02/2012)



A Mud volcano at Lashadar with slurry of mud and water seeping from the crater with precipitated salt seen around the crater (N09$^0$42’00.4” EO11$^0$10’30.0”; photo taken: 19/02/2012)



A volcano of water variety at Lashadar with reddish water seeping from the crater (N09$^0$42’01.8” EO11$^0$10’37.2”; photo taken: 19/02/2012)



Plate 80: A mud volcano at Lakaturu with slurry of mud and water seeping from the crater with precipitated salt seen around the crater (N09$^0$42’11.9” EO11$^0$07’44.8”; photo taken: 20/02/2012)



A mud volcano at Lakaturu with slurry of mud and water seeping from the crater with precipitated salt seen around the crater (N09$^0$42’12.6” EO11$^0$07’42.5”; photo taken: 20/02/2012)



A mud volcano at Lakaturu with slurry of mud and water seeping from the crater with precipitated salt seen around the crater (N09$^0$42’12.4” EO11$^0$07’42.8”; photo taken: 20/02/2012)



A mud volcano at Lakaturu with slurry of mud and water seeping from the crater with precipitated salt seen around the crater (N09$^0$42’12.0” EO11$^0$07’42.7”; photo taken: 20/02/2012)



A mud volcano at Lakaturu with slurry of mud and water seeping from the crater with precipitated salt seen around the crater (N09$^0$42’12.0” EO11$^0$07’42.7”; photo taken: 20/02/2012)



A mud volcano at Lakaturu with slurry of mud and water seeping from the crater with precipitated salt seen around the crater (N09$^0$42’12.2” EO11$^0$07’42.9”; photo taken: 20/02/2012)



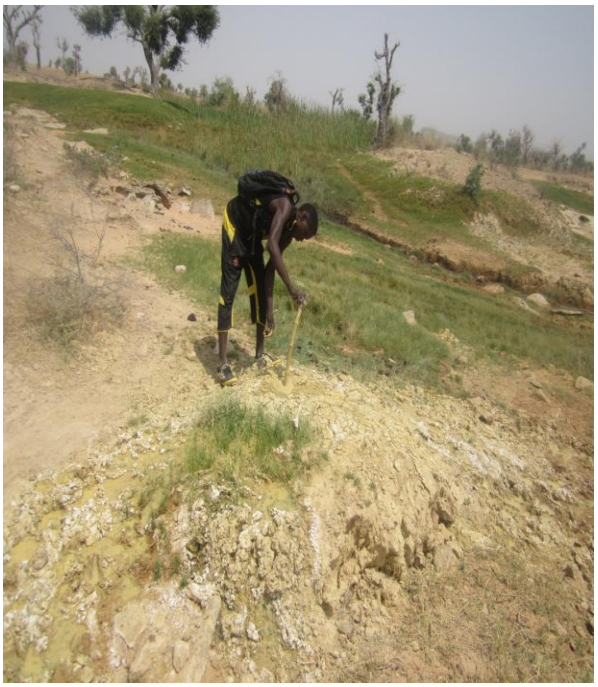
A mud volcano at Lakaturu with slurry of mud and water seeping from the crater with precipitated salt seen around the crater (N09$^0$42’12.1” EO11$^0$07’42.5”; photo taken: 20/02/2012)



A mud volcano at Lakaturu with slurry of mud and water seeping from the crater with precipitated salt seen around the crater (N09$^0$42’10.8” EO11$^0$07’43.1”; photo taken: 20/02/2012)



A mud volcano at Lakaturu with slurry of mud and water seeping from the crater with precipitated salt seen around the crater (N09$^0$42’10.8” EO11$^0$07’42.8”; photo taken: 20/02/2012)



A mud volcano at Lakaturu with slurry of mud and water seeping from the crater with precipitated salt seen around the crater (N09$^0$42’11.2” EO11$^0$07’43.0”; photo taken: 20/02/2012)



A mud volcano at Lakaturu with slurry of mud and water seeping from the crater with precipitated salt seen around the crater (N09$^0$42’12.6” EO11$^0$07’42.5”; photo taken: 20/02/2012)



Women scraping the areas around mud volcanoes at Lakaturu in search of potash used for cooking after being filtered from the sediments n around the crater (N09$^0$42’10.7” EO11$^0$07’43.3” ; photo taken: 20/02/2012)



A volcano of water variety seeping out water of brownish – reddish colour from the crater with grasses and precipitated salt seen around the crater at Digga (N09$^0$39’52.0” E011$^0$07’56.4” ; photo taken: 20/02/2012)



A mud volcano at Digga with slurry of mud and water seeping from the crater with precipitated salt seen around the crater (N09$^0$39’49.6” E011$^0$07’59.5”; photo taken: 20/02/2012)



A volcano of water variety seeping out water of brownish – reddish colour from the crater with grasses and precipitated salt seen around the crater at Digga (N09$^0$39’51.0” E011$^0$08’03.3” ; photo taken: 20/02/2012)



A mud volcano at Kurum with slurry of mud and water seeping from the crater with precipitated salt seen around the crater (N09$^0$46’16.4” E011$^0$03’04.6”; photo taken: 21/02/2012)



A mud volcano at Kurum with slurry of mud and water seeping from the crater with precipitated salt seen around the crater (N09$^0$46’17.2” E011$^0$03’04.9”; photo taken: 21/02/2012)

)



A mud volcano at Kurum with slurry of mud and water seeping from the crater with precipitated salt seen around the crater (N09$^0$46’16.3” E011$^0$03’05.2”; photo taken: 21/02/2012)



A mud volcano at Kurum with slurry of mud and water seeping from the crater with precipitated salt seen around the crater (N09$^0$46’16.5” E011$^0$03’06.1”; photo taken: 21/02/2012)



A mud volcano at Kurum with slurry of mud and water seeping flowing from the crater (N09$^0$46’17.1” E011$^0$03’05.7”)



A mud volcano at Kurum with slurry of mud and water seeping from the crater (N09$^0$46’17.9” E011$^0$03’05.0”; photo taken: 03/09/2013)



A mud volcano at Kurum with slurry of mud and water seeping from the crater (N09$^0$46’18.1” E011$^0$03’05.8”; photo taken: 03/09/2013)



A Mud volcano at Kurum with slurry of mud and water seeping from the crater (N09$^0$46'18.2" E011$^0$03'06.1"; photo taken: 03/09/2013)



A mud volcano at Kurum with slurry of mud and water seeping from the crater with precipitated salt seen around the crater (N09$^0$46'18.3" E011$^0$03'06.7"; photo taken: 03/09/2013)



Villagers at Kurum making potash from scraped sands within the vicinity of the mud volcanoes (N09$^0$46'18.5" E011$^0$03'06.9"; photo taken: 21/02/2012)



A dormant mud volcano at Todi, showing the angle of slope, with cone still intact but no mud is flowing out of the crater (N09$^0$44'55.2" E011$^0$07'55.2"; photo taken: 22/02/2012)



A mud volcano at Todi with slurry of mud and water seeping from the crater with whitish precipitates seen around the crater (N09$^0$45’01.6” E011$^0$07’56.6”; photo taken: 22/02/2012)



A mud volcano at Todi with slurry of mud and water seeping from the crater with whitish precipitates seen around the crater (N09$^0$45’03.7” E011$^0$07’53.5”; photo taken: 22/02/2012)



A mud volcano at Todi with slurry of mud and water seeping from the crater with whitish precipitates seen around the crater (N09$^0$44’59.2” E011$^0$07’46.2”; photo taken: 22/02/2012)



A volcano of water variety at Todi with water seeping from the crater with precipitated salt seen around the crater (N09$^0$44’00.7” E011$^0$07’44.9”; photo taken: 22/02/2012)



A volcano of water variety at Todi with water seeping from the crater with precipitated salt seen around the crater (N09$^0$44’01.6” E011$^0$07’41.8”; photo taken: 22/02/2012)



A volcano of water variety at Todi with water seeping from the crater with precipitated salt seen around the crater (N09$^0$44’06.2” E011$^0$07’40.9”; photo taken: 22/02/2012)

# APPENDIX C

**Physico - chemical parameters of water from onshore mud volcanoes in Nigeria**

| Location ID | Sample ID | Geog. Cordinates | pH | Temp °C | TDS mg/l | EC uS/cm | TH mg/l $Caco_3$ | $Na^+$ | $K^+$ mg/l | $Ca^{2+}$ mg/l | $Mg^{2+}$ mg/l | Fe mg/l | $Cl^-$ mg/l | $HCO_{3-}$ mg/l | $CO_3^{2-}$ mg/l | $SO_4^{2-}$ mg/l | $SiO_2$ mg/l |
|---|---|---|---|---|---|---|---|---|---|---|---|---|---|---|---|---|---|
| Lakaturu | K 1 | N09$^0$42'12.9" E11$^0$07'42.5" | 8.62 | 24.9 | 2729 | 2100 | 829 | 781 | 29 | 32 | 2.75 | 0.22 | 325 | 1235 | 88.8 | 12.6 | 23.2 |
| Chengau | K 2 | N09$^0$39'17.1" E11$^0$06'42.7" | - | 26.4 | 2717 | - | - | 852 | 23 | 15 | 2.45 | 4.56 | 123 | 1501 | 168 | 13.9 | 14.4 |
| Jenye | K 3 | N09$^0$39'47.4" E11$^0$04'39.6" | - | 25.8 | 4208 | - | - | 1058 | 13 | 10 | 1.19 | 0.26 | 202 | 1747 | 137 | 12.6 | 9.49 |
| Gujuba | K 4 | N09$^0$38'52.2" E11$^0$04'09.2" | 8.73 | 22.1 | 3637 | 2400 | 1110 | 1178 | 18 | 21 | 2.72 | 4.55 | 246 | 1903 | 240 | 16.9 | 7 |
| Laturu | K 5 | N09$^0$42'10.1" E11$^0$11'31.8" | 7.94 | 41.9 | 448 | 324 | 155 | 50 | 31 | 17 | 3.07 | 0.24 | 6 | 293 | 3 | 12.9 | 32 |
| Pamadu | K 6 | N09$^0$40'44.1" E11$^0$03'56.1" | 8.01 | 22.8 | 776 | 256 | 108 | 188 | 20 | 22 | 7.82 | 0.67 | 5 | 495 | 3 | 12.5 | 22.2 |
| Kurum | K 7 | N09$^0$46'16.1" E11$^0$03'04.9" | 8.58 | 25.6 | 2280 | 2430 | 979 | 688 | 41 | 35 | 10.4 | 0.02 | 228 | 1171 | 72 | 12.7 | 22.3 |
| Todi | K 8 | N09$^0$44'59.0" E11$^0$07'55.1" | 8.99 | 22.5 | 12757 | 2670 | 1180 | 4789 | 134 | 17 | 20 | 0.13 | 2625 | 3111 | 2040 | 13.2 | 8.12 |
| Sasanyi | K 9 | N09$^0$56'11.6" E11$^0$12'12.6" | - | 22.0 | 653 | - | - | 84 | 9 | 46 | 4.67 | 2.23 | 48 | 415 | 3 | 13.2 | 28.4 |
| Lachikoltok | K 10 | N09$^0$54'18.8" E11$^0$14'32.5" | 7.99 | 22.1 | 456 | 222 | 102 | 41 | 32 | 41 | 6.9 | 5.74 | 6 | 262 | 3 | 12.9 | 45.6 |
| Digga | K 11 | N09$^0$39'49.6" E11$^0$07'59.5" | - | 26.2 | 2078 | - | - | 600 | 14 | 8 | 1.16 | 0.73 | 141 | 1196 | 84 | 12.9 | 20.4 |
| Lashadar | K 12 | N09$^0$14'47.5" E11$^0$10'15.6" | 8.53 | 25.5 | 1132 | 1150 | 478 | 310 | 17 | 13 | 1.43 | 0.22 | 98 | 647 | 3 | 13.4 | 30.2 |
| Lakomji | K 13 | N09$^0$41'05.9" E11$^0$14'09.0" | - | 41.2 | 249 | | | 19 | 20 | 29 | 4.46 | 0.02 | 5 | 126 | 3 | 13.9 | 29.4 |
| Lallapido | K 14 | N09$^0$43'11.6" E11$^0$08'59.5" | 8.70 | 26.1 | 1126 | 1770 | 713 | 327 | 21 | 15 | 3.66 | 0.07 | 100 | 561 | 72 | 14.4 | 12.4 |

# APPENDIX D

**CENTRUM BADAŃ I DOZORU GÓRNICTWA PODZIEMNEGO Sp. z o.o.**
**Ośrodek Badań Środowiska i Zagrożeń Naturalnych**
43-143 LĘDZINY, ul. LĘDZIŃSKA 8, NIP PL6460008992
tel. 32-324-22-40, fax 32-216-66-66, http://www.cbidgp.pl e-mail: obsizn@cbidgp.pl
SR w Katowicach, Wydz. Gosp. Krajowego Rejestru Sądowego nr KRS 0000067459, Kapitał Zakładowy 3.700.000,00 zł

AB 418

**OŚRODEK BADAŃ ŚRODOWISKA I ZAGROŻEŃ NATURALNYCH**

**Posiada akredytację AB 418 w zakresie:**

**Badań i pomiarów w środowisku pracy:**
- pobierania próbek powietrza,
- oznaczania stężeń substancji chemicznych i pyłowych,
- pomiaru hałasu, drgań, oświetlenia, pól elektromagnetycznych.

**Badań i pomiarów w środowisku ogólnym:**
- pobierania próbek gazów odlotowych,
- oznaczania stężeń substancji chemicznych i pyłowych w gazach odlotowych,
- pomiaru emisji do powietrza, hałasu, pól elektromagnetycznych.

**Pobierania próbek:**
- wód powierzchniowych, podziemnych, przeznaczonych do spożycia,
- ścieków,
- osadów ściekowych.

**Badań fizyko-chemicznych:**
- wód i ścieków,
- wyciągów wodnych,
- osadów i odpadów,
- gleb/gruntów,
- produktów naftowych,
- substancji chemicznych.

**Badań mikrobiologicznych:**
- wód,
- osadów ściekowych.

**Badań spalin pojazdów górniczych.**

# SPRAWOZDANIE Z BADAŃ NR 1619/ZL/13

wykonanych zgodnie ze zleceniem nr - z dnia 2013-04-05

Nr zlecenia wg CBiDGP: 4/13/00699

**UNIWERSYTET ŚLĄSKI WYDZIAŁ NAUK O ZIEMI**
**KATEDRA GEOLOGII PODSTAWOWEJ**
**41-200 SOSNOWIEC, ul. BĘDZIŃSKA 60**

Zgodnie ze zleceniem i przeprowadzonymi uzgodnieniami wykonano badania w 14 próbkach.

Liczba stron zawartych w sprawozdaniu: 15.

Sprawozdanie sporządził:

Inspektor ds. Badań Środowiska
i Zagrożeń Naturalnych

mgr Małgorzata Dyllus

Sprawozdanie autoryzował:

Kierownik Pracowni
Analiz Fizykochemicznych i Biologicznych

Irena Malczyk

Zatwierdził:

KIEROWNIK
Laboratorium Analiz Chemicznych

mgr Magdalena Śmigiel

Lędziny, dn. 2013-04-18



Załącznik nr 2/1 do PO-17, wydanie VI z 08.04.2013r.

Nazwa klienta: UNIWERSYTET ŚLĄSKI WYDZIAŁ NAUK O ZIEMI KATEDRA GEOLOGII PODSTAWOWEJ
41-200 SOSNOWIEC, BĘDZIŃSKA 60

Miejsce poboru próbek: Nigeria - źródła występujące w środowisku osadowym — Próbki pobrał: Klient

Data dostarczenia próbek: 2013-04-05 — Próbki dostarczył: Klient

Stan próbek: dobry

| | | | | | |
|---|---|---|---|---|---|
| | | | | Numer próbki | **1908/ZL1/13** |
| | | | | Data/godzina pobrania próbki | |
| | | | | Miejsce pobrania próbki | **LAKATURU** |
| | | | | Rodzaj próbki | Woda |
| S.j.* | Parametr | Metoda badawcza/ Metoda oznaczenia | Jednostka | Zakres wykonania oznaczenia | Wyniki badań |
| A | Chlorki | PN-ISO 9297:1994 Miareczkowo | [mg/l Cl] | 5.0 - 50000 | 325 ±9 |
| A | Siarczany | PN-ISO 9280:2002 Wagowo | [mg/l $SO_4$] | 10.0-5000 | 12.6 ±1.9 |
| A | Wodorowęglany | PB-58/07.2008 wyd. I z dnia 11.07.2008r. Obliczeniowo | [mg/l] | 6.10 - 6100 | 1235 ±83 |
| A | Węglany | PB-58/07.2008 wyd. I z dnia 11.07.2008r. Obliczeniowo | [mg/l] | 3.0 - 3000 | 88.8 ±6.0 |
| A | Krzemionka ogólna | PN-EN ISO 11885:2009 ICP-OES | [mg/l $SiO_2$] | 0.10-100 | 23.2 ±3.7 |
| A | Potas | PN-EN ISO 11885:2009 ICP-OES | [mg/l] | 1.0-10000 | 29.2 ±5.3 |
| A | Sód | PN-EN ISO 11885:2009 ICP-OES | [mg/l] | 1.0-100000 | 781 ±141 |
| A | Żelazo ogólne | PN-EN ISO 11885:2009 ICP-OES | [mg/l] | 0.010 - 500 | 0.22 ±0.04 |
| A | Wapń | PN-EN ISO 11885:2009 ICP-OES | [mg/l] | 0.10 - 10000 | 32.0 ±5.1 |
| A | Magnez | PN-EN ISO 11885:2009 ICP-OES | [mg/l] | 0.10 - 5000 | 2.75 ±0.40 |

Nazwa klienta: UNIWERSYTET ŚLĄSKI WYDZIAŁ NAUK O ZIEMI KATEDRA GEOLOGII PODSTAWOWEJ
41-200 SOSNOWIEC, BĘDZIŃSKA 60

Miejsce poboru próbek: Nigeria - źródła występujące w środowisku osadowym — Próbki pobrał: Klient

Data dostarczenia próbek: 2013-04-05 — Próbki dostarczył: Klient

Stan próbek: dobry

| | | | | | Numer próbki | 1909/ZL1/13 |
|---|---|---|---|---|---|---|
| | | | | | Data/godzina pobrania próbki | |
| | | | | | Miejsce pobrania próbki | CHENGAU |
| | | | | | Rodzaj próbki | Woda |
| S.j.* | Parametr | Metoda badawcza/ Metoda oznaczenia | Jednostka | Zakres wykonania oznaczenia | Wyniki badań | |
| A | Chlorki | PN-ISO 9297:1994 Miareczkowo | [mg/l Cl] | 5.0 - 50000 | 123 | ±3 |
| A | Siarczany | PN-ISO 9280:2002 Wagowo | [mg/l $SO_4$] | 10.0-5000 | 13.9 | ±2.1 |
| A | Wodorowęglany | PB-58/07.2008 wyd. I z dnia 11.07.2008r. Obliczeniowo | [mg/l] | 6.10 - 6100 | 1501 | ±101 |
| A | Węglany | PB-58/07.2008 wyd. I z dnia 11.07.2008r. Obliczeniowo | [mg/l] | 3.0 - 3000 | 168 | ±11 |
| A | Krzemionka ogólna | PN-EN ISO 11885:2009 ICP-OES | [mg/l $SiO_2$] | 0.10-100 | 14.4 | ±2.3 |
| A | Potas | PN-EN ISO 11885:2009 ICP-OES | [mg/l] | 1.0-10000 | 22.7 | ±4.1 |
| A | Sód | PN-EN ISO 11885:2009 ICP-OES | [mg/l] | 1.0-100000 | 852 | ±153 |
| A | Żelazo ogólne | PN-EN ISO 11885:2009 ICP-OES | [mg/l] | 0.010 - 500 | 4.56 | ±0.91 |
| A | Wapń | PN-EN ISO 11885:2009 ICP-OES | [mg/l] | 0.10 - 10000 | 15.1 | ±2.4 |
| A | Magnez | PN-EN ISO 11885:2009 ICP-OES | [mg/l] | 0.10 - 5000 | 2.45 | ±0.40 |

Nazwa klienta: UNIWERSYTET ŚLĄSKI WYDZIAŁ NAUK O ZIEMI KATEDRA GEOLOGII PODSTAWOWEJ
41-200 SOSNOWIEC, BĘDZIŃSKA 60

Miejsce poboru próbek: Nigeria - źródła występujące w środowisku osadowym — Próbki pobrał: Klient

Data dostarczenia próbek: 2013-04-05 — Próbki dostarczył: Klient

Stan próbek: dobry

| | | | | | |
|---|---|---|---|---|---|
| | | | | Numer próbki | 1910/ZL1/13 |
| | | | | Data/godzina pobrania próbki | |
| | | | | Miejsce pobrania próbki | JENYE |
| | | | | Rodzaj próbki | Woda |
| S.j.* | Parametr | Metoda badawcza/ Metoda oznaczenia | Jednostka | Zakres wykonania oznaczenia | Wyniki badań |
| A | Chlorki | PN-ISO 9297:1994 Miareczkowo | [mg/l Cl] | 5.0 - 50000 | 202 ±6 |
| A | Siarczany | PN-ISO 9280:2002 Wagowo | [mg/l $SO_4$] | 10.0-5000 | 12.6 ±1.9 |
| A | Wodorowęglany | PB-58/07.2008 wyd. I z dnia 11.07.2008r. Obliczeniowo | [mg/l] | 6.10 - 6100 | 1747 ±117 |
| A | Węglany | PB-58/07.2008 wyd. I z dnia 11.07.2008r. Obliczeniowo | [mg/l] | 3.0 - 3000 | 137 ±9 |
| A | Krzemionka ogólna | PN-EN ISO 11885:2009 ICP-OES | [mg/l $SiO_2$] | 0.10-100 | 9.49 ±1.52 |
| A | Potas | PN-EN ISO 11885:2009 ICP-OES | [mg/l] | 1.0-10000 | 12.5 ±2.3 |
| A | Sód | PN-EN ISO 11885:2009 ICP-OES | [mg/l] | 1.0-100000 | 1058 ±190 |
| A | Żelazo ogólne | PN-EN ISO 11885:2009 ICP-OES | [mg/l] | 0.010 - 500 | 0.26 ±0.05 |
| A | Wapń | PN-EN ISO 11885:2009 ICP-OES | [mg/l] | 0.10 - 10000 | 10.2 ±1.6 |
| A | Magnez | PN-EN ISO 11885:2009 ICP-OES | [mg/l] | 0.10 - 5000 | 1.19 ±0.20 |

| CBiDGP Sp. z o.o. | Sprawozdanie z badań<br>Nr 1619/ZL/13<br><br>z dnia 2013-04-18 | Strona: 5<br><br>Stron: 15 |
|---|---|---|
| Załącznik nr 2/1 do PO-17, wydanie VI z 08.04.2013r. | | |

Nazwa klienta: UNIWERSYTET ŚLĄSKI WYDZIAŁ NAUK O ZIEMI KATEDRA GEOLOGII PODSTAWOWEJ
41-200 SOSNOWIEC, BĘDZIŃSKA 60

Miejsce poboru próbek: Nigeria - źródła występujące w środowisku osadowym — Próbki pobrał: Klient

Data dostarczenia próbek: 2013-04-05 — Próbki dostarczył: Klient

Stan próbek: dobry

| | | | | | | |
|---|---|---|---|---|---|---|
| | | | | Numer próbki | 1911/ZL1/13 | |
| | | | | Data/godzina pobrania próbki | | |
| | | | | Miejsce pobrania próbki | GUJUBA | |
| | | | | Rodzaj próbki | Woda | |
| S.j.* | Parametr | Metoda badawcza/ Metoda oznaczenia | Jednostka | Zakres wykonania oznaczenia | Wyniki badań | |
| A | Chlorki | PN-ISO 9297:1994 Miareczkowo | [mg/l Cl] | 5.0 - 50000 | 246 | ±7 |
| A | Siarczany | PN-ISO 9280:2002 Wagowo | [mg/l $SO_4$] | 10.0-5000 | 16.9 | ±2.5 |
| A | Wodorowęglany | PB-58/07.2008 wyd. I z dnia 11.07.2008r. Obliczeniowo | [mg/l] | 6.10 - 6100 | 1903 | ±128 |
| A | Węglany | PB-58/07.2008 wyd. I z dnia 11.07.2008r. Obliczeniowo | [mg/l] | 3.0 - 3000 | 240 | ±16 |
| A | Krzemionka ogólna | PN-EN ISO 11885:2009 ICP-OES | [mg/l $SiO_2$] | 0.10-100 | 7.00 | ±1.12 |
| A | Potas | PN-EN ISO 11885:2009 ICP-OES | [mg/l] | 1.0-10000 | 18.4 | ±3.3 |
| A | Sód | PN-EN ISO 11885:2009 ICP-OES | [mg/l] | 1.0-100000 | 1178 | ±212 |
| A | Żelazo ogólne | PN-EN ISO 11885:2009 ICP-OES | [mg/l] | 0.010 - 500 | 4.55 | ±0.91 |
| A | Wapń | PN-EN ISO 11885:2009 ICP-OES | [mg/l] | 0.10 - 10000 | 21.0 | ±3.4 |
| A | Magnez | PN-EN ISO 11885:2009 ICP-OES | [mg/l] | 0.10 - 5000 | 2.72 | ±0.40 |

| CBiDGP Sp. z o.o. | Sprawozdanie z badań<br>Nr 1619/ZL/13<br><br>z dnia 2013-04-18 | Strona: 6<br><br>Stron: 15 |
|---|---|---|
| Załącznik nr 2/1 do PO-17, wydanie VI z 08.04.2013r. | | |

Nazwa klienta: UNIWERSYTET ŚLĄSKI WYDZIAŁ NAUK O ZIEMI KATEDRA GEOLOGII PODSTAWOWEJ
41-200 SOSNOWIEC, BĘDZIŃSKA 60

Miejsce poboru próbek: Nigeria - źródła występujące w środowisku osadowym — Próbki pobrał: Klient

Data dostarczenia próbek: 2013-04-05 — Próbki dostarczył: Klient

Stan próbek: dobry

| | | | | | | |
|---|---|---|---|---|---|---|
| | | | | Numer próbki | 1912/ZL1/13 | |
| | | | | Data/godzina pobrania próbki | | |
| | | | | Miejsce pobrania próbki | LETURU | |
| | | | | Rodzaj próbki | Woda | |
| S.J.* | Parametr | Metoda badawcza/ Metoda oznaczenia | Jednostka | Zakres wykonania oznaczenia | Wyniki badań | |
| A | Chlorki | PN-ISO 9297:1994 Miareczkowo | [mg/l Cl] | 5.0 - 50000 | 6.0 | ±0.2 |
| A | Siarczany | PN-ISO 9280:2002 Wagowo | [mg/l $SO_4$] | 10.0-5000 | 12.9 | ±1.9 |
| A | Wodorowęglany | PB-58/07.2008 wyd. I z dnia 11.07.2008r. Obliczeniowo | [mg/l] | 6.10 - 6100 | 293 | ±20 |
| A | Węglany | PB-58/07.2008 wyd. I z dnia 11.07.2008r. Obliczeniowo | [mg/l] | 3.0 - 3000 | <3.0[1)] | |
| A | Krzemionka ogólna | PN-EN ISO 11885:2009 ICP-OES | [mg/l $SiO_2$] | 0.10-100 | 32.0 | ±5.1 |
| A | Potas | PN-EN ISO 11885:2009 ICP-OES | [mg/l] | 1.0-10000 | 30.6 | ±5.5 |
| A | Sód | PN-EN ISO 11885:2009 ICP-OES | [mg/l] | 1.0-100000 | 50.1 | ±9.0 |
| A | Żelazo ogólne | PN-EN ISO 11885:2009 ICP-OES | [mg/l] | 0.010 - 500 | 0.24 | ±0.05 |
| A | Wapń | PN-EN ISO 11885:2009 ICP-OES | [mg/l] | 0.10 - 10000 | 16.6 | ±2.7 |
| A | Magnez | PN-EN ISO 11885:2009 ICP-OES | [mg/l] | 0.10 - 5000 | 3.07 | ±0.50 |

Nazwa klienta: UNIWERSYTET ŚLĄSKI WYDZIAŁ NAUK O ZIEMI KATEDRA GEOLOGII PODSTAWOWEJ
41-200 SOSNOWIEC, BĘDZIŃSKA 60

Miejsce poboru próbek: Nigeria - źródła występujące w środowisku osadowym — Próbki pobrał: Klient

Data dostarczenia próbek: 2013-04-05 — Próbki dostarczył: Klient

Stan próbek: dobry

| | | | | | |
|---|---|---|---|---|---|
| | | | | Numer próbki | 1913/ZL1/13 |
| | | | | Data/godzina pobrania próbki | |
| | | | | Miejsce pobrania próbki | PAMADU |
| | | | | Rodzaj próbki | Woda |
| S.j.* | Parametr | Metoda badawcza/ Metoda oznaczenia | Jednostka | Zakres wykonania oznaczenia | Wyniki badań |
| A | Chlorki | PN-ISO 9297:1994 Miareczkowo | [mg/l Cl] | 5.0 - 50000 | <5.0[1)] |
| A | Siarczany | PN-ISO 9280:2002 Wagowo | [mg/l $SO_4$] | 10.0-5000 | 12.5 ±1.9 |
| A | Wodorowęglany | PB-58/07.2008 wyd. I z dnia 11.07.2008r. Obliczeniowo | [mg/l] | 6.10 - 6100 | 495 ±33 |
| A | Węglany | PB-58/07.2008 wyd. I z dnia 11.07.2008r. Obliczeniowo | [mg/l] | 3.0 - 3000 | <3.0[1)] |
| A | Krzemionka ogólna | PN-EN ISO 11885:2009 ICP-OES | [mg/l $SiO_2$] | 0.10-100 | 22.2 ±3.6 |
| A | Potas | PN-EN ISO 11885:2009 ICP-OES | [mg/l] | 1.0-10000 | 20.2 ±3.6 |
| A | Sód | PN-EN ISO 11885:2009 ICP-OES | [mg/l] | 1.0-100000 | 188 ±34 |
| A | Żelazo ogólne | PN-EN ISO 11885:2009 ICP-OES | [mg/l] | 0.010 - 500 | 0.67 ±0.13 |
| A | Wapń | PN-EN ISO 11885:2009 ICP-OES | [mg/l] | 0.10 - 10000 | 22.3 ±3.6 |
| A | Magnez | PN-EN ISO 11885:2009 ICP-OES | [mg/l] | 0.10 - 5000 | 7.82 ±1.30 |

Nazwa klienta: UNIWERSYTET ŚLĄSKI WYDZIAŁ NAUK O ZIEMI KATEDRA GEOLOGII PODSTAWOWEJ
41-200 SOSNOWIEC, BĘDZIŃSKA 60

Miejsce poboru próbek: Nigeria - źródła występujące w środowisku osadowym — Próbki pobrał: Klient

Data dostarczenia próbek: 2013-04-05 — Próbki dostarczył: Klient

Stan próbek: dobry

| | | | | | |
|---|---|---|---|---|---|
| | | | | Numer próbki | 1914/ZL1/13 |
| | | | | Data/godzina pobrania próbki | |
| | | | | Miejsce pobrania próbki | KURUM |
| | | | | Rodzaj próbki | Woda |
| S.J.* | Parametr | Metoda badawcza/ Metoda oznaczenia | Jednostka | Zakres wykonania oznaczenia | Wyniki badań |
| A | Chlorki | PN-ISO 9297:1994 Miareczkowo | [mg/l Cl] | 5.0 - 50000 | 228 ±6 |
| A | Siarczany | PN-ISO 9280:2002 Wagowo | [mg/l $SO_4$] | 10.0-5000 | 12.7 ±1.9 |
| A | Wodorowęglany | PB-58/07.2008 wyd. I z dnia 11.07.2008r. Obliczeniowo | [mg/l] | 6.10 - 6100 | 1171 ±79 |
| A | Węglany | PB-58/07.2008 wyd. I z dnia 11.07.2008r. Obliczeniowo | [mg/l] | 3.0 - 3000 | 72.0 ±4.8 |
| A | Krzemionka ogólna | PN-EN ISO 11885:2009 ICP-OES | [mg/l $SiO_2$] | 0.10-100 | 22.3 ±3.6 |
| A | Potas | PN-EN ISO 11885:2009 ICP-OES | [mg/l] | 1.0-10000 | 40.6 ±7.3 |
| A | Sód | PN-EN ISO 11885:2009 ICP-OES | [mg/l] | 1.0-100000 | 688 ±124 |
| A | Żelazo ogólne | PN-EN ISO 11885:2009 ICP-OES | [mg/l] | 0.010 - 500 | 0.024 ±0.005 |
| A | Wapń | PN-EN ISO 11885:2009 ICP-OES | [mg/l] | 0.10 - 10000 | 34.5 ±5.5 |
| A | Magnez | PN-EN ISO 11885:2009 ICP-OES | [mg/l] | 0.10 - 5000 | 10.4 ±1.7 |

Nazwa klienta: UNIWERSYTET ŚLĄSKI WYDZIAŁ NAUK O ZIEMI KATEDRA GEOLOGII PODSTAWOWEJ
41-200 SOSNOWIEC, BĘDZIŃSKA 60

Miejsce poboru próbek: Nigeria - źródła występujące w środowisku osadowym — Próbki pobrał: Klient

Data dostarczenia próbek: 2013-04-05 — Próbki dostarczył: Klient

Stan próbek: dobry

| | | | | | Numer próbki | 1915/ZL1/13 |
|---|---|---|---|---|---|---|
| | | | | | Data/godzina pobrania próbki | |
| | | | | | Miejsce pobrania próbki | TODI |
| | | | | | Rodzaj próbki | Woda |
| S.J.* | Parametr | Metoda badawcza/ Metoda oznaczenia | Jednostka | Zakres wykonania oznaczenia | Wyniki badań | |
| A | Chlorki | PN-ISO 9297:1994 Miareczkowo | [mg/l Cl] | 5.0 - 50000 | 2625 | ±74 |
| A | Siarczany | PN-ISO 9280:2002 Wagowo | [mg/l $SO_4$] | 10.0-5000 | 13.2 | ±2.0 |
| A | Wodorowęglany | PB-58/07.2008 wyd. I z dnia 11.07.2008r. Obliczeniowo | [mg/l] | 6.10 - 6100 | 3111 | ±208 |
| A | Węglany | PB-58/07.2008 wyd. I z dnia 11.07.2008r. Obliczeniowo | [mg/l] | 3.0 - 3000 | 2040 | ±137 |
| A | Krzemionka ogólna | PN-EN ISO 11885:2009 ICP-OES | [mg/l $SiO_2$] | 0.10-100 | 8.12 | ±1.30 |
| A | Potas | PN-EN ISO 11885:2009 ICP-OES | [mg/l] | 1.0-10000 | 134 | ±24 |
| A | Sód | PN-EN ISO 11885:2009 ICP-OES | [mg/l] | 1.0-100000 | 4789 | ±862 |
| A | Żelazo ogólne | PN-EN ISO 11885:2009 ICP-OES | [mg/l] | 0.010 - 500 | 0.13 | ±0.03 |
| A | Wapń | PN-EN ISO 11885:2009 ICP-OES | [mg/l] | 0.10 - 10000 | 16.7 | ±2.7 |
| A | Magnez | PN-EN ISO 11885:2009 ICP-OES | [mg/l] | 0.10 - 5000 | 20.0 | ±3.2 |

Nazwa klienta: UNIWERSYTET ŚLĄSKI WYDZIAŁ NAUK O ZIEMI KATEDRA GEOLOGII PODSTAWOWEJ
41-200 SOSNOWIEC, BĘDZIŃSKA 60

Miejsce poboru próbek: Nigeria - źródła występujące w środowisku osadowym — Próbki pobrał: Klient

Data dostarczenia próbek: 2013-04-05 — Próbki dostarczył: Klient

Stan próbek: dobry

| | | | | | |
|---|---|---|---|---|---|
| | | | | Numer próbki | 1916/ZL1/13 |
| | | | | Data/godzina pobrania próbki | |
| | | | | Miejsce pobrania próbki | SANSANYI |
| | | | | Rodzaj próbki | Woda |
| S.J.* | Parametr | Metoda badawcza/ Metoda oznaczenia | Jednostka | Zakres wykonania oznaczenia | Wyniki badań |
| A | Chlorki | PN-ISO 9297:1994 Miareczkowo | [mg/l Cl] | 5.0 - 50000 | 48 ±1 |
| A | Siarczany | PN-ISO 9280:2002 Wagowo | [mg/l $SO_4$] | 10.0-5000 | 13.2 ±2.0 |
| A | Wodorowęglany | PB-58/07.2008 wyd. I z dnia 11.07.2008r. Obliczeniowo | [mg/l] | 6.10 - 6100 | 415 ±28 |
| A | Węglany | PB-58/07.2008 wyd. I z dnia 11.07.2008r. Obliczeniowo | [mg/l] | 3.0 - 3000 | <3.0[1)] |
| A | Krzemionka ogólna | PN-EN ISO 11885:2009 ICP-OES | [mg/l $SiO_2$] | 0.10-100 | 28.4 ±4.5 |
| A | Potas | PN-EN ISO 11885:2009 ICP-OES | [mg/l] | 1.0-10000 | 9.40 ±1.69 |
| A | Sód | PN-EN ISO 11885:2009 ICP-OES | [mg/l] | 1.0-100000 | 84.1 ±15.1 |
| A | Żelazo ogólne | PN-EN ISO 11885:2009 ICP-OES | [mg/l] | 0.010 - 500 | 2.23 ±0.45 |
| A | Wapń | PN-EN ISO 11885:2009 ICP-OES | [mg/l] | 0.10 - 10000 | 46.4 ±7.4 |
| A | Magnez | PN-EN ISO 11885:2009 ICP-OES | [mg/l] | 0.10 - 5000 | 4.67 ±0.70 |

| CBiDGP Sp. z o.o. | Sprawozdanie z badań<br>Nr 1619/ZL/13<br><br>z dnia 2013-04-18 | Strona: 11<br><br>Stron: 15 |
|---|---|---|
| Załącznik nr 2/1 do PO-17, wydanie VI z 08.04.2013r. | | |

Nazwa klienta: UNIWERSYTET ŚLĄSKI WYDZIAŁ NAUK O ZIEMI KATEDRA GEOLOGII PODSTAWOWEJ
41-200 SOSNOWIEC, BĘDZIŃSKA 60

Miejsce poboru próbek: Nigeria - źródła występujące w środowisku osadowym — Próbki pobrał: Klient

Data dostarczenia próbek: 2013-04-05 — Próbki dostarczył: Klient

Stan próbek: dobry

| | | | | | | |
|---|---|---|---|---|---|---|
| | | | | Numer próbki | 1917/ZL1/13 | |
| | | | | Data/godzina pobrania próbki | | |
| | | | | Miejsce pobrania próbki | LACHIKOLTOK | |
| | | | | Rodzaj próbki | Woda | |
| S.J.* | Parametr | Metoda badawcza/ Metoda oznaczenia | Jednostka | Zakres wykonania oznaczenia | Wyniki badań | |
| A | Chlorki | PN-ISO 9297:1994 Miareczkowo | [mg/l Cl] | 5.0 - 50000 | 6.0 | ±0.2 |
| A | Siarczany | PN-ISO 9280:2002 Wagowo | [mg/l $SO_4$] | 10.0-5000 | 12.9 | ±1.9 |
| A | Wodorowęglany | PB-58/07.2008 wyd. I z dnia 11.07.2008r. Obliczeniowo | [mg/l] | 6.10 - 6100 | 262 | ±18 |
| A | Węglany | PB-58/07.2008 wyd. I z dnia 11.07.2008r. Obliczeniowo | [mg/l] | 3.0 - 3000 | <3.0[1)] | |
| A | Krzemionka ogólna | PN-EN ISO 11885:2009 ICP-OES | [mg/l $SiO_2$] | 0.10-100 | 45.6 | ±7.3 |
| A | Potas | PN-EN ISO 11885:2009 ICP-OES | [mg/l] | 1.0-10000 | 32.4 | ±5.8 |
| A | Sód | PN-EN ISO 11885:2009 ICP-OES | [mg/l] | 1.0-100000 | 40.6 | ±7.3 |
| A | Żelazo ogólne | PN-EN ISO 11885:2009 ICP-OES | [mg/l] | 0.010 - 500 | 5.74 | ±1.15 |
| A | Wapń | PN-EN ISO 11885:2009 ICP-OES | [mg/l] | 0.10 - 10000 | 40.5 | ±6.5 |
| A | Magnez | PN-EN ISO 11885:2009 ICP-OES | [mg/l] | 0.10 - 5000 | 6.90 | ±1.10 |

Nazwa klienta: UNIWERSYTET ŚLĄSKI WYDZIAŁ NAUK O ZIEMI KATEDRA GEOLOGII PODSTAWOWEJ
41-200 SOSNOWIEC, BĘDZIŃSKA 60

Miejsce poboru próbek: Nigeria - źródła występujące w środowisku osadowym — Próbki pobrał: Klient

Data dostarczenia próbek: 2013-04-05 — Próbki dostarczył: Klient

Stan próbek: dobry

| | | | | | |
|---|---|---|---|---|---|
| | | | Numer próbki | | 1918/ZL1/13 |
| | | | Data/godzina pobrania próbki | | |
| | | | Miejsce pobrania próbki | | DIGGA |
| | | | Rodzaj próbki | | Woda |
| S.J.* | Parametr | Metoda badawcza/ Metoda oznaczenia | Jednostka | Zakres wykonania oznaczenia | Wyniki badań |
| A | Chlorki | PN-ISO 9297:1994 Miareczkowo | [mg/l Cl] | 5.0 - 50000 | 141 ±4 |
| A | Siarczany | PN-ISO 9280:2002 Wagowo | [mg/l $SO_4$] | 10.0-5000 | 12.9 ±1.9 |
| A | Wodorowęglany | PB-58/07.2008 wyd. I z dnia 11.07.2008r. Obliczeniowo | [mg/l] | 6.10 - 6100 | 1196 ±80 |
| A | Węglany | PB-58/07.2008 wyd. I z dnia 11.07.2008r. Obliczeniowo | [mg/l] | 3.0 - 3000 | 84.0 ±5.6 |
| A | Krzemionka ogólna | PN-EN ISO 11885:2009 ICP-OES | [mg/l $SiO_2$] | 0.10-100 | 20.4 ±3.3 |
| A | Potas | PN-EN ISO 11885:2009 ICP-OES | [mg/l] | 1.0-10000 | 14.2 ±2.6 |
| A | Sód | PN-EN ISO 11885:2009 ICP-OES | [mg/l] | 1.0-100000 | 600 ±108 |
| A | Żelazo ogólne | PN-EN ISO 11885:2009 ICP-OES | [mg/l] | 0.010 - 500 | 0.73 ±0.15 |
| A | Wapń | PN-EN ISO 11885:2009 ICP-OES | [mg/l] | 0.10 - 10000 | 8.26 ±1.30 |
| A | Magnez | PN-EN ISO 11885:2009 ICP-OES | [mg/l] | 0.10 - 5000 | 1.16 ±0.20 |

Nazwa klienta: UNIWERSYTET ŚLĄSKI WYDZIAŁ NAUK O ZIEMI KATEDRA GEOLOGII PODSTAWOWEJ
41-200 SOSNOWIEC, BĘDZIŃSKA 60

Miejsce poboru próbek: Nigeria - źródła występujące w środowisku osadowym

Próbki pobrał: Klient

Data dostarczenia próbek: 2013-04-05

Próbki dostarczył: Klient

Stan próbek: dobry

| | | | | | | |
|---|---|---|---|---|---|---|
| | | | | Numer próbki | 1919/ZL1/13 | |
| | | | | Data/godzina pobrania próbki | | |
| | | | | Miejsce pobrania próbki | LASHADAR | |
| | | | | Rodzaj próbki | Woda | |
| S.J.* | Parametr | Metoda badawcza/ Metoda oznaczenia | Jednostka | Zakres wykonania oznaczenia | Wyniki badań | |
| A | Chlorki | PN-ISO 9297:1994 Miareczkowo | [mg/l Cl] | 5.0 - 50000 | 98 | ±3 |
| A | Siarczany | PN-ISO 9280:2002 Wagowo | [mg/l $SO_4$] | 10.0-5000 | 13.4 | ±2.0 |
| A | Wodorowęglany | PB-58/07.2008 wyd. I z dnia 11.07.2008r. Obliczeniowo | [mg/l] | 6.10 - 6100 | 647 | ±43 |
| A | Węglany | PB-58/07.2008 wyd. I z dnia 11.07.2008r. Obliczeniowo | [mg/l] | 3.0 - 3000 | <3.0[1)] | |
| A | Krzemionka ogólna | PN-EN ISO 11885:2009 ICP-OES | [mg/l $SiO_2$] | 0.10-100 | 30.2 | ±4.8 |
| A | Potas | PN-EN ISO 11885:2009 ICP-OES | [mg/l] | 1.0-10000 | 16.5 | ±3.0 |
| A | Sód | PN-EN ISO 11885:2009 ICP-OES | [mg/l] | 1.0-100000 | 310 | ±56 |
| A | Żelazo ogólne | PN-EN ISO 11885:2009 ICP-OES | [mg/l] | 0.010 - 500 | 0.22 | ±0.04 |
| A | Wapń | PN-EN ISO 11885:2009 ICP-OES | [mg/l] | 0.10 - 10000 | 13.2 | ±2.1 |
| A | Magnez | PN-EN ISO 11885:2009 ICP-OES | [mg/l] | 0.10 - 5000 | 1.43 | ±0.20 |

| CBiDGP Sp. z o.o. | Sprawozdanie z badań<br>Nr 1619/ZL/13<br><br>z dnia 2013-04-18 | Strona: 14<br><br>Stron: 15 |
|---|---|---|
| Załącznik nr 2/1 do PO-17, wydanie VI z 08.04.2013r. | | |

Nazwa klienta: UNIWERSYTET ŚLĄSKI WYDZIAŁ NAUK O ZIEMI KATEDRA GEOLOGII PODSTAWOWEJ
41-200 SOSNOWIEC, BĘDZIŃSKA 60

Miejsce poboru próbek: Nigeria - źródła występujące w środowisku osadowym — Próbki pobrał: Klient

Data dostarczenia próbek: 2013-04-05 — Próbki dostarczył: Klient

Stan próbek: dobry

| | | | | | |
|---|---|---|---|---|---|
| | | | | Numer próbki | 1920/ZL1/13 |
| | | | | Data/godzina pobrania próbki | |
| | | | | Miejsce pobrania próbki | LAKOMJI WARM SPRING |
| | | | | Rodzaj próbki | Woda |
| S.J.* | Parametr | Metoda badawcza/ Metoda oznaczenia | Jednostka | Zakres wykonania oznaczenia | Wyniki badań |
| A | Chlorki | PN-ISO 9297:1994 Miareczkowo | [mg/l Cl] | 5.0 - 50000 | 5.0 ±0.1 |
| A | Siarczany | PN-ISO 9280:2002 Wagowo | [mg/l $SO_4$] | 10.0-5000 | 13.9 ±2.1 |
| A | Wodorowęglany | PB-58/07.2008 wyd. I z dnia 11.07.2008r. Obliczeniowo | [mg/l] | 6.10 - 6100 | 126 ±8 |
| A | Węglany | PB-58/07.2008 wyd. I z dnia 11.07.2008r. Obliczeniowo | [mg/l] | 3.0 - 3000 | <3.0[1)] |
| A | Krzemionka ogólna | PN-EN ISO 11885:2009 ICP-OES | [mg/l $SiO_2$] | 0.10-100 | 29.4 ±4.7 |
| A | Potas | PN-EN ISO 11885:2009 ICP-OES | [mg/l] | 1.0-10000 | 20.0 ±3.6 |
| A | Sód | PN-EN ISO 11885:2009 ICP-OES | [mg/l] | 1.0-100000 | 18.6 ±3.4 |
| A | Żelazo ogólne | PN-EN ISO 11885:2009 ICP-OES | [mg/l] | 0.010 - 500 | 0.018 ±0.004 |
| A | Wapń | PN-EN ISO 11885:2009 ICP-OES | [mg/l] | 0.10 - 10000 | 28.5 ±4.6 |
| A | Magnez | PN-EN ISO 11885:2009 ICP-OES | [mg/l] | 0.10 - 5000 | 4.46 ±0.70 |

| CBIDGP Sp. z o.o. | Sprawozdanie z badań<br>Nr 1619/ZL/13<br><br>z dnia 2013-04-18 | Strona: 15<br><br>Stron: 15 |
|---|---|---|
| Załącznik nr 2/1 do PO-17, wydanie VI z 08.04.2013r. | | |

Nazwa klienta: UNIWERSYTET ŚLĄSKI WYDZIAŁ NAUK O ZIEMI KATEDRA GEOLOGII PODSTAWOWEJ
41-200 SOSNOWIEC, BĘDZIŃSKA 60

Miejsce poboru próbek: Nigeria - źródła występujące w środowisku osadowym — Próbki pobrał: Klient

Data dostarczenia próbek: 2013-04-05 — Próbki dostarczył: Klient

Stan próbek: dobry

| | | | | | |
|---|---|---|---|---|---|
| | | | | Numer próbki | 1921/ZL1/13 |
| | | | | Data/godzina pobrania próbki | |
| | | | | Miejsce pobrania próbki | SAMPLE 14 |
| | | | | Rodzaj próbki | Woda |
| S.j.* | Parametr | Metoda badawcza/ Metoda oznaczenia | Jednostka | Zakres wykonania oznaczenia | Wyniki badań |
| A | Chlorki | PN-ISO 9297:1994 Miareczkowo | [mg/l Cl] | 5.0 - 50000 | 100 ±3 |
| A | Siarczany | PN-ISO 9280:2002 Wagowo | [mg/l $SO_4$] | 10.0-5000 | 14.4 ±2.2 |
| A | Wodorowęglany | PB-58/07.2008 wyd. I z dnia 11.07.2008r. Obliczeniowo | [mg/l] | 6.10 - 6100 | 561 ±38 |
| A | Węglany | PB-58/07.2008 wyd. I z dnia 11.07.2008r. Obliczeniowo | [mg/l] | 3.0 - 3000 | 72.0 ±4.8 |
| A | Krzemionka ogólna | PN-EN ISO 11885:2009 ICP-OES | [mg/l $SiO_2$] | 0.10-100 | 12.4 ±2.0 |
| A | Potas | PN-EN ISO 11885:2009 ICP-OES | [mg/l] | 1.0-10000 | 21.2 ±3.8 |
| A | Sód | PN-EN ISO 11885:2009 ICP-OES | [mg/l] | 1.0-100000 | 327 ±59 |
| A | Żelazo ogólne | PN-EN ISO 11885:2009 ICP-OES | [mg/l] | 0.010 - 500 | 0.073 ±0.015 |
| A | Wapń | PN-EN ISO 11885:2009 ICP-OES | [mg/l] | 0.10 - 10000 | 14.8 ±2.4 |
| A | Magnez | PN-EN ISO 11885:2009 ICP-OES | [mg/l] | 0.10 - 5000 | 3.66 ±0.60 |

Wodorowęglany: na podstawie zasadowości złożonej i ogólnej. Węglany: na podstawie zasadowości złożonej i ogólnej.
Niepewność: niepewność rozszerzona wykonania oznaczenia dla p=95% i współczynnika rozszerzenia k=2.
* S.j. - symbol jakości metody badawczej: A - metoda akredytowana przez PCA, test zamieszczona w zakresie akredytacji PCA nr AB 418.
1) < - poniżej oznaczalności

Laboratorium oświadcza, że wyniki odnoszą się wyłącznie do badanej(ych) próbki(ek). Niniejsze sprawozdanie z badań bez pisemnej zgody laboratorium nie może być powielane inaczej niż w całości.
Daty wykonania poszczególnych badań są identyfikowalne poprzez zapisy prowadzone w laboratorium.

*KONIEC SPRAWOZDANIA*